Comparison of bus network structures versus urban dispersion : a monocentric analytical approach : evidences from Barcelona's bus network

Hugo Badia Rodríguez

PhD THESIS

Comparison of bus network structures versus urban dispersion: A monocentric analytical approach

Evidences from Barcelona's bus network

Author:

Hugo Badia Rodríguez

Comparison of bus network structures versus urban dispersion: A monocentric analytical approach

Evidences from Barcelona's bus network

Author:

Hugo Badia Rodríguez

This thesis is submitted in satisfaction of the requirements for the degree of
Doctor of Philosophy in Civil Engineering

Civil Engineering School of Barcelona
Technical University of Catalonia - Barcelona Tech

Supervisors:

Dr. Miquel Àngel Estrada Romeu

Dr. Francesc Robusté Antón

Fall 2016

UNIVERSITAT POLITÈCNICA DE CATALUNYA
BARCELONATECH
Escola Tècnica Superior d'Enginyers
de Camins, Canals i Ports de Barcelona

"Quan surts per fer el viatge cap a Ítaca,
has de pregar que el camí sigui llarg,
ple d'aventures, ple de coneixences.
Has de pregar que el camí sigui llarg,
que siguin moltes les matinades
que entraràs en un port que els teus ulls ignoraven,
i vagis a ciutats per aprendre dels que saben."

Excerpt from the song *"Viatge a Ítaca"*, Lluís Llach, 1975;
adaptation of Konstantinos Kavafis' poem *"Ithaca"*, 1911.

Abstract

Comparison of bus network structures versus urban dispersion: A monocentric analytical approach

Evidences from Barcelona's bus network

Hugo Badia Rodríguez

Doctor of Philosophy in Civil Engineering

This thesis discusses which transit network structure is the best option to serve urban mobility. As a consequence of the evolution of urban form, cities have undergone a dispersion process of their activities. This fact has caused a change in mobility needs in the last few decades. Mobility networks and services should progressively adapt to the new demand patterns, especially the bus transit network, which has more flexibility to reorganize the deployment of resources at an affordable cost. Three base transit network structures are compared: a radial scheme, a direct trip-based network, and a transfer-based system. An analytical model is used to estimate the behavior of these structures for idealized monocentric mobility patterns with several degrees of concentration. This is made atop two street patterns, grid and ring-radial.

The thesis aimed at determining the right range of situations for the applicability of each bus network structure, and providing guidelines about the transit network planning process. It turns out that the best structure is not always the same, and depends on the mobility spatial pattern. A radial network is the best alternative in very concentrated cities; however, a direct trip-based system is more suitable for intermediate degrees of dispersion. A transfer-based structure is the best option when the activities are more decentralized. Nevertheless, the decentralization degree that justifies a specific transit structure is not constant. This degree depends on the characteristics of the city, transport technology and users. The street pattern atop the network is designed also affects on the range of applicability, especially on the cut-off point between direct services and transfer-based networks. However, the different network structures follow the same behavior in front of urban dispersion and changes on input parameters in both street patterns.

The analysis of O-D matrixes gives a first approximation about in which decentralized scenario a city is. Therefore, given that decentralization, the arising question is what network structure is the most suitable alternative for its transit system. Barcelona (Spain) is an instance where a change of bus network structure from direct services to a transfer-based scheme is justified. The analytical network design model is applied to design a transfer-based bus network for this city. It provides a layout plan that is used as a design target to develop the detailed real master plan. The eventually proposed network, called the *Nova Xarxa*, covers the whole city by 28 corridors with easy understanding, non-circuitous lines, higher frequencies and ubiquitous transfer points. The final design improves the level of service, reducing by 4.12% total travel time for the pre-existing bus demand. However, the new bus network design has an important handicap, a greater number of transfers.

The *Nova Xarxa* is being deployed in a multiple-step implementation process. It is an opportunity to test the conventional wisdom that states that transit riders are averse to

transfers and that consequently bus networks should be designed to limit their number. In order to answer this question, this thesis examines data from the first three deployment phases of the *Nova Xarxa*. It is found that the lines of the *Nova Xarxa* are already carrying more passengers than the old lines they replaced. Furthermore, this demand has increased disproportionately with the number of lines opened for service in each phase, revealing the existence of network effect. At the end of 2015, the percentage of trips that involved a transfer was approximately 26%, and it will reach 44% once the *Nova Xarxa* is completed in 2018. Therefore, the numbers disprove the conventional wisdom.

Keywords: *Public transport; bus system; transit network design; bus network design; bus network structure; transfer-based network; hybrid network; analytical network design model; network effect; urban mobility; urban dispersion.*

Dr. Miquel Estrada

Associate Professor of Transportation
Civil Engineering - UPC Barcelona Tech
November, 2016

Dr. Francesc Robusté

Professor of Transportation
Civil Engineering - UPC Barcelona Tech
November, 2016

Resumen

Comparación de estructuras de red de autobuses frente a la dispersión urbana: Un enfoque analítico monocéntrico

Evidencias de la red de autobuses de Barcelona

Hugo Badia Rodríguez

Doctor en Ingeniería Civil

Esta tesis analiza que estructura de red de transporte público es la mejor opción para servir la movilidad urbana. Como consecuencia de la evolución de la estructura urbana, las ciudades han experimentado un proceso de dispersión de sus actividades. Este hecho ha causado un cambio en la necesidades de movilidad en las últimas décadas. Las redes y servicios de movilidad deben progresivamente adaptarse a los nuevos patrones de demanda, especialmente la red de transporte público de autobús, la cual tiene más flexibilidad para reorganizar la utilización de los recursos a un coste razonable. Tres estructuras base de red de transporte público son comparadas: un esquema radial, una red basada en conexiones directas, y un sistema basado en transferencias. Un modelo analítico es usado para estimar el comportamiento de estas estructuras para idealizados patrones monocéntricos de movilidad con diferentes grados de concentración. Esto es realizado sobre dos patrones de calles, una malla rectangular y otra radial-circular.

La tesis pretendía determinar el correcto rango de situaciones para la aplicabilidad de cada estructura de red de autobuses, y proporcionar directrices sobre el proceso de planificación de la red de transporte público. Resulta que la mejor estructura no siempre es la misma, y depende del patrón espacial de la movilidad. Una red radial es la mejor alternativa en ciudades muy concentradas; sin embargo, un sistema basado en viajes directos es más adecuado para grados intermedios de dispersión. Una estructura basada en la transferencia es la mejor opción cuando las actividades están más descentralizadas. Sin embargo, el grado de descentralización que justifica una estructura específica de transporte público no es constante. Este grado depende de las características de la ciudad, la tecnología del transporte y los usuarios. El patrón de calles sobre el que la red está diseñada también afecta al rango de aplicabilidad, especialmente al punto de cambio entre los servicios directos y redes basadas en transferencias. Aún así, las diferentes estructuras de red siguen el mismo comportamiento frente a la dispersión urbana y cambios en los parámetros de entrada en ambos patrones de calles.

El análisis de matrices O-D da una primera aproximación sobre en qué escenario de descentralización una ciudad se encuentra. Por lo tanto, dada esta descentralización, la pregunta que surge es qué estructura de red es la alternativa más adecuada para su sistema de transporte público. Barcelona (España) es un ejemplo donde se justifica un cambio de estructura de red de autobuses desde servicios directos a un esquema basado en transferencias. El modelo analítico para el diseño de red se aplica para diseñar una red de autobuses basada en transferencias para esta ciudad. Esto proporciona un plan de diseño que se utiliza como objetivo para desarrollar un plan maestro real detallado. La red finalmente propuesta, denominada *Nova Xarxa*, cubre toda la ciudad con 28 corredores de fácil comprensión, líneas no tortuosas, frecuencias más altas y puntos de transferencia ubicuos. El diseño final mejora el nivel de servicio, reduciendo un 4.12%

el tiempo total de viaje de la demanda del autobús preexistente. Sin embargo, el nuevo diseño de la red de autobuses tiene una desventaja importante, un mayor número de transferencias.

La *Nova Xarxa* está siendo desplegada en base a un proceso de implementación de varias etapas. Es una oportunidad para poner a prueba la sabiduría convencional que indica que los usuarios del transporte público son reacios a transferir y que en consecuencia las redes de autobuses deben ser diseñadas para limitar su número. Con el fin de responder a esta pregunta, esta tesis analiza datos de las tres primeras fases de despliegue de la *Nova Xarxa*. Se halla que las líneas de la *Nova Xarxa* ya están llevando más pasajeros que las viejas líneas que reemplazaron. Además, esta demanda se ha incrementado de manera desproporcionada con el número de líneas implementadas en cada fase, revelando la existencia del efecto red. A finales de 2015, el porcentaje de viajes que suponían una transferencia fue de aproximadamente un 26%, y alcanzará el 44% una vez que se haya completado la *Nova Xarxa* en 2018. Por lo tanto, los números desmienten la sabiduría convencional.

Palabras clave: *Transporte público; sistema de autobuses; diseño de red de transporte público; diseño de red de autobuses; estructura de red de autobuses; red basada en transferencias; red híbrida; modelo analítico de diseño de red; efecto red; movilidad urbana; dispersión urbana.*

Dr. Miquel Estrada

Profesor Agregado de Transportes
Ingeniería Civil - UPC Barcelona Tech
Noviembre, 2016

Dr. Francesc Robusté

Catedrático de Transportes
Ingeniería Civil - UPC Barcelona Tech
Noviembre, 2016

Resum

Comparació d'estructures de xarxa d'autobusos enfront de la dispersió urbana: Un enfocament analític monocèntric

Evidències de la xarxa d'autobusos de Barcelona

Hugo Badia Rodríguez

Doctor en Enginyeria Civil

Aquesta tesi analitza quina estructura de xarxa de transport públic és la millor opció per servir la mobilitat urbana. Com a conseqüència de l'evolució de l'estructura urbana, les ciutats han experimentat un procés de dispersió de les seves activitats. Aquest fet ha causat un canvi en les necessitats de la mobilitat a les últimes dècades. Les xarxes i serveis de mobilitat deuen progressivament adaptar-se als nous patrons de demanda, especialment la xarxa de transport públic d'autobús, la qual té més flexibilitat per reorganitzar la utilització dels recursos a un cost raonable. Tres estructures base de xarxa de transport públic són comparades: un esquema radial, una xarxa basada en connexions directes, i un sistema basat en transferències. Un model analític és utilitzat per estimar el comportament d'aquestes estructures per idealitzats patrons monocèntrics de mobilitat amb diferents graus de concentració. Això és realitzat sobre dos patrons de carrers, una malla rectangular i una altra radial-circular.

La tesi pretenia determinar el correcte rang de situacions per l'aplicabilitat de cada estructura de xarxa d'autobusos, i proporcionar directrius sobre el procés de planificació de la xarxa de transport públic. Resulta que la millor estructura no sempre és la mateixa, i depèn del patró espacial de la mobilitat. Una xarxa radial és la millor alternativa en ciutats molt concentrades; no obstant això, un sistema basat en viatges directes és més adequat per graus intermedis de dispersió. Una estructura basada en transferències és la millor opció quan les activitats estan més descentralitzades. Encara que el grau de descentralització que justifica una estructura específica de transport públic no és constant. Aquest grau depèn de les característiques de la ciutat, la tecnologia del transport i els usuaris. El patró de carrers sobre el que la xarxa està dissenyada també afecta el rang d'aplicabilitat, especialment al punt de canvi entre els serveis directes i xarxes basades en transferències. No obstant això, les diferents estructures de xarxa segueixen el mateix comportament enfront de la dispersió urbana i canvis en els paràmetres d'entrada en tots dos patrons de carrers.

L'anàlisi de matrius O-D dóna una primera aproximació sobre en què escenari de descentralització una ciutat es troba. Per tant, donada aquesta descentralització, la pregunta que sorgeix és quina estructura de xarxa és l'alternativa més adient pel seu sistema de transport públic. Barcelona (Espanya) és un exemple a on es justifica un canvi d'estructura de xarxa d'autobusos des de serveis directes a un esquema basat en transferències. El model analític per al disseny de xarxa s'aplica per dissenyar una xarxa d'autobusos basada en transferències per aquesta ciutat. Això proporciona un pla de disseny que s'utilitza com a objectiu per desenvolupar un pla mestre real detallat. La xarxa finalment proposada, denominada *Nova Xarxa* cobreix tota la ciutat amb 28 corredors de fàcil comprensió, línies no tortuoses, freqüències més altes i punts de transferència ubics. El disseny final millora el nivell de servei, reduint un 4.12% el temps total de viatge de la demanda de l'autobús preexistent. No obstant

això, el nou disseny de la xarxa d'autobusos té un desavantatge important, un major nombre de transferències.

La *Nova Xarxa* està sent desplegada d'acord amb un procés d'implementació de diverses etapes. És una oportunitat per posar a prova la saviesa convencional que indica que els usuaris del transport públic són reticents a transferir i que en conseqüència les xarxes d'autobusos deuen ser dissenyades per limitar el seu nombre. Amb la finalitat de respondre a aquesta pregunta, aquesta tesi analitza les dades de les tres primeres fases de desplegament de la *Nova Xarxa*. Es troba que les línies de la Nova Xarxa ja estan portant més passatgers que les velles línies que van reemplaçar. A més, aquesta demanda s'ha incrementat de manera desproporcionada amb el nombre de línies implementades en cada fase, revelant l'existència de l'efecte xarxa. A finals del 2015, el percentatge de viatges que suposaven una transferència va ser d'aproximadament un 26%, i assolirà el 44% una vegada que s'hagi completat la *Nova Xarxa* en 2018. Per tant, els nombres desmenteixen la saviesa convencional.

Paraules clau: *Transport públic; sistema d'autobusos; disseny de xarxa de transport públic; disseny de xarxa d'autobusos; estructura de xarxa d'autobusos; xarxa basada en transferències; xarxa híbrida; model analític de disseny de xarxa; efecte xarxa; mobilitat urbana; dispersió urbana*

Dr. Miquel Estrada

Professor Agregat de Transports
Enginyeria Civil - UPC Barcelona Tech
Novembre, 2016

Dr. Francesc Robusté

Catedràtic de Transports
Enginyeria Civil - UPC Barcelona Tech
Novembre, 2016

Publications derived from this thesis

The results of this thesis have already been published in three papers in SCI Journals with high impact factor:

- Estrada, M., Roca-Riu, M., **Badia, H.**, Robusté, F., Daganzo, C.F., 2011. Design and implementation of efficient transit networks: Procedure, case study and validity test. *Transportation Research Part A* 45 (9), 935-950. [Impact factor: 2.354, JCR - Thomson Reuters. Quantil Q1 in Transportation Science & Technology area.] (In *Proceedings of the 19th International Symposium on Transportation and Traffic Theory*. Berkeley, California.)

- **Badia, H.**, Estrada, M., Robusté, F., 2014. Competitive transit network design in cities with radial street patterns. *Transportation Research Part B* 59, 161-181. [Impact factor: 3.894, JCR - Thomson Reuters. Quantil Q1 in Transportation Science & Technology area.] (**Finalist of Young Researcher of the Year Award** of International Transport Forum of OECD.)

- **Badia, H.**, Estrada, M., Robusté, F., 2016. Bus network structure and mobility pattern: A monocentric analytical approach on a grid street pattern. *Transportation Research Part B* 93, 37-56. [Impact factor: 3.769, JCR - Thomson Reuters. Quantil Q1 in Transportation Science & Technology area.]

In addition, another SCI paper is currently under review, and some more papers will be written from unpublished results of this thesis.

- **Badia, H.**, Argote-Cabanero, J., Daganzo, C.F., (2017). How network structure can boost and shape the demand for bus transit. Submitted in *Transportation Research Part A*. [Impact factor: 1.994, JCR - Thomson Reuters. Quantil Q1 in Transportation Science & Technology area.]

Finally, some of these results have been accepted for presentation in two conferences:

- **Badia, H.**, 2016. Diseño de redes de autobús frente a la dispersión de la movilidad urbana. In *Proceedings of the XII Congreso de Ingeniería del Transporte*. Valencia, Spain. (In Spanish) (**Winner of Young Researcher Excellence Network Award** of Foro de Ingeniería del Transporte - FIT.)

- **Badia, H.**, Argote-Cabanero, J., Daganzo, C.F., 2017. Network effects in bus transit: Evidence from Barcelona's *Nova Xarxa*. In *Proceedings of the 96th Transportation Research Board Annual Meeting*. Washington, D.C.

Acknowledgements

First of all, I should indicate that this thesis has been funded by the Spanish Ministry of Education by means of a FPU grant (Formación de Profesorado Universitario - University Faculty Training), with the reference number AP2010-4544. This support has been essential for a complete dedication to this thesis to obtain the best results. In addition, complementary grants of the FPU program allowed me to do two abroad stages: one in Delft University of Technology (reference Est13/00284) and other in University of California, Berkeley (reference EST14/00438).

En segon lloc vull destacar el suport dels meus directors de tesi Prof. Miquel Estrada i Prof. Francesc Robusté. Pels seus consells, comentaris, correccions, aportacions, etc., en definitiva, pel seu acompanyament durant aquests anys a l'hora d'encarar la tesi doctoral.

I also want to thanks the opportunity that Prof. Daganzo and Prof. Cassidy gave me to do a PhD stage at UC Berkeley. This opportunity allowed me to work together with Prof. Carlos Daganzo and Dr. Juan Argote, a productive collaboration that is part of this thesis. Fue un verdadero placer trabajar y aprender con vosotros.

I express my gratitude to Prof. Van Nes for hosting me at TU Delft and allowing me to enjoy the big family of the Transport & Planning Department. Thanks to Xavi, Han, Xiao, Kai, Lin and many others for giving me those very nice months.

Obviamente, no me puedo olvidar de mencionar a todos los compañeros del CENIT y de la UPC que me han acompañado durante estos años haciendo más soportable el largo periodo que ha supuesto completar esta tesis: Quique, Mireia, Javi, Pau, Albert, Siscu, Carles, Òscar, Beti, Deme, Vero, Pilar, César, Marcel, Víctor, Aleix, Sara, Jaume, Ester y muchos otros. En especial, quiero destacar la labor de Sandra, un apoyo fundamental para enfrentarse a la agotadora burocracia que nos envuelve.

Finalmente, agradecer el permanente apoyo de mi familia, mi madre, mi padre, mis abuelos, mi hermano Santi, Àngels, y mis sobrinos Matilde y Blai, ambos nacidos durante el desarrollo de esta tesis.

Muchas gracias a todos y buena suerte / Many thanks to all of you and good luck,

Hugo

Barcelona, madrugada del 11 de noviembre de 2016

Contents

List of Figures

List of Tables

Part I: THESIS APPROACH

Chapter 1

Introduction

Transportation has a relevant impact in the economy, as well as in social, political and environmental aspects. The economic competitiveness of a city and its social equity might be determined by its transport supply. Among the different transport modes, the convenience of transit systems versus automobile in urban areas is clearly accepted. Transit systems are a key strategy to overcome the mobility problems caused by the private vehicle. The congestion states achieved by car, urban space degradation, air and noise pollution, travel time growth, and the inefficient use of space and energy have led to an unsustainable scenario (Cervero, 1998).

A good design of these transit systems is essential to guarantee their efficiency and effectiveness in order to be an attractive and a competitive transport mode. Among the different aspects that one can consider for a well-designed transit network, its network structure stands out, i.e., how the different transit lines that compose the system are arranged over the city. This structure should be the most suitable with regard to transit system cost and level of service to satisfy the urban mobility patterns. These patterns have changed at the same time as the urban form where activities have followed a process of decentralization. As a consequence, a discussion appears about what network structure is the best solution to satisfy the new mobility requirements (Dodson et al., 2011).

In this line, this thesis connects the urban mobility pattern evolution and the transit network design problem in order to contribute and clarify the previous discussion. Therefore, the best transit network structure is found out as a function of the urban mobility pattern that the network has to serve.

1.1. Urban form evolution and mobility patterns

The urban spatial structure has evolved from initial centralized scenarios to a complete dispersion in those cities that present the maximum degree of evolution. Rodrigue et al. (2006) summarized this evolution in three phases: the pre-industrial phase when the city was highly centralized, in this case, the major part of activities take place in a central business district (CBD) or city center that was limited to a small area; the second phase was the result of the industrial revolution, an intermediate scenario where some of these activities started to scatter over adjacent areas of the CBD; and the last, the contemporary stage, is a dispersed urban form, where a high number of activities are relocated in new peripheral areas far away from the CBD.

Anas et al. (1998) presented a similar evolution of the city in the last two centuries from a centralized to a decentralized scenario due to changes in technology, telecommunications and transportation. From the called *nineteenth century city*, characterized by a compact core surrounded by residential areas, CBD's have been expanding. At first, activities from the center spread outward around it; after, new poles of activities appear, forming subcenters or, in a metropolitan scale, edge cities. Initially, these new poles presented a clustered form, and as the time went by, they also reached a scenario of dispersion. However, this evolution presents different degrees of development in each city. In general, American cities present a high degree of dispersion while European cities still maintains strong centers.

In line with this historical evolution of the urban form, each city presents a particular process of decentralization. Bertaud (2004) exposed that all city was originally monocentric and they have progressively evolved to polycentric patterns. The existing urban spatial structures that we can find are different stages of that evolution. As the previous authors explained, the CBD has lost its primacy in benefit of new clusters of activities. However, the idealized polycentrism as a group of self-sufficient urban villages aggregated to conform the city does not exist in the real world. Each cluster performs in the same way as the traditional center since these clusters attract trips from everywhere of the city. Nevertheless, among the different clusters, the CBD remains the most relevant, forming the mono-polycentric model proposed by this author: city with more than one attractant pole of demand, where the extended traditional center is still predominant, attracting most of the trips. Finally, the author concluded that there would be two types of cities in the future, one that retains a strong center and one completely dispersed with no centrality.

Lee (2007) identified three distinctive patterns in American urban areas based on two of the dimensions of the urban sprawl phenomenon, concentration and centralization. These three types of city are: (i) monocentric city, where the urban core remains stable although with a certain level of deconcentration in its adjacent areas, but with a little level of decentralization; (ii) polycentric city, where the activities that are decentralized from the CBD are reconcentrated in suburban centers at the same time; and (iii) dispersed city, characterized by the absence of a clear structure, where decentralized activities from the CBD are not regrouped in other centers, in this case, the decentralization is accompanied by a deconcentration process. The most generalized pattern in European cities is the first of the previous patterns, since the traditional city centers remain as the most significant pole of activities and new poles are usually dependent on them. As Riguelle et al. (2007) and Bontje and Burdack (2005) showed, polycentrism is weak in these cities due to the prestige of their historical centers. Jobs remain concentrated in the city center, but it tends to decentralization.

Other authors studied urban spatial structures from different cities by means of diverse tools of analysis of employment and population distributions. Giuliano and Small (1991), Baumont et al. (1999), Craig and Ng (2001), Griffith and Wong (2007) and Pereira et al. (2013) reinforced the idea that the monocentrism is still predominant, the clusters of high demand are located around the traditional CBD. However, the deconcentration process is a general tendency since new centralities have appeared. Their densities are higher in comparison with their surroundings, but not in comparison with the whole city.

The urban form and the mobility pattern are connected (Aguilera, 2005). Due to this process of urban decentralization, the vector of displacements have been changing from a centripetal pattern, where all trips have their origins or destinations in the city center, to decentralized scenarios, where a high percentage of trips connect peripheral areas without depending on the CBD. In addition, there is a reciprocal relationship between the urban form and the transportation networks. The former constrains the development of the transport network, and the latter allows the development of a specific urban form. As it is shown in Pucher and Lefevre (1996) and Giuliano and Narayan (2003), American cities present a more dispersed structures because of a more extended use of the automobile. However, in European cities, higher modal splits of transit systems have retained the monocentric urban structures.

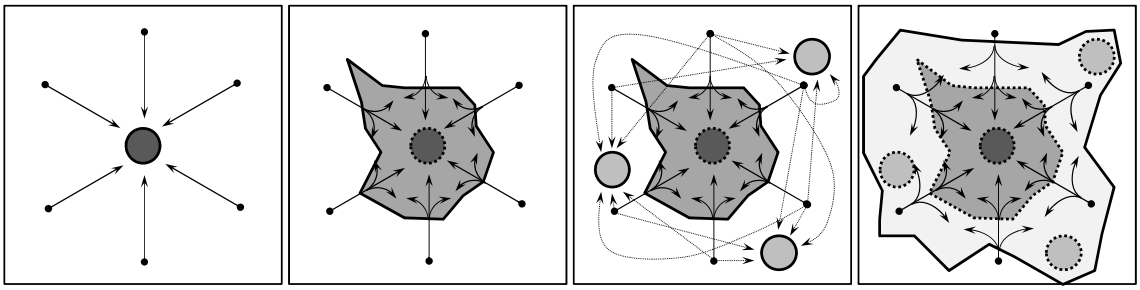

(a) Monocentric city, centralization and concentration

(b) CBD extension, Deconcentration - and low decentralization

(c) Polycentric city, decentralization - and low deconcentration

(d) Dispersed city, decentralization and deconcentration

Figure 1.1. Urban form evolution and mobility patterns associated.

It is important to emphasize that when we refer to the urban form evolution, the words *dispersion*, *(de)concentration* and *(de)centralization* are used interchangeably along most of the document. This is a consequence of the approach assumed in this dissertation to represent the urban form and the related mobility patterns, where in practice those three terms can be considered synonymous.

1.2. Transit network design

Transit systems should adapted to the evolution of the urban spatial structure. In a centralized urban form, the best solution is evidently a radial structure, where all lines of the network are focused on the city center. However, when this scenario changes due to urban sprawl, modifications on the network are needed to serve new mobility requirements. The traditional solution has been the development of new lines overlapped with the existing lines in order to connect new centralities with the rest of the city. The last objective is to satisfy new displacements reducing the number of transfers. The transfer is considered by many planners as an important dissuasive element for the promotion of transit usage. For example, some transit

network design models introduce the minimization of the number of transfers in its objective function (Zhao, 2006) or as a constraint with regard to the maximum number of transfers (Baaj and Mahmassani, 1995). This approach conforms direct trip-based network structures. However, these types of network design present some characteristics that set out doubts about their suitability. Thompson (1977), Mess (2000) and Nielsen et al. (2005) emphasize the weaknesses of this strategy of network design:

- Diffuse system as a sum of many lines that operate independently to each other without working as a real network. Each line connects directly many pairs origin-destination.
- Absence of hierarchy in the network design. Lines dispersed over a high number of streets; fact that makes it difficult to the implementation of operating measures widely.
- Low readability that makes the use of the transit network difficult, especially for unusual users.
- As the system works by direct services, the transfer process is not well-designed. Therefore, transfers are so expensive and the network dissuades to make non-direct trips.
- Complex routes to cover a large extension, that is, a great number of origin-destination pairs. This aspect lengthens the in-vehicle distance traveled.
- Low efficiency of the resources since these are diluted in many independent lines.
- Other factors related to these deficiencies are: low commercial speed, long travel times, low regularity and reliability, low frequencies and the long waiting times.

On the other hand, the same authors propose an alternative way to design the transit networks. These authors support a network reconfiguration based on simple structures where the transfer would be an essential step of the user transit chain. The success of these networks is based on the network effect exposed in Mees (2000). This network effect is the result of the synergies among the different lines of the system by means of transfers, fact that improved the efficiency (less resources) and effectiveness (more users) of the transit networks. The characteristics of this transfer-based network structure are widely explained in Nielsen et al. (2005), and in a summarized way in Nielsen et al. (2006):

- Simple network structures adapted to urban street patterns. Important measure to improve the operation from the agency point of view and the usage for users.
- Continuous and linear corridors to improve the operational efficiency with regard to commercial speed, reliability and regularity.
- Transit services concentrated on a limited number of road corridors. That is, one section-one line strategy, where every transit corridor is traversed by only one transit line.
- As a consequence of the previous aspects, resources are deployed in less streets. Therefore, an easier introduction of operational measures along the network and higher frequencies.
- From the user point of view, the main improvement is a greater network readability. This makes the combination of lines easier by means of transfers; the most important change about how the network works.

- By means of well-designed transfers, people can reach everywhere from any origin; moving away from the previous many-to-many configurations to all-to-all configurations.

Figure 1.2 shows the graphical description of these two network design approaches made in Nielsen et al. (2005).

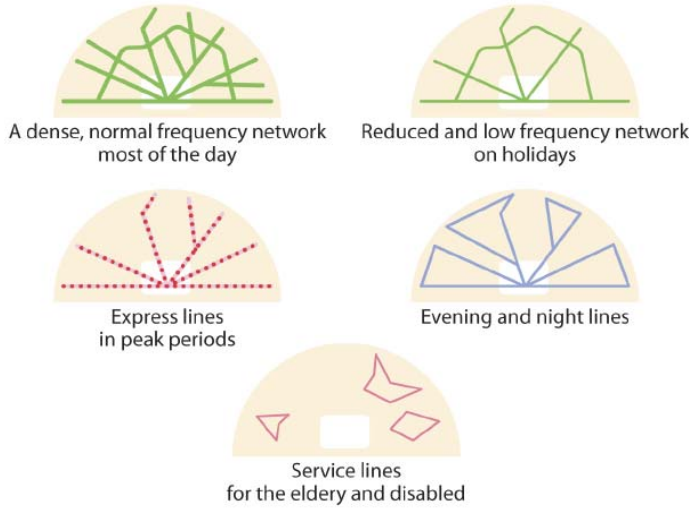

(a) The tailor-made approach

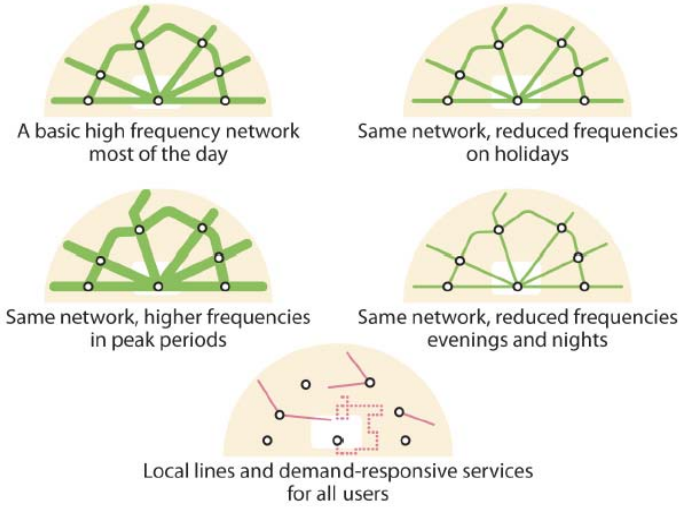

(b) The ready-made approach

Figure 1.2. Diagram of the two transit network design approaches compared. (Source: Nielsen et al., 2005)

Some authors analyzed the discussion about these two network design approaches by means of analytical models. Thompson (1977) did a simple comparison between four different structures: radial, ubiquitous (the highest degree of a direct trip-based system, where there is a direct line from each origin to any destination), grid and timed transfer (these two last represent two different transfer-based schemes). His main conclusion is that a transfer-based system provides a better service for peripheral trips than the traditional radial scheme, and, at the same time, is cheaper than a ubiquitous scheme. As a consequence, in a city decentralization process, these alternative structures are gaining applicability.

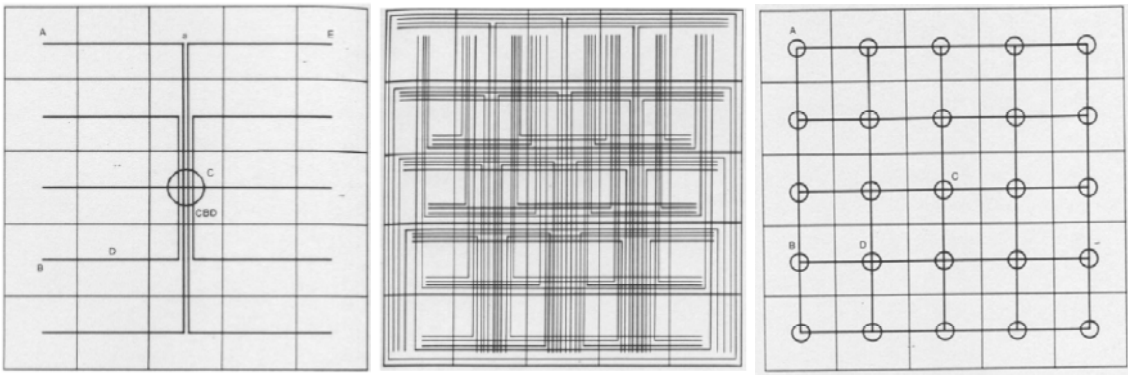

(a) Radial network *(b) Ubiquitous network* *(c) Grid network*

Figure 1.3. Three of the transit network structures analyzed in Thompson (1977). (Source: Thompson, 1977)

Other authors, Jara-Diaz and Gschwender (2003), studied the same problem in a simple spatial system, just composed by five nodes that form a cross. Two different strategies to serve the demand are compared, direct trips by means of lines that connect the different pairs O-D demanded, or by only two perpendicular corridors with a transfer point at their intersection. Their conclusion was that working with two corridors became more convenient with the demand disparity, and it is conditioned by the level of demand and unit user and agency costs. In the same line, other contributions from the same authors present similar results: considering financial constraints (Jara-Diaz et al., 2014) or one isolated line (Jara-Diaz et al., 2012).

On the other hand, Newell (1979) stated that a central area, where the major part of activities are concentrated, is generally found in cities due to economies of scale. Therefore, the transit system has to focus on that space. For this reason, he maintained the idea that a radial system concentrated around a central corridor would be the best strategy against alternative networks as the grid proposed in Holroyd (1967).

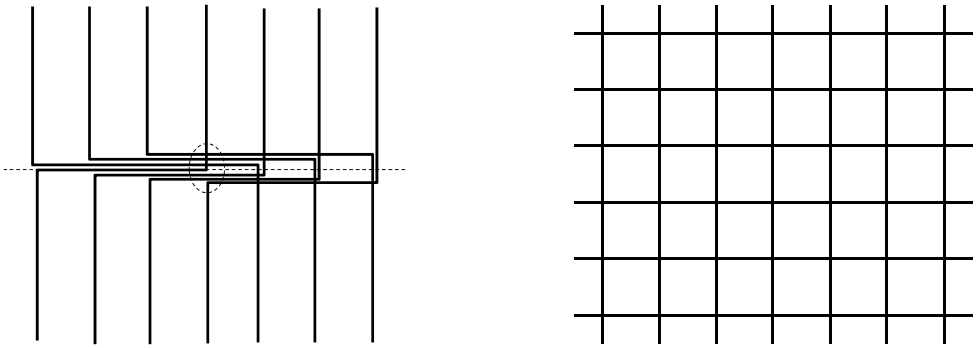

(a) Hub and spoke network *(b) Gird network*

Figure 1.4. Transit network structures compared in Newell (1979).

Other contributions justified the convenience of transfer-based transit systems by means of the analysis of real networks. Thompson and Matoff (2003) compared nine transit networks from different American cities based on supply, ridership, efficiency and effectiveness. They observed that those that had implemented a transfer-based network had had a better performance on most measures and they had not lost productivity. In Brown and Thompson (2008), a multivariate analysis of twenty metropolitan areas in USA refuted the idea that a decentralized network design, non focused only in the traditional center, produces a reduction of its productivity or an under-use of their resources.

Mees (2000) made an exhaustive comparison about urban form and transit system between two cities, Melbourne and Toronto. His conclusion was that the main reason why ridership in Toronto was higher than Melbourne was not the characteristics of their urban form, which were similar, but their transit system orientation and its consequences. Toronto presented a grid transit network structure following its street pattern, composed by integrated services with high frequencies that favor the network effect. Similar comparisons between Boston and Toronto (Schimek, 1997) or Broward (Florida) and Tarrant (Texas), made by Brown and Thompson (2012), gave similar conclusions.

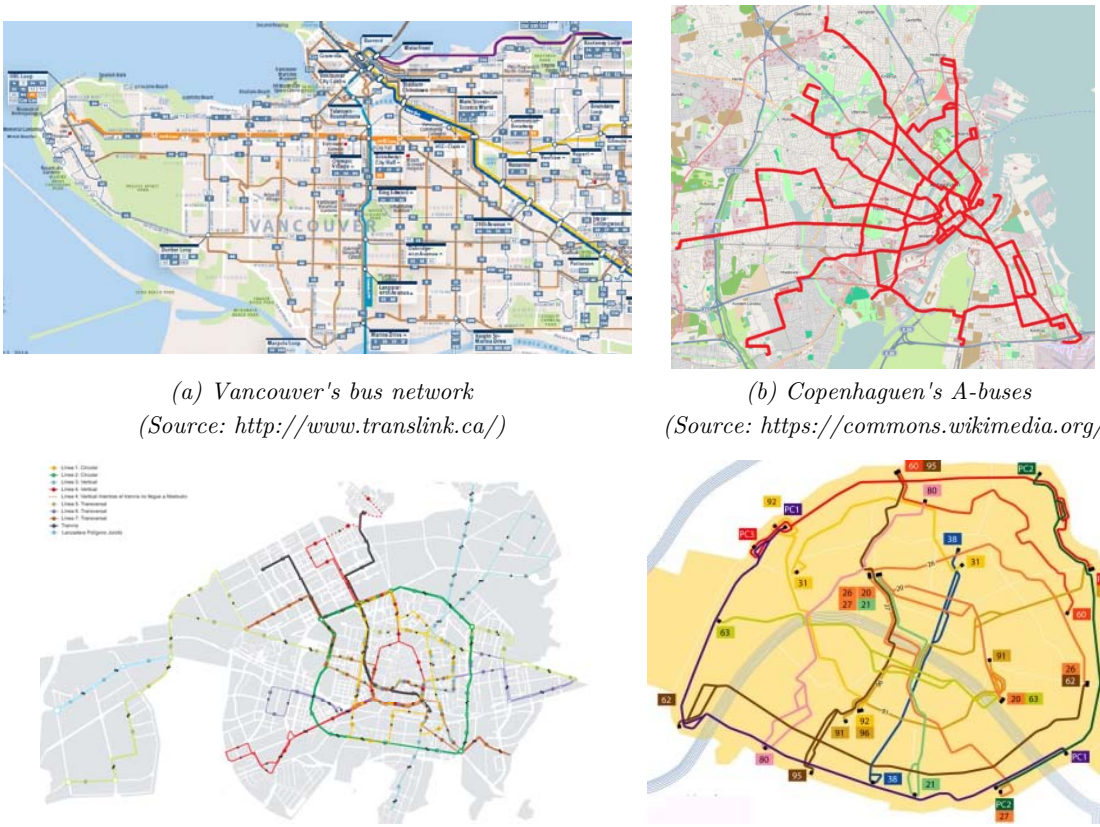

(a) Vancouver's bus network (Source: http://www.translink.ca/)

(b) Copenhaguen's A-buses (Source: https://commons.wikimedia.org/)

(c) Vitoria's bus network (Source: Rueda, 2010)

(d) Plan "Le Mobilien" for Paris

Figure 1.5. Four real or planned transfer-based bus networks.

While transfer-based networks have been developed in some American cities (Chicago, San Francisco, Portland, etc.) and widely in Canadian cities like Vancouver (Figure 1.5a), Toronto or Montreal, they are not common in European cities. In line with the implementation of buses with high level of service (Heddebaut, 2010), in the last years, some European cities have partially implemented it in some corridors, but not as a complete network. Some exceptions like Blue-buses from Stockholm or A-buses (Figure 1.5b) from Copenhagen are transit networks with a simple structure adapted to their urban street patterns. However, these represent the highest level of a wider hierarchical transit system since the previous network has not been removed completely. Therefore, they are a mix between a transfer-based and a direct trip-based networks. In the same line, there was a proposal for Paris, *"Le Mobilien"*. As Figure 1.5d shows, this is a wide plan for a reconfiguration of the transit system in which there is a simple and hierarchical group of lines with a high level of service (Labbouz et al., 2006; González, 2008). An exemption is the case of Vitoria (Spain), where the old network was completely replaced by a transfer-based network with a ring-radial scheme (Figure 1.5c). Rueda et al. (2009) summarized

the changes made with the new network and its advantages: few lines, higher frequencies, higher commercial speeds, shorter total travel times, and an increasing of the level of demand.

1.3. Thesis goals

Among the different aspects commented above about the transit network design, this dissertation focuses its attention on the network structure and its relationship with the urban sprawl process that affects the mobility patterns. Due to this process of deconcentration and decentralization, the vector of displacements changes from centripetal patterns, where every trip has its origin or destination in the city center, to dispersed scenarios, where a high percentage of trips connect peripheral areas without depending on the traditional CBD.

Given this phenomenon, transit systems should evolve with urban form changes to respond new mobility requirements. Figure 1.6 summarizes the dissertation framework followed with regard to urban form evolution and the transit network structure related to the different phases of that evolution. As it has been commented previously, in a centralized city, the best solution would be a radial structure. However, when this scenario is overcome, new lines are implemented to serve new centralities by direct connections. This strategy conforms the network structure that is called along the dissertation direct trip-based structure. That is, its main objective is to satisfy the highest percentage of displacements by means of direct trips. The last stage of its development is a ubiquitous system where from any zone of the city there is at least one line to reach any other zone.

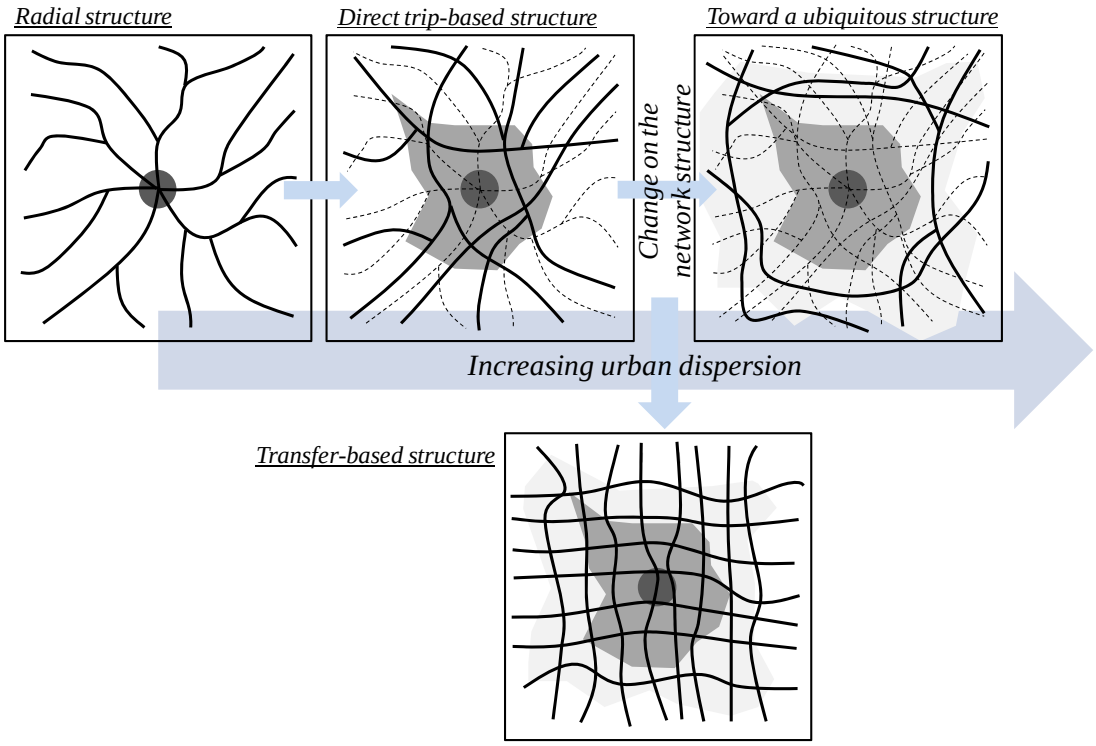

Figure 1.6. Dissertation framework with respect to urban form and transit network evolution.

However, **this thesis wants to check if there is a certain degree of demand dispersion from which developing more direct services is no longer the best decision.** From that dispersion degree on, **a reorganization of the transit lines in order**

to design a simple structure and clear points of interchange between lines (named along the document transfer-based structure) **is the most efficient way to operate the transit system. The main goal of this dissertation is to obtain when and where each type of network structure is more suitable to serve a specific demand pattern.**

In summary, the main questions that this dissertation addresses are:

- General insights about **the behavior of transit systems versus urban form evolution**, focusing the attention on the network structure.
- **Range of applicability for different transit network structures** and how these ranges change with regard to city, demand and transit characteristics. Therefore, guidelines are provided to determine the best network structure for different scenarios of study.
- Parsimonious methodology **to obtain a first approximation about what transit network would be the most suitable alternative in real cities**, i.e., whether a city has reached the threshold of urban dispersion that justifies a change on the transit network structure.
- **Redesign of a real transit system based on a transfer-based structure**, comparing the new design with the old one to validate the previous theoretical results. In addition, its implementation gives the opportunity to examine with real data the benefits of the new design.

First, in order to make all this, an analytical model is developed. It is based on continuous approximations and geometrical probability. This model gives the theoretical results to understand the transit system behavior and general guidelines about well-designed networks. Secondly, a simple methodology is defined to compare the analytical results with the urban dispersion levels in real cities. Finally, by means of macrosimulation and real demand data analysis, a real case study serves to evaluates the benefits, improvements and better performance because of a change in the bus network structure.

The comparison made in this thesis improves and goes in depth the previous works of Thompson (1977) and Jara-Diaz and Gschwender (2003). The former only considered the last stage of a direct trip-based network, the ubiquitous, therefore, the lack of an analysis where that structure is concentrated around the main attraction poles leaves the door open for a deeper comparison. The latter analyzed a network composed by two perpendicular corridors, what is the same as two one-dimension analyses overlapped. As a consequence, they did not consider some important aspects in the comparison, such as the spatial coverage or the trip length, and did not identify the degree of dispersion from which a transfer-based network is better. An extension of the analysis to a two-dimension network would be necessary.

1.4. Thesis contents

The structure of this dissertation is composed by four parts. The first one provides for the reader an overview about the discussion of how transit network design should be faced. In addition, Chapter 1 shows the relationship between urban form evolution and transit network

structure. On the other hand, Chapter 2 presents the State of the Art of transit network design models, where a set of discrete and analytical models are discussed. Moreover, this chapter reviews the different existing approaches to compare distinct urban spatial structures and to measure the dimensions of the urban sprawl process.

The second part includes the theoretical analysis made with regard to transit network structure. Chapter 3 presents the analytical model developed to make the comparison among different structures on two different street patterns. This chapter explains its characteristics: geometrical schemes, decision variables, input parameters, objective function, and agency and user costs. In Chapter 4, the results of the comparison among network structures in idealized cities for different scenarios of the urban form evolution are exhaustively presented. In this chapter, the range of applicability for each structure and the respective cut-off urban dispersion degree between each pair of them are identified. Finally, Chapter 5 analyses real mobility patterns from some real cities by means of origin-destination matrixes. As a result of this analysis, the urban dispersion degree is obtained and compared with the previous analytical results. In this way, a parsimonious methodology approximately determines which is the best network structure in real urban scenarios.

After that, Part III analyses a real case study, the Barcelona's bus network. Chapter 6 designs a new bus network for Barcelona with the goal to transform the pre-existing network from a direct trip-based structure to a transfer-based one. After defining the new design, this chapter includes a macroanalysis of demand over the former and new bus networks to measure their performances. Chapter 7 closes this third part. Once the new network has been partially implemented, an extended analysis of its demand provides an opportunity to evaluate its goodness related to the level of demand, mainly a consequence of the network effect.

Then, the most important conclusions of this dissertation are summarized in Part IV (Chapter 8). It also includes possible extensions of the research content of this thesis. Finally, other information of interest is extended in different appendices such as an exhaustive derivation of model's formulae, a sensitivity analysis of that model, and additional data of the theoretical results and Barcelona's bus network.

Chapter 2

State of the Art

This second chapter provides an overview of two of the main aspects to make possible this dissertation: (i) models that face the transit network design problem, a essential tool to make a comparison among different possible network structures or strategies; and (ii) methodologies to measure the dispersion degree in urban areas, the phenomenon that supports the discussion about the transit network design. Section 2.1 summarizes the main transit network design models and Section 2.2 the different ways used in order to understand the urban form. Finally, Section 2.3 ponders what type of approach would be the most useful to deal with the thesis' objectives.

2.1. Transit network design problem

Transit system planning is a complex process that Ceder and Wilson (1986) divides in five sequential tasks. These tasks are aggregated by Desaulniers and Hickman (2007) in three main steps. Table 2.1 summarizes these tasks and steps and their respective outputs. These sequential tasks are interdependent among them, a fact that converts the planning process in a complex problem. Therefore, the different models involved in this process deal with one or two of these tasks but not the whole process at the same time. An additional aspect that increases the problem complexity is the different stakeholders with opposed interests. There are at least two, transit agency and users. This fact converts the problem in multiobjective. The models search for a balanced solution that meets the budget constraints of the agency and the level of service perceived by users.

Table 2.1. Steps and tasks that compose the planning process in transit systems.

Step	Task	Output
Strategic	*Network design*	Definition of network structure, routes and stops
Tactical	*Frequencies setting*	Determination of service frequencies
	Timetable development	Elaboration of service timetables, departure times and arrival times
Operational	*Bus scheduling*	Estimation of fleet needed to serve the different periods during the day
	Driver scheduling	Allocation of driver crew on vehicles related to labor constraints

There is a wide range of models that solve the planning problem. Guilhaire and Hao (2008) classify the different models that deal with the first two steps regarding the tasks that they address. There are three types of basic problems: network design (TNDP), frequencies setting (TNFSP) and timetable development (TNTP). Moreover, there are two types as a result of the combination of two basic problems: network design-frequencies setting (TNDFSP), and frequencies setting-timetable development (TNSP). Finally, a sixth problem is stated as a combination of the three basic problems at the same time (TNDSP), i.e., strategic and tactical steps. These models are distinguished by (Fan and Machemehl, 2004): objective function, decision variables, input parameters, constraints, demand behavior, solving methodology and outputs.

Among the different components of the transit system planning process, this thesis focuses its attention on the two first ones: network design and frequencies setting. By means of network geometrical characteristics and its frequency of service, it is possible to obtain the system costs performance. From this point, we can make a comparison among alternative network structures. Below, this section goes in depth into the developed models until now that solve both tasks, either individually (TNDP or TNFSP) or together (TNDFSP). These models are grouped in two families: discrete and analytical models. The reader can find a wide review of both two groups of models in Kepaptsoglou and Karlaftis (2009).

2.1.1. Discrete models

These models simplify the reality by means of a graph that represents the street network. This graph is composed by nodes, where the demand is generated and attracted and are possible candidates to stop, and links, the streets that connect the nodes and are possible sections of transit lines. Their characteristics are treated in a disaggregated way. The objective function and route construction criteria define the optimal network, number of routes and stops and links that compose each of them. The resultant problem is *NP-Hard*, a complexity that increases with the network size. Therefore, combinatorial optimization techniques are used for its solution. Some of its benefits are: direct adaptation to the available streets and a more exhaustive data processing, related to demand by means of real O-D matrixes and different characteristics for each street section. However, a discrete analysis implies the management of a large amount of data not always easy to get. Then, a representative group of this type of models are presented (Figure 2.1).

Lampkin and Saalmans (1967) proposed a sequential model. In the first step, an heuristic algorithm constructs the routes iteratively, paying attention on the maximum number of passengers carried from a O-D matrix by direct connections. The second step determines the

frequency for each of the previous routes by Greedy heuristic, minimizing the total travel time constrained by a maximum fleet. In Mandl (1980), the model only defines the routes. The author developed and heuristic algorithm that constructs the routes considering a constant and equal frequency for all the lines. Initially, the routes are also generated iteratively connecting pairs of nodes to maximize the number of users. The passenger assignment is made based on an *all-or-nothing* method. Then, the model evaluates possible changes on the network in order to reduce the total travel time. This model was applied in a real network with 15 nodes and 16,000 users per day.

Discrete models

Mathematical	*Heuristics*	*Tabu search; simulated annelling*	*Genetic algorithm*	*Hybrid models*
Hasselström (1981)	Lampkin and Saalsmans (1967); Mandl (1980); Ceder and Wilson (1986); Israeli and Ceder (1989, 1995); Ceder and Israeli (1998); Van Nes et al. (1988); Ceder (2003)	Fan and Machemehl (2004, 2006a, 2006b)*; Zhao and Zeng (2006)*	Pattniak et al. (1998); Tom and Mohan (2003)	Baaj and Mahmassani (1990, 1991, 1992, 1995); Shih and Mahmassani (1994); Shih et al. (1998)

** both models also used Genetic algorithms*

Figure 2.1. Discrete transit network design models classified based on solving methodology.

Hasselström (1981) proposed a model that determines routes and frequencies in a simultaneous way. Its objective function maximizes the level of service assuming a endogenous demand that varies with the supply in function to a gravitatory model. Two steps compose the optimization process. First, the model considers all links to generate a group of feasible routes that connect all O-D pairs. Secondly, the model chooses a number of those routes by means of the frequencies setting. Linear programming is used to solve that second task. However, the possible solutions are conditioned by a maximum budget, minimum level of frequency in each zone of the territory, and the range of values of those frequencies. This model is able to give answers in real problems such as Goteborg where there were 60 transit lines.

A similar model to Hasselström (1981) is the model developed in Van Nes et al. (1988). This model also determines routes and frequencies simultaneously. Again, its objective is to maximize the direct trips. However, the problem is subject to a constraint on the number of vehicles. The demand also varies with the level of service. An heuristic solves the problem: feasible routes start with frequency zero, and that value increases based on an effectiveness related to attracted passengers. If that effectiveness reaches a minimum, the model assigns that frequency to the route. At the end of this process, only those routes with non-null frequency compose the network.

Ceder and Wilson (1986) developed two mathematical formulations in order to face the network design problem. In one of them, the goal is to minimize in isolation the user cost. In its objective function, the travel time is evaluated as the excess time (travel and transfer times) that one route implies with regard to the minimum time of a direct connection. There are constraints related to maximum time to connect a pair O-D against the direct connection, the route length and the number of routes. The second formulation introduces new costs in the objective function. From the user point of view, waiting times, from the agency, operational and capital costs of its fleet. In this case, additional constraints are considered, minimum frequency per route and maximum fleet.

After, this model is studied in Israeli and Ceder (1989, 1995) and Ceder and Israeli (1998). The network design problem is reformulated as a multiobjective problem with two goals: total user cost and fleet. The models have constraints related to the served demand from a constant

O-D matrix and minimum frequencies. An heuristic algorithm solves these models. Its steps are: (i) construction of routes from the node with the maximum number of generated trips; (ii) removal of redundant routes; (iii) to remove routes that do not meet the constraints; (iv) calculation of the objective function; (v) choosing the most closed node to continuous the route; (vi) to verify the constraints until they are not satisfied; (vii) to find another origin node; (viii) finishing after all the nodes are analyzed.

Baaj y Mahmassani (1990, 1991, 1992, 1995) proposed an heuristic algorithm based on artificial intelligence. Three steps compose it: route generation, frequencies setting and a fine-tuning algorithm improves the system effectiveness. The first step takes into account user and agency costs, i.e., travel time and resources invested. It connects the pairs O-D with the highest demands. Then, the frequency of each line is estimated in function to the demand carried. Giving a first approximation of the network, the model analyses the effectiveness of that network with regard to the number of direct trips, waiting time or number of transfers, etc. Finally, another heuristic improves the routes to increase the global system effectiveness.

Subsequently, other works such as Shih and Mahmassani (1994) and Shih et al. (1998) gave continuity to the previous model. These works introduced advanced concepts in the formulation: coordination between routes, variable vehicle size or services on demand. There is an important inconvenient, a difficult application to real problems due to its complexity and the dependence to expertise of planners, demand patterns, land uses and constraints on resources.

Another way to solve the network design problem is by means of genetic algorithms. An example of that is Pattnaik et al. (1998). This algorithm defines a group of routes following a two-step process. The first step generates a group of routes, that is, the optimal solution of the network. Secondly, a genetic algorithm evaluates the previous solution to improve the network in size and routes. Its objective function minimizes the total system costs as a sum of agency costs and travel times for passengers. The solution is constrained to feasible headways and vehicle occupancies. Tom and Mohan (2003) proposed a similar model whose main contribution is a new code scheme for the genetic algorithm and the introduction of frequency as a decision variable.

Other models introduce operating strategies in the transit network design problem. Ceder (2003) took into account short-turning services. The solving methodology has two steps. Initially, the model selects a group of routes among the feasible routes and transfer points that supply a certain connectivity. Moreover, the frequencies are determined. The objective function balances agency, user and society costs. Finally, when the demand for each route is known, the resources are readjusted using short-turning strategies.

In Fan and Machemehl (2004, 2006a, 2006b), the network design and frequencies setting problem was formulated with an objective function that minimizes the sum of access, waiting and in-vehicle times, agency costs related to number of vehicles, and costs derived from unsatisfied demand. The optimization is constrained by feasible range of headways, maximum load of vehicles, maximum fleet, feasible route length, maximum number of routes and maximum unsatisfied demand. A solving methodology composed by three steps is used for two different scenarios, fixed or variable demand. The first step defines the group of candidate routes that meet the route length constraint. The second step studies the network structure to determine the frequencies. Finally, metaheuristics select a group of feasible routes. Five different

algorithms are used: tabu search, simulated annealing, genetic algorithm, random search and local search.

Other examples, such as Zhao and Zeng (2006) and Zhao (2006), used a integrated method between simulated annealing and genetic algorithms. Its objective function minimizes the number of transfers and maximizes the spatial coverage. This computational tool is effective for real problems.

2.1.2. Analytical models

Analytical models study the transport systems based on continuous approximations and characterizing the territory by an aggregated way. The first step is to define a simple network scheme that makes the estimation of costs and level of service easy with a small number of decision variables. By means of an objective function, the models obtain the optimal values of those decision variables, i.e., the theoretical optimal network configuration. These models simplify the real world in order to evaluate costs and benefits of a network in a compact way. The data collection is easy due to the aggregated approach, and the small number of variables makes to solve the problem easy with a low computational cost. However, once the network is optimized, an adaptation to the real street layout is needed. Then, a set of the most characteristic models are presented. Their main differences are: network scheme and objective function.

Analytical models

Linear		*Parallel lines*				*Hub & spoke*	*Radial*		*Ring-radial*	*Grid*		*Hybrid*
Saka (2001)	Park et al. (2008)	Byrne and Vuchic (1972)	Byrne (1976)	Wirasinghe (1980)	Kuah and Perl (1988)	Newell (1979)	Byrne (1975)	Tirachini et al. (2009)	Vaughan (1986)	Holroyd (1967)	Aldaihani et al. (2004)	Daganzo (2010)

Figure 2.2. Analytical transit network design models classified based on network structure.

Holroyd (1967) proposed one of the first analytical models. His model optimizes the transit line spacing, where the lines compose a grid network. The author assumed a uniform headway and demand density in the city. The objective function captures waiting time, operating costs and effective access time. This last time is the difference between the total travel time using the network and that time if the trip is door-to-door.

Byrne and Vuchic (1972) analyzed a network composed by parallel lines that connect a rectangular territory where one of its extremes is the CBD (a perpendicular line with respect to the transit lines). Byrne (1975) readapted the previous model to radial lines gathered in the CBD of a territory, which is a circular sector. The objective in both cases is to find the optimal combination between line position and headway with a minimum global system cost. The CBD attracts all trips and the objective function considers user and agency costs. Regarding the former, access, waiting and in-vehicle time are taken into account. An operating cost related to the number of vehicles is considered for the latter. Two decision variables define the network: the relative position among lines and the headway of service. Both variables can vary over the territory but not along the route.

Byrne (1976) introduced a new aspect to the model presented in Byrne and Vuchic (1972): the commercial speed is not the same for all the lines. This factor changes the previous results, the distance between lines are no longer constant. Therefore, users do not choose the closest line if

that line is slow. Obviously, this phenomenon has a greater impact with the distance from the CBD, when the in-vehicle time has a greater presence. The higher the speed is, the longer the line spacing and the lower the headway. Furthermore, lines with a slow speed are shorter because they are never used from a certain distance to the CBD.

As Section 1.2 introduces, Newell (1979) made an analytical comparison between two network topologies that Figure 1.4 shows. The goal was to know which of them is the optimal way to serve a specific demand pattern. The model evaluates the access, waiting and transferring costs from the user point of view, and operating cost from the agency. The sum of those cost is minimized. He stated that a higher number of passengers justifies a better level of service. Therefore, as the demand is concentrated around a central corridor, the network has to be focused on that corridor.

Wirasinghe (1980) proposed an intermodal model that defines a group of bus lines to feed a rail corridor. Those feeder lines are arranged over a grid street layout. The goal is to determine the location of rail stations, and bus routes and frequencies. The decision variables are: density of feeder lines, buses per line and rail station density. The costs evaluated are: access, waiting and in-vehicle in both modes, and operating costs. Regarding in-vehicle time, the model includes the lost times at bus stops. Operating costs are related to route length and rail stations. The demand is fixed but varies over the territory. The author used the model for two different scenarios. One that assumes pre-fixed rail stations and the model optimizes the feeder bus lines. The other is a general case where the locations of those stations are also optimized. The solving methodologies used are a trial and error method, graphical representation or numerical integration. As the optimal values of line density and number of vehicles depend on a cube root of a group of parameters, the variability of their optimal values is low. This fact shows the model's robustness. The model was applied in Calgary (Canada) in order to define a feeder system for a new light rail transit line whose stations were already fixed.

Vaughan (1986) developed a model for a ring-radial network. In this case, all of destinations are not in the CBD. Generated and attracted demand are uniformly and independently distributed over a circular city. The decision variables are line spacings and headways. They vary between radial and circular lines and with the distance from the city center. Regarding user costs, this model evaluates all the steps of the user transit chain: access in origin and destination, waiting time in origin and transfer stops, and in-vehicle time between origin and intermediate transfer stop and from that last point to the destination. Users can reach any destination from any origin by means of one transfer always following the shortest path. The agency cost are not included in the objective function. Only a constraint related to the number of vehicles is considered, but not related to the vehicle capacity.

Until that moment, the analytical models only considered as decision variables the line spacing and the headway. However, the stop spacing had been neglected. Kuah and Perl (1988) introduced that variable in their model. This model designs feeder bus lines to connect a rail corridor. The network scheme is similar to Byrne and Vuchic (1972). However, the destination is now a rail corridor as Wirasinghe (1980) and not the CBD. Headways and line spacings vary among the different bus lines, and stop spacings also along each line. Its objective function minimizes the travel time and the agency investment. Regarding travel time, that function includes access, waiting and the lost times due to stops (acceleration, deceleration and boarding passengers). In-vehicle time and bus-rail transfer time are not added since they are constant. The agency investment is derived from distance travelled and spent time at stops.

The results are coincident with Wirasinghe (1980). The line spacing and the headways depend on a cubic root of different input parameters. However, the stop spacing presents a lower robustness since it depends on a square root. The model was applied in an idealized case study with three different demand distributions: uniform, and other two decreasing with the distance from the city center. As a conclusion, higher levels of demand reduce the line and stop spacings and headways.

In the last decades new models have been developed. These have introduced a wide range of aspects in their formulations. Saka (2001) is an example of that. The objective is to determine the optimal stop spacing in one transit line. The model evaluates the effects of that stop spacing on the fleet, the headway, and the travel time. This time includes the time spent due to stops: acceleration and deceleration, time at stop, delays due to traffic signals; these times are added to the travel time needed to run all line without those obstacles. The objective function minimizes the fleet, assuming constraints on the headway and a maximum stop spacing.

Aldaihani et al. (2004) proposed a model to design a hierarchical transit system. This system combines fixed routes that shape a grid network and on-demand services in the different areas between the fixed lines. This on-demand service increases the accessibility to the main network. The number of transfers in this structure is so high. Beyond transfers that a grid network implies, there are additional transfers between the two levels of the system. The goal of this approach is to find the optimal number of zones and total fleet. The objective function minimizes the costs derived from both services and the costs that users spend in the system (in-vehicle and waiting times). The approach assumes that on-demand trips are not shared by more than one user, and trip density is uniform and constant over the territory.

Other authors developed different approaches to compare alternative system structures. Park et al. (2009) compared a corridor with branched lines in both extremes and other option with a central corridor fed by other lines in its extremes. From the user point of view, the branched service is better, since it does not imply transfers. However, if the central corridor supplies a level of service that balances out the transfer cost, the best option changes. On the other hand, the agency prefers feeder lines to make operation easy and reduce costs. Tirachini et al. (2010) made an analytical comparison among transit modes (bus, tram and metro) that connect a circular territory with its CBD by radial lines. A bus rapid transit (BRT) is the best alternative in most of scenarios.

Recently, Daganzo (2010) proposed a new model where the network scheme is a combination of a central grid and a branching of the central corridors in the periphery. This scheme is a mixture between the grid of Holroyd (1967) and the hub-and-spoke of Newell (1979). The objective function minimizes a combination of agency and user costs. The agency supports fixed and maintenance costs of infrastructure and fleet, and the operating cost derived from the kilometers travelled. Users spend access, waiting, in-vehicle and transferring times. The approach assumes uniform demand distribution and a commercial speed reduced by stop times and boarding and alighting of passengers. There are three decision variables: central grid size, stop spacing (coincident with line spacing) and headway. The stop spacing is constant along the city, the headway along the central grid, but decreases with the distance from the center in the branched sections.

2.2. Urban form representation

A minor branch of this dissertation is the analysis of urban dispersion and how to describe and measure it. A simple way to obtain an idea about the urban form is based on three-dimensional graphics. These represent the density of one variable over the territory, a two-dimensional space. Bertaud (2001) showed the population distribution for different cities. A visual comparison reveals that those built-up areas are different. However, this method is not a measurable way to compare them, and it is conditioned by the level of detail of the territorial zonification. *Choropleth* maps are a similar option and present the same limitations.

Anas et al. (1998) summarized three alternatives used for this purpose. Two of them are based on a mathematical description of points distributions in space: point pattern analysis and fractals. The former consists of spatial point distribution analysis the analysis in a study territory. This analysis shows clusterization or randomness of those points over the space. After that, the resultant arrangement is compared with theoretical patterns. Examples of this methodology are Getis (2010) where the author identified population clusters, and Duranton and Overman (2008) where economic theories of location were evaluated. On the other hand, the methodology based on fractals is used to describe boundaries of a territory such as coastlines, and Batty and Longley (1987) applied it to measure the urban boundaries. The third alternative summarized in Anas et al. (1998) is based on cluster analysis. To consider a certain area as a cluster, its gross density or absolute value of one variable has to exceed fixed thresholds of those measures. An example of that is Giuliano and Small (1991), where this methodology indentifies subcenters in the Los Angeles region.

In addition, Anas et al. (1998) presented the analysis of urban form by means of density functions. This approach was firstly proposed by Clark (1951). The proposed model assumes a monocentric city and describes the population distribution over a region by a negative exponential tendency with the distance from the CBD. Heikkila et al. (1989) extended that description to polycentric cities, where each center is independently treated. However, authors like Craig and Ng (2001) considered the interaction between the central business district and the subcenters. They analyzed an urban area using quantile smoothing splines to identify employment subcenters besides the CBD. Those subcenters influence surrounding areas and condition the employment gradient with the distance from that CBD.

Other perspective to face the analysis of urban form is the spatial autocorrelation. The explanatory spatial data analysis (ESDA) have two branches, one global and other local. The former describes the distribution of one variable over space. That is, whether the value of that variable is similar or different between any zone and its surroundings. On the other hand, a local analysis identifies the existence of clusters of high or low value of one variable in the territory. Depending on the number of high demand clusters, this analysis determines the urban structure, i.e., mono or polycentric city. Moran's I coefficient in its global or local expression and its scatterplot and cluster map associated (Anselin, 1993 and 1995) are a suitable tool for the spatial autocorrelation analysis. Other measure is G-statistic presented in Getis and Ord (1992) and Ord and Getis (1995). ESDA has been used in different studies about the distribution in urban areas of employment in Baumont et al. (2004) or trips in Mazzulla and Forciniti (2012).

Malpezzi and Guo (2001) included other methodologies to describe or measure urban form. The simplest measure is the average density of one variable and others associated to that

density. Other possibilities are inequality measures such as Gini coefficient used in Small and Song (1994) and Theil index, or a compactness index in Bertaud and Malpezzi (1999) related to distance from the CBD. Other authors proposed centralization indexes like modified Wheaton index (Wheaton, 2004) or area based centralization index in Massey and Denton (1988). These last authors also proposed a concentration measure, the delta index.

Galster et al. (2001) stated urban form and its evolution to more dispersed scenarios has an impact in eight dimensions of land use patterns: density, continuity, concentration, clustering, centrality, nuclearity, mixed uses and proximity. The analysis of them defines the urban sprawl degree. The authors proposed different ways to measure each of those dimensions by means of indexes or clustering methods based on thresholds. However, the evolution of these dimension conditions the rest of them. Therefore, the analysis of a smaller number of them can give a good approximation to understand the stage of urban dispersion in a city. For that reason, other authors reduced the number of dimensions to measure the urban dispersion and to compare urban areas.

As an example of those authors is Tsai (2005), who considered four dimensions: population, density, equal distribution degree and clustering degree. This last dimension is analyzed by coefficients of spatial autocorrelation and determines the urban spatial structure, monocentric or polycentric. For the distribution, the author used the Gini coefficient to know if the city is concentrated or deconcentrated. That is, the variable is located around the main poles or is completely sprawled. Another example is Lee (2007), he described the urban spatial structure in U.S. metropolitan areas only by two dimensions: centralization and concentration. The former informs if the employment or population is closed to the CBD and it is measured by indexes previously commented like modified Wheaton index, area based centralization index, or weighted average distance from the CBD (Galster et al., 2001). The latter dimension is coincident to Tsai (2005). In this case, two indexes are used, Gini coefficient again and Delta index.

Finally, other authors defined one index that combines two dimensions. This index is the product of independent measures for each of the dimensions considered. Pereira et al. (2013) defined the urban centrality index. This is a combination of an unequal distribution coefficient and a spatial separation index, i.e., product of concentration and centralization. The authors use a location coefficient for the former, and a normalized Venables index for the latter. Both were used to analyses the industrial specialization and distribution in Florence (1948) and Midelfart-Knarvik et al. (2002) respectively.

2.3. Summary

This section emphasizes the benefits and disadvantages of the different transit network design models. On the one hand, discrete models present an exhaustive data processing related to demand pattern and street layout. Their resultant networks are directly adapted to streets, being a good tool to design a network in a specific case study. However, the large volume of data and the long computational time needed make its application in real case studies more difficult and reduce the benefits of the discretization effort. Moreover, the results from a discrete model are not easy to extrapolate among different scenarios. As a consequence, they are a tedious approach to understand the general behavior of transport systems versus changes on input parameters or decision variables. In addition, as Daganzo (2010) argued, discrete models

focus their attention on solving methodologies rather than their resultant network designs. Therefore, they do not give guidelines about the design problem.

On the other hand, analytical models are simple and useful tools to obtain those guidelines from a strategic point of view. In comparison with the other family of models, in this case, the small volume of input data and the short number of variables allow us to solve the problem in a simple way. Although their results are the initial layout for the subsequent adaptation to real streets. Some authors emphasized the advantages of this type of models. Ceder and Wilson (1986) commented that these models are suitable for screening and policy analyses, Vaughan (1987) stated that the suitability of these models is to discover fundamental relationships between variables and describe the behavior of transport systems. Recently, Daganzo et al. (2012) explored the benefits of these parsimonious models for large scale transportation systems to answer big picture questions. The authors exposed five types of benefits: fewer data requirements, reduced computational complexity, improved system representation, transparency, and insightfulness.

The goal of this thesis is to discuss about transit network structures in general terms. That is, to understand the behavior of different structures versus urban dispersion in a wide range of scenarios. Analytical models are used in this thesis, a decision reinforced by the benefits commented above. In addition to its ease of use in front of changes on case study characteristics, these models are a good way to compare structures. An analytical model assumes beforehand that structure, and therefore, it is possible to develop models for the different structures under comparison. However, the resultant networks in discrete models have complex and diffuse structures that makes difficult a clear comparison between direct trip-based networks and transfer-based ones.

Once the type of transit network design model is assumed, the second aspect to be discussed is the methodology to measure urban dispersion. Visual tools like three-dimensional graphics or *choropleth* maps of one urban variable are a first approximation to capture urban form. However, these descriptive analysis are not an option to evaluate in a measurable way spatial structures in order to be compared with the results of the transit network design model. A similar problem happens in thresholds methods, which are highly conditioned by the value of those thresholds to define clusters. Explanatory spatial data analysis improves the previous methodologies since arbitrary thresholds are not needed. In this case, statistical significance determines clusters. Furthermore, global coefficients associated give a quantifiable way to capture the dispersion in a case study.

Other alternatives such as density functions are too accurate to compare their descriptions with the results from an analytical model. Most of these models assume uniform demand distributions over the whole city or inside a small number of zones that compose the territory. This assumption makes to work with complex curves to represent the demand distribution poorly useful.

On the other hand, working with indexes that measure urban dispersion degree is a simple and measurable way to be compared with analytical results. However, among different dimensions of that urban phenomenon, the analytical model is able to include a small number of them in the analysis. Therefore, reasonable methodological frameworks to analyze urban form are those proposed by Tsai (2005) and Lee (2007). They reduce the number of dimensions, focusing on

concentration and decentralization. However, Tsai (2005) also incorporates spatial autocorrelation analysis to know the urban structure.

As a summary, on the one hand, to obtain an approximation of urban structure, explanatory spatial data analysis gives information about one city is monocentric or polycentric. On the other hand, indexes are a suitable way to measure urban dispersion degrees related to those dimensions taken into account in the transit network design model.

Part II: THEORETICAL ANALYSIS

Chapter 3

Transit network design model*

In this chapter the methodological approach for designing transit networks is presented in detail. This model determines the optimal network configurations for different network structures on distinct street patterns for a wide range of scenarios conditioned by city, transit technology and user characteristics. This dissertation opts for an analytical model due to the advantages that these models present to obtain general insights about the behavior of transit systems in a simple way in a wide range of scenarios. As it is shown in Section 2.1.2, this type of models has been widely used in the transit network design problem by many authors, and at the same time, in other transportation fields, for example, logistics (Daganzo, 2005) or traffic (Vaughan, 1987; Miyagawa, 2009).

The base of the model of this thesis is the hybrid model presented in Daganzo (2010), which is modified to: (i) distinguish different degrees of demand dispersion, (ii) estimate in a more exhaustive way some partial costs, (iii) adapt it to different network structures, and finally, (iv) adapt these concepts on a ring-radial street pattern. The street patterns atop the networks are adapted, how the demand and its dispersion are represented, the network structures compared, the basics and assumptions considered in the analytical model and its formulation are explained in detail below.

* Most of the contents of this chapter are included in Badia et al. (2014, 2016) and Badia (2016).

3.1. Street patterns

One of the requirements of the guidelines for a new transit network design framework presented in Section 1.2 is the adaptation of its structure to the street pattern. For this reason, a first step is knowing the basic street patterns that are found in the cities. In Bauer (2009), from an urban point of view, there are two main categories with regard to the city layout: (i) regular, when streets follow a pattern characterized by a simple and constant geometrical layout in a wide extension of the city as a result of its planning, and (ii) irregular, when that street pattern does not follow any particular structure, streets form a scheme lacking of organization, that is, arisen in an unplanned way.

Regular cities present different configurations. Dickinson (1961) made a two-categories classification where distinguished between radial or rectangular patterns. The former is composed by streets that leave from the city center and continuous to the periphery, and, in some cases, by circular streets concentric to that center, allowing transverse connections. The latter is simply a grid, where orthogonal streets conform the road network. These are the two main patterns that are repeated in the main classifications, however, some of them consider someone more. Lynch (1962) included the linear city, Sitte (1945) mentioned the triangular scheme, Unwin (1914) referenced also circular and diagonal configurations, and Abercrombie (1933) incorporated hexagonal structures. On the other hand, from a morphological point of view, similar classifications are made about transport networks. Van Nes (2002) summarized this classification in six topologies: linear, radial, circular, radial/circular, rectangular and triangular. All of them already included in the previous references about the city layouts.

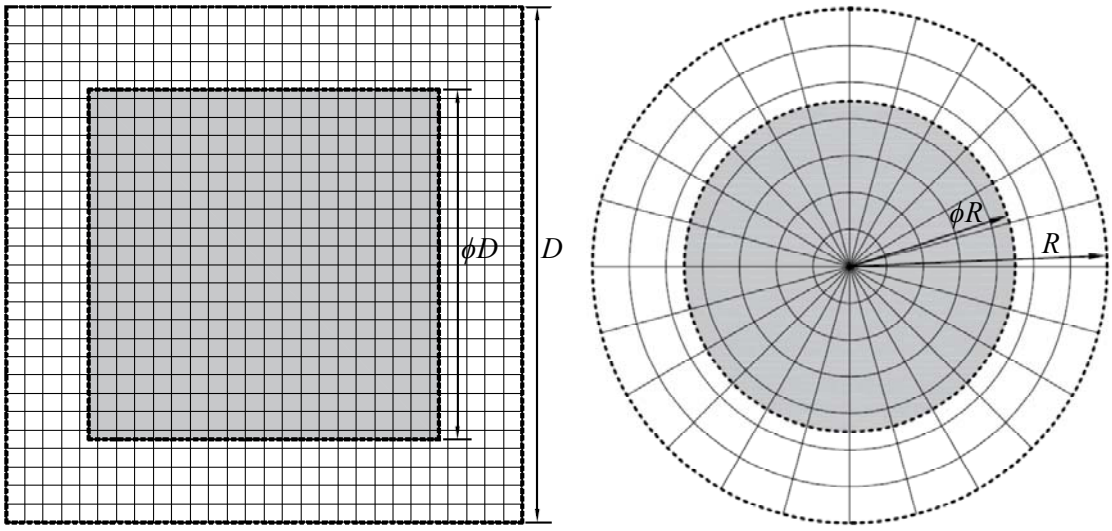

(a) Grid street pattern *(b) Ring-radial street pattern*

Figure 3.1. Street patterns atop the network structures are adapted.

Although all these patterns are analyzed from a theoretical point of view, if the attention is focused on real cities, the regular cities can be reduced to the most simplified classification: radial and rectangular schemes, in other words, ring-radial and grid street patterns. The rest of configurations either not conform a network by themselves (linear or circular schemes) or are not found commonly as a general layout for an urban area (triangular, diagonal or hexagonal). However, these specific configurations can appear in a small region of a wider city without disturbing its general structure. For example, diagonal streets or triangular configurations are

found in cities like Barcelona, Paris, New York or Palma, without breaking their widespread street patterns.

Based on the previous information, a grid and a ring-radial street patterns are just considered in this thesis. Therefore, the initial analytical model is adapted to design transit networks atop both patterns. As Figure 3.1 shows, the former is defined as a square city of side D (km) with a infinite grid in the whole extension, the latter is a circular city of radius R (km) whose street layout is an infinite ring-radial mesh.

3.2. Demand representation

Regarding the level of demand and its spatial distribution, all analytical models assume some simplifications of the reality. On one hand, the average hourly demand of the transit system is λ (p/h) and the demand at rush hour is Λ (p/rh). These values are supposed to be constant, they do not vary with the level of service or other factors related to the transit supply.

On the other hand, to represent the demand pattern, a trade-off between the simplicity of the analytical models and the detail of representing real mobility patterns is needed. Most of analytical models assumed uniform and independent distribution of generated and attracted trips over the whole area of study (Holroyd, 1967; Vaughan, 1986; Aldaihani et al., 2004; Daganzo, 2010; Nourbakhsh and Ouyang, 2012). However, this alternative makes it impossible to analyze different degrees of demand decentralization. Other authors as Vaughan (1987) considered more complex demand curves where generation and attraction curves of demand were non-uniform and non-independent. This more realistic representation implies a high complexity, and as a consequence, this type of models would lose its main benefit, its compactness and simplicity. In addition, the results on the network configuration are not so significant if the goal is obtaining general insights.

Intermediate approximations have been used in other studies. In these cases, the uniform distribution is accepted, although the city is divided in zones with different demand densities. Moreover, the independence between origins and destinations is maintained. Smeed (1965) and Tan (1966) divided the territory in two areas, one central and the remainder periphery. All destinations are located in the central area since they are related to workplaces. The origins are home-based and are located in the peripheral area. This approach represents in a simple way the commuting. Fairthorne (1964) used a more generalized approach, considering workplaces and homes in both areas but with different densities. More recent studies assumed similar approaches. In Tsekeris and Geroliminis (2013), the generated demand is distributed over the whole city but with high density in the central area, while the demand is only attracted by the central area. The same is assumed in Li et al. (2013), where the CBD attracts all trips.

Therefore, in order to represent different scenarios of demand dispersion without losing a simple and clear formulation, the model used in this dissertation divides the city in two areas. A central one and the remaining peripheral area between the boundary of that central area and the city boundary. This is also shown in Figure 3.1, the former is a central square of side ϕD for a grid street pattern and a central circle of radius ϕR for a ring-radial. The parameter ϕ varies from 0 to 1. The generated demand is uniformly distributed over both areas but with different densities. The central density is greater than the peripheral density by a factor f_d. If this factor is equal to one, the demand is uniformly distributed over the whole city. If f_d is higher, the

central area presents a greater capacity to generate demand. However, only the central area is attractant, where the attracted demand is uniformly distributed. In addition, we maintain the independence between both demand curves. In this way, two types of trips exist with regard to the origin's location: (i) those whose origins belong to the central area, whit a probability ρ, and (ii) those whose origins are peripheral, with a complementary probability $(1-\rho)$. The value of ρ depends on the central area's size and the previous generated demand densities factor between both areas, that is, $\rho = f_d\phi^2/[1+\phi^2(f_d-1)]$.

In this way, these hypotheses allow us to determine the degree of demand dispersion easily by means of two factors. On one hand, the size of the attractant central area represents in a simple way the different phases of the urban form evolution commented in Chapter 1. A small central area (low values of ϕ) is equivalent to a scenario where the CBD is the destination of all trips. A large central area, when ϕ tends to 1, represents a dispersed urban form where CBD has lost its relevance with the appearance of new non-clustered centralities far away from it. Intermediate values of ϕ represent different demand decentralization degrees between these extremes, when the CBD starts to scatter on its surrounding. On the other hand, the different capacity of trip generation between central and peripheral areas allows distributing the relevance of each area in the mobility.

This monocentric approach takes into account different scenarios of CBD's extension, but not a polycentric city where different centers are distinguished. This is an approximation where secondary poles appear and foment the occupancy of the territory between the CBD and itself, to finally become part of that extended CBD. Therefore, it is a monocentric approximation related to the prevalence of the traditional center in urban mobility exposed in Section 1.1.

3.3. Transit network structures

Regarding the transit network structure, from the point of view of the strategy of service, Vuchic (2005) proposed a classification of four types of networks: radial as a set of lines that converge on a central point; radial/circumferential as a radial network complemented with circular lines that allow transversal trips and transfers with the radial lines; grid as two groups of parallel lines perpendicular to each other; and ubiquitous composed by different types of lines that are branched to serve major origin-destination pairs by direct connections. Radial/circumferential and grid are two mesh networks, each one adapted to the most generalized street patterns exposed in Section 3.1. This classification is in line with the previous discussion about the transit network design problem in Section 1.2, which is followed in this dissertation.

Three basic network structures are compared along the thesis: a radial scheme, a direct trip-based structure and a transfer-based one. This comparison is made atop the street layouts in Figure 3.1. Below, the schemes that represent the different structures are shown. It includes the arrangement of lines and the decision variables that configure each network structure. Both geometrical scheme and the frequency of service determine the transit system cost from the agency point of view.

3.3.1. Service operation: headways or schedules

A transit service can be operated by schedules or in headways. In the former, users know the moment when transit vehicles should arrive at their transit stops, and adapt their arrival based on that information. In the latter, users arrive at stop randomly due to the lack of vehicle arrival information. If trips are direct, a user only has to wait at an initial stop. In this case, he/she can adapt his/her arrival at that stop. However, if a transfer is needed, a user has to wait at an intermediate stop where he/she cannot decide when he/she arrives. This is conditioned by the arrivals of the first and the second bus at the interchange point. Therefore, we only consider the possibility to work with both types of service operation in transit network structures that do not need transferring to complete the trips. Consequently, radial and transfer-based networks can only work in headways, but direct trip-based structure can combine both service operations.

The approach followed to combine schedules and headways services is the same as Tirachini et al. (2010), for which three parameters are defined: (i) H_s that is the cut-off headway between both types of service, which determines the boundary between inner and outer zones, that work in headways and by schedules respectively, (ii) safety waiting time h_s is a fixed value for all stops that works by schedules, the user arrives some minutes before the arrival time of the vehicle, and (iii) home waiting time as an opportunity cost, which is a variable time defined as the product of the headway of service at stop and the factor f_s. This factor has a value lesser than 0.5 since waiting at home/work is less negatively perceived than at transit stop. Therefore, Function (3.1) determines the waiting time at bus stop w_s for a line with a headway H_l. and Figure 3.2 shows the evolution of that waiting time with regard to the headway of service.

$$w_s = \begin{cases} H_l/2, & if\ H_l < H_s \\ h_s + f_s H_l, & if\ H_l \geq H_s \end{cases} \tag{3.1}$$

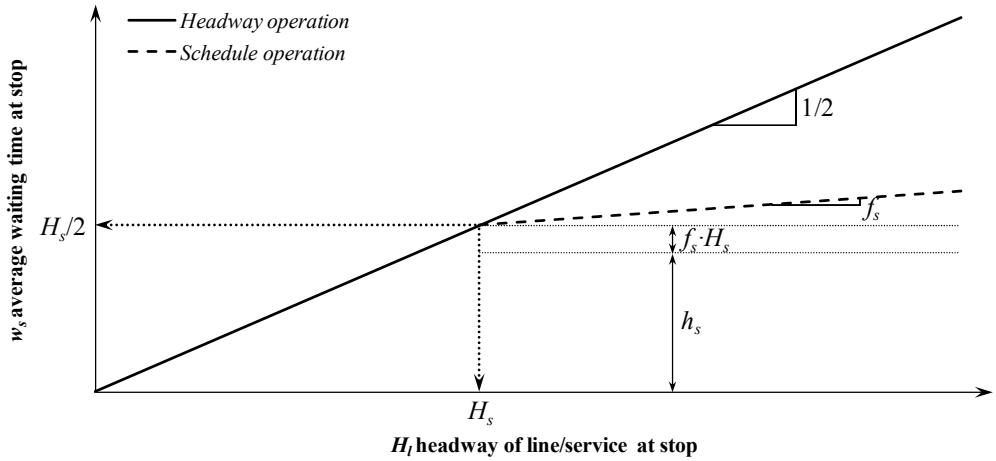

Figure 3.2. Waiting time versus headway of service at stop with regard to type of service operation.

In a direct trip-based network, another parameter ε_H is used to determine the boundary between both types of operation. The system operates in headways in the central area inside that cordon, and by schedules outside. This boundary is the square cordon of side $\varepsilon_H D$ for a grid street pattern and a circle of radius $\varepsilon_H R$ for a radial street pattern. If ε_H is equal to 1, all the network works in headways. On the contrary, the service is mixed.

3.4. Adaptation of network structures atop a grid street pattern

3.4.1. Geometry and operation

Figure 3.3 shows the structures studied atop a grid street pattern: radial, direct trip-based one and two transfer-based systems, a grid and the hybrid scheme presented in Daganzo (2010). Decision variables of the radial scheme are the stop spacing s, which determines the route branching, and the headway H at central point of the city for each direction (N-S and W-E). For the grid structure, the stop spacing s, which is coincident with the line spacing, and two headways are distinguished; H_c is the headway for lines that cross the attractant central area defined in Section 3.3 and H_p is the headway for the rest of the lines. This distinction guarantees a better deployment of resources. In the case of the hybrid network, three decision variables define it: the stop spacing s, the headway H for corridors at its central grid, and the parameter α that determines the size of that grid. This last variable is the ratio between the side of the central gridded square and the side of the city. Therefore, radial and grid network can be represented by hybrid scheme letting $\alpha = 0$ and $\alpha = 1$ respectively. These schemes are based on Daganzo (2010).

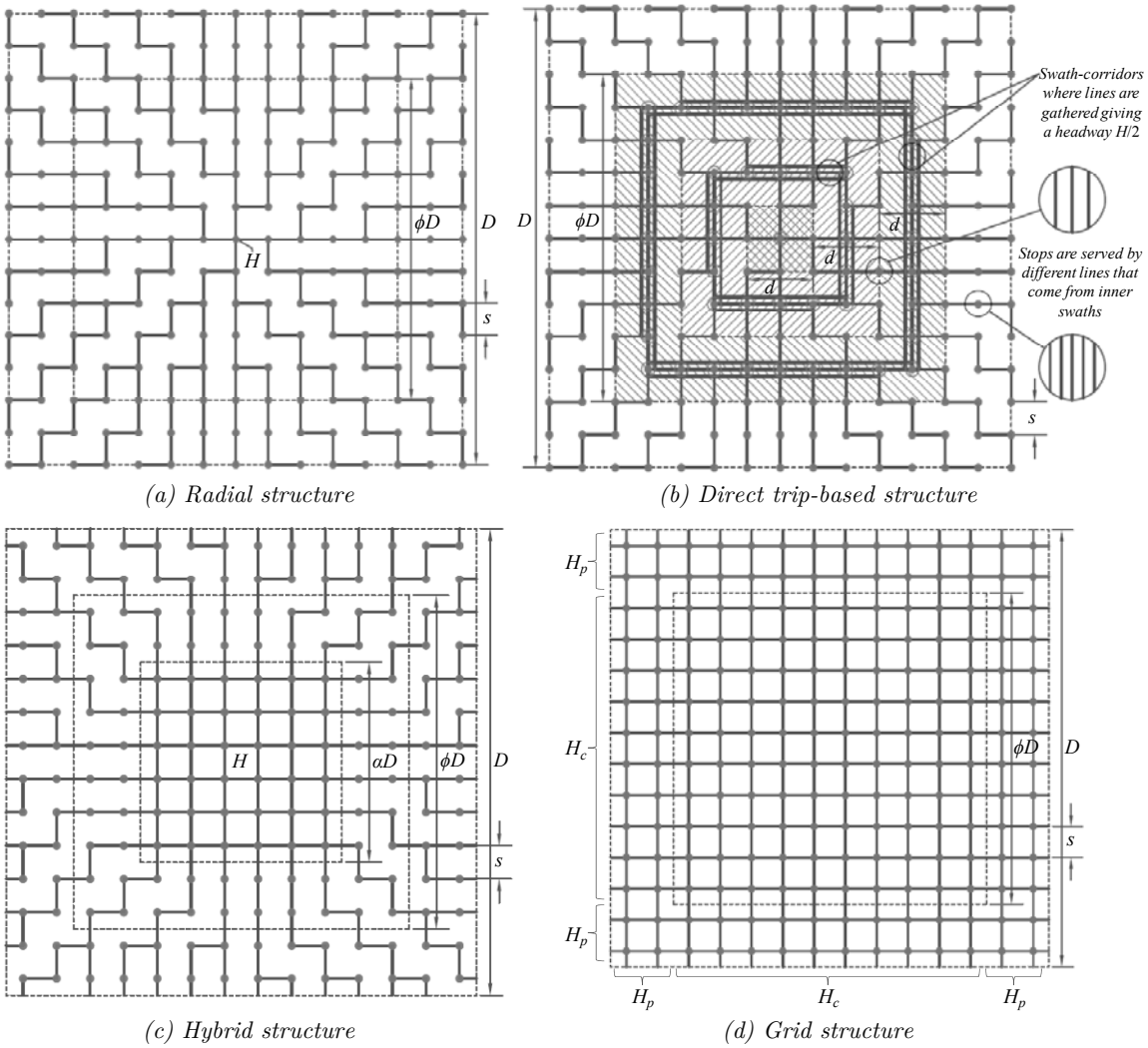

Figure 3.3. Different network structures compared atop a grid street pattern.

The direct trip-based scheme deserves further explanation. Its main goal is connecting the attractant central area directly (without transfers) with the whole city. This system is an evolution of the radial network, where new lines are created to serve new attractant spaces resulting from the CBD's scattering. The resultant structure is like a superposition of different radial networks, each centered in one of the different attractant poles. The last stage of this structure is a ubiquitous system where every zone of the city is connected directly to every zone at least by one line; this happens when the attracted demand is distributed over the whole city ($\phi = 1$).

For the idealization of this direct trip-based structure, defining a network scheme that satisfies that main goal is needed. Firstly, the demand poles are defined, dividing the continuous attractant space into subareas. Then, the lines that connect each of them with the rest of the city. The routing of these lines should avoid reiterative connections and try to cover the maximum area of service without tangled paths or loops. Therefore, the network is composed by different group of lines, each connect one subarea with the whole city. The lines of the same group are gathered in the subarea that they serve, and are dispersed out of this subarea to cover the rest of the territory. After considering different possibilities, we choose the structure presented in Figure 3.3b since it accomplishes the previous requirements.

The central attractant area is divided into different concentric swaths of width *d*. The central swath, a square of side *d*, is served by means of a radial network as in Figure 3.3a, whose lines are branched over the territory determined by the stop spacing *s*. The next swath is already connected to the central one by that radial network; however, new lines are needed to connect it to the rest of the city. To explain how the lines are arranged, we divide the swath into four zones, called swath-quadrants, and the area to be connected into four external-quadrants. These represent the area between the inner boundary of the swath and the city boundary. Figure 3.4 shows these divisions, where we focus our attention on how the transit lines connect the East swath-quadrant.

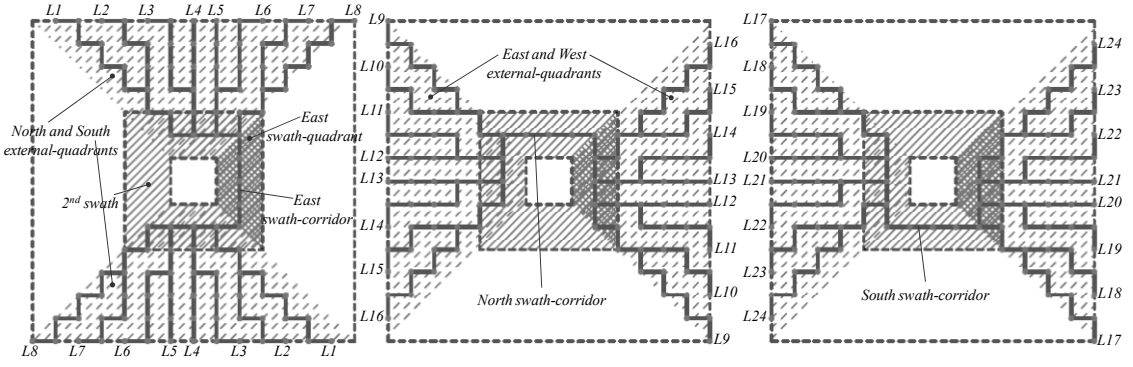

Figure 3.4. Detail of a direct trip-based network structure: how lines are arranged to connect the East swath-quadrant of the second swath to its external-quadrants by means of East, North and South swath-corridors.

Figure 3.4 shows three of the four groups of lines that serve the second swath and how they are arranged. Lines of the same group are gathered in one swath-quadrant and are distributed in the respective adjacent swath-quadrants for the next branching over the external-quadrants that they serve. This branching follows the same routing as the radial network of the central swath. The lines gathered in the East swath-quadrant (Figure 3.4a) are distributed over the North and

South swath-quadrants and serve the respective external-quadrants. In this way, this group of lines completely connects the East swath-quadrant to these external-quadrants. To connect the West and East external-quadrants, we do not create new lines: alternatively, we use the lines gathered in the North and South swath-quadrants, as Figures 3.4b and 3.4c show respectively. Both groups of lines complement each other. Line L9 complements line L17; line L10 complements line L18; and successively until line L16 complements line L24. As a result, the East swath-quadrant is connected to the four external-quadrants.

By symmetry, rotating 90°, 180° and 270° each component of Figure 3.4, we obtain the lines that connect the other three swath-quadrants. For the remainder of swaths, the same explanation is valid. The lines are arranged in the same way, but they serve a smaller external area, since each swath is already connected to all its inner ones such as the swath explained before with regard to the central swath.

To summarize, the geometrical scheme of this structure is defined by two decision variables: stop spacing s and corridor spacing d, which is equivalent to swath width. In the external area of the city, which does not attract trips, transit corridors are not introduced due to their uselessness. On the other hand, the decision variable that defines the temporal coverage is H. This is the headway to the central point of the radial network, and, at the same time, is the resultant headway of those lines that belong to the same group; that is, the lines gathered in a swath-corridor of one swath-quadrant and serve its respective adjacent external-quadrants. This assumption guarantees the same level of service frequency for all the attractant area. Simultaneously, as Figure 3.4 shows, the swath-corridor is also partially crossed by lines that connect the same and the opposite external-quadrants. As a consequence, the resultant headway on these corridors is $H/2$.

3.4.2. User transit chain

The other component of the total system cost is the user cost. This is determined by the transit chain followed by passengers. The steps of that chain are the access time from the origin to the transit stop, where the user waits to get on the transit vehicle, after the in-vehicle time spent to move from the initial stop to the final stop, where the user gets off and walks to its destination (egress time). However, in those structures where transfers are needed, additional steps are included. The previous in-vehicle step is divided into different sections and between two of them a transfer is added. A transfer implies a cost derived of a possible walking time and an extra waiting time until the arrival of the next vehicle. Some criteria are assumed to define this path, which is an essential step to derive the user costs later in Appendixes B and C.

- Access and egress cost: The user takes the bus at the closest stop to his/her origin and gets off at the closest stop to his/her destination, conditioned by the variable s. There is only one exception in a direct trip-based network; the initial or final stop is the closest stop located at one of the swath-corridors where the lines are gathered, conditioned by the variable d. In this network, we assume that the user does not make transfers.
- Waiting cost: It is conditioned by the previous assumption. However, the headway varies smoothly among nearby stops. One exception exists in the complete grid network atop a grid street layout, where stops in some peripheral areas are served by two perpendicular

lines with different headway. In these stops, users choose the path of the line with the minimum headway.

- In-vehicle cost: The user opts for the shortest path that the network structure allows between its origin and destination.
- Transfer cost: The user chooses the path with the minimum number of transfers.

Generally, assumed the first two criteria, there is a path that accomplishes the third and fourth criteria, which presents the shortest total travel time. Figure 3.5 shows the path for different origin-destination pairs for the four structures analyzed atop a grid street pattern. In a radial network, the path that connects any origin-destination pair accomplishes the four criteria, either by direct trips if origin and destination belongs to the same line (O_1-D_1), or by one transfer at central stop (O_2-$D_{2,1}$ or O_2-$D_{2,2}$). It is possible to observe that some trips are longer than the real distance due to the structure itself. The user must arrive to the center of the network to take the line that serves the destination, for example O_2-$D_{2,1}$ pair.

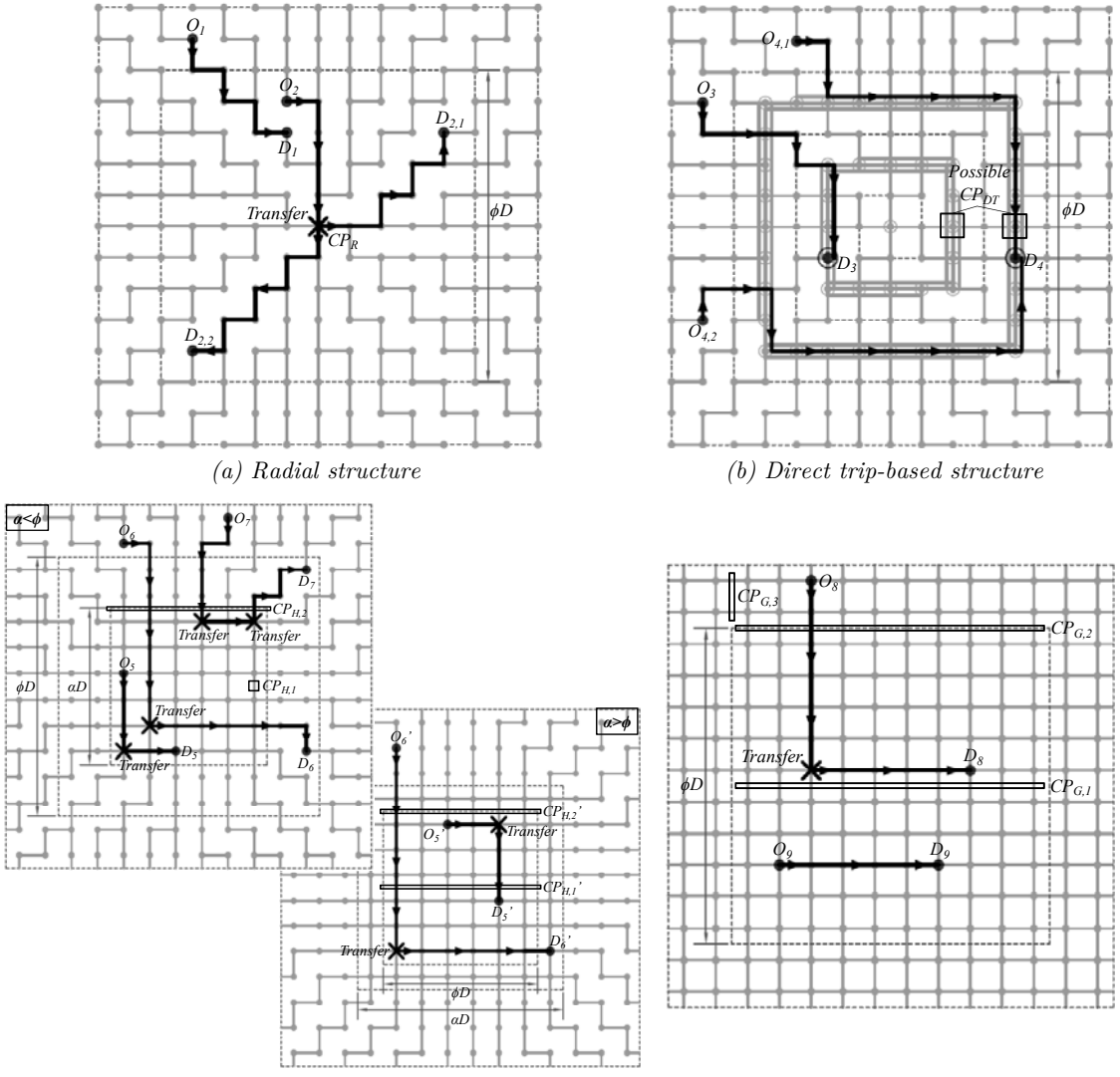

(a) Radial structure

(b) Direct trip-based structure

(c) Hybrid structure

(d) Grid structure

Figure 3.5. Paths and critical loaded points of the structures studied atop a grid street pattern.

In a grid, the best path for any origin-destination pair is the shortest in a L_1 metric, and at the same time, it presents the minimum number of transfers, zero or one. In the area served by central and peripheral lines, the users take the line that implies the shortest waiting time, by definition H_c is always lower than H_p. The trip O_8-D_8 is an example of this. As the hybrid network is a mix scheme, it presents the same type of paths as the grid structure when origin and destination are located in its central grid (O_5-D_5 and O_5'-D_5'), or as the radial network when one of them is in the peripheral branching (O_6-D_6 and O_6'-D_6'). Although with one exemption, some trips need a second transfer, being O_7-D_7 an example. These last trips only exist when the variable α is smaller than the parameter ϕ. This relationship conditions the types of trip that exist.

In a direct trip-based network, the third and fourth criteria are coincident when the destination is located in the same quadrant as the origin or in adjacent quadrants, for example O_3-D_3 and $O_{4,1}$-D_4 trips. However, this does not happen when both extremes of the trip belong to opposite quadrants ($O_{4,2}$-D_4). In this case, some of direct trips that go through the destination swath are longer than alternative paths that cross the city center where the users must make one transfer. The best alternative depends on different aspects like commercial speed, transfer penalty, the user perception of in-vehicle and transfer times, and in what swath the destination is. For simplicity, we consider as general criterion, that users choose the direct trip, although this is longer, since the main objective of this network is to guarantee direct connections between origins and destinations.

3.5. Adaptation of network structures atop a ring-radial street pattern

3.5.1. ***Geometry and operation***

Atop a ring-radial street pattern, three structures are compared: a radial scheme, a direct trip-based one and a hybrid network as a transfer-based system. Figure 3.6 shows the geometry of that hybrid network. This consists of two types of bidirectional corridors, radial or pendular lines (periphery-center-periphery) and circular or ring lines (concentric to the center). The territory is covered by two distinct areas, combining the scheme of Vaughan's model (1986) in the central area and Newell's hub and spoke scheme (1979) in the peripheral band.

The resulting network configuration is defined by four decision variables. Three of these are spatial variables that determine its topology: the angle between radial lines (or between stops of circular lines) in the central area θ (radians), circular line spacing (or stop spacing in radial lines) s (km), and the central area size $\alpha=r_c/R$, where r_c (km) is the radius of the inner area and R (km) the corresponding radius of the city. The fourth variable is the headway of service H (h) in the lines of the central area. The spacings, which are referenced throughout the document, are equivalent to a linear distance between circular lines or radial stops, and an angle between radial lines or circular stops.

In that central area, the network scheme is adapted to the urban structure with centripetal (radial lines) and transverse (circular lines) connections. This central region from a supply point of view, whose area is $\pi(\alpha R)^2$, is extended on an area equal to or smaller than the central attractant region from a demand point of view, whose area is $\pi(\phi R)^2$, i.e., $\alpha \leq \phi$. The remainder

city is served by the branching of radial lines. Circular lines do not have sense out of the attractant area since nobody would use them. In consequence to this scheme, temporal coverage (headways) is constant in the central area. However, spatial coverage varies, the stop spacing in the ring direction increases linearly with the distance from the center and proportionally to θ. Its stops present double coverage, i.e., they are served by one radial and one circular line, which allows transfers.

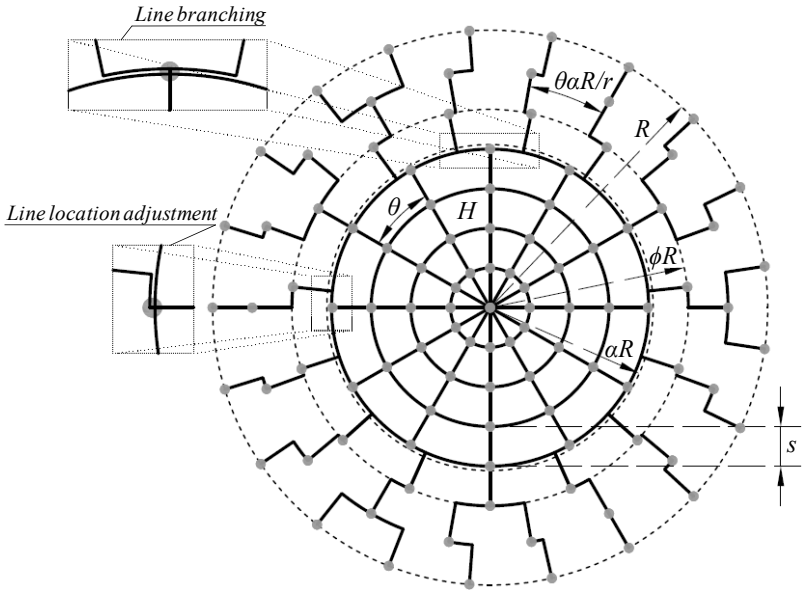

Figure 3.6. Network scheme, geometric decision variables and parameters of the ring-radial hybrid model.

On the other hand, in the peripheral band, corridors branch out to ensure a constant spatial accessibility; keeping the radial line spacing equal to the spacing at the central area boundary αR. However, it causes vehicular scattering, and as a result, a decrease in temporal coverage with the distance from the center. This peripheral area has stops with single coverage and centripetal connections (radial lines), and users cannot make transfers in them. There is a breakdown between the characteristics of these two zones, and the model evaluates the optimum percentage of both areas through the variable α.

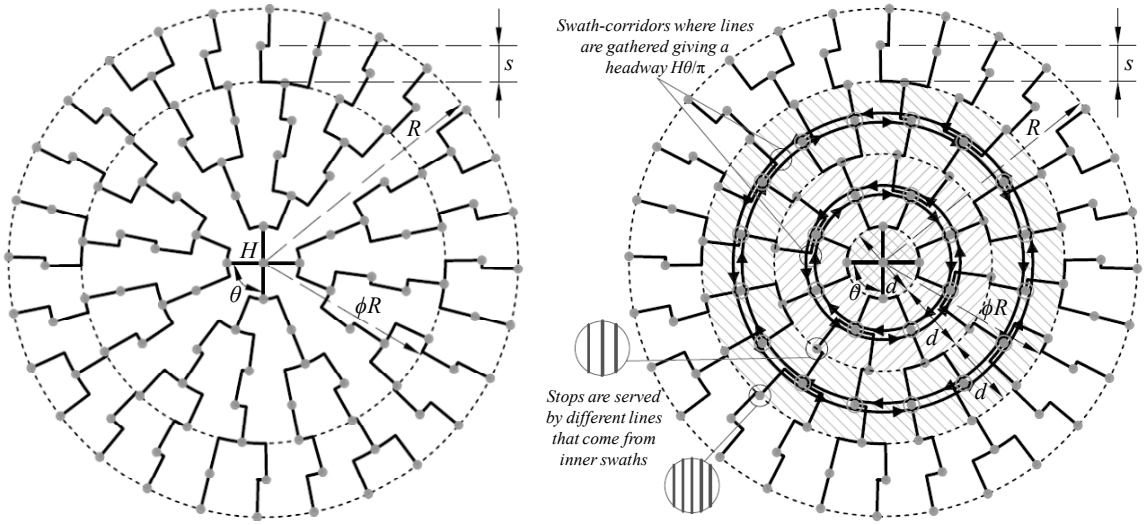

(a) Radial structure *(b) Direct trip-based structure*

Figure 3.7. Network scheme, decision variables and parameters of the radial and direct trip-based structures atop a ring-radial street pattern.

Figure 3.7a presents the radial scheme, which is a particular case of the hybrid structure for $\alpha = 0$. Therefore, it follows the same behavior as the peripheral section of that previous structure. In this case, only radial lines serve the city and these start to branch out from its center. Its decision variables are s, θ and H. Variables s and θ define the geometry of the network and the radial lines' branching that guarantees the same spatial coverage along the city. H is the headway of one corridor at central point of the network. The temporal coverage decreases with the distance from that center.

At the same time, that radial network is the starting point for the direct-trip based structure (Figure 3.7b). As in a grid street layout, the central attractant area is divided into concentric circular swaths. The central one is served by the radial network. The remainder of swaths are connected directly by means of additional group of lines gathered in each of them. In Figure 3.8 the route layout of some lines that connect one swath is plotted. One of these lines crosses the external area between the city boundary and the connected swath following the same routes of the radial network. Once the line arrives at the swath, this runs longitudinally the swath-corridor defining approximately a semi circle. After that, the line crosses the external area again but in the opposite side of the city. In this way, this line connect half of the swath with its area of influence in the external area. The other half of the swath is connected by a symmetrical line that runs over the other semi circle. For example, Figure 3.8 shows three of these pairs of lines L1-L4, L2-L5 and L3-L6 that go into the second swath at the same point. If this process is repeated for all the lines that arrive to the swath in the remainder points of entrance, this swath would be connected with the whole city by direct services. The inner area of the swath is already connected by means of the lines that serve inner swaths.

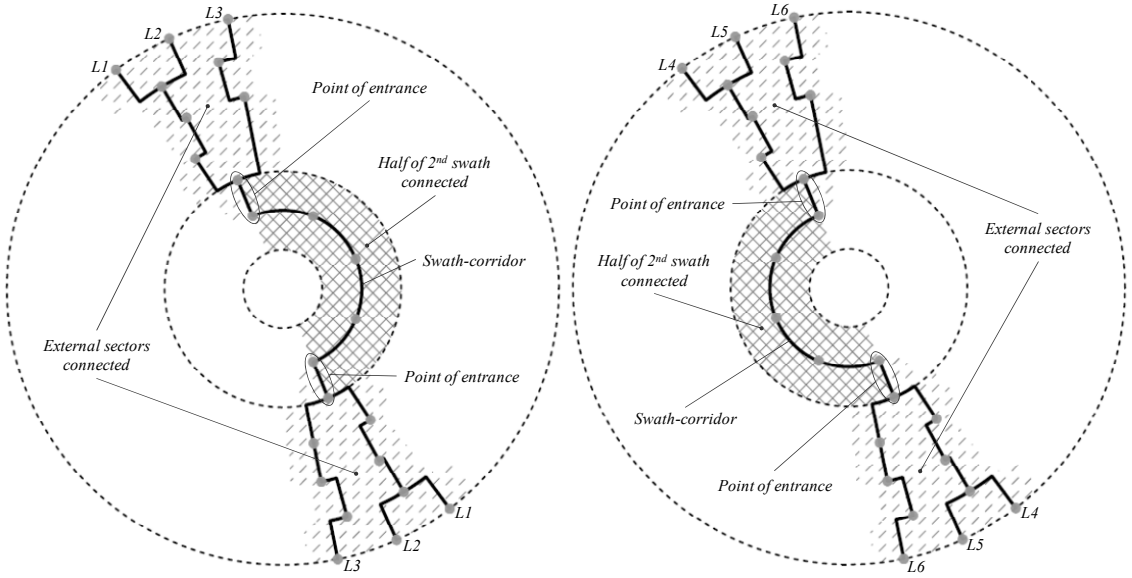

Figure 3.8. Detail of a direct trip-based network structure: how lines are arranged to connect the second swath to its external area.

Four decision variables determine the network configuration for this structure. Three from the previous radial network (s, θ and H), and an additional one that defines the swath width d. Focusing on the initial radial network, H is the headway for each corridor at city center. However, due to the line branching, the headway increases with regard to the distance from that center. To maintain the vehicle flow, at a distance r, the headway is $(r/s)H$. Regarding the remainder of swaths, it is assumed that the same level of service is provided from the frequency point of view. That is, a line that serve a swaths located at a distance r has on average a

headway $(r/s)H$. In the swath-corridor, the resultant headway is the addition of the different overlapped lines. From Figure 3.8, it is possible to deduce that the number of overlapped lines is π/θ_r; where θ_r is the angle between radial lines at a distance r from the city center. Knowing that $\theta_r = \theta s/r$, the resultant headway in each swath corridor is $H\theta/\pi$ in order to conserve the spatial coverage.

3.5.2. User transit chain

To determine the path followed by users, the same criteria as in the grid street pattern are considered here: access and egress at the closest stop to origin and destination, shortest path, and minimum number of transfers. Moreover, similar exemptions are assumed for the derivation of user costs.

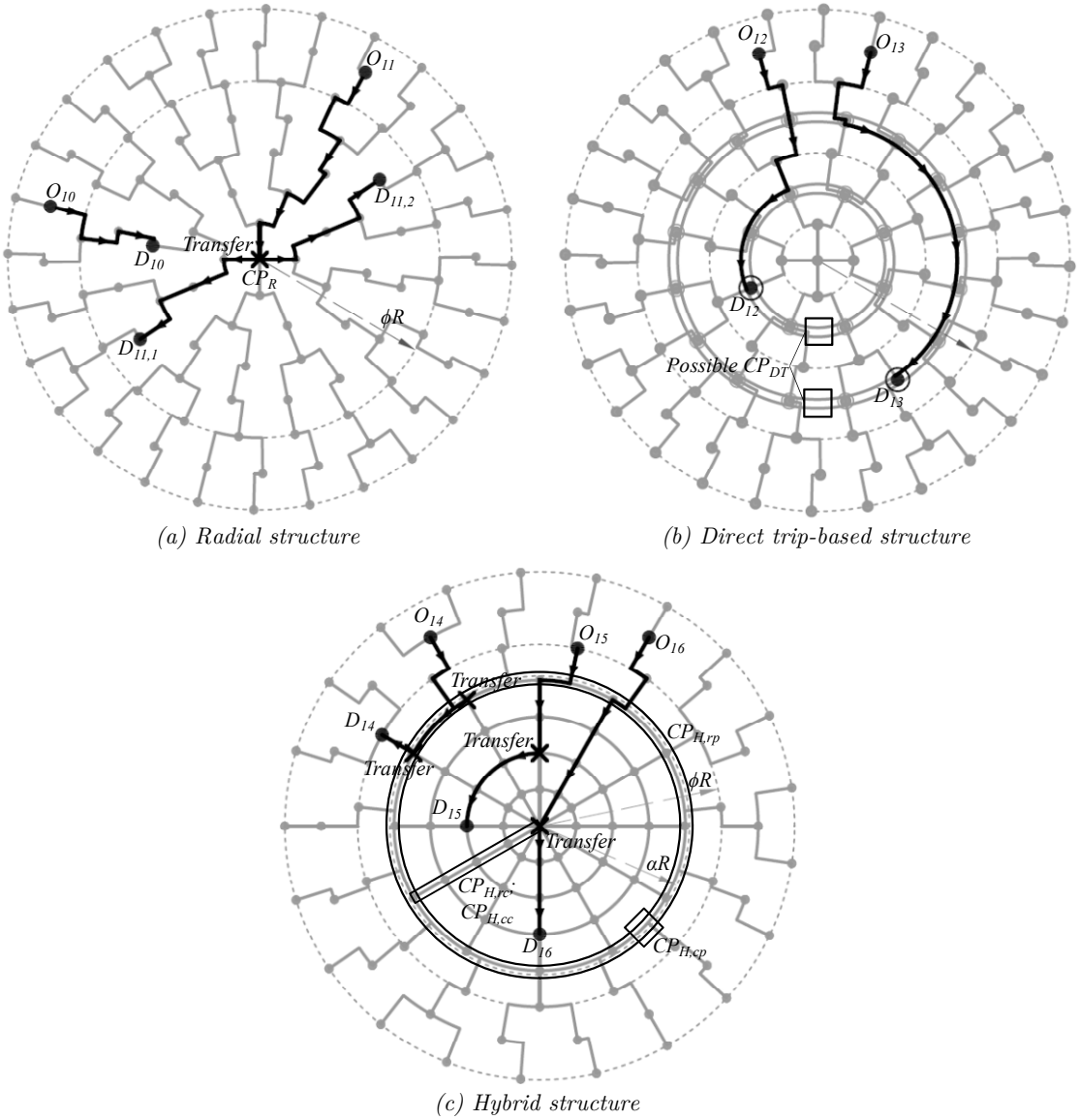

(a) Radial structure

(b) Direct trip-based structure

(c) Hybrid structure

Figure 3.9. Paths and critical loaded points of the structures studied atop a ring-radial street pattern.

Figure 3.9 shows the different types of trips for the three basic network structures compared. In the radial network, all the criteria are coincident since there is only one path to connect any

pair origin-destination. This trip can be direct (O_{10}-D_{10}) or by one transfer made at the city center (O_{11}-$D_{11,1}$). In this last case, this network presents circuitous trips whose length is considerable longer than the real distance between origin and destination, for example the case O_{11}-$D_{11,2}$.

For the other two structures, the previous criteria cannot be always achieved at the same time. To obtain a simple formulation without a comparison between different possible alternative routes in every possible network configuration, the routing strategy of users is simplified. In a direct trip-based network, as in the previous grid street pattern, users get off the bus in stops located at the swath-corridor although this decision implies a longer egress time. To get the most closest stop to the destination, the trip would imply a transfer, the step of the transit chain that this structure wants to avoid. The same reason is assumed to justify that the criterion of minimum transfers prevails over the shortest path. For trip O_{12}-D_{12}, both criteria are coincident. However, when origin and destination are distanced by an angle greater than 2 radians, the shortest path goes through the city center, but the path with a minimum number of transfers by the respective swath-corridor. Users are supposed to choose this second option, trip O_{13}-D_{13}.

On the other hand, in the hybrid network, the shortest path criterion prevails over the minimum number of transfers. This happens for trips that have two characteristics: origin and destination belong to the branched section of the radial lines, and the angular distance between them is smaller than 2 radians. Trip O_{14}-D_{14} in Figure 3.9c is an example of this. Three sections compose it: from the origin to the most external circular line, where the user transfers to reach the radial line that serves the destination, and a second transfer is needed. For the remainder trips, these two criteria are coincident. If the angular distance is smaller than 2 radians and at least one of the extremes is located in the central ring-radial mesh, the trip combines one radial and one circular line (trip O_{15}-D_{15}). However, when that angular distance is greater, in spite of the origin and destination location, the trip only uses radial lines, passing through the city center, where users make the unique transfer (trip O_{16}-D_{16}).

3.6. Basics of the analytical transit network design model

In this section, the key elements of the analytical model are presented such as its input parameters, the objective function that minimizes the total system cost, the partial costs that are considered, and finally, the constraints that control the network configurations. The model presents coincident input parameters for all structures and a common objective function where the same agency and user partial costs are included.

3.6.1. Input parameters

A short number of inputs parameters are necessary to characterize the territory, the demand and the transport technology. Some of them have been already commented in the previous sections for defining city and transit network configuration and the rest complete the parameters used in this model.

- Size of the territory that has to be served is defined by the parameter D (km) that is the side of the square city in a grid and by the radius R (km) of the circle for a ring-radial city. (Explained in Section 3.1)
- Demand at rush hour Λ (p/h), the amount of passengers that use the transit system during its most demanded hour, and average hourly demand λ (p/h), the amount of passengers that use the transit system during a day assigned per each hour of service. (Explained in Section 3.2)
- Urban dispersion defined by ϕ, which determines the central attractant area's size, and f_d, which indicates the ratio between the generated demand density at central and peripheral areas. (Explained in Section 3.2)
- Vehicle capacity C (p/veh), maximum number of passengers that a vehicle can carry.
- Occupancy safety factor SF, which takes into account possible peaks of demand during the rush hour.
- Cruising speed v (km/h), this is the maximum speed that a vehicle can achieve in the road network taking into account the lost time due to traffic lights and other types of disturbances, but not because of transit stops and boarding and alighting processes.
- Dwell time τ (h), a fixed time that one vehicle spends when it has to stop at transit station or stop defined as the sum of the time devoted accelerating and decelerating, opening and closing doors, and other possible operational times like holding times to guarantee a certain level of reliability.
- Boarding and alighting time τ' (h), time spent by one passenger to get on and get off a transit vehicle.
- Value of time μ (€/h), the monetary cost for one user that spends one hour of his/her time in the transit system.
- Pedestrian speed w (km/h).
- Transfer penalty δ (km), as a walking distance between the loading areas of the lines that are combined.
- Agency unit costs of infrastructure $€_L$ (€/km-h), operation $€_V$ (€/veh-km) and fleet $€_M$ (€/veh-h).
- Time perception weights for the respective user costs: access w_A, waiting w_W, riding w_T and transferring w_t.
- Cut-off headway between both types of service operation H_s. (Explained in Section 3.3.1)
- Safety waiting time h_s. (Explained in Section 3.3.1)

- Factor of opportunity cost f_s. (Explained in Section 3.3.1)

3.6.2. Objective function and constraints

To determine the best network structure, we compare the total system cost of each member belonging to the same family design concept (grid or ring-radial street pattern). Therefore, the model seeks to obtain the network configuration that minimizes that cost, where the resources invested by agency and travel time of users are considered. From the agency point of view, the model computes three costs: (i) infrastructure length L (km), with regard to its construction and maintenance, (ii) operation of the service, caused by the kilometers traveled, energy, wear of the vehicles, etc., which are captured by parameter V (veh-km/h), which is the distance travelled by all vehicles in one hour of service, and (iii) number of vehicles M (veh), this includes the acquisition of the fleet and the crew needed to operate the network. On the other hand, user cost is proportional to the travel time needed to accomplish each component of the user transit chain, such as access A (h), waiting W (h), riding in-vehicle T (h) and transferring. The in-vehicle time is the result to divide the average in-vehicle distance per trip E (km) by the commercial speed of the transit system v_c (km/h). Regarding transfers, two types of costs are considered: a waiting time included in the total waiting time W, and a walking penalty that depends on the average number of transfers per trip e_T, a fixed distance δ per transfer and the pedestrian speed w.

The identification of the most competitive transit network should satisfy a proper trade-off between the user and agency perspectives. Therefore, all network costs are included in the objective function Z (h) (3.2) to be minimized. The term Z represents the sum of C_A (h), which is the agency cost of service supplied in one hour prorated by the number of users, plus C_U (h), which is the average user cost per trip weighted by their respective time perceptions (access w_A, waiting w_W, riding w_T and transferring w_t). In the objective function, all the costs have to be expressed in the same units, in this case, hours per passenger. For this reason, the different agency costs are multiplied by their respective unit monetary costs per km-h ($€_L$), veh-km ($€_V$) or veh-h ($€_M$), and expressed in terms of equivalent hours of passenger by means of the factor $1/\lambda\mu$.

$$min\{Z = C_A + C_U = [€_L L + €_V V + €_M M]/\lambda\mu + [w_A A + w_W W + w_T T + w_t(\delta/w)e_T]\} \tag{3.2}$$

In a grid street layout, subject to:

$$\begin{aligned} &s > 0;\ H > 0;\ s/D \le \phi;\ O \le C,\ \textit{for radial network} \\ &d \ge s > 0;\ H > 0;\ s/D \le \phi/2;\ d/D \le \phi/2;\ O \le C,\ \textit{for direct trip-based network} \\ &s > 0;\ H_p \ge H_c > 0;\ s/D \le \phi;\ O \le C,\ \textit{for grid network} \\ &s > 0;\ H > 0;\ s/D \le min\{\alpha;\phi\};\ O \le C,\ \textit{for hybrid network} \end{aligned} \tag{3.2a}$$

In a ring-radial street layout, subject to:

$$\begin{aligned} &s > 0;\theta > \pi/2;\ H > 0;\ s/R \le \phi;\ O \le C,\ \textit{for radial network} \\ &d \ge s > 0;\theta > \pi;\ H > 0;\ s/R \le \phi;\ d/R \le \phi;\ O \le C,\ \textit{for direct trip-based network} \\ &s > 0;\theta > \pi;\ H > 0;\ s/R \le \alpha;\ O \le C,\ \textit{for hybrid network} \end{aligned} \tag{3.2b}$$

In addition, constraints (3.2a and 3.2b) related to the decision variables and the vehicle capacity conditions the optimal solution. All decision variables have to be positive for physical

reasons, and maximum vehicle occupancy O (p/veh) has to be lower than the vehicle capacity C. Moreover, a ratio between stop or corridor spacing and the length of the side of the central attractant area, or the central grid for the hybrid network, must be respected as a consequence of how the formulation is derived. This method is sufficiently flexible as we can take further constraints into account for particular case studies. For example, we may consider the limit values of decision variables, a maximum fleet, minimal accessibility or maximal network length, etc. However, these restrictions may particularly affect the benefits that can be achieved.

The objective function for all network structures is convex as it can be seen in Appendix D that includes a sensitivity analysis of this model; that is, the local optimum found is the global solution. This characteristic and the small number of decision variables make its minimization trivial. Therefore, its optimization is performed easily by means of a grid search.

To estimate the occupancy, the most loaded points are compared in each network. Figures 3.5 shows the location of these points in the different networks atop a grid street pattern. The same happens in Figure 3.9 for the structures compared atop a ring-radial street layout. The central point in a radial scheme (CP_R) for both street patterns. For a direct trip-based network, the critical point belongs to one swath that can be the most external one when the attractant area is small, or an intermediate swath when this area is larger. In the hybrid network, the critical points differ with regard to the street pattern. Atop a grid, it depends on the ratio between α and ϕ. If α is greater, the critical points are located at the boundary ϕD and at the central point of the corridors that cross the attractant area, points $CP_{H,2}{}'$ and $CP_{H,1}{}'$ respectively. On the contrary, at the boundary αD ($CP_{H,2}$) and at the central point of the most external corridors ($CP_{H,1}$). Atop a ring-radial mesh, two types of critical points are identified: in radial lines and in circular lines. In both cases, one critical point is located in the central mesh boundary, $CP_{H,rp}$ in radial lines and $CP_{H,cp}$ in the most external circular. Depending on the central area size, there are two more critical points, one in a middle position of a radial line ($CP_{H,rc}$), and other in an intermediate circular line ($CP_{H,cc}$). Finally, there are three critical points in a grid structure (only atop a grid street pattern), the middle point ($CP_{G,1}$) and the point at the central attractant area boundary ($CP_{G,2}$) of one central corridor, and the point $CP_{G,3}$ of the peripheral corridors.

3.7. Partial costs

This section presents the different agency and user costs included in the objective function. All of them are expressed in a compact form as a function of decision variables. On the one hand, Tables 3.1, 3.2, 3.3 and 3.4 directly displays the formulae for the radial, direct trip, hybrid and grid networks respectively atop a grid street layout. On the other hand, Tables 3.5, 3.6 and 3.7 summarize the formulae for the radial, direct trip and hybrid structures respectively atop a ring-radial pattern. However, the exhaustive derivation of these partial costs is placed in Appendix B (grid) and C (ring-radial) for each of the street layouts. Appendix D includes a sensitivity analysis of all these partial costs with regard to changes on the decision variables.

3.7.1. Atop a grid street pattern

Table 3.1. Formulation of partial costs, commercial speed and occupancy constraint for radial network structure atop a grid street pattern.

Partial cost	*Radial network*
L	$L = D^2/s$
V	$V = 6D/H$
M	$M = V/v_c$
v_c	$v_c = 1/[1/v_{FFS} + \tau/s + \tau'(1+e_T)\Lambda/V]$
A	$A = s/w$
W	$W = H\left[15D(1+2\phi+2\phi^2) - 15s(1+\phi) - \rho\left(15D + s(1+\phi)\right)\right]/45s(1+\phi)$
E	$E = \left[15D(1+2\phi+2\phi^2) - 15s(1+\phi) - \rho\left(15D + s(1+\phi)\right)\right]/30(1+\phi)$
T	$T = E/v_c$
e_T	$e_T = 1 - s(3+\rho)/3\phi D$
O	$O = (SF)H\Lambda[6\phi D - s(3+\phi^2)]/24\phi D$

Table 3.2. Formulation of partial costs, commercial speed and occupancy constraint for direct trip-based network structure atop a grid street pattern.

Partial cost	*Direct trip-based network*
L	$L = D^2/s + (\phi^2 D^2 - d^2)/d$
V	$V = [\phi D^2(6+\phi) - d^2]/dH$
M	$M = V/v_c$
v_c	$v_c = 1/[1/v + \tau/s + \tau'\Lambda/V]$
A	$A = (3s+d)/4w$
W	*if* $\varepsilon_H \geq 1$, $W = H[5(1+\phi+\phi^2) - \rho(5-\phi-\phi^2)]D/15(1+\phi)s$ *if* $\phi \leq \varepsilon_H < 1$, $W = \left[h_s(1-\varepsilon_H^2) + H\left(2f_s(1-\varepsilon_H^3) + (\varepsilon_H^3 - \phi^3)\right)D/3s\right](1-\rho)/(1-\phi^2) + 2\phi DH\rho/5s$ *if* $\varepsilon_H < \phi$, $W = [h_s + 2f_s(1+\phi+\phi^2)DH/3(1+\phi)s](1-\rho) + \left[h_s(\phi^4 - \varepsilon_H^4) + 2H\left(2f_s(\phi^5 - \varepsilon_H^5) + \varepsilon_H^5\right)D/5s\right]\rho/\phi^4$
E	$E = [15(1-\rho) + 2\phi(1+\phi)(10+\rho)]D/30(1+\phi)$
T	$T = E/v_c$
e_T	$e_T = 0$
O	*if* $\left(2d\rho + \sqrt{3\phi^2D^2\rho + d^2\rho^2}\right)/6\rho \leq \phi D/2$, $O = (SF)\,H\Lambda d\left[d\rho(9\phi^2D^2 - \rho d^2) + \rho^{1/2}(3D^2 + d^2)^{3/2}\right]/27\phi^4D^4\rho$ *if* $\left(2d\rho + \sqrt{3\phi^2D^2\rho + d^2\rho^2}\right)/6\rho > \phi D/2$, $O = (SF)\,H\Lambda d(\phi D - d)[\phi^2D^2(1-\rho) + 4d\rho(\phi D - d)]/2\phi^4D^4$

Table 3.3. Formulation of partial costs, commercial speed and occupancy constraint for hybrid network structure atop a grid street pattern.

Partial cost	*Hybrid network*
L	$L = D^2(1+\alpha^2)/s$
V	$V = 2\alpha D^2(3-\alpha)/sH$
M	$M = V/v_c$
v_c	$v_c = 1/[1/v_{FFS} + \tau/s + \tau'(1+e_T)\Lambda/V]$
A	$A = s/w$
	If $\alpha > \phi$
W	$W = H[\phi^2 D^2[(2+\alpha^3)(1-\rho) + 3\alpha(1+\rho) - 6\alpha\phi^2] - 3\phi Ds[\phi(1+\alpha^2)(1-\rho) + 2\alpha(\rho-\phi^2)] + 3\alpha s^2(1-\phi^2)\rho]/6\alpha\phi^2(1-\phi^2)D^2$
E	$E = D[(6\alpha + \phi^2 + \alpha^2\phi^2)(1-\rho) + 8\alpha\phi(\rho-\phi^2)]/12\alpha(1-\phi^2)$
T	$T = E/v_c$
e_T	$e_T = 1 - s[\phi^2 D(1+\alpha^2)(1-\rho) + 2\alpha\phi D(\rho-\phi^2) - \alpha s(1-\phi^2)\rho]/\alpha\phi^2(1-\phi^2)D^2$
O	$O = [H\Lambda s/8\alpha\phi(1-\phi^2)D]max\{2\alpha(1-\rho)(2-\phi^2-\alpha^2); (1-\rho)(\alpha+\phi)(2-\alpha^2) + 2\alpha(\rho-\phi^2)\}$
	If $\alpha \leq \phi$
W	$W = \rho W_c + (1-\rho)W_p$
	where:
	$W_c = H\big[D^2\big(\phi^4(8\phi+3\alpha) + \alpha^3(3\alpha^2-2\phi^2) - \alpha^3(\phi+\alpha)\big) - 2Ds\big(\phi^3(2\phi+\alpha) + \alpha^3(2\alpha+\phi)\big) + 6\alpha^3 s^2\big]/12\alpha\phi^4 D^2$
	$W_p = H\big[D\big(\phi^3(8\phi+11\alpha) + \phi^2\alpha(4+3\alpha) - \alpha^3(\phi+\alpha)\big) - 2s\big(\phi^2(2\phi+3\alpha) + \alpha^2(3\phi-2\alpha)\big)\big]/12\alpha\phi^2(\alpha+\phi)D$
E	$E = D\big[\big(\alpha^3(2\phi^2(1+\rho) - \alpha^2\rho) + \phi^4(12\phi-7\alpha)\big)(1+\phi) + 6\phi^4(1-\rho)\big]/12\phi^4(1+\phi)$
T	$T = E/v_c$
e_T	$e_T = 1 + [D(\phi^2-\alpha^2) + 2\alpha s](\phi^2 - \rho\alpha^2)/2\phi^4 D - [2\phi^3 D - \rho\alpha^2 s]s/\phi^4 D^2$
O	$(H\Lambda/2\alpha\phi^2 D)max\big\{\big[D\alpha(\phi^2-\alpha^2)(\phi^2-\rho\alpha^2) + 4s\big(\phi^2\alpha^2(1+\rho) + 3(\phi^4 - \rho\alpha^4)\big)\big]/16\phi^2;\ s(\phi^2-\alpha^2\rho)\big\}$

Table 3.4. Formulation of partial costs, commercial speed and occupancy constraint for grid network structure atop a grid street pattern.

Partial cost	*Grid network*
L	$L = 2D^2/s$
V	$V = 4D^2\big[(1-\phi)H_c + \phi H_p\big]/sH_cH_p$
M	$M = V/v_c$
v_c	$v_c = 1/[1/v_{FFS} + \tau/s + \tau'(1+e_T)\Lambda/V]$
A	$A = s/w$
W	$W = H_c\big[\phi^2 D^2\big(1+3\phi+\rho(1-\phi)\big) - 2\phi Ds(\rho+\phi) + \rho s^2(1+\phi)\big]/2\phi^2 D^2(1+\phi) + H_p(1-\phi)(1-\rho)/2(1+\phi)$
E	$E = D[3+3\phi+4\phi^2 - \rho(3-\phi)]/6(1+\phi)$
T	$T = E/v_c$
e_T	$e_T = 1 - s[2\phi D(\phi+\rho) - s\rho(1+\phi)]/\phi^2(1+\phi)D^2$
O	$O = (SF)(\Lambda s/4D)max\big\{H_c[1+3\phi+\rho(1-\phi)]/2\phi(1+\phi);\ H_c(1-\rho)/\phi;\ H_p(1-\rho)/(1+\phi)\big\}$

3.7.2. Atop a ring-radial street pattern

Table 3.5. Formulation of partial costs, commercial speed and occupancy constraint for radial network structure atop a ring-radial street pattern.

Partial cost	*Radial network*
L	$L = \pi[(4+\theta)R(R+s) - 2\theta s^2]/4s\theta$
V	$V = \pi[(4+\theta)R - \theta s]/\theta H$
M	$M = V/v_c$
v_c	$v_c = 1/[1/v + \tau/l_s + \tau'(1+e_T)\Lambda/V] = 1/[1/v + \tau\pi R(R+s)/L\theta s^2 + \tau'\Lambda(1+e_T)/V]$ *where:* $l_s = L\theta s^2/\pi R(R+s)$ *is the average infrastructure length per stop*
A	$A = s(1+\theta)/2w$
W	$W = H\big[15\pi R(1+2\phi+2\phi^2) - 30\theta s(1+\phi) - \rho\big(15\pi R + 2\theta s(1+\phi)\big)\big]/45\pi s(1+\phi)$
E	$E/v_c = (4+\theta)[15\pi R(1-\phi)(1+2\phi+2\phi^2-\rho) - 2\theta s(15-18\phi^2+\rho+2\rho\phi)]/90\pi(1-\phi^2)$
T	$T = E/v_c$
e_T	$e_T = 1 - 2s\theta(3+\rho)/3\pi\phi R$
O	$O = (SF)H\Lambda\theta[3\pi\phi R - \theta s(3+\rho)]/6\pi^2\phi R$

Table 3.6. Formulation of partial costs, commercial speed and occupancy constraint for direct trip-based network structure atop a ring-radial street pattern.

Partial cost	*Direct trip-based network*
L	$L = \pi[(4+\theta)R(R+s) - 2\theta s^2]/4s\theta + \pi(4\phi^2R^2 - d^2)/4d$
V	$V = \pi\big[4\phi R^2\big((4+\theta)(2-\phi) + 2\pi\phi\big) - d\big(2d(\pi-2) - \theta(d-4s)\big)\big]/4d\theta H$
M	$M = V/v_c$
v_c	$v_c = 1/[1/v + \tau/l_s + \tau'(1+e_T)\Lambda/V] = 1/[1/v + \tau\pi[4dR(R+s) + s(4\phi^2R^2 - d^2)]/4L\theta ds^2 + \tau'\Lambda/V]$ *where:* $l_s = 4L\theta ds^2/\pi[4dR(R+s) + s(4\phi^2R^2 - d^2)]$ *is the average infrastructure length per stop*
A	$A = [s(1+2\theta) + d]/4w$
W	*if* $\varepsilon_H \geq 1$, $W = H[5(1-\rho) + \phi(1+\phi)(5+\rho)]R/15(1+\phi)s$ *if* $\phi \leq \varepsilon_H < 1$, $W = \Big[h_s(1-\varepsilon_H^2) + H\Big(2f_s(1-\varepsilon_H^3) + (\varepsilon_H^3 - \phi^3)\Big)R/3s\Big](1-\rho)/(1-\phi^2) + 2\phi RH\rho/5s$ *if* $\varepsilon_H < \phi$, $W = [h_s + 2f_s(1+\phi+\phi^2)RH/3(1+\phi)s](1-\rho) + \big[h_s(\phi^4 - \varepsilon_H^4) + 2H\big(2f_s\big(\phi^5 - \varepsilon_H^5\big) + \varepsilon_H^5\big)R/5s\big]\rho/\phi^4$
E	$E = \big[(20+5\theta)(1-\rho) + 2\phi(1+\phi)\big(5\pi + \rho(4+\theta-\pi)\big)\big]R/30(1+\phi)$
T	$T = E/v_c$
e_T	$e_T = 0$
O	*if* $\big(2d\rho + \sqrt{12\phi^2R^2\rho + d^2\rho^2}\big)/6\rho \leq \phi R$, $O_i = (SF)\,H\Lambda\theta d\big[d\rho(36\phi^2R^2 - \rho d^2) + \rho^{1/2}(12\phi^2R^2 + \rho d^2)^{3/2}\big]/216\pi\phi^4R^4\rho$ *if* $\big(2d\rho + \sqrt{12\phi^2R^2\rho + d^2\rho^2}\big)/6\rho > \phi R$, $O_e = (SF)\,H\Lambda\theta d(2\phi R - d)[\phi^2R^2(1-\rho) + \rho d(2\phi R - d)]/4\pi\phi^4R^4$

Table 3.7. Formulation of partial costs, commercial speed and occupancy constraint for hybrid network structure atop a ring-radial street pattern.

Partial cost	*Hybrid network*
L	$L = \pi\left[4s\left((1+\alpha^2)R + (1-\alpha)s\right) + \theta\alpha R\left((1+3\alpha^2)R + (1+3\alpha)s\right)\right]/4\alpha s\theta$
V	$V = \pi R[4s + \alpha\theta(2s + (1+\alpha)R)]/\theta sH$
M	$M = V/v_c$
v_c	$v_c = 1/[1/v + \tau/l_s + \tau'(1+e_T)\Lambda/V] = 1/[1/v + \tau\pi[(1+\alpha^2)R + (1-\alpha)s + 2\alpha^2 R]/L\alpha\theta s + \tau'\Lambda(1+e_T)/V]$ *where:* $l_s = L\alpha\theta s/\pi[(1+\alpha^2)R + (1-\alpha)s + 2\alpha^2 R]$ *is the average infrastructure length per stop*
A	$A = [\alpha R\theta(6\phi^2 - \alpha^2 - \rho\alpha^2)/12\phi^2 + s/2]/w$
W	$W = \rho W_c + (1-\rho)W_p$ *where:* $W_c = H\left[4\pi\phi^2(\phi^3+\alpha^3)R + 3\alpha R\left((4-\theta)\phi^4 - (4+\theta)\alpha^2(2\phi^2-\alpha^2)\right) - 4\alpha^4 s(4-\theta)\right]/12\pi\alpha\phi^4 R$ $W_p = H\left[2\pi\phi^2\left(2\phi^2 + (4\phi^3+\alpha^3)(1+\phi)\right) + 3\alpha(1+\phi)\left(4(\phi^2-\alpha^2) - \theta(\phi^2+\alpha^2)\right)\right]/12\pi\alpha\phi^2(1+\phi)$
E	$E = \left[\rho E_c + (1-\rho)E_p\right]$ *where:* $E_c = R[5\pi\alpha R\theta\phi^2(2\phi^3 - 3\alpha\phi^2 + \alpha^3) + 4s(10\pi\phi^5 - 15\alpha\phi^4 + 10\alpha^3\phi^2 - 3\alpha^5)]/30\pi\phi^4 s$ $E_p = R\left[\pi\alpha R\theta\left(2\phi^2 + (1+\phi)(4\phi^3 - 6\alpha\phi^2 + \alpha^3)\right) + 8s\left(\pi\phi^2 + (1+\phi)(2\pi\phi^3 - 3\alpha\phi^2 + \alpha^3)\right)\right]/12\pi\phi^2(1+\phi)s$
T	$T = E/v_c$
e_T	$e_T = 1 + [4(\phi^2-\alpha^2) - \theta(\phi^2+\alpha^2)]/2\pi\phi^2 - \rho\alpha^2[R(4+3\theta)(\phi^2-\alpha^2) + 4\alpha s(4-\theta)]/6\pi\phi^4 R$
O	$O = (SF)max\left\{H\theta\Lambda(1-\rho\alpha^2/\phi^2)/\pi;\ H\Lambda[4R^2(\phi^2-\rho\alpha^2) + \rho s(4\alpha R - s)][4R^2(\phi^2-\alpha^2) + s(4\alpha R - s)]/32\pi^2\phi^4R^4;\ H\theta\Lambda[4\phi^2 + \rho(\pi\phi^2 - 2\phi^2 - 2\alpha^2)]^2/16\pi^2\phi^4\rho, if\ R\sqrt{\rho(4\phi^2 + 2\rho\phi^2 - \pi\rho\phi^2 - 2\rho\alpha^2)}/2\rho < \alpha R;\ H\Lambda s\left(2\rho s + \sqrt{\rho(12\phi^2R^2 + \rho s^2)}\right)\left(12\phi^2R^2 + s\sqrt{\rho(12\phi^2R^2 + \rho s^2)} - \rho s^2\right)/108\pi^2\phi^4R^4\rho, if\ s/3 + \sqrt{12\rho\phi^2R^2 + \rho^2 s^2}/6\rho < \alpha R\right\}$

Chapter 4

Comparison of transit network structures*

This chapter provides a comparison among the performance of main transit network structures commented along the thesis in an idealized case study. Its main objective is to identify which of them is the best strategy to serve a given city with a specific urban dispersion degree. The analytical model from Chapter 3 is the tool used to obtain the results as well as the behavior and network performance for those structures in a non-specified city presented in Section 4.1.

This analysis shows the behavior of the different structures versus the demand decentralization process. First, the analysis is made in detail in the base scenario of study. We identify the demand decentralization degrees of change from which the best network structure will be another. Secondly, the thesis analysis how that decentralization degree of change varies when the main input parameters vary from that base scenario. All this is initially made on a grid street layout in Section 4.2, and after on a ring-radial one in Section 4.3. In this way, the study finds out the areas of applicability for the different network structures. Then, Section 4.4 compares the results in both street patterns. Finally, Section 4.5 highlights the most important conclusions of this chapter.

* The results presented in this chapter are also included in Badia et al. (2016) and Badia (2016).

4.1. Base case study

The characteristics of the city, demand, users and transport technology used in the base case study are addressed in this section. Table 4.1 summarizes all parameters. The dimensions of the territory are a side of length $D = 7$ km for a square city and a radius $R = 4$ km for a circular. These dimensions give a territory with a similar extension around 50 km^2 in both cases. The average hourly transit demand λ is 20,000 pax/h, but at rush hour the demand Λ is 50,000 pax/rh. That city size and its transit demand level are an approximation from a real city like Barcelona. The value of time of transit users μ is 15 €/h (Gutiérrez-Domènech, 2008). The walking speed w is 4.5 km/h, which is determined in TRB (2003) for a high-intermediate level of service. The walking transfer penalty δ is 0.3 km. It is assumed that the walking, waiting and transferring times are worse perceived than the in-vehicle time. While this last time is not penalized, the others are increased by the factors 2.2, 2.1 and 2.5 respectively (TRB, 2003).

Table 4.1. Characteristics of the base case study.

Input parameter	Variable	Units	Value
Demand at rush hour	Λ	p/rh	50,000
Average hourly demand	λ	p/h	20,000
Square city dimension	D	km	7
Circular city dimension	R	km	4
Value of time	μ	€/h	15
Equivalent penalty distance per transfer	δ	km	0.3
Cruising speed	v	km/h	30
Walking speed	w	km/h	4.5
Unit infrastructure cost	$€_L$	€/km-h	76
Unit distance cost	$€_V$	€/veh-km	0.85 or 1.1*[a]
Unit vehicle cost	$€_M$	€/veh-h	35 or 36*[a]
Vehicle capacity	C	p/veh	80 or 150*[a]
Occupancy safety factor	SF	-	1.2
Dwell time	τ	s	35
Boarding (and alighting) time	τ'	s	3
Time perception weight of access	w_A	-	2.2
Time perception weight of waiting	w_W	-	2.1
Time perception weight of travelling	w_T	-	1.0
Time perception weight of transferring	w_t	-	2.5
Cut-off headway between types of service	H_s	min	12
Safety waiting time	h_s	min	5
Home waiting time factor	f_s	-	1/12

*[a] First value corresponds to a standard bus and second to an articulated bus.

Regarding the transport technology, the transit services are supplied by a high performance bus (HPB), which is described in Heddebaut et al. (2010) or widely in COST (2010). In this case, we assume a segregated infrastructure with proper stop management and traffic light coordination in favor of the bus. For this reason, the cruising speed v (reduced by traffic lights, congestion, and other factors for surface transportation) is assumed high and its value is 30 km/h. The dwell time at stop τ is 35 s and the boarding (and alighting) time per passenger τ' is 3 s (TRB, 2003).

In addition, we consider two types of vehicles: standard buses or articulated buses. The former is cheaper, but the latter is suitable to serve network configurations or urban centralization scenarios with a high passenger load at the critical points of the network. In any case, the fleet

is composed only by one type of vehicle, all standard or all articulated. Their vehicle capacities C are 80 and 150 pax/veh respectively (Vuchic, 2007). On the other hand, the safety factor of the occupancy (SF) is supposed to be 1.2. That is, due to an irregular allocation of passengers among the vehicles, some of them carry until a 20% more than the occupancy at the most loaded points compared.

In order to evaluate the operation of the network and the depreciation of its resources (infrastructure or vehicles), it is essential to know their unit monetary values. For the infrastructure, this is $€_L$=76 €/km-h. For the other two agency costs, the values are different for standard and articulated buses. In the former, they are $€_V$=0.85 €/veh-km and $€_M$=35 €/veh-h. However, these values for the latter are $€_V$=1.1 €/veh-km and $€_M$=36 €/veh-h. These numbers are obtained from various sources: ATC (2006), MCRIT and GEE (2010), and TMB (2009). The unit costs are estimated per hour of service; it is considered that the service is provided 365 days per year and 18 hours per day.

The input parameters related to the system operation, in headways or by schedules, are H_s = 12 min (Tirachini et al., 2010), h_s = 5 min, and f_s = 1/12. Based on these values, users arrive at the stop randomly for headways lower than 12 minutes. However, if the headway of service at one stop exceeds that threshold, users know the moment when buses pass by the stop, and they arrive only 5 minutes before that time. Users wait at home the remainder time between two buses. That time is perceived in a better way than if users are waiting in the street. For this reason, that time is multiplied by a factor 1/12 and not by 1/2 like an operation in headways.

Finally, as the comparison is made for different scenarios of urban dispersion, the parameters ϕ and f_d adopt different values to represent them. The former ranges from low values around 0.1 to 1. The latter from 1, when the generated demand is uniformly distributed over the whole city, to 30.

4.2. Comparison atop a grid street pattern

4.2.1. Comparison in the base case study

In this section, the behavior of the different structures with regard to demand decentralization is shown. First, this behavior is analyzed in detail considering a constant generated demand density over the whole city. This assumption allows that the decentralization degree is just defined by the parameter ϕ. After, we distinguish the generated demand density between the central area and the periphery, showing how a higher concentration of origins in that central area changes the results of the model. The results presented below are complemented by additional outcomes of partial agency and user costs in Appendix E.

Uniform generated demand density over the whole city

As the generated demand density is constant over the whole city, the ratio between the central and the peripheral densities is $f_d = 1$. Therefore, the weight of the trips whose origin is located at central area central is $\rho = \phi^2$. Figure 4 shows the total, agency and user costs with regard to the demand decentralization degree ϕ for the different transit network structures: radial (Ra), direct trip-based network (DT), grid (Gr) and hybrid (Hy).

As observed in Figure 4.1a, the best transit structure is not always the same: it depends on mobility requirements. There are different cut-off points between the total cost curves of the different transit network structures. These points determine the ranges of applicability of each structure; that is, which is the optimal alternative for each stage of the demand dispersion process.

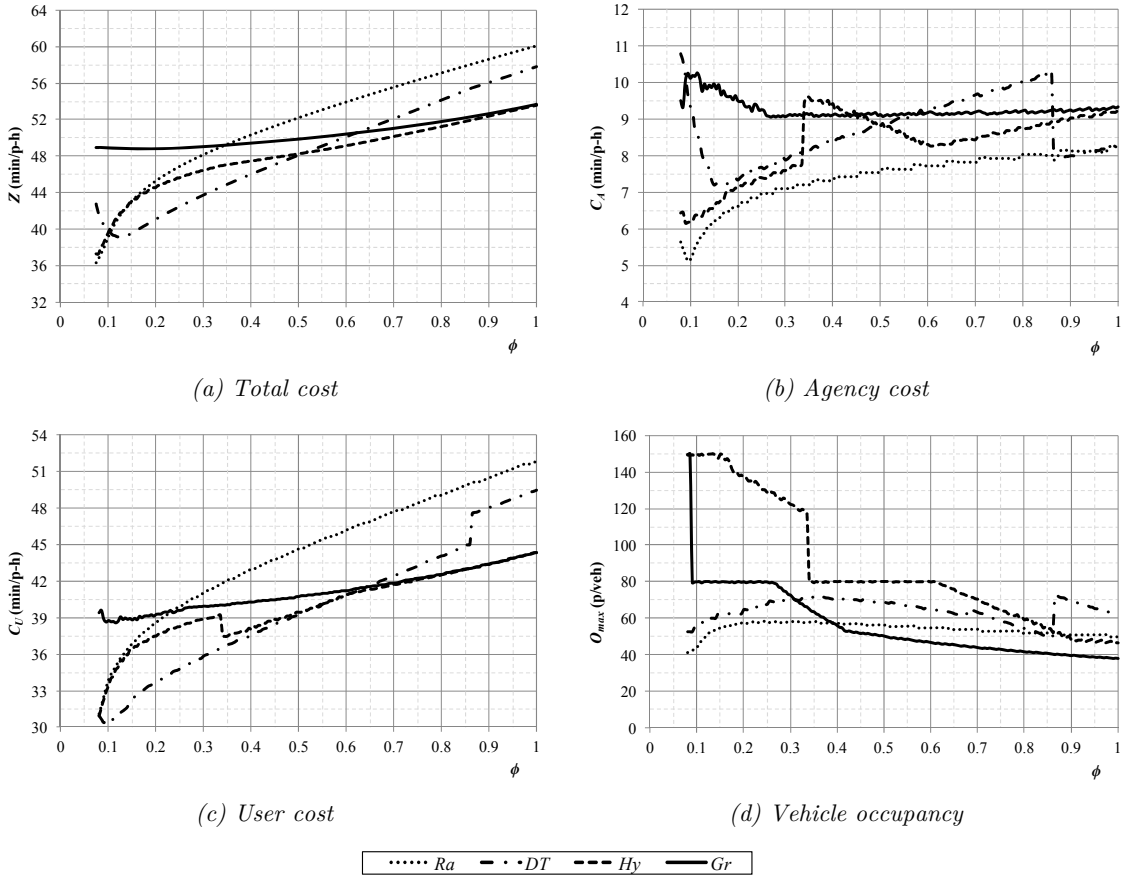

Figure 4.1. Evolution of costs and vehicle occupancy with regard to the demand decentralization degree parameter ϕ in a grid street pattern.

A radial network is the most suitable alternative when the vector of displacements is centripetal, i.e., people want to travel to a small central area. However, its total cost increases sharply when the demand starts to scatter. Therefore, the transit system needs a change of its network structure. Two options are possible: either a direct trip-based structure by means of the introduction of new lines over the radial network, or a hybrid scheme with an initial transformation of the central part of the network to a grid. As Figure 4.1a shows, the former is the best solution, since it keeps the total costs lower than the corresponding values of the latter. This strategy supposes a greater agency investment, which is compensated by the reduction of the increasing user cost that demand decentralization implies.

From that point on, the direct trip-based structure continues to remain the best alternative until the demand decentralization reaches a higher degree. In our case study, this value is 0.52. If that decentralization degree is exceeded, a change from a direct trips strategy to a hybrid network is the best decision. This change guarantees that the transit network works in the most efficient way. The hybrid network is the best for higher levels of decentralization.

All structures present increasing cost with demand dispersion. These curves vary smoothly. However, the evolution of the agency and user costs (Figures 4.1b and 4.1c respectively) shows break points and changing tendencies along the decentralization process. Three factors explain these changes: (i) geometrical decision variable constraints, (ii) the vehicle capacity constraint, and (iii) which type of service operation is used. For low values of ϕ around 0.1, the stop/line spacings are restricted to short distances, as Figure 4.2a shows. Its main consequence is a sharp growth in agency cost.

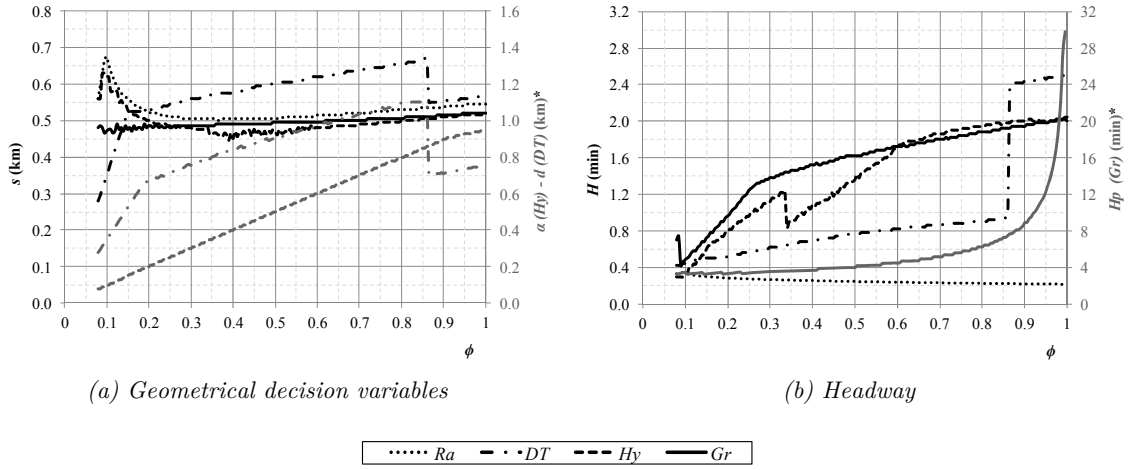

(a) Geometrical decision variables *(b) Headway*

* *Gray curves are related to the vertical axes on the right. Their line style to the network structure of the respective decision variable.*

Figure 4.2. Evolution of decision variables with respect to the demand decentralization degree parameter ϕ in a grid street pattern.

The second factor (ii) produces the jumps at $\phi = 0.09$ and 0.34 in the grid and the hybrid network respectively (Figures 4.1b and 4.1c). For lower values, the high pressure on the small attractant area forces these networks to work with articulated vehicles (higher vehicle capacity). However, when the attracted demand is spread over a larger area, the occupancy at the most loaded points decreases, and a change of vehicle size is possible. As Jara-Diaz (2003) and Jansson (1980) have shown, if the objective function includes the user cost, working with smaller vehicles is appropriate due to a better trade-off between agency and user costs. The former increases due to a larger fleet, and the latter reduces because of lower headways (Figure 4.2b). In both networks, from these decentralization degrees, they work at capacity, reducing progressively the agency costs until the vehicle occupancy is no longer a constraint: $\phi = 0.27$ and 0.61, respectively.

The final factor (iii) only affects the direct trip-based structure. At a decentralization degree of around 0.86, the agency and user cost curves change sharply. From this stage, this structure starts to work by schedules in most of its stops. Therefore, almost all trips then work by schedules.

Figure 4.2 shows the evolution of the decision variables for all network structures. Their curves are also conditioned by the previous factors; hence, some abrupt changes are manifested. Figure 4.3 includes two metrics of the network performance from the user point of view: average number of transfers per trip, and average in-vehicle travel time per trip. This information allows us to understand the main weaknesses and advantages of each network. The most important weakness of the radial structure is the length of its trips, as these pivot around the city center.

This fact increases in a constant way, and is clearly greater than the other structures. Moreover, the number of transfers increases rapidly at the initial steps of the demand decentralization, until it reaches similar values to transfer-based networks.

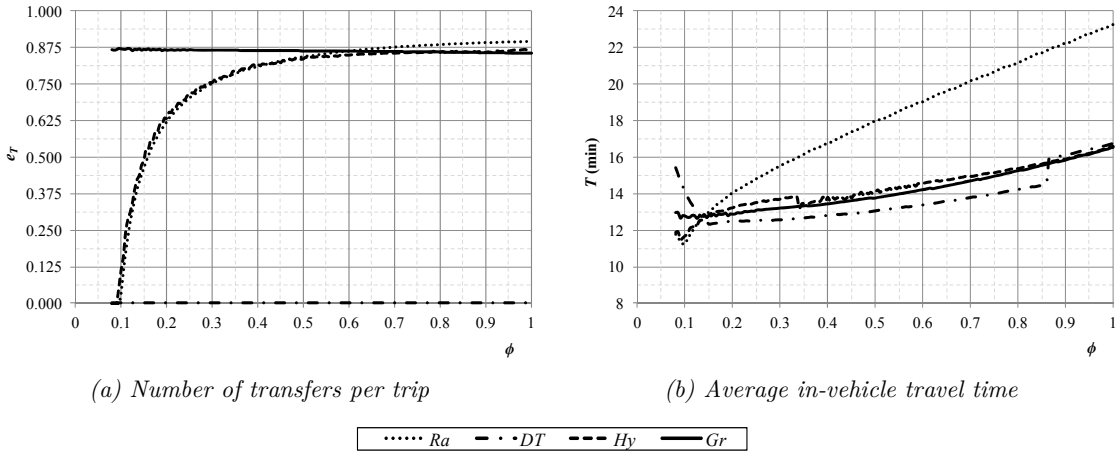

(a) Number of transfers per trip *(b) Average in-vehicle travel time*

Figure 4.3. Evolution of the number of transfers per trip and the average in-vehicle travel time with respect to the demand decentralization degree parameter ϕ in a grid street pattern.

The main inconvenience of a direct trip-based network is that, to avoid transfers, the network configuration tends to longer stop and corridor spacings and higher headways, as Figure 4.2 shows. Therefore, users progressively lose spatial and temporal coverage to guarantee direct connections. Otherwise, a larger volume of resources would be needed to serve the attractant areas directly with the whole city when the demand dispersion grows. However, there is a dispersion degree from which this tendency is no longer sustainable. As a consequence, the system starts to work with mixed services, and the network configuration changes to closer stops at the expense of service frequencies.

A transfer-based network structure has constant spatial coverage; however, the headway of service increases, since there are more corridors where the fleet is allocated. Its main weakness is that the transfer is an essential step of the transit chain. Between the hybrid and the grid structures, the former is always a better alternative. The hybrid network is focused on its central grid, which evolves with the size of the central attractant area. Figure 4.2a shows it with increasing values of α. This fact allows the number of transfers to be kept low, and better deployment of resources. The number of transfers in a grid is practically constant in any mobility pattern, and different headways for central and peripheral corridors are insufficient to compensate the double coverage for all stops, one horizontal and one vertical corridor.

Different generated demand densities between central and peripheral areas

We now let the value of f_d change from 1, as in the previous section, to 30, a scenario where the central area has a higher trip generation capacity than the rest of the city. Figure 4.4a shows that the total system cost decreases when the central area is denser. However, as Figure 4.4b shows, the area of applicability among the different structures is practically constant, since the decreasing tendency of the total cost is similar in all structures. The value of ϕ, where a change of structure is justified, varies between 3.4 – 7.1%, from $f_d = 1$ to $f_d = 30$, between the radial and the direct trip-based networks and between this second and the hybrid scheme, respectively.

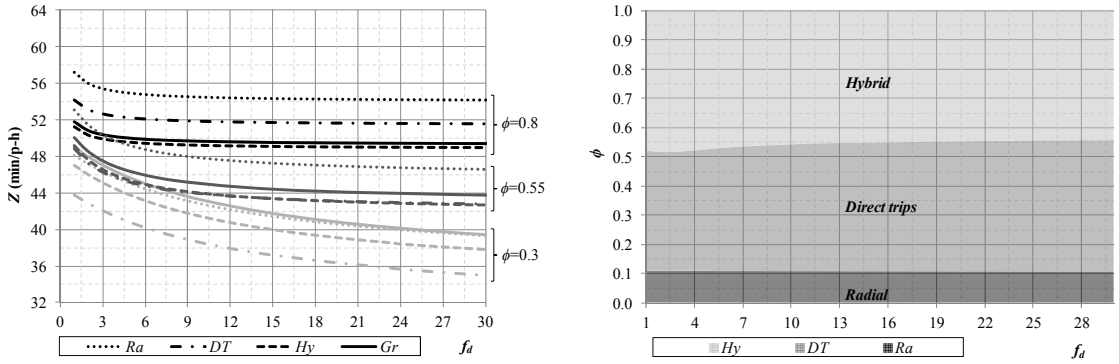

(a) Total cost *(b) Area of applicability*

Figure 4.4. Total cost and area of applicability with regard to the factor between central and peripheral generated demand densities f_d in a grid street pattern.

Therefore, regarding the demand representation, the results show that the size of the central area is the most important determinant of the applicability of each structure. That is, the area where we have to develop swath-corridors or a central grid. However, the fact that greater or fewer users come from the periphery or travel within the central area is not as relevant. The introduction of more complex demand representation, which now depends on a second parameter, does not provide important insights.

4.2.2. Variations in the demand decentralization degree of change of structure due to input parameters variations

The previous section showed that the best transit network structure is not always the same: it depends on how the demand is spread over the city, i.e., whether it is concentrated or dispersed. Therefore, there is a demand decentralization degree that justifies a change to the transit network structure. We now analyze how the cut-off point of change among the different structures varies with regard to four main characteristics: level of transit demand, city size, transfer penalty and ratio between agency and user unit costs. We use the previous base scenario of Section 4.1, where we only work with ϕ to determine the urban decentralization degree. For the case of the level of transit demand, the ratio Λ/λ is always considered equal to 2.5. On the other hand, the city size is represented by the square dimension D.

The structures analyzed here are: radial (Ra), direct trip-based (DT) or hybrid (Hy). The grid structure is removed in this part of the analysis since it is never the best solution, which was shown in the previous section. The results are presented in two different figures. Figure 4.5 shows the values of ϕ of change between different network structures. Not all the boundaries between structures are included on the figures; only those that have relevance, since they delimit structures that interchange the position of minimum cost. On the other hand, Figure 4.6 presents the area of applicability of each structure when each of the four input parameters analyzed is examined independently.

The results of Section 4.2.1 are reinforced here. The radial structure is the most suitable solution for high levels of demand concentration. When this alternative is overtaken, the solution lies in introducing new lines to conform to a direct trip-based structure. The boundary between radial and hybrid networks is not relevant unless the transfer penalty is low, as Figures 4.5b and 4.6d show. In this case, the purpose of a direct trip-based structure loses its meaning.

Subsequently, when the demand decentralization reaches higher values, transit systems have to face a reorganization of their network structures to implement a transfer-based structure.

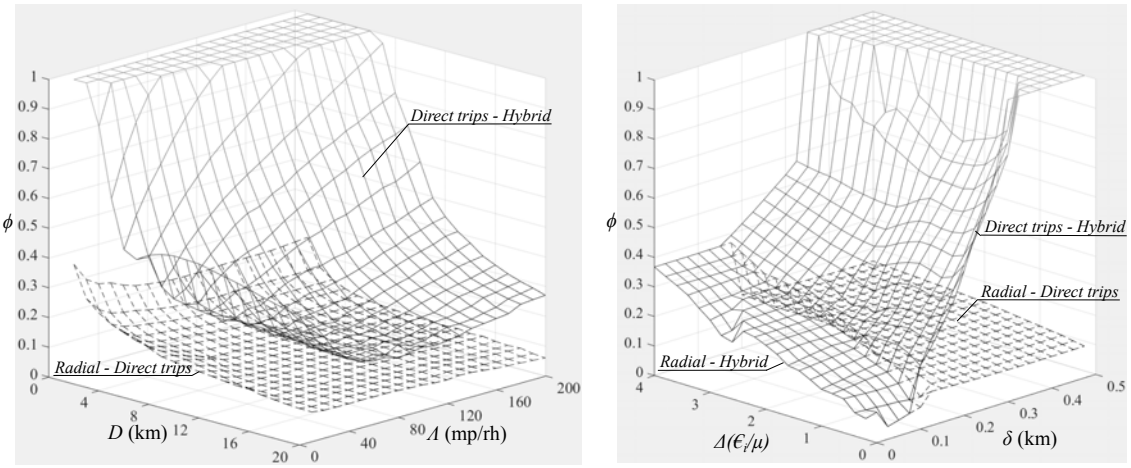

(a) Level of demand Λ and square dimension D *(b) Transfer penalty δ and unit costs $\Delta(€_i/\mu)$*

Figure 4.5. Evolution of the demand decentralization degree ϕ as a cut-off point between transit network structures with respect to the four input parameters analyzed in a grid street pattern.

Figure 4.5a shows how the areas of applicability change when the transit demand and city size vary. Regarding the level of demand, the direct trip-based structure increases its area of applicability when demand grows. First, this network has a lower ratio of C_U/C_A than the radial network. Secondly, against the hybrid structure, increasing demand justifies the development of more independent lines, maintaining a suitable spatial and temporal coverage to connect all trips directly for higher demand decentralization degrees. However, this tendency changes for low levels of demand. The direct trip-based structure gains applicability versus the hybrid network, since the former operates by schedules in these scenarios – a type of service that reduces the agency investment at the expense of the users.

On the other hand, radial and the direct trip-based structures reduce their applicability when the city is larger. The former is penalized because that factor highlights one of its weaknesses, the trip length. The latter would need a large number of lines to supply a good level of service, and as a consequence, a huge volume of resources. On the contrary, the synergies among transit lines in a transfer-based structure allow better performance to be supplied with limited increases in investment.

The higher the value of one of these parameters, the smaller the effects that the other produces when it changes. This phenomenon is more evident for the demand variations conditioned by the city size. For small cities, demand growth increases the suitability of direct trips. However, this fact happens in a moderate way when the city is larger. In this instance, the direct trip-based structure gains applicability for low levels of demand.

Figure 4.5b focuses attention on the transfer penalty, to evaluate the interchange stop design, and the ratio between unit agency costs and the value of time, i.e., $€_i/\mu$ where i is L, V or M. These ratios vary from the base scenario by multiplying them by a factor of 0.2–4. In this way, different scenarios are considered: those where the value of time prevails over the unit costs of infrastructure, kilometers traveled and fleet, and those where the value of time is undervalued versus the unit agency costs.

As observed, the former has a greater impact on the cut-off point between the direct trip-based structure and the hybrid scheme. There exists a range of transfer penalties, which approximately varies from 0.1–0.45 km, where this cut-off point varies sharply. Beyond this range, one of these structures is never the best solution: direct trips when the transfer cost is lower, or a hybrid network when the penalty is higher. Changes due to unit costs are moderate. Figure 4.6d shows that for scenarios where the user cost prevails, a greater agency investment is justified; therefore, direct connections are supplied without losing other performances of the transit system. The network completely operates in headways for higher levels of dispersion.

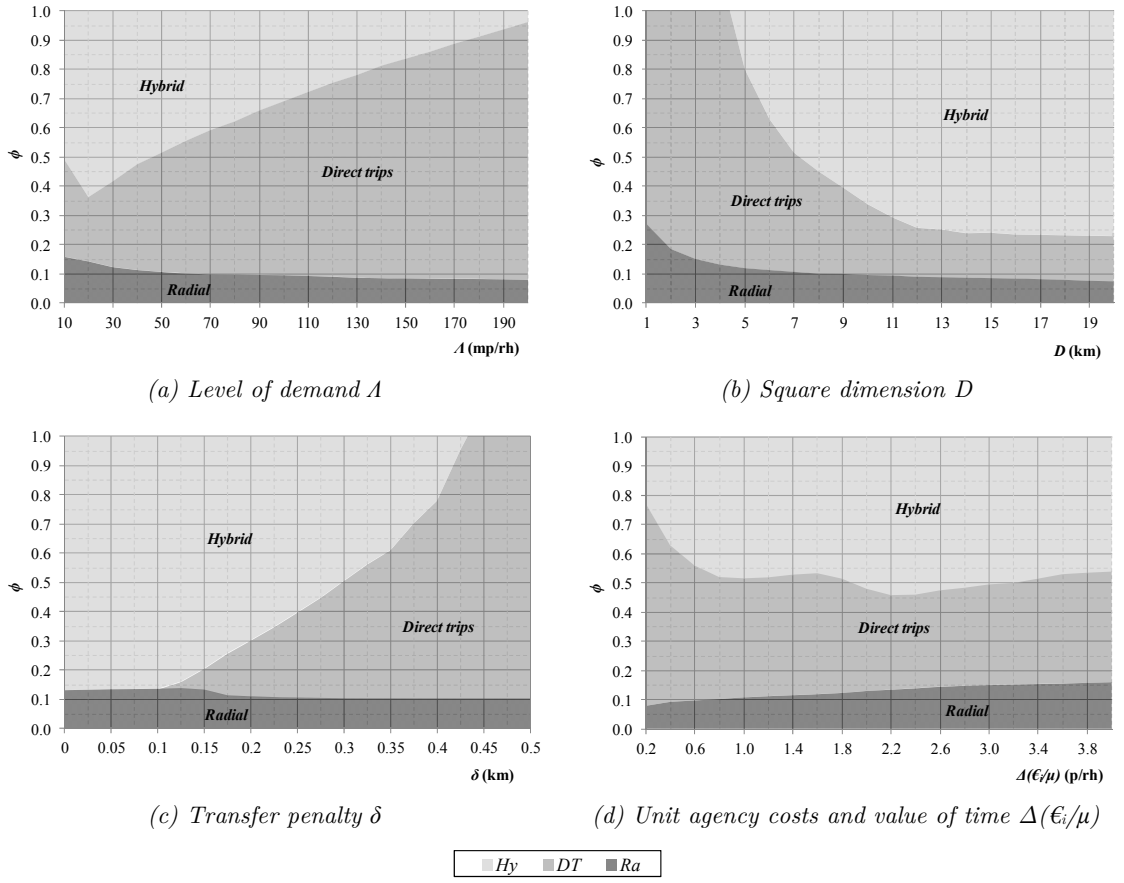

(a) Level of demand Λ

(b) Square dimension D

(c) Transfer penalty δ

(d) Unit agency costs and value of time Δ(€ᵢ/μ)

Figure 4.6. Area of applicability with regard to the four input parameters analyzed for the base scenario of Section 4.1 in a grid street pattern.

Regarding the radial structure, its applicability is practically constant. The most significant change takes place when the agency costs gain relevance against the user costs, especially when this structure competes with the hybrid scheme. The reason is the low agency investment that characterizes the radial network.

4.3. Comparison atop a ring-radial street pattern

4.3.1. Comparison in the base case study

The same analysis as in the grid street pattern is made on the ring-radial now in the same base case study. Initially, varying the parameter ϕ, while f_d is equal to 1. After, the analysis

introduces this second parameter. Appendix E also includes additional results from the analysis in this street pattern.

Constant generated demand density over the whole city

In this case, three network structures are considered: one radial (*Ra*), one direct trip-based network (*DT*) and one transfer-based structure such as the hybrid scheme (*Hy*). The behavior of these structures is similar to in the grid street pattern case. Again, the most competitive network varies in function to the demand dispersion degree of the city. Figure 4.7a shows the existence of cut-off points among the three structures with regard to the total system cost. The transition is the same as the previous case: a radial scheme for concentrated demands, direct trips in intermediate scenarios and a transfer-based structure when the decentralization is higher. The intersection between the curves of the two first structures happens when $\phi = 0.11$. The hybrid scheme is the best solution from values of $\phi \geq 0.60$.

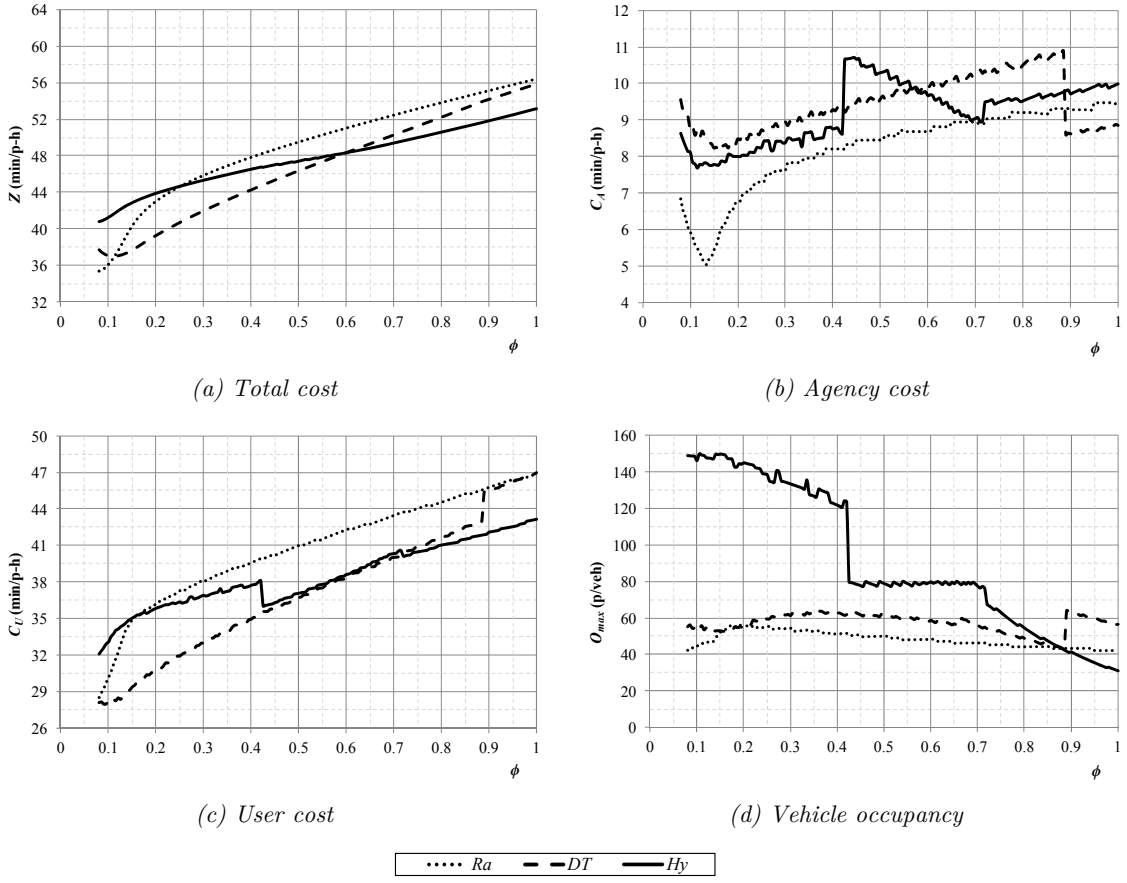

Figure 4.7. Evolution of costs and vehicle occupancy with regard to the demand decentralization degree parameter ϕ in a ring-radial street pattern.

Newly, urban dispersion increases the costs of mobility; and the same break points appears in the agency and user costs as Figures 4.7b and 4.7c show. Obviously, the same reasons produce the changes on the tendencies of those curves. For high demand concentration, constraints on the spacing variables in the three structures (Figures 4.8a). For the hybrid scheme, Figure 4.7d shows capacity problems until $\phi = 0.43$ that forces the system to work with articulated buses. From that degree of dispersion until $\phi = 0.70$, the system works with standard buses but at capacity, preventing the hybrid network from reaching a better configuration. The last break

point happens in the direct trip-based structure at $\phi = 0.89$ when the service operation changes from headways to schedules (Figure 4.8c).

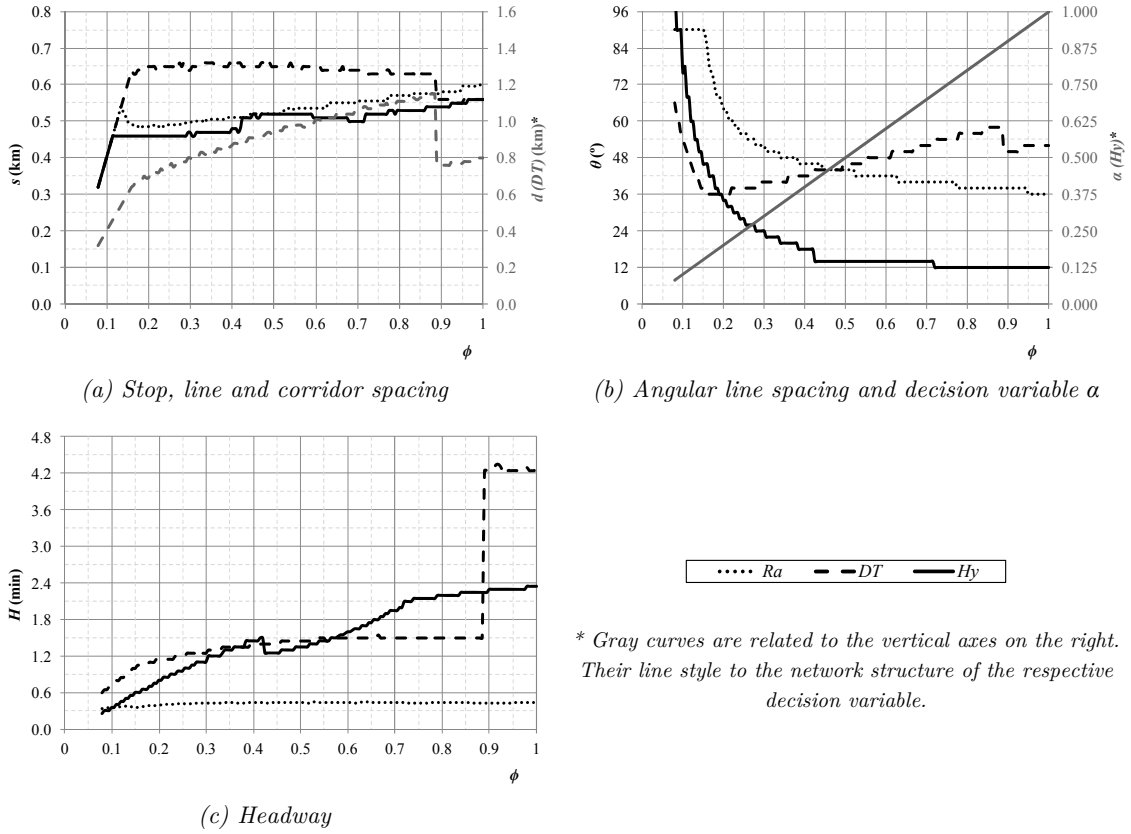

(a) Stop, line and corridor spacing

(b) Angular line spacing and decision variable α

(c) Headway

* *Gray curves are related to the vertical axes on the right. Their line style to the network structure of the respective decision variable.*

Figure 4.8. Evolution of decision variables with respect to the demand decentralization degree parameter ϕ in a ring-radial street pattern.

Each structure presents the same advantages and weaknesses as atop a grid street layout. Long trips and a high percentage of transfers in a radial network are identified (Figure 4.9). For a direct trip-based structure, the advantage of its direct connections is penalized by a loss of the other performances. Figure 4.8 shows a lower spatial coverage and worse frequencies per line until the system works by schedules.

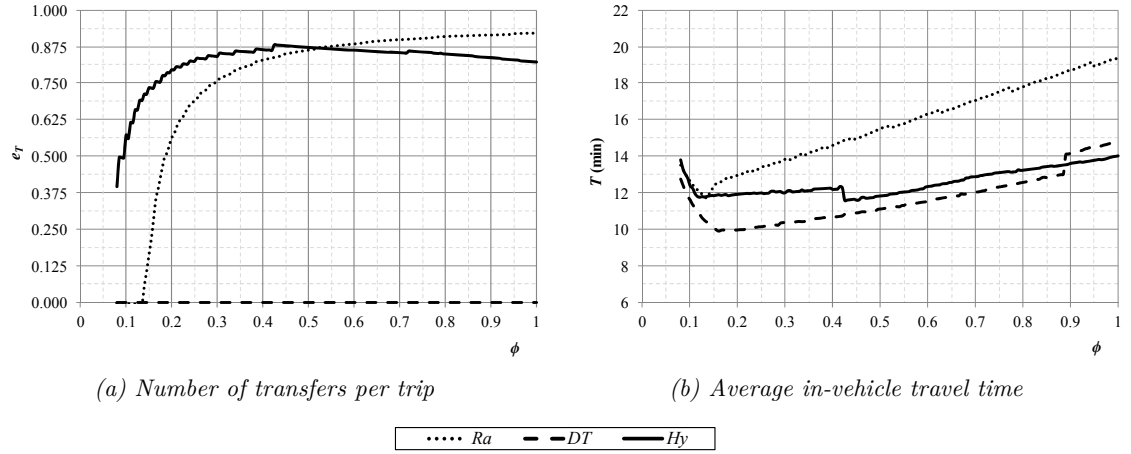

(a) Number of transfers per trip

(b) Average in-vehicle travel time

Figure 4.9. Evolution of the number of transfers per trip and the average in-vehicle travel time with respect to the demand decentralization degree parameter ϕ in a ring-radial street pattern.

Finally, a network based on transfers has a large number of transfers, however, this fact allows maintaining a more balanced distribution of the different times of each step of the user transit chain. Shorter access and waiting times compensate the additional time that a transfer implies.

Unlike Section 4.2.1, in this comparison, the total cost of the hybrid structure does not tend to the radial scheme when the demand is concentrated. Atop a grid street layout, when one horizontal corridor and one vertical compose the central mesh of the hybrid scheme, that structure is the same as a radial. However, atop a ring-radial street pattern, these two structures never coincide. A hybrid scheme has at least one circular line, but this type of line does not exist in a radial network. In addition, the same fact causes a significant number of transfers in the hybrid case although the attracted demand is quite concentrated.

Different generated demand densities between central and peripheral areas

The denser the central area is, the cheaper the transit system. This reduction in the cost is greater in the hybrid scheme especially when the central area is small, such as Figure 4.10 shows for $\phi = 0.3$. This last fact increases the area of applicability of the hybrid structure. The dispersion degree of change between that structure and the direct trip-based decreases around a 30% from the most decentralized scenario of the generated demand ($f_d = 1$) and the most centralized analyzed ($f_d = 30$). The increasing of that degree for low values of f_d is a consequence of capacity constraints. In these cases, the critical point is in radial lines at boundary of the ring-radial mesh, crossed by all the demand generated in the periphery. However, when the generated demand tends to be concentrated in the center, that critical point moves to an inner point of that mesh. In the periphery, the demand is worse distributed among lines than in the mesh due to the line branching. For this reason, in those scenarios, the maximum occupancy is higher. Therefore, the hybrid network configuration is further away from the non-constrained optimum solution. In addition, the circular lines have a higher participation on the central trips than in the peripheral, as consequence, less users take the radial lines when a higher percentage of generated demand is central. On the other hand, the other significant boundary, between radial and direct trip-based network, only grows an 11.8%.

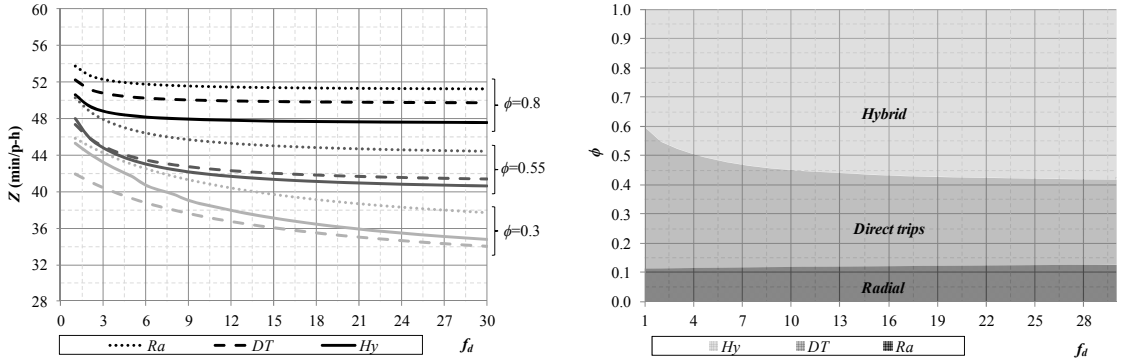

(a) Total cost *(b) Area of applicability*

Figure 4.10. Total cost and area of applicability with regard to the factor between central and peripheral generated demand densities f_d in a ring-radial street pattern.

Again, the analysis in this street pattern concludes that the parameter ϕ is more relevant than the parameter f_d. Knowing the parameter f_d of one city, it is not possible to determine what network structure is the most suitable solution. However, if the value of ϕ is known, only this parameter defines the best alternative practically in all the cases.

4.3.2. Variations in the demand decentralization degree of change of structure due to input parameters variations

Section 4.3.1 shows that the comparison among the different transit network structures on a ring-radial street pattern has similar results to the grid. That is, each structure has a range of dispersion degrees where this is the best alternative. Then, this section studies the changes on the areas of applicability for the different structures when the main input parameters of the model vary from the above base scenario. These parameters are the same as Section 4.2.2: demand where Λ/λ is always 2.5, city size symbolized by the circular dimension R, transfer penalty and unit costs. The work focuses its attention on the parameter ϕ again.

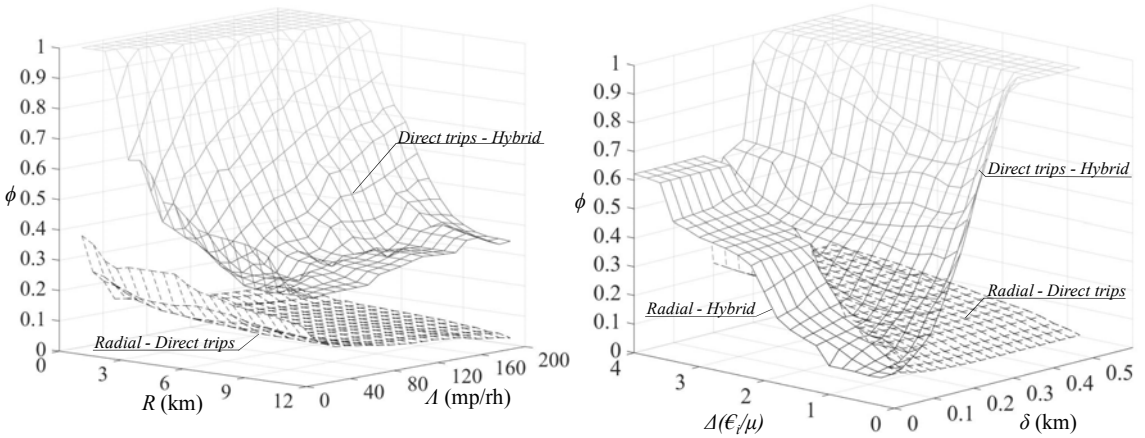

(a) Level of demand Λ and circular dimension R *(b) Transfer penalty δ and unit costs $\Delta(€_i/\mu)$*

Figure 4.11. Evolution of the demand decentralization degree ϕ as a cut-off point between transit network structures with respect to the four input parameters analyzed in a ring-radial street pattern.

To avoid a reiterative explanation, we derive the reader to Section 4.2.2. Figure 4.11 exhibits a similar evolution in the values of the cut-off points of change between each pair of network structures to this evolution in Figure 4.5. And the same happens in Figure 4.12, where each input parameter is varied in a isolated way in the base scenario.

In summary, three areas of applicability are identified: (i) a high degree of concentration where a radial network is the most reasonable solution, (ii) intermediate levels of dispersion where direct connections satisfy the mobility requirements in a agency investment, and (iii) high levels of dispersion where the most efficient alternative is a transfer-based network. The radial scheme gains applicability for small cities, high agency costs and low transfer penalties. In the case of direct services, small cities, higher levels of demand (or too low levels) and costly transfers promote the usage of this strategy. In opposite scenarios, transfer-based structure is the alternative that increases its applicability.

4.4. Comparison between grid and ring-radial street patterns

The evolution of the best transit network structure with regard to urban mobility dispersion follows the same behavior independently of the street pattern where the network is designed. The area of applicability of each structure varies in a similar way versus changes on the main input parameters of the analytical model. However, the degree of dispersion from which a

change between two structures is justified does not need to be coincident in each street pattern. This fact specially happens in the boundary between the areas of applicability of direct trip-based systems and hybrid networks.

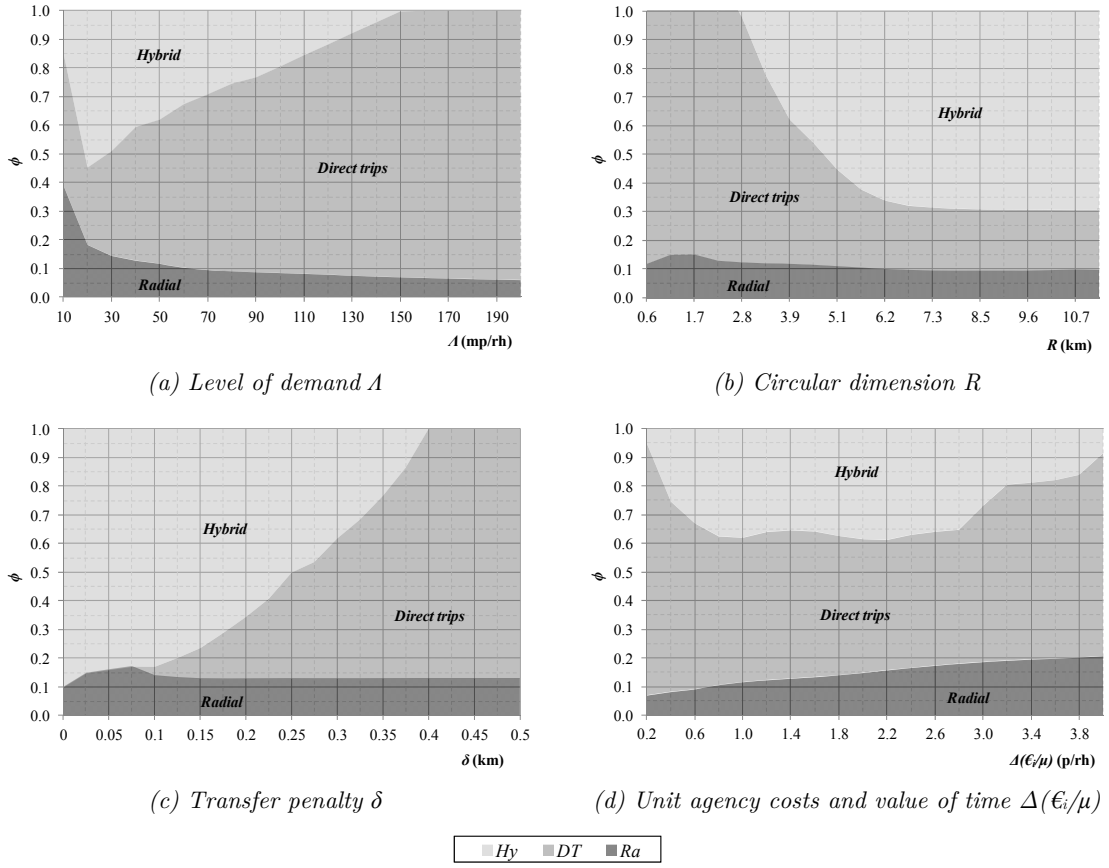

(a) Level of demand Λ *(b) Circular dimension R*

(c) Transfer penalty δ *(d) Unit agency costs and value of time Δ(€ᵢ/μ)*

Figure 4.12. Area of applicability with regard to the four input parameters analyzed for the base scenario of Section 4.1 in a ring-radial street pattern.

Figure 4.13 compares the value of ϕ of change between direct trip and transfer-based structures for each street layout analyzed. This is made in different scenarios of demand, city size, transfer penalty and ratio between unit agency costs and value of time. In Figure 4.13a, the generated demand is uniformly distributed along the city, i.e., $f_d = 1$. On the other hand, Figure 4.13b assumes a higher generated demand density in the central area than in the periphery. In that case, $f_d = 30$, in other words, the central density is 30 times higher than the peripheral.

It is easy to see that most of points are above the bisecting line in Figure 4.13a, and below that line in Figure 4.13b. This is a consequence of the worse allocation of resources in ring-radial hybrid networks for more decentralized generated demand. As Section 4.3 already comments, the peripheral demand in those networks is only supported by radial lines while the circular lines carry a small number of passengers from the central area. For that reason, the more centralized the generated demand is, the better the distribution of users among radial and circular lines. On the other hand, atop a grid street pattern, horizontal and vertical lines always present a good balance of the resources invested among them.

Figure 4.14 makes the same comparison but between radial scheme and direct trip-based network. In this case, we find points above and below the bisecting line in the same proportion,

and this does not change significantly among different scenarios of generated demand centralization.

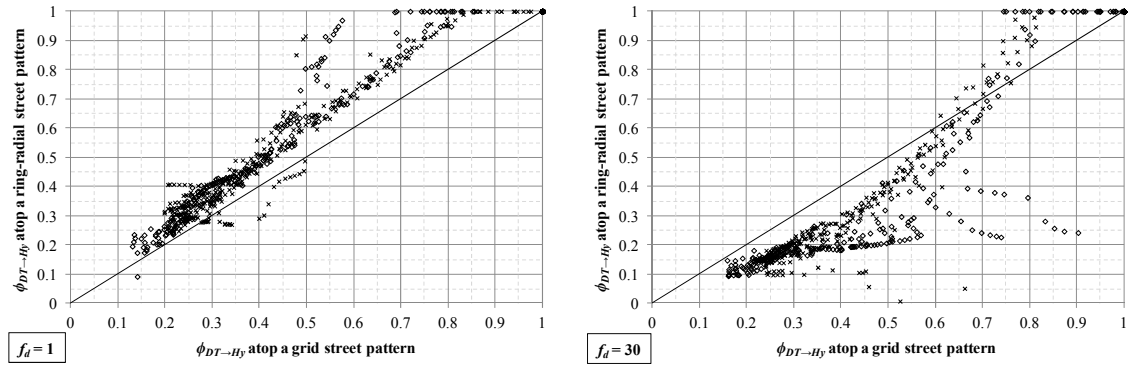

(a) $f_d = 1$ (b) $f_d = 30$

Figure 4.13. Comparison between grid and ring-radial street patterns of their points of change ϕ between direct trip and transfer-based networks.

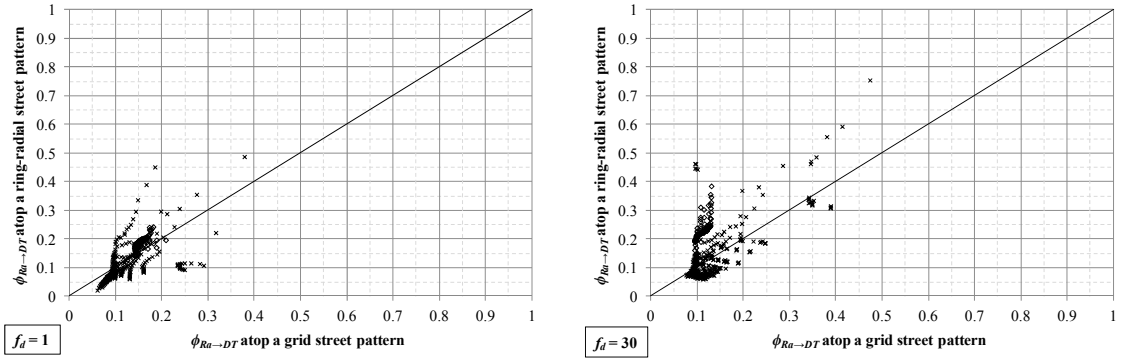

(a) $f_d = 1$ (b) $f_d = 30$

Figure 4.14. Comparison between grid and ring-radial street patterns of their points of change ϕ between radial and direct trip-based networks.

4.5. Conclusions

The analysis developed throughout this chapter confirms that the best transit network structure is not always the same: it depends on the mobility pattern of the city. We have identified the relationship between the demand requirements and the applicability of different transit network structures atop two different street patterns. In both cases, a comparison among three base network structures identifies three different scenarios of demand decentralization. Each is related to one of these structures: (i) high demand concentration in the central district, where a radial system is the most suitable solution; (ii) an intermediate scenario when the demand starts to scatter around that central district, where the best alternative is the development of new lines to connect directly the new attractant areas; and finally (iii) a dispersed demand pattern, where the hybrid scheme as a transfer-based structure is the most efficient alternative.

The reasons that justify these changes of network structure are the strengths and weaknesses that characterize each of the previous three structures. The radial network is cheap from the agency point of view, but the number of transfers and the trip length increase sharply with the

demand decentralization. A service based on direct connections removes the transfers completely and limits further increases of trip length. However, keeping those direct trips in a decentralization process implies great investment, at the same time as negatively affecting the spatial and temporal coverage. In dispersed scenarios, the hybrid network allows better utilization of the resources by means of transfers. Although, at the same time, transfers are its main disadvantage.

On the other hand, the size of the central area is the most important factor that determines the applicability of each structure. There exists a size of this area above which the development of the direct trip-based network is not the most efficient measure. However, a change of structure to a hybrid scheme is the best decision. Therefore, parameter ϕ is more relevant than f_d in representing the demand decentralization degree.

The other aspect from our results is that the point of change among the different transit network structures is not constant, and all three aforementioned phases do not always exist. This depends on the characteristics of the city, the transit system and the demand. The most important variations are produced by the city size and the transfer penalty. Large cities and well-designed transfers need a transfer-based network implementation for lower degrees of dispersion. However, in some scenarios, the level of demand also plays a significant role. High levels of demand justify greater investment in direct services for higher scenarios of decentralization; on the contrary, the transit system works by schedules when the number of users is low.

Chapter 5

Application of analytical results in real cities*

The previous chapter gives general insights about the discussion of what transit network structure is the most suitable solution to satisfy particular urban mobility requirements. Based on the city's characteristics, the analytical model gives the area of applicability of the three basic network structures compared. However, new questions are open: in what scenario are the real cities? That is, how should be the transit network faced given the current situation of urban areas? Is there a predominant solution given the prevailing city characteristics?

The goal of this chapter is transferring the previous analytical results to real cities. That is, determining by means of the analytical model what network structure is the best solution for a particular case study. Here, we present a simple methodology to translate the analytical results. Obviously, the next results are an approximation and not a specific network design for each city studied. A more exhaustive analysis for a real bus network will be made in the next chapter. The results of this chapter are a first approximation of the actual situation of cities.

The next section presents the methodological framework followed along the chapter to extrapolate the theoretical results to the real word. Then, Section 5.2 analyses three cities from the mobility point of view. After that, the current situation of those cities is compared with the

* The contents of Chapter 5 are introduced in Badia (2016).

analytical results in Section 5.3. The most important conclusions are summarized in the final section.

5.1. Methodological framework

A methodological framework to measure the urban dispersion degree is presented in order to be compared with the analytical results. The base information used in this analysis is an O-D matrix from a city. This matrix gives information about the capacity of trip generation and attraction for the different zones of transport in which the city is divided into. Two levels compose the analysis. First, we check that the city presents a similar characteristics as the approach assumed in the analytical model of Chapter 3: (i) a monocentric city at least with regard to the attracted demand, and (ii) the city works as a whole, people travels from any part of the city to any other. Therefore, the first step is to know the urban structure and the displacement pattern. Secondly, we estimate the level of dispersion in a comparable way to the corresponding parameters of the analytical model.

As Tsai (2005), spatial autocorrelation coefficients define the urban spatial structure: monocentric or polycentric. Here, we use global and local Moran's I (Anselin, 1993 and 1995). The global indicator gives information about the continuity or discontinuity of one variable over a territory. In this case, we analyze whether zones with similar levels of density of trips are surrounded by zones with similar densities; or, conversely, there are zones with dissimilar trip densities intermingled. Moran's I coefficient varies from -1 to +1. If this value tends to +1, the city presents a high spatial autocorrelation. The local indicators and the cluster maps associated show the clusters of high or low demand and possible outliers in the city. This analysis determines whether a city is monocentric (one cluster of high demand) or polycentric (more than one cluster of high demand).

Figure 5.1. Moran's I coefficient with regard to the urban spatial structure and mobility pattern.

An additional analysis seeks to know if the city works as a whole or by independent districts. Figure 5.2 shows a simple representation of these two behaviors. With this aim, it is checked if the global center of gravity (CoG) of the trips coincides with the local ones for each zone of the city. For the generated demand, we compare the center of gravity of the total trips generated against the centers of gravity of the origins of all the trips attracted by each zone of the city. On the other hand, for the attracted demand, the comparison is made between the center of gravity of the total attracted trips versus the centers of gravity of the destinations of all the trips generated by each zone. If global and partial centers of gravity coincide, it is assumed that the city works as a whole. Otherwise, we distinguish independent districts where most of generated trips have their destination in the same district.

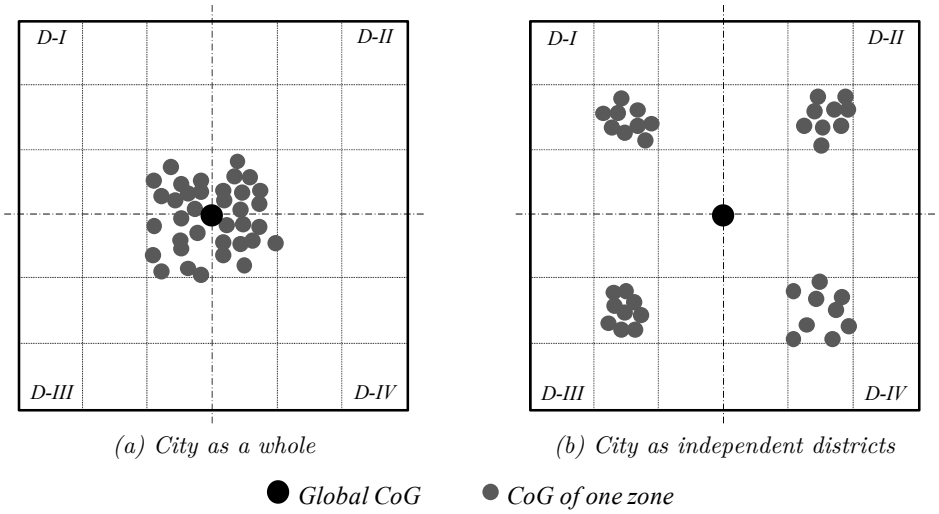

Figure 5.2. Representation of the mobility pattern for a whole city and independent districts.

In a second step, the task is to determine the dispersion degree of mobility. Different methodologies have been used to analyze and quantify the urban dispersion phenomenon. These are summarized in Section 2.2. Among all of them, in order to make an easy comparison between the dispersion degree of real cities and the simple representation of that dispersion in the analytical model, the best alternative is to work with indexes that can be directly compared to the parameters ϕ and f_d.

Different dimensions of the urban dispersion are quantified by means of indexes (Galster et al., 2001). However, some of them are not considered in this thesis, for example, mixed uses or proximity. Others such as continuity, nuclearity or clustering are fixed in the model; we assume a continuous occupancy of the territory with a mononuclear pattern. Here, the dimensions analyzed are a partial combination of those used in Tsai (2005) and Lee (2007). Size and density are defined in the analytical model by the input parameters of space dimension D or R and the level of transit demand (that is the population that concerns to this study). The other two dimensions that the dissertation takes into account are concentration and centralization by means of ϕ and f_d. We choose a Gini coefficient GC, which is defined in Equation (5.1), to determine the concentration. To quantify the centralization, among the different alternatives, we use the area based centralization index ACI (Massey and Denton, 1988) since the city is worked by a zonification. This last index is calculated by Equation (5.2).

$$GC = \sum_{i=1}^{n} D_i A_{i-1} - \sum_{i=1}^{n} D_{i-1} A_i \tag{5.1}$$

$$ACI = \sum_{i=1}^{n} D_{i-1} A_i - \sum_{i=1}^{n} D_i A_{i-1} \tag{5.2}$$

In the previous Equations (5.1) and (5.2), D_i is the cumulative portion of demand in zone i, and A_i the cumulative proportion of associated land area. The Gini coefficient varies from 0 (minimum concentration) to 1 (maximum concentration). The area based centralization index adopts the same range of values, representing the maximum decentralization the value 0 and the maximum centralization the value 1.

Figure 1.1 in Chapter 1 represents urban form evolution due to deconcentration or decentralization processes. Depending on how the city evolves, these dimensions can vary in different amounts or directions. However, in the model's representation of the demand pattern

(monocentric city with a variable extension of its central area), both two dimensions are related. On the one hand, when the central attractant area spreads, the city loses concentration at the same time it is decentralized. Therefore, the Gini coefficient and the area based centralization index are lower when ϕ grows. On the other hand, with regard to the generated demand, the higher f_d is, the more concentrated and centralized that demand. As a consequence, both indexes increase with the value of f_d.

To explain how these indexes are connected with the parameters that represent the demand in the analytical model, the thesis proposes the Lorenz curve (Lorenz, 1905) associated with the Gini coefficient and a similar one associated with the *ACI*. The demand information is distinguished between the generated and the attracted trips in each zone, and these have a different Lorenz curve as Figure 5.3 shows. The model's assumes that the attracted demand presents a higher degree of concentration/centralization than the generated. The former is completely located in a central attractant area. The latter, although can have a higher density in that area, is distributed over all the city. Therefore, the size of the central attractant area, the value of ϕ, is given by the real attractant demand distribution. Once the value of ϕ is known, the real generated demand distribution determines the parameter f_d.

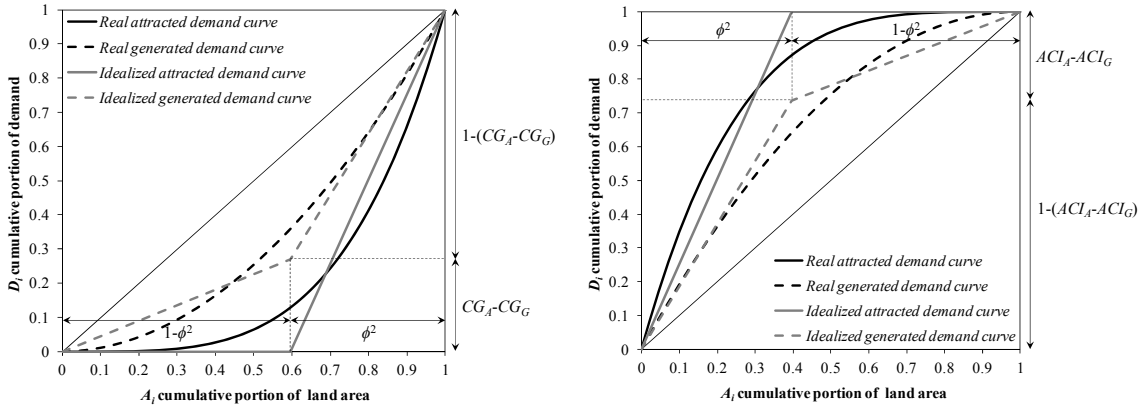

(a) Lorenz curves associated to GC *(b) Curves associated to ACI*

Figure 5.3. Relationship between the associated curves of concentration and centralization indexes with regard to the demand representation of the analytical model.

To obtain the Lorenz curve of the idealized attracted demand, we assume that its Gini coefficient is the same as that coefficient for the real attracted demand curve GC_A. Figure 5.3 shows that the Lorenz curve of the idealized attracted demand has two regions. A flat one of value 0 until a portion of land area 1-ϕ^2, and a second section whose value ranges from 0 to 1, where all the demand is uniformly attracted in a potion of area ϕ^2. Knowing that, the value of ϕ is calculated by Equation (5.3).

$$\phi_{GC} = \sqrt{1 - GC_A} \tag{5.3}$$

The idealized Lorenz curve for the generated demand has the same GC_G as the real curve of generation. Figure 5.3 displays it. This curve also has two sections, one in the first potion of land area 1-ϕ^2. It is easily derived considering that it must generate a portion of demand GC_A-GC_G. The second section generates the remainder portion of demand in a portion of land area ϕ^2. Finally, the value of the parameter f_d is obtained by Equation (5.4).

$$f_{d,GC} = (1 - GC_A + GC_G)(1 - \phi^2)/(GC_A - GC_G)\phi^2 \tag{5.4}$$

The same process is followed to obtain the values of ϕ and f_d from the area based centralization index. Equations (5.5) and (5.6) calculate these parameters respectively. To estimate this index, it is necessary to fix a center from which the distance is calculated. This center is assumed the respective global center of gravity for attracted and generated demand.

$$\phi_{ACI} = \sqrt{1 - ACI_A} \tag{5.5}$$

$$f_{d,ACI} = (1 - ACI_A + ACI_G)(1 - \phi^2)/(ACI_A - ACI_G)\phi^2 \tag{5.6}$$

As the model represents the mobility pattern, if the generated demand was more concentrated/centralized than the attracted, the previous analysis and formulation would be applicable replacing the attracted demand distribution by the generated.

5.2. O-D matrix analysis

Once the methodology used for analyzing the demand behavior has been presented in Section 5.1; Section 5.2 focuses its attention in the analysis of O-D matrixes from three Spanish cities: Barcelona, Palma and Terrassa. Only a portion of each municipality is included in the analysis, those zones that are mainly composed by built-up areas, present a continuous development over the territory, and at the same time, are served by the current bus network with a certain level of service. Table 5.1 summarizes the characteristics of these cities.

Table 5.1. Demand, size and number of transport zones of the studied cities.

City	Barcelona	Palma	Terrassa
Population 2015	1,604,555	400,578	215,214
Total area (km^2)	102.15	208.63	70.20
Number of transport zones	199	71	42
Analyzed area (km^2)	77.14	43.23	29.22
Number of transport zones analyzed	196	54	37

5.2.1. Barcelona[1]

The attracted demand in Barcelona shows a high spatial autocorrelation. Its Moran's I[2] is so high, almost 0.7. Most of zones with the highest densities are located around the traditional center. As cluster map[3] in Figure 5.5a shows, that center conforms the unique cluster of high attracted demand that there is in the city. Figure 5.4a distinguishes approximately different annuli with decreasing density from that center to the periphery. In the North area, the furthest zones from that center compose a large cluster of low demand. The centers of gravity appears in the same Figure 5.4a, all of them, whether global or local, are located in the cluster of high demand. The deviation among them is 446 meters.

[1] The Barcelona's O-D matrix used is EMO'01, an obligatory mobility survey that considers all the transport modes. It was conducted in 2001 by INE and IDESCAT.

[2] The spatial weights matrix used along the study to estimate the coefficient of spatial autocorrelation is based on queen contiguity with an order of contiguity 1; that is, these weights indicate whether a zone of transport share or not a boundary with the others.

[3] These maps are carried out with *GeoDa* software, using a significance level $p = 0.05$.

On the other hand, the generated demand has a more irregular distribution. Although there is a certain degree of spatial autocorrelation, the value of Moran's I is lower than 0.4. As Figure 5.5b shows, there are more than one cluster of high demand (even some outlier), and they are not coincident with the highest for the attracted demand. However, the centers of gravity are located around to the same area with a deviation of 612 meters.

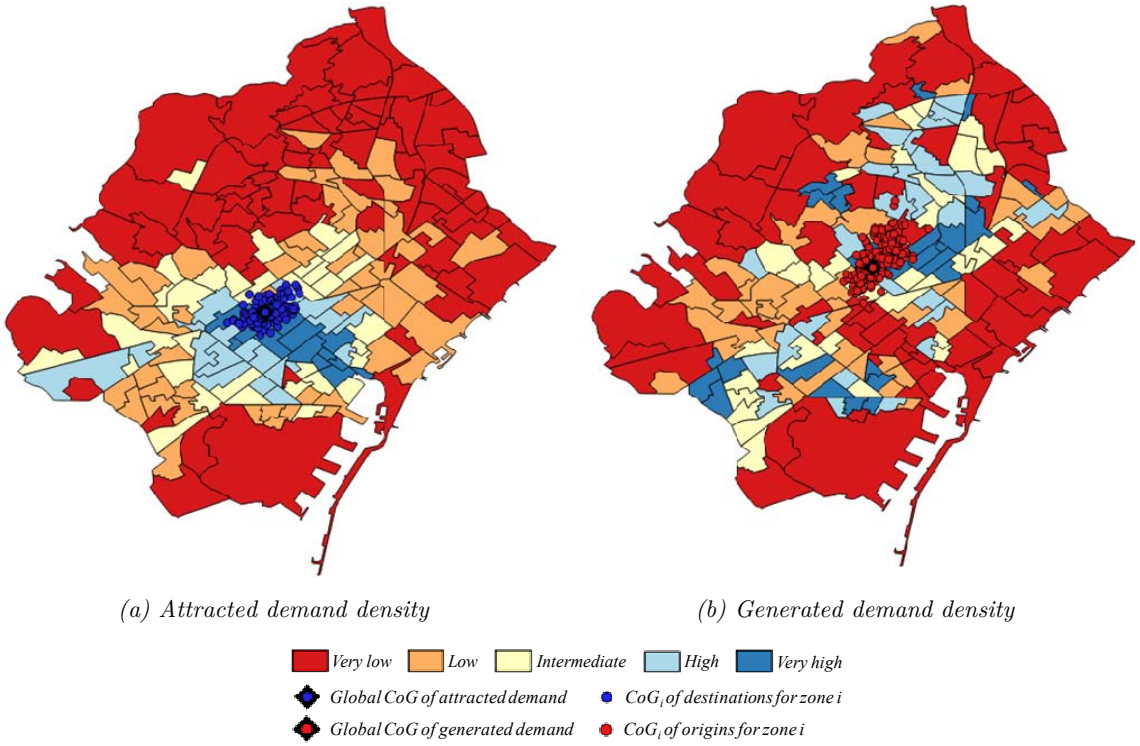

(a) Attracted demand density *(b) Generated demand density*

Figure 5.4. Demand density distribution and CoG of mobility for Barcelona.

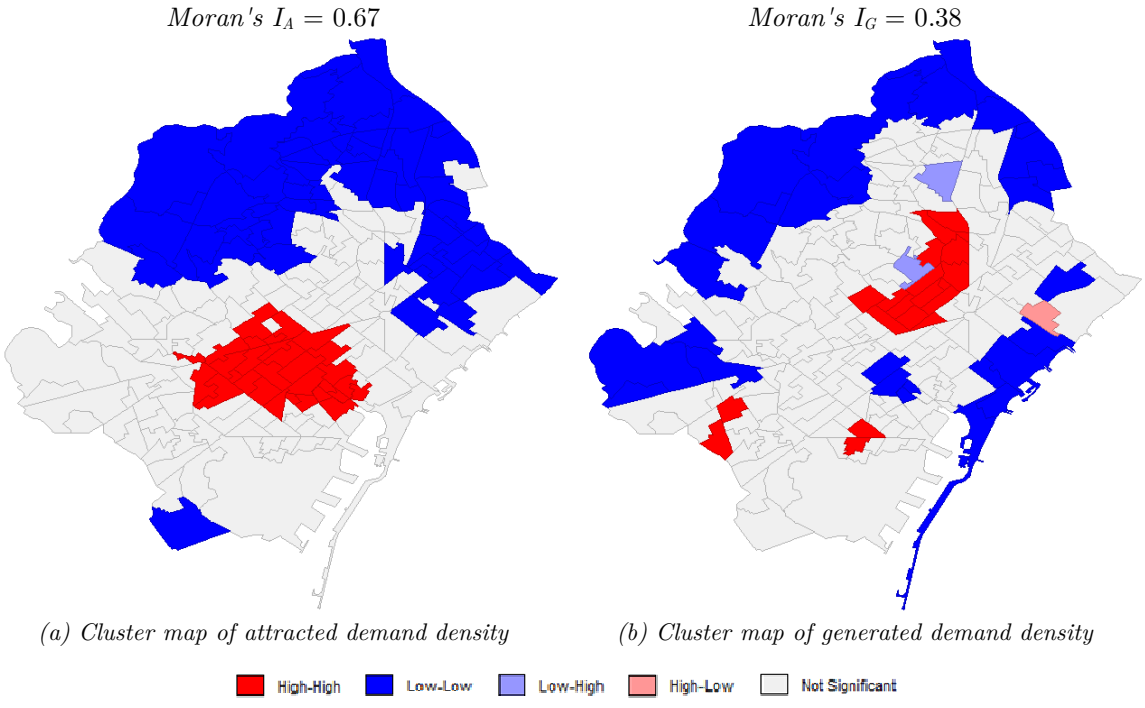

(a) Cluster map of attracted demand density *(b) Cluster map of generated demand density*

Figure 5.5. Cluster map of demand density for Barcelona.

In summary, the attracted demand has a monocentric structure with a predominant center where most of trips have their destination. However, the generated has a more irregular distribution. The origins come from distant areas of the city. The GC and the ACI reinforce all this; their values are: $GC_A = 0.55$, $GC_G = 0.50$, $ACI_A = 0.40$ and $ACI_G = 0.27$. The former shows the highest concentration of destinations, especially in the zones with the highest densities as Figure 5.6a reflects. The latter, displayed in Figure 5.6b, confirms that the zones with the highest attracted demand densities are closer to each other and to the respective CoG. For the generation, the demand grows with the distance from its CoG by a smaller rate. This fact justifies that the densest zones are more dispersed.

Finally, the value of ϕ for Barcelona varies from 0.67 to 0.77 depending on it is calculated based on the Gini coefficient or the area based centralization index. Obviously, the GC gives lower values of ϕ than the ACI. The former orders the zones of transport by demand density while the latter by distance from the CoG. Therefore, in the Lorenz curve, the densest areas are ordered one after the other, however, in the curve associated to ACI, there are zones with lower demand among those areas with high demand. For the same reason, the value of f_d is higher when it is estimated based on the concentration dimension instead of based on the centralization dimension. Its values are 23.35 and 4.49 respectively.

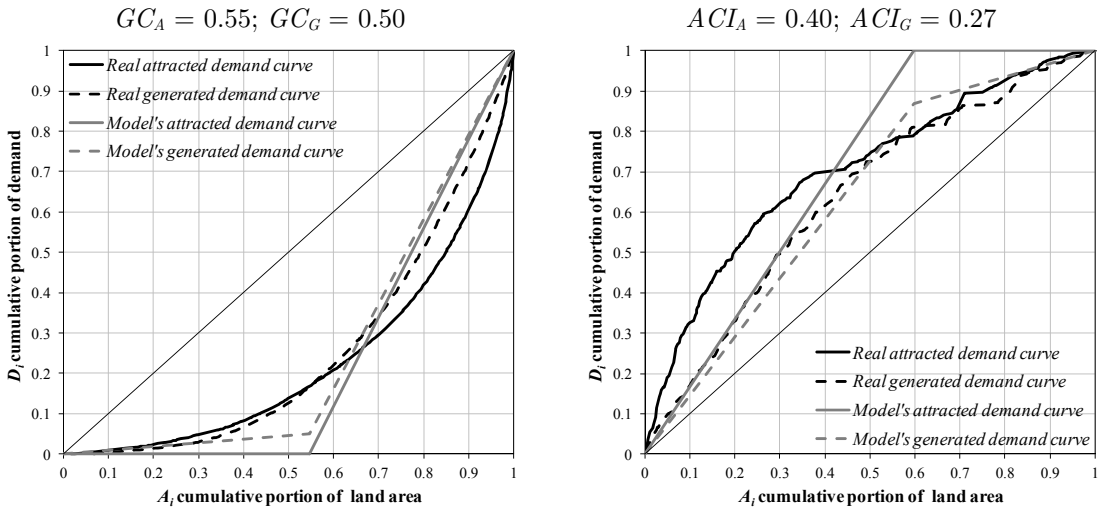

(a) Lorenz curves associated to GC *(b) Curves associated to ACI*

Figure 5.6. Associated curves of demand concentration and centralization for Barcelona.

For the dimension of trip concentration, the central attractant area spreads over the 45% of the total extension of the city, concentrating the 83% of the destinations. A similar percentage of origins is in that area. On the other hand, the dimension of centralization gives a central attractant area extended in a 52%, where around 80% of origins and destinations are located.

5.2.2. Palma[4]

Palma's O-D matrix is practically symmetric. The behavior of generated and attracted demand is very similar. Their respective Moran's I are 0.50 and 0.51, fact that confirms the

[4] The O-D matrix used from Palma is estimated in its Urban Mobility Plan of 2003.

existence of spatial autocorrelation. This city is monocentric, with only one cluster of high demand (Figure 5.8). In addition, Figure 5.7 shows that most of centers of gravity of origins and destinations are located around the global centers. Their deviations are 496 and 487 respectively.

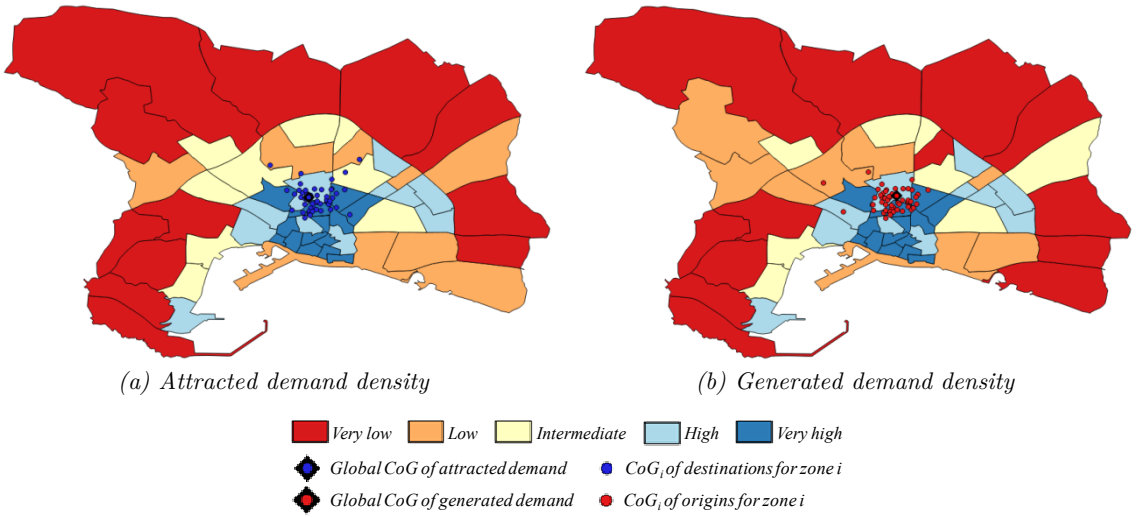

(a) Attracted demand density *(b) Generated demand density*

Figure 5.7. Demand density distribution and CoG of mobility for Palma.

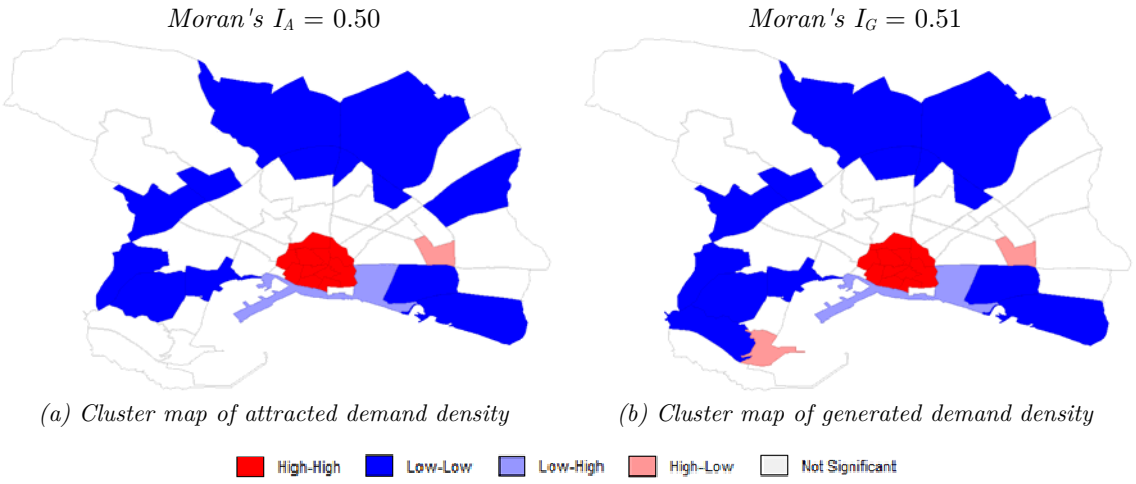

(a) Cluster map of attracted demand density *(b) Cluster map of generated demand density*

Figure 5.8. Cluster map of demand density for Palma.

The curves in Figure 5.9 exhibit the same distribution of demand either generated or attracted. The concentration degree is $GC_A = 0.53$ and $GC_G = 0.54$, and the level of centralization is $ACI_A = 0.44$ and $ACI_G = 0.43$. The 25% of the densest areas are also the closest to the global CoG. From that point on, zones with higher and lower densities are mixed in an intermediate area of the city. This fact put distance between the curves associated to each dimension.

From the previous results, ϕ is 0.68 or 0.75 for concentration or centralization respectively. Therefore, the central attractant area encompasses 46-56% of the city and around 82% of trips start or finish there. Finally, as the O-D matrix is practically symmetric, the idealized curves of generated demand density and attracted are very near to each other. This is the reason that the value of f_d is so high, 103 with regard to concentration and 477 with regard to centralization.

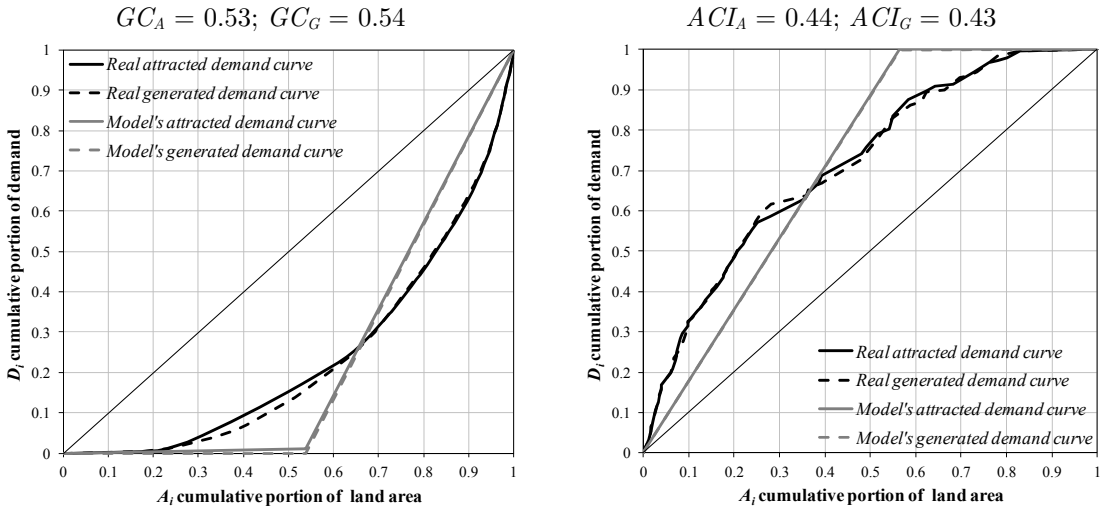

(a) Lorenz curves associated to GC *(b) Curves associated to ACI*

Figure 5.9. Associated curves of demand concentration and centralization for Palma.

5.2.3. Terrassa[5]

Although in this case the O-D matrix is not symmetric, the zones with the highest densities of origins have also the highest densities of destinations (Figure 5.10). The demand distribution presents spatial autocorrelation with a Moran's I equal to 0.54 and 0.53 for attracted and generated demand respectively. Terrassa is also a monocentric city such as the local analysis reflects in Figure 5.11. The global and local CoG are located in that center, although with deviations around 629 - 645 meters among themselves.

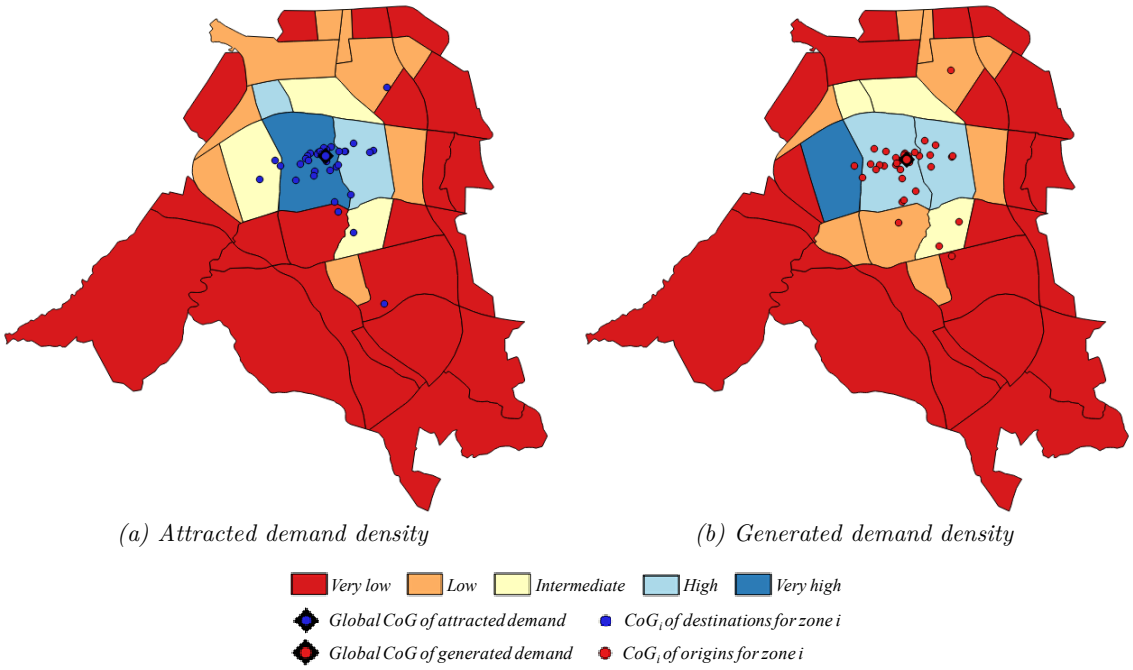

(a) Attracted demand density *(b) Generated demand density*

Figure 5.10. Demand density distribution and CoG of mobility for Terrassa.

[5] The Terrassa's O-D matrix used here only considers bus demand. The matrix is obtained from boardings and alightings in the bus network during working days of the year 2014.

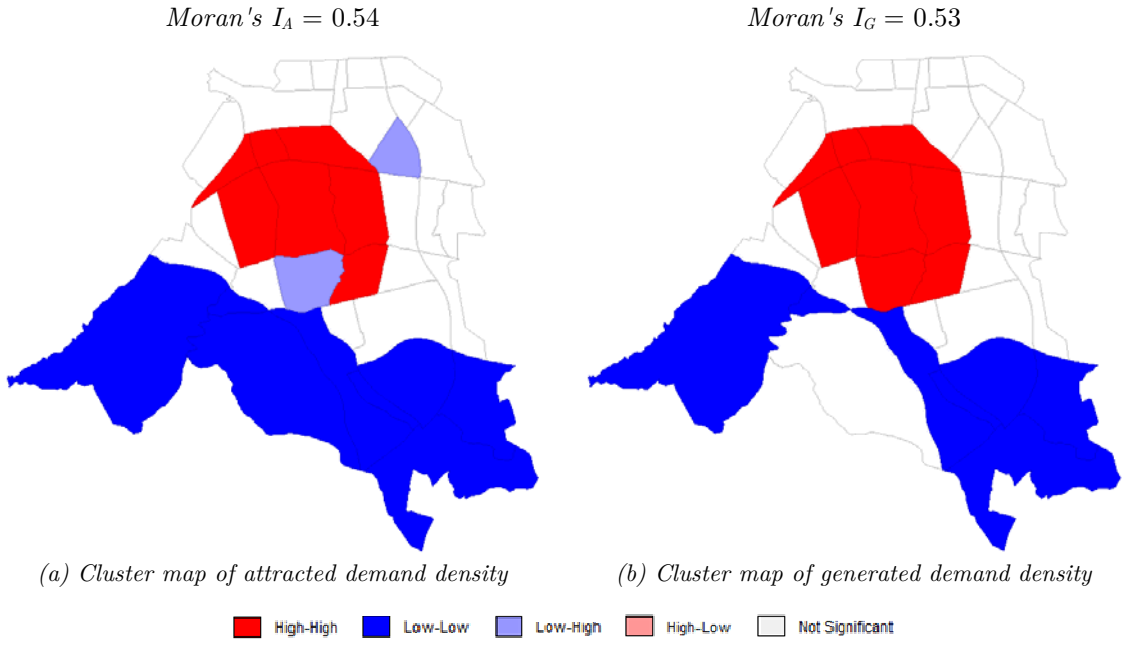

(a) Cluster map of attracted demand density *(b) Cluster map of generated demand density*

Figure 5.11. Cluster map of demand density for Terrassa.

For the generated and attracted demand distribution, the Gini coefficient is 0.67 and the ACI is 0.64. Two values closer than in the other cities. That is, the densest areas tend to be closer to the CoG. From that values, ϕ is 0.58-0.60. The central attractant area is 33-36% of the city and has 84-86% of origins and destinations. Again, as generation and attraction curves are practically coincident, the values of f_d are too high: 883 and 1,932 for concentration and centralization.

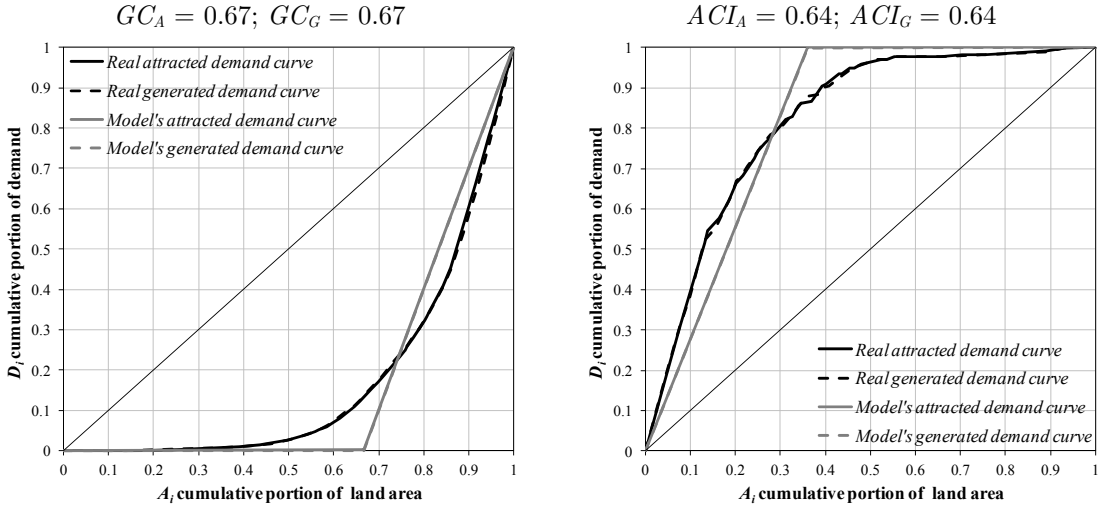

(a) Lorenz curves associated to GC *(b) Curves associated to ACI*

Figure 5.12. Associated curves of demand concentration and centralization for Terrassa.

5.3. Comparison between real data and analytical results

Now, the results from the O-D matrix analysis are compared versus the theoretical results from the model of previous chapters. First, additional information about the previous cities is

given in Table 5.2: street pattern, size, level of demand and modal split. Regarding other input parameters of the model, this section assumes the same values as the base scenario of Section 4.1. Secondly, for each city, the analytical model determines the area of applicability for the different network structures with regard to the parameters ϕ and f_d. Finally, knowing the actual mobility dispersion degrees from Section 5.2, the thesis identifies the best network structure in each case study.

Table 5.2. Demand and dimensional characteristics of the studied cities.

City	Barcelona	Palma	Terrassa
Street pattern	Grid	Ring-radial	Grid
Λ (p/rh)	45,000*[a]	13,000*[b]	3,500*[c]
λ (p/h)	20,000*[a]	8,000*[b]	2,000*[c]
Equivalent D or R (km)	8.8	3.7	5.4
Rush hour demand density (p/km^2 rh)	583	301	120
Hourly demand density (p/km^2 h)	259	185	69
Modal split of Bus (%)	14*[a]	11*[b]	5*[c]

*[a] Data from TMB (2009) and Ajuntament de Barcelona - Direcció de Serveis de Mobilitat (2012-2015); *[b] Values estimated from the annual report published by the transit agency EMT (EMT, 2015) and Urban mobility plan (Ajuntament de Palma, 2003); *[c] Values estimated from the O-D matrix used in Section 5.2.3 and reports of the mobility survey EMQ'06 (ATM, 2006).

Regarding the bus network structure that we find in these cities, Barcelona is a clear example of a direct trip-based structure, where a high number of lines supplies a wide number of direct connections among different areas of the city. In addition, this city has a wide radial metro network. The Barcelona's bus network is discussed in detail in Chapter 6. Palma is an intermediate case between a radial network and direct services. This network is a radial system in a changing process to a direct trip-based structure. Its bus network is mainly composed by radial lines complemented by other lines with tangential routes that connect different neighborhoods with relevant poles of demand (basically hospitals). Finally, Terrassa is essentially a radial network, all lines go from a peripheral area to the city center, and some of them continue to another external zone.

Figure 5.13 exhibits the area of applicability for the different network structures in function to the parameters ϕ and f_d. In addition, each graph includes the urban dispersion scenario that can be considered for each city. This current scenario is determined in the previous section by the range of values of ϕ estimated from concentration and centralization dimensions. As it is explained in Sections 4.2.1 and 4.3.1, ϕ is the parameter that determines the best network alternative. In general, f_d is not relevant. However, its range of values tested in each city are conditioned by that value of the concentration dimension in Section 5.2.

From these results, we conclude that the best structure for the three cities analyzed is the same: a hybrid network. As all of the cities have a high degree of dispersion, at first glance, cities would be predestinated to justify a change of structure. Barcelona has a high level of demand, however, due to a large are of service, the best alternative is to work with transfers. The other two networks serve smaller territories, but the level of demand are also lower. Therefore, the characteristics of these cities lead to the same conclusion, up to the point that in Palma direct connections are never a suitable solution. Even in a small city such as Terrassa, whose size is almost three times smaller than Barcelona, the area of applicability of a direct trip-based structure is little. The main reason is the low level of demand. This fact does not

justify direct connections for higher dispersion degrees, that is, to gain applicability in front of a transfer-based structure. At the same time, the radial network increases its usefulness due to shorter trips and low investment justified when the number of users is small.

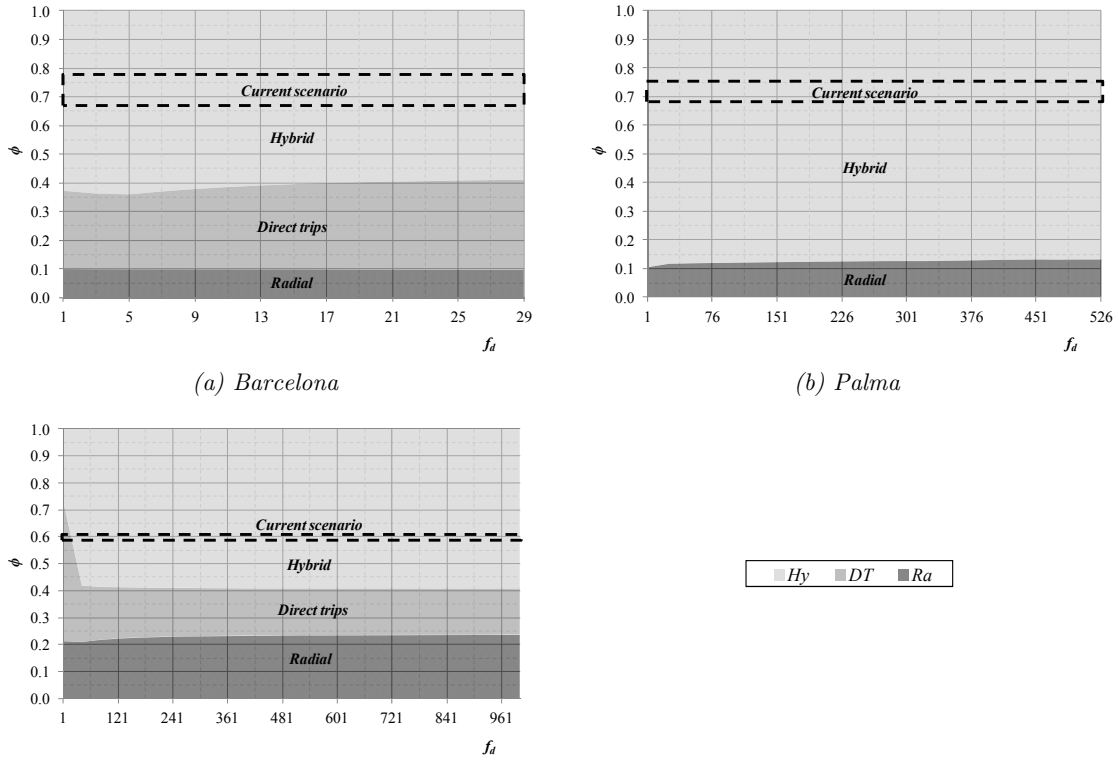

(a) Barcelona *(b) Palma*

(c) Terrassa

Figure 5.13. Area of applicability of each network structure and the current scenario of demand dispersion in the three cities analyzed.

5.4. Conclusions

This chapter presents a methodology to translate the theoretical results of the analytical model presented in Chapter 3 to real cities. The objective is that the analytical approach becomes an useful tool to understand the real situation of the current cities in order to face the transit network design problem. That is, to obtain a first approximation about how city planners have to conceive the redesign of the bus systems.

By means of this theoretical framework, three cities have been analyzed. In all these cases, the best solution is a transfer-based structure. Either by high dispersion degrees, large city areas or low levels of demand, the best alternative is always the same. However, a more extensive analysis that includes a greater number of O-D matrixes would be necessary to obtain a more general conclusion.

In any case, the study of Barcelona, Palma and Terrassa reinforces the idea that a change in the network structures from direct services or radial schemes to transfer-based strategies is a good solution in the current urban context. This fact is identified in several American cities but not too much in European urban areas, as it has been mentioned in Chapter 1.

Part III: CASE STUDY

Chapter 6

Barcelona's bus network redesign*

In this third part of the document, the thesis focuses its attention on a real case study: the Barcelona's urban bus network. The analysis made in Chapter 5 with regard to the Barcelona's mobility is a first justification that a change on the bus network structure would be the best decision to improve the efficiency of its bus system. In this chapter, the thesis analyzes this possibility in detail. A transfer-based network is compared with a network based on direct services such as the pre-existing Barcelona's bus network. The final objective is to confirm if a change on the bus network structure is a good decision for the city.

The first step of this comparison is the design of a transfer-based network for Barcelona. A two-step design method is used, where an analytical model defines an idealized geometric network layout that is a design target to develop a real detailed master plan. The analytical model for the hybrid scheme presented in Chapter 3 is used for this purpose. As this city is rectangular and not squared (its parallel dimension to the sea is double than the perpendicular), that model is adapted for a rectangular grid to obtain a more accurate design. Regarding the direct trip-based alternative, it is assumed that the pre-existing network is an optimized enough candidate of this type of structure.

Then, simulations of the networks give accurate estimations of their system costs and their levels of service in different scenarios of supply and demand. In this way, the thesis identifies the best alternative to satisfy the mobility requirements in Barcelona. Furthermore, these

* This chapter summarizes the work done during three years in CENIT (Center for Innovation in Transport) in two projects ordered by TMB (Transports Metropolitans de Barcelona) and Barcelona's Council to redesign the urban bus network. Some of these contents are presented in Estrada et al. (2011).

simulations check that the analytic model predictions are reasonably accurate and that the proposed urban bus network would work well.

Section 6.1 presents the pre-existing Barcelona's bus network. The alternative transfer-based network is designed in Section 6.2. That section includes the idealized system from which the two-step design method is then applied to Barcelona; results include the idealized target arising from the optimization, and the modified master plan that conforms to the peculiarities of the city. Section 6.3 simulates several scenarios and discusses the results. Finally, Section 6.4 summarizes the most relevant results.

6.1. Pre-existing Barcelona's bus network

Barcelona's urban bus network was a clear example of the traditional network design presented in Section 1.2 of Chapter 1, called direct trip-based network. Its network planners designed it with an important idea in mind: avoiding transfers, i.e., serving most origin-destination pairs with direct connections. For that reason, the resultant network was composed by a high number of lines, around hundred, where centripetal services predominated. Among all of them, 63 urban lines stood out; the others were 9 interurban and 26 neighborhood lines. Figure 6.1 shows the map of this network. From this map, we observe some of the weaknesses commented in Section 1.2: diffuse system, circuitous routes, and low readability where transfer stops are not clearly indicated. As a consequence, the percentage of transfer trips was only 11% (TMB, 2016).

Figure 6.1. Pre-existing Barcelona's bus network map. (Source: TMB, 2009)

This network needed 855 buses during the rush hour, however, 761 only served the 63 urban lines. Despite all this fleet, most of the lines had low frequencies, other of the disadvantages of this type of network. Figure 6.2a shows the headways for those 63 lines, and half of them had headways above 10 minutes. On average, the headway of these lines is 12.30 minutes. The reminder lines had even higher headways. Other problem of this network was the inefficient exploitation of resources due to the high number of lines. Figure 6.2b exhibits that a 20% of

lines carried a 50% of demand. The network allocated resources in lines with low demand, and as a consequence, underemployed vehicles. Finally, a short spacing around 300-350 m was an important factor that limited the bus commercial speed. In this study, the commercial speed during the rush hour is assumed to be 10.10 km/h.

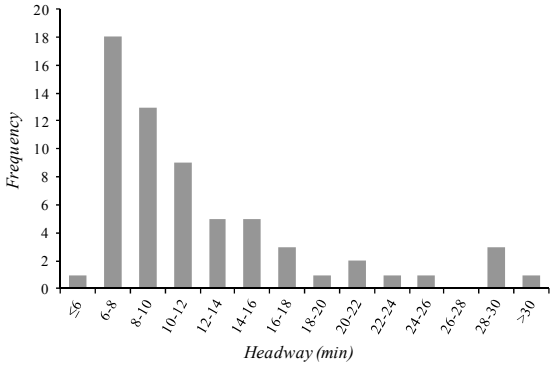

(a) Headways histogram of 63 urban lines

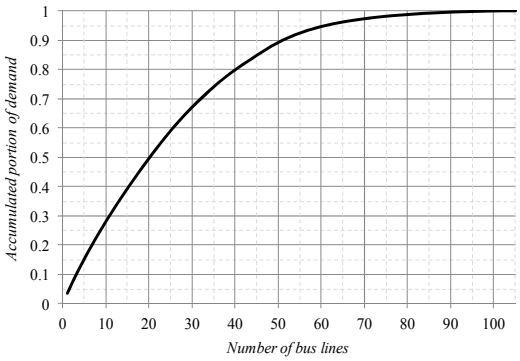

(b) Demand distribution over all bus lines

Figure 6.2. Characteristics of headway and demand distribution in the pre-existing Barcelona's bus network.

At the same time, the Barcelona's transit system is composed by different rail modes. The main one is the metro network, composed by five lines with a clear radial scheme, four of them cross the same central pole *Catalunya* square. All the headways are less than four minutes. On the other hand, three underground rail lines and six tram lines supply urban services, although they have mainly an interurban range. The former have headways around five minutes and the latter twelve minutes.

6.2. A transfer-based bus network for Barcelona

This section describes how the master plan for a transfer-based bus network in Barcelona is developed and summarizes its features: the idealized scheme in Section 6.2.1, the input data and some analysis simplifications introduced in Section 6.2.1, the optimization results in Section 6.2.2, and the master plan in Section 6.2.3.

6.2.1. The idealized system

Figure 6.3 depicts the idealized system for a rectangular hybrid network atop a grid street pattern. Now, the service region is a rectangle of sides D_H and D_V and six decision variables shape the network configuration. The additional variables distinguish the design in both directions in order to reach a better adaptation to a rectangular city. The geometrical decision variables are the line spacing between horizontal lines s_H and between vertical lines s_V, and the stop spacing s, the same in both directions. The line spacings are an integer multiple of the stop spacing; i.e., $s_H = p_H s$ and $s_V = p_V s$, where p_H and p_V are integers. In addition, parameters α_H and α_V determine the size of the central grid in horizontal and vertical direction respectively. Again, all the lines operate in the central grid with a common headway H.

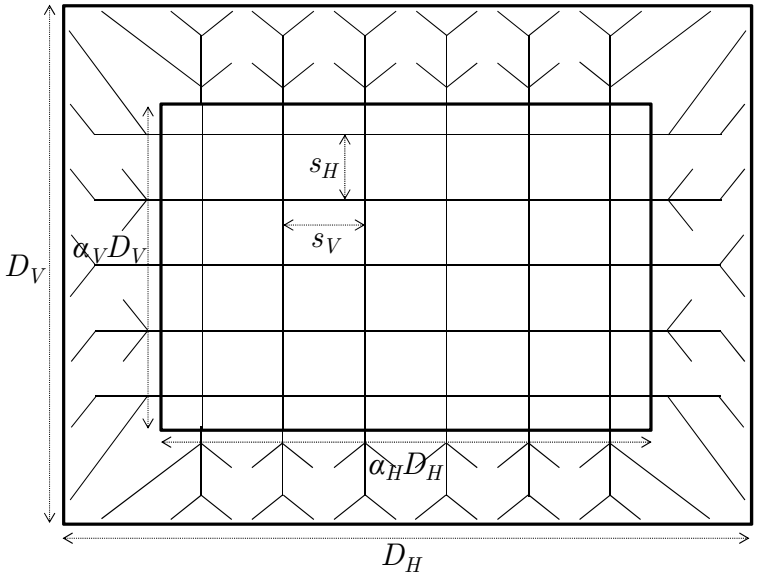

Figure 6.3. The hybrid concept in a rectangular zone.

In this case, the model allows different behavior in horizontal and vertical direction, and the existence of two types of stops: transfer and simple stops. The former are served by two perpendicular lines, and the latter only for one line. If $p_H = p_V = 1$, as in the previous Part II, every stop in the central grid is a transfer point. Otherwise, only a portion of stops is a transfer stop. Figure 6.4 shows three examples $(p_H,p_V) = \{(1,1); (1,2) ; (2,2)\}$, called complete, horizontal semi-alternate or alternate respectively.

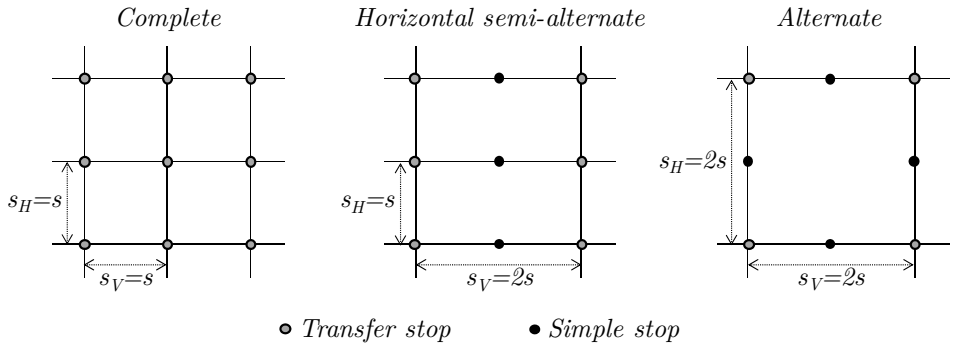

Figure 6.4. Three possible central grid lattice of lines and stops.

The same objective function (6.1) as the previous work is used here. Formulae for the different partial costs included in the objective function are presented in Appendix F. Regarding constraints, the model adds a new one: a minimum headway H_{min}. This is a constraint imposed by the transit agency in Barcelona due to operational reasons. This decision facilitates the provision of regular headways and reduces the risk of bus bunching events. Moreover, the model distinguishes the peak vehicle occupancy during rush hour in both directions O_H and O_V. Allowing different values for s_H and s_V, transportation capacity in the two directions can be better matched with the demand. If both line spacings are forced to be equal then the occupancy of the parallel lines to the long side of the rectangle would be higher than the perpendicular lines at their critical load points. As a result, vehicle capacity constraints would be only reached for the horizontal lines.

$$min\{Z = C_A + C_U = [\epsilon_L L + \epsilon_V V + \epsilon_M M]/\lambda\mu + [w_A A + w_W W + w_T T + w_t(\delta/w)e_T]\} \quad (6.1)$$

Subject to:

$$s > 0; s_H = p_H s; s_V = p_V s; p_H, p_V \text{ integer};\ H > H_{min}; s_H/D_H \leq \alpha_H; s_V/D_V \leq \alpha_V; \\ O_H \leq C; O_V \leq C;\ \alpha_H D_H/s_H + \alpha_V D_V/s_V \leq N \quad (6.1a)$$

The last constraint is related to the total number of lines in the central grid. The study is made for two different scenarios. One with a constraint in the maximum number of transit corridors N, and other where that number is not previously determined.

The solution of this problem for a specific application yields an idealized design. From this sketch, the analyst should then construct a detailed transit network that uses the available streets, hits the major demand generators and attractors to the extent possible, but still resembles to the ideal as much as possible. This second step is an art more than a science, but the process can be carried out fairly easily by hand. Next sections show both the process and the result of these two steps for Barcelona's vision of a city-wide transfer-based network.

6.2.2. Input data

Table 6.1 includes the input parameters used for the optimization step. Most of them change with respect to the base case study in Table 4.1. The values are adapted for specific data from Barcelona. Some of these deserve comment. The study focus its attention in a central core of the city with an extension of 50 km^2. Figure 6.5 shows the transport zones that belongs to that area (178 zones in dark gray) and the remainder zones of the city (20 zones in light gray that complete the whole territory of service). As the study is focused on the central city area, we consider an uniform distribution over the whole territory for generated and attracted demand. For that reason, all the study and its formulation assume a parameter ϕ equal to 1.

Table 6.1. Barcelona's characteristics.

Input parameter	Variable	Units	Value
Demand at rush hour	Λ	p/rh	45,000
Average hourly demand	λ	p/h	20,000
Horizontal city dimension	D_H	km	10
Vertical city dimension	D_V	km	5
Value of time	μ	€/h	15
Equivalent penalty distance per transfer	δ	km	0.1*[a]
Cruising speed	v	km/h	21.4 or 16*[b,* c]
Walking speed	w	km/h	4.5
Unit infrastructure cost	$€_L$	€/km-h	80*[a]
Unit distance cost	$€_V$	€/veh-km	5.2*[a]
Unit vehicle cost	$€_M$	€/veh-h	60.2*[a]
Vehicle capacity	C	p/veh	150
Dwell time	τ	s	31*[a]
Boarding (and alighting) time	τ'	s	1.5*[a]
Time perception weight of access	w_A	-	2.25
Time perception weight of waiting	w_W	-	1
Time perception weight of travelling	w_T	-	1
Time perception weight of transferring	w_t	-	2.25
Minimum headway	H_{min}	min	3*[a]

*[a] Data given by TMB (transit agency); *[b] Data given by Barcelona's municipality; *[c] Commercial speed varies from a high speed scenario with segregated bus lanes or a low speed scenario with pre-existing circulation conditions.

The maximum possible cruising speed depends on the operating conditions. If the bus runs on segregated bus lanes, this speed is assumed the average speed for cars, that is, $v = 21.4$ km/h. On the contrary, if the bus continues to work in similar conditions to the pre-existing bus service, the cruising speed is $v = 16.0$ km/h. The transit agency avoids lower headways than 3 minutes for operational reasons. The transfer penalty is a distance of 100 m, equivalent to 3 minutes, the same value used by the Barcelona's transit agency. The other technical parameters are those for the bus in Barcelona.

Figure 6.5. Rectangular approximation of the central core of Barcelona city and its transport zonification.

The pre-existing bus network was characterized by short stop spacing and direct connections. Therefore, users used to short walking distances and few transfers at the expense of low frequencies and low commercial speed. However, the analytical model gives networks with opposite characteristics. To limit the change on the network characteristics in the new design, only access and transfer times are penalized by a time perception factor, 2.25 for both. The goal is to limit the walking distance and the number of transfers in order to avoid a negative user reaction.

Related to the constraint of a maximum number of corridors, two different networks are proposed: one constrained to 11 corridors, and other not constrained. The final goal in the former is to develop a high performance bus service as an intermediate level between metro system and conventional bus. However, the city decision makers were not willing to allocate a large pavement space for the exclusive use of buses due to the consequences on private vehicle mobility. For that reason, an important political constraint was the maximum number of corridors that could be used, $N = 11$. As a consequence of that decision, an important portion of the pre-existing conventional bus would continue in service. On the other hand, an unconstrained scenario proposes a new complete grid network. In this case, the last objective is not an intermediate service between conventional bus and metro. The new bus network would replace most of the old bus lines. However, just a portion of the whole network would have segregated bus lanes. Therefore, in this case, the commercial speed remains in the background.

6.2.3. Optimization results

Regarding the optimization problem, some simplifications are assumed in order to reduce the search space. The model only considers three possible central grid's configurations, the same as Figure 6.4. A complete grid where every stop is served by two perpendiculars lines; an alternate configuration where one simple stop is introduced between each pair of transfer stops; and a horizontal semi-alternate scheme. On the one hand, the alternate puts the network closer to users and reduces the agency investment due to lower number of corridors. On the other hand, the horizontal semi-alternate allows a better allocation of resources among horizontal and vertical corridors, an important factor related to capacity considerations. In addition, the central grid is forced to be homothetic with the service region: $\alpha_H = \alpha_V = \alpha$.

Table 6.2. Results derived from the application of the analytical model in Barcelona.

Line lattice layout	Constrained scenario ($N \leq 11$)*[a]	Unconstrained scenario with high speed*[a]	Unconstrained scenario with low speed*[b]
α	0.82	0.89	0.89
H (min)	3.0	5.0	5.0
s (km)	0.69	0.48	0.49
s_H (km)	0.69	0.48	0.49
s_V (km)	1.38	0.48	0.49
A (min)*[c]	25.88 (11.50)	14.40 (6.40)	14.70 (6.53)
W (min)	2.77	4.75	4.74
T (min)	23.07	23.74	28.42
v_c (km/h)	13.01	12.56	10.49
e_T	0.83	0.90	0.89
$P_0/P_1/P_2$	0.22/0.74/0.05	0.13/0.86/0.02	0.13/0.85/0.02
Number of horizontal corridors	5	9	9
Number of vertical corridors	6	19	18
L (km)	91	187	183
M (veh-h/h)	299	379	444
V (veh-km/h)	3,886	4,756	4,659
Average user cost C_U (min)*[c]	54.19 (39.83)	45.57 (37.59)	50.53 (40.88)
Agency cost per user C_A (min)	9.08	12.48	13.12
Agency cost per hour of service (€/h)	45,456	62,457	65,585
System unit cost per user Z (min)	63.27	58.05	63.65
C_U/C_A	5.97	3.65	3.85
O_H (p/veh)	149	142	145
O_V (p/veh)	149	74	75

*[a] Cruising speed $v = 21.4$ km/h; *[b] Cruising speed $v = 16.0$ km/h; *[c] Numbers in parentheses consider an unpenalized access cost.

Table 6.2 shows how the optimized networks perform. The semi-alternate configuration provides the best alternative in the constrained scenario, where the constraint on number of corridors is binding. The same happens with the headway constraint since its value in the central grid reaches 3 minutes. That grid covers a 68% of the total region. The stop spacing is so long in comparison with the pre-existing bus network. A characteristic that produces a high access cost. In this case, the agency cost is small compared about to the total cost; the ratio is approximately 1/7. In monetary units, the agency unit operating cost per user is 2.27 €/p, and the total hourly cost, 45,456 €/h. Finally, in a semi-alternate alternative buses are predicted to

reach 149 passengers in both directions, i.e., the same use for all buses that operate at full capacity at critical points.

Regarding the unconstrained scenario, the results are presented for two different cruising speeds. In both cases, the network characteristics are very similar and the network size is larger than the constrained scenario. The optimal number of corridors is around 27-28 and the central grid covers a 80% of the territory served. Moreover, that grid is complete. As a consequence, buses of horizontal lines have an occupancy around 95% while buses in the perpendicular direction only carries half of their capacity. The existence of more corridors allows shorter spacings and higher headways, therefore, a greater distribution of total travel time among the different steps of the transit chain.

The difference between cruising speeds mainly implies a longer in-vehicle time for users and more vehicles per hour for agency. In addition, the larger network development implies a greater investment for the agency and a more compensate balance between its cost versus user cost. Now, the agency bears more than one fifth of the total cost, spending 3.12-3.28 €/p and 62,457-65,585 €/h. In high speed conditions, the sum of that cost to user cost gives a lower value than the constrained network. Obviously, this unconstrained proposal is the best solution from the results of the analytical model. However, if the cruising speed does not improve, the total cost in both scenarios is similar.

6.2.4. The master plan

After the theoretical network layout, a detailed route map for Barcelona is meticulously developed by hand. The idea is to follow the guidelines from the previous section as much as possible, using only the available streets. Drawing the individual lines is easy in the central *Eixample* district where streets follow a perfect grid, but this district represents only 30% of the total service area. In the rest of the city, particularly on its hilly areas, routes have to depart from the ideal. In some cases, the direction of traffic would have to be reversed in some streets to accommodate the system. Routes are also modified to serve near hospitals, universities, intermodal stations and other key demand points.

New networks need a fleet that has to come from the pre-existing conventional bus. The objective is to improve the transit system by means of a reorganization of the service, but not by more vehicles and a greater agency budget. Therefore, at the same time that the new lines are designed, the old bus services are reduced. The study focuses its attention on the urban lines that compete with the new networks. However, interurban or neighborhood lines are not considered.

The pre-existing bus network is modified based on three criteria: (i) elimination of pre-existing lines overlapped with new lines; (ii) elimination of those sections of pre-existing lines partially overlapped with new lines; and finally, (iii) reduction of service in those pre-existing lines that loose passengers due to implementation of new lines. Simulations of Section 6.3 help to make decisions for this last criterion. Frequencies of those pre-existing lines are diminished in recognition of the new passenger flows. An iterative process is carried out to determine final bus frequencies, with a constraint that headways cannot exceed a maximum threshold of $H_{max} = 20$ minutes. The O-D matrix in these scenarios is split among bus lines with an *all-or-nothing* method that includes the generalized cost of travel from zone to zone on the best route.

Constrained scenario: 11 corridors

Figure 6.6 shows the 11 corridors for the constrained scenario, 5 running East-West and 6 North-South. Because Barcelona's central business district is not in the center of the service region (it is much closer to the sea than to the hills) the central grid area is displaced toward the seafront. Furthermore, because the seafront is a demand generator, the peripheral lines running toward the sea are joined by a transversal line running along the coast. The average quantitative measures of the design are close to the ideal. The central grid area is about 66% of the whole, corresponding to $\alpha = 0.81$ (vs. $\alpha = 0.85$); the average East-West line spacing is 0.67 km and 1.14 km North-South (vs. 0.69 km and 1.38 km); and the average stop spacing is 0.54 km. (vs. 0.69 km). The municipality and the transit agency also request slightly shorter stop spacing in the central area than that recommended by the model.

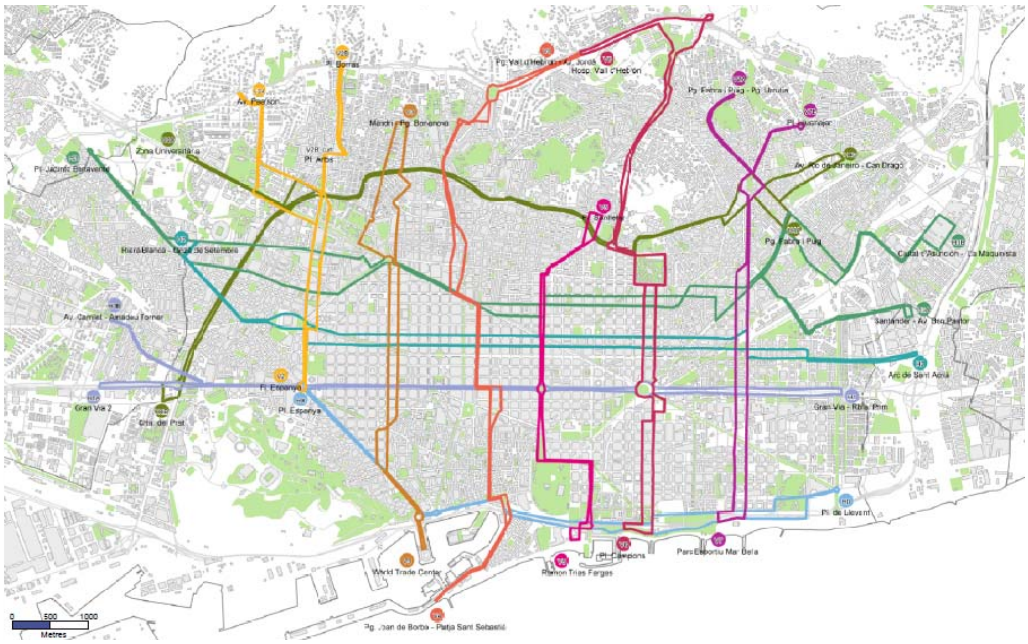

(a) Total network

(b) Horizontal corridors

(c) Vertical corridors

Figure 6.6. Proposed network of 11 corridors for Barcelona.

The agency metrics are also similar: the total network length is 220 km of one-way infrastructure (vs. 182 km); the maximum number of buses in use is 292 (vs. 299); and the number of vehicle-km in the peak hour is 3,814 (vs. 3,886). As these lines will run on segregated bus lanes with operating measures, the commercial speed would be the same as the analytical model predictions, 13 km/h. Table 6.3 summarizes the different lines that compose the network

and their length, headway and fleet. The 292 vehicles are obtained from the old bus network. With that objective in mind, 7 lines are removed, the route is cut in 8 lines, and 20 lines reduce the frequency of service (to 20 minutes in most of them). For additional information about the network of 11 corridors and the changes on the pre-existing conventional bus lines, the reader can look up CENIT (2010).

Table 6.3. 11 lines that compose the proposed constrained bus network for Barcelona.

Line	Length	Headway	Fleet	Line	Length	Headway	Fleet
H0	16.92	3	26	V2A	8.97	6	7
H1A	19.76	6	15	V2B	9.56	6	7
H1B	20.13	6	15	V3	12.63	3	19
H2	21.55	3	33	V4	19.02	3	29
H3A	25.62	6	20	V5	11.10	3	17
H3B	28.92	6	22	V6	19.83	3	31
H4A	19.65	6	15	V7A	12.68	6	10
H4B	21.95	6	17	V7B	12.02	6	9

Unconstrained scenario: 28 corridors

Figure 6.7 presents an alternative proposal of 28 corridors. This is the result of the unconstrained scenario where the cruising speed is low. Although in theory 9 would be horizontal and 18 vertical, in the resultant design, there are only 8 and 17 respectively. The remainder lines are converted into three diagonal lines. The reason is to serve three of the most emblematic streets of the city (Diagonal, Paral · lel and Meridiana Avenue). This network maintains most of the 11 corridors from the other proposal and adds 17 more.

In this case, the final design differs from the theoretical sketch more than the previous proposal. The central grid covers practically the total region, α tends to 1 (vs. $\alpha = 0.89$). On the one hand, that central area is also displaced toward the seafront. On the other hand, the complex street pattern in the hilly side of the city does not give alternatives with continuity beyond the streets chosen. Due to these facts, the line spacing is a bit longer than the theoretical design (0.49 km): 0.67 km between horizontal lines and 0.56 km between vertical lines. However, as in the previous proposal, there is a requirement that the stop spacing has to be shorter than the result of the model. In this case, as the new network substitutes most of the conventional bus, the stop spacing is only a bit longer than the old bus system around 0.38 km.

In this network, the commercial speed is considered 10.24 km/h since the new lines will operate in similar conditions to the pre-existing bus lines. In those conditions, to final speed is a bit lower than the speed estimated in the model. Table 6.4 includes the main properties of these lines. The total length is 525 km (vs. 366), the adaptation to the real street pattern out of the central *Eixample* district and the extension to near municipalities generate longer lines. As a consequence, more fleet is needed, 573 buses (vs. 444), and more kilometers are travelled, 5,748 (vs. 4,659). In this proposal, the pre-existing bus network is extensively reduced: 44 lines are removed and 11 are modified. This reduction of services allows serving the new lines without a growth in the total bus fleet. A more extended explanation of this proposal and the changes on the pre-existing bus network is compiled in CENIT (2013).

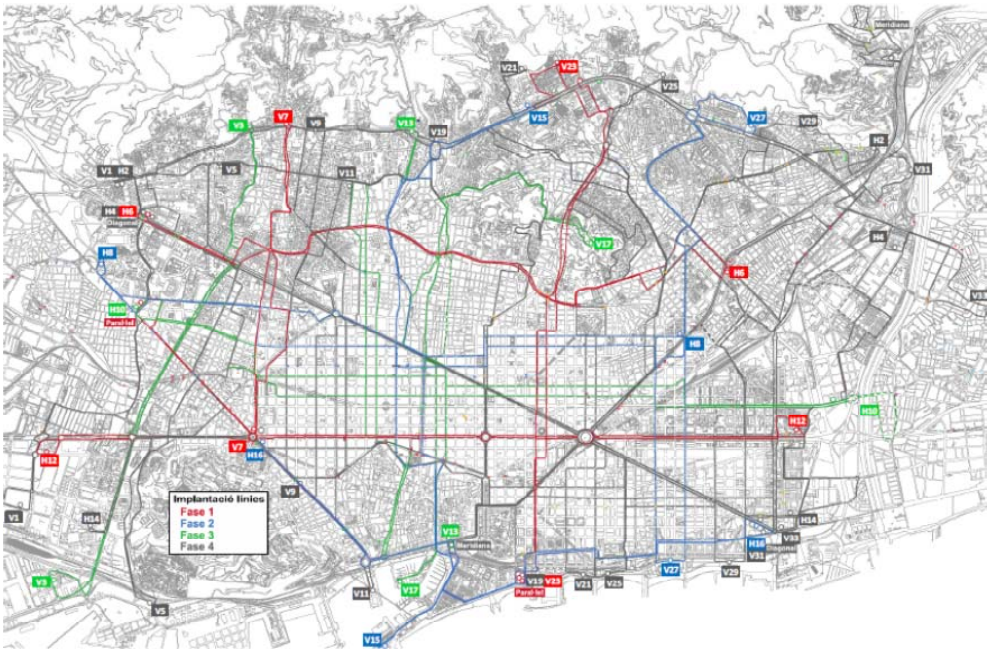

(a) Total network (Source: TMB, 2012)

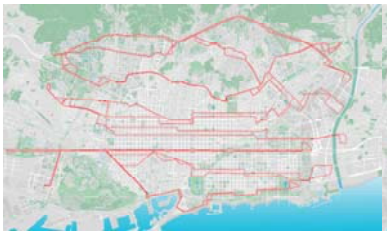

(b) Horizontal corridors

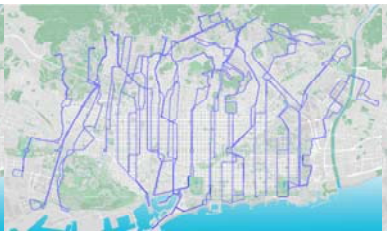

(c) Vertical corridors

(d) Diagonal corridors

(Source: Ajuntament de Barcelona and TMB, 2012)

Figure 6.7. Proposed network of 28 corridors for Barcelona.

Table 6.4. 28 lines that compose the proposed unconstrained bus network.

Line	Length	Headway*[a]	Fleet	Line	Length	Headway*[a]	Fleet
H2	26.2	8	16	V13	16.3	4	29
H4	27.0	5	34	V15	19.5	4	34
H6	19.3	5	23	V17	17.5	6	17
H8	27.9	5	37	V19	22.6	6	23
H10	21.4	3	39	V21	18.5	6	16
H12	21.6	3	47	V23	22.0	8	16
H14	25.4	5	30	V25	17.4	8	12
H16	14.7	8	11	V27	16.8	8	11
V1	13.8	8	9	V29	19.0	8	15
V3	16.0	5	21	V31	13.6	8	10
V5	15.4	8	12	V33	16.5	8	11
V7	9.7	7	10	D20	16.4	4	21
V9	11.4	8	9	D30	19.5	4	28
V11	13.1	5	16	D40	26.4	8	16

*[a] Final headways were readjusted by the transit agency

6.3. Simulation of the transit system

The following sections examine the simulated performance of the transit system, focusing on the user experience. These simulations are used to test both the model predictions and the usefulness of the proposed designs in two scenarios: only considering bus supply and demand, and another where the analysis includes all the transit system supplied and its demand. Figure 6.8 shows the different transit networks that are built for those simulations. Regarding commercial speed, the simulations consider that pre-existing bus runs at 10.10 km/h, bus network of 11 corridors at 13 km/h and bus network of 28 corridors at 10.24 km/h. The O-D matrix used in this analysis is EMIT'07, most recent mobility survey[6] including all transport modes.

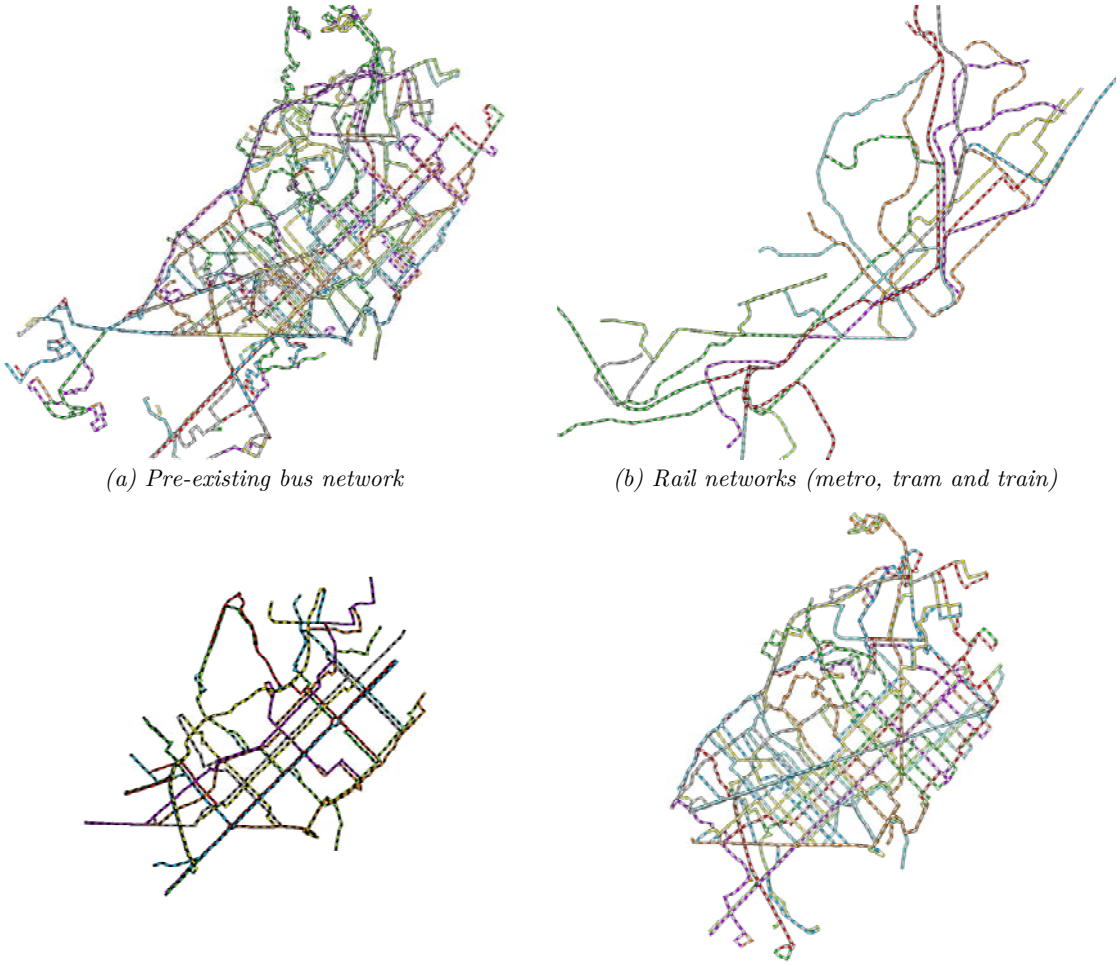

(a) Pre-existing bus network

(b) Rail networks (metro, tram and train)

(c) Bus network of 11 corridors

(d) Bus network of 28 corridors

Figure 6.8. Transit networks simulated.

6.3.1. Model verification test

The model of Section 6.2 assumes that origins and destinations are uniformly and independently distributed in the service region. Although this is somewhat unrealistic, in reality

[6] TMB, the major bus operator, conducted in 2007 a wide mobility survey (EMIT'07) to characterize the overall demand in Barcelona of all the transit modes and private vehicles.

demand tends to focus in a central area. Taking into account this fact, this section compares the predictions of the analytic model with that uniform demand (Scenarios A0 and B0 for constrained and unconstrained designs respectively) with two simulated scenarios for each proposed network. On the one hand, Scenarios A1 (for the system in Figure 6.6) and B1 (for the system in Figure 6.7) spread the total demand of the idealized model evenly among 178×178 transportation zone pairs (central core in Figure 6.5), as in the idealized model. Thus, comparisons of A0 vs. A1 and B0 vs. B1 test the validity of the supply-side approximations in the analytic model. On the other hand, Scenarios A2 for 11 corridors and B2 for 28 corridors divide the demand of the idealized model across the 178×178 zones in proportion to the O-D demand flows in Barcelona's mobility survey (EMIT'07) including all modes, which is not uniform. By including all modes, this distribution describes where people want to travel, which seems appropriate to evaluate realistically a system intended to serve all types of trips. Thus, a comparison of A0 vs. A2 and B0 vs. B2 should jointly test the effects of the demand uniformity assumption and the supply-side idealizations in the analytic model. In all of the simulations, the route assignment method used is an *all-or-nothing* for consistency with the analytic model. This method is chosen because it does not disperse trips among the different possible routes to connect one O-D pair. All passengers choose the path with the minimum generalized cost.

First, user metrics are discussed in the proposal of 11 corridors (Table 6.5). Therefore, Scenarios A0 and A1-A2 are compared. The agreement between A0 and A1 is relatively good. The model predicts particularly well most of the metrics despite the small discrepancies, all level of service measures are predicted to within 10%. Except for the walking time (and walking distance) and the number of transfers. The discrepancies are only due to the route choice of users. They prefer to walk more to reach one stop that allows them a direct trip, therefore, the number of transfers made in the network is smaller. The agreement between A0 and A2 is not as good, mainly by discrepancies around 20% in the trip length. One reason for this is that the actual trips in Barcelona are considerably shorter than assumed (5.00 km vs. 5.95 km) and concentrated at the center. As one would expect, scenario A2 then yields considerably lower and better metrics than scenario A1 (and A0), with the exception of the door-to-door travel speed. This is a consequence of a greater ratio between access and in-vehicle distances.

Table 6.5. Comparison of user metrics in different scenarios of 11 corridors.

User metric	Scenario A0: Model predictions	Scenario A1: Uniform demand simulation	Scenario A2: Non-uniform demand distribution
In-vehicle distance (km)	5.00	5.28	4.09
Walking distance (km) *[a]	0.95	1.11	0.90
Total travel distance (km)	5.95	6.38	5.00
Walking time (min)*[a,b]	12.61 (28.37)	14.4 (32.4)	12.64 (28.44)
Waiting time (min)	2.77	2.87	2.41
In-vehicle time (min)	23.07	23.96	18.69
Number of transfers	0.83	0.61	0.50
Total travel time (min)*[b]	38.45 (54.21)	41.23 (59.23)	33.74 (49.54)
Door-to-door speed (km/h)*[b]	9.29 (6.59)	9.29 (6.46)	8.89 (6.06)

*[a] This metric includes access, egress and transfer distances; *[b] Numbers in parentheses consider an access cost penalized by a factor $w_A = 2.25$.

Secondly, Table 6.6 summarizes the user metrics in the proposal of 28 corridors. In these simulations, the headway is homogeneous and its value is 5 minutes, equal to the result of the analytical model. On the one hand, the metrics between Scenarios B0 and B1 also match so well. However, the same discrepancies appear related to walking time or distance and the

number of transfers. On the other hand, the agreement between B0 and B2 is worsen again due to the greater concentration of real demand.

Table 6.6. Comparison of user metrics in different scenarios of 28 corridors.

User metric	Scenario B0: Model predictions	Scenario B1: Uniform demand simulation	Scenario B2: Non-uniform demand distribution
In-vehicle distance (km)	4.97	4.90	3.97
Walking distance (km) *[a]	0.58	0.84	0.64
Total travel distance (km)	5.55	5.74	4.61
Walking time (min)*[a,b]	7.72 (17.37)	11.21 (25.22)	8.48 (19.08)
Waiting time (min)	4.74	3.98	3.78
In-vehicle time (min)	28.42	28.69	23.24
Number of transfers	0.89	0.52	0.46
Total travel time (min)*[b]	40.88 (50.53)	43.88 (57.89)	35.50 (46.10)
Door-to-door speed (km/h)*[b]	8.15 (6.59)	7.85 (5.96)	7.79 (6.00)

*[a] This metric includes access, egress and transfer distances; *[b] Numbers in parentheses consider an access cost penalized by a factor $w_A = 2.25$.

6.3.2. Expected system performance

In addition to the above scenarios used for model verification, some benchmark simulations are also run to test the system performance and compare it with the pre-existing transport system to know if the proposals of this chapter are an improvement or not. In this section, all zones of transport in Figure 6.5 are included in the simulations. The first comparison only considers the bus system and its demand: Scenario C0 consists of the pre-existing bus network, Scenario C1 examines the future bus network composed by 11 new corridors and a slightly modified version of the conventional bus system, and Scenario C2 simulates the grid network of 28 lines and the small portion of the pre-existing bus network that remains. Table 6.7 summarizes the main user metrics in those scenarios. In the next, the remainder transit modes are considered and all the transit demand is assigned: Scenario D0 consists of the pre-existing transit system (bus, metro, tram and train) with the total transit demand, and Scenarios D1 and D2 add the rail system to the previous Scenarios C1 and C2 respectively. Their results are shown in Table 6.8.

In this section, the headway of service among the 28 corridors is distinguished such as Table 6.4 shows. The O-D matrix in these scenarios is split among transit lines by means of a choice model (*stochastic user equilibrium*) that includes the generalized cost of travel from zone to zone in the different possible paths.

First, note the smaller travel distance in Scenarios C0-C2 versus Scenarios D0-D2. This occurs because the pre-existing bus system, with its low commercial speed, mostly attracts short trips. Longer trips tend to be made either on metro or with private vehicles. A comparison of C0 vs. C1 and C2 reveals that the proposed networks increase the door-to-door speed of all bus trips by 16.32% and 4.05% respectively. The growth in the former case is greater since we put attention in the speed in the 11 corridors. Furthermore, both networks reduce the total travel time by 9.11% and 9.09% respectively. Based on this metric, both proposals have the same level of service. However, if the walking distance is penalized, the 11 corridors are less suitable. In this case, the second network improves more the level of service due to a better distribution of time among the different steps of the user transit chain. 11 corridors are faster but the travel distance also, specially due to access distance.

Table 6.7. Comparison of user metrics in different bus scenarios.

User metric	Scenario C0: Current bus	Scenario C1: Future 11 corridors	Scenario C2: Future 28 corridors
In-vehicle distance (km)	3.64	3.71	3.47
Walking distance (km) *a	0.74	0.93	0.67
Total travel distance (km)	4.38	4.63	4.14
Walking time (min)*a,*b	10.44 (23.49)	12.90 (29.02)	9.37 (21.08)
Waiting time (min)	4.59	3.29	3.61
In-vehicle time (min)	21.62	17.12	20.34
Number of transfers	0.10	0.41	0.26
Total travel time (min)*b	36.65 (49.70)	33.31 (49.43)	33.32 (45.03)
Door-to-door speed (km/h)*b	7.17 (5.29)	8.34 (5.62)	7.46 (5.52)

*a This metric includes access, egress and transfer distances; *b Numbers in parentheses consider an access cost penalized by a factor $w_A = 2.25$.

On the other hand, when all the transit modes are considered, the improvements of the new bus lines go in the same line, but the changes are smaller. From Scenario D0 to D1, the door-to-door speed increases by 6.84%, and the total travel times decreases by 4.63% on the condition that access time is not penalized. From Scenario D0 to D2, the door-to-door speed is similar (1.49% higher) and the total travel times is 4.12% smaller. Finally, the simulations reveal that both new bus networks capture nearly all the demand from the pre-existing bus system and a small portion from the metro lines.

Table 6.8. Comparison of user metrics in different transit system scenarios.

User metric	Scenario D0: Current bus	Scenario D1: Future 11 corridors	Scenario D2: Future 28 corridors
In-vehicle distance (km)	4.42	4.42	4.31
Walking distance (km) *a	0.85	0.95	0.82
Total travel distance (km)	5.27	5.37	5.13
Walking time (min)*a,*b	12.07 (27.16)	13.40 (30.15)	11.62 (26.15)
Waiting time (min)	3.89	2.98	3.29
In-vehicle time (min)	15.38	13.51	15.14
Number of transfers	0.15	0.31	0.20
Total travel time (min)*b	31.34 (46.43)	29.89 (46.64)	30.05 (44.58)
Door-to-door speed (km/h)*b	10.09 (6.81)	10.78 (6.91)	10.24 (6.90)

*a This metric includes access, egress and transfer distances; *b Numbers in parentheses consider an access cost penalized by a factor $w_A = 2.25$.

6.4. Conclusion

This chapter demonstrates the feasibility of a transfer-based system for Barcelona. For the current transit demand, the proposed networks improve the level of service. The network of 11 corridors bases its success on the commercial speed, this is the fastest option. However, this proposal does not solve one of the disadvantages of the pre-existing bus network, the inefficient exploitation of a portion of its resources. A high percentage of the old bus lines would continue working with low frequencies of service. Therefore, there would be vehicles with a low occupancy dispersed in those lines. On the other hand, the 28 corridors also reduce the total travel time, especially if the access cost is penalized. The advantage of this network is the complete reorganization of the bus system, removing most of the old lines. This second proposal reduce the total travel time at the same time that it is closer to the user. Although the speed

would be still too low. In any case, these comparisons guarantee that a change in the bus network structure improves user performance for the current transit demand. However, these metrics are conservative because our analysis ignores the induced demand the system would attract from the better readability and easy usage of a transfer-based network.

This analysis also demonstrates that a hybrid network with some asymmetry in design can be adapted to a real city with a two-step (analysis/design) method. The real-life design results from this process are shown to be robust and near-optimal. The analytic model was found to make reasonably accurate predictions. These would improve if more streets were available so that the actual system could more closely resemble the ideal.

Finally, the municipality and the transit agency decided to implement the network composed by 28 lines. The new network, called the *Nova Xarxa*, has followed a gradual implementation process at the same time that the pre-existing bus network has been dismantled. This process started in 2012 and will finish around 2018. The next chapter analyses real demand data from the lines that belong to the three first implementation phases.

Chapter 7

Network effect in the new Barcelona's bus network*

This chapter presents an empirical analysis of a transfer-based bus network, the *Nova Xarxa* in Barcelona. It attempts to prove two ideas contrary to conventional wisdom: (a) that transit passengers are much less averse to transfers than assumed in current planning practice, and (b) that properly designed transfer-based networks can be very appealing and even attract more demand than their conventional counterparts. To do so, the analysis examines the jumps in demand as new lines and connections were opened in this transfer-friendly network.

The *Nova Xarxa* is an instance in which a complete direct-service network is being replaced by a transfer-based network that meets three conditions: (i) provide full area coverage with easy transfers and non-circuitous routings; (ii) be easy to understand (e.g. a pure grid); and (iii) operate with high frequency. These features should reduce riders' aversion to transfers and encourage usage. The *Nova Xarxa*'s rollout started in 2012, and after several intermediate deployment phases should be completed in 2018. This gradual deployment has created an excellent natural experiment to test the validity of ideas (a) and (b) above with the longitudinal data that it has generated.

The chapter describes these tests. The next section provides information about the implementation process of the *Nova Xarxa* and the efforts put on the design at transfer stops.

* This chapter is the result of my collaboration with Prof. C.F. Daganzo and Dr. J. Argote-Cabanero during my stage at University of California, Berkeley. The results are presented in Badia et al. (2017).

Section 7.2 describes the evolution of bus boardings in the *Nova Xarxa* from 2012 to 2015, which unveils a significant network effect. Then, Section 7.3 presents the results of a demand analysis that estimates transfers and establishes the validity of ideas (a) and (b). Finally, Section 7.4 presents some conclusions.

7.1. The *Nova Xarxa*: transfer design and implementation

As of 2015, thirteen of these lines have been opened to the public. Figure 7.1 shows the 2015 network. In comparison with the old system (Figure 6.1), the new map show that from a user's perspective, the *Nova Xarxa* already exhibits properties (i) and (ii) above, unlike the old system. It has and will continue to have full coverage with non-circuitous routes that are clearly shown on the map.

Figure 7.1. Maps of the Nova Xarxa in 2015. (Source: http://www.tmb.cat/)

Property (ii), understandability, is further reinforced by navigational aids on the street and in the buses. Figure 7.2 shows the instructions and diagrams that are provided at transfer locations, and signals on streets to guide users in the path between stops at interchange point. These diagrams include: the lines that serve the transfer point, their directions, the station locations, and the recommended walking paths for connecting passengers.

Now consider property (iii), high frequency. The *Nova Xarxa* will eventually be served with an average headway of 6.18 min, for more detailed information see Table 6.4. Contrast this with the old bus network with an average headway of 12.30 min. Thus, the *Nova Xarxa* will deliver nearly twice the service frequency of the old network.

Figure 7.2. Transfer point information examples. (Source: http://www.tmb.cat/)

7.1.1. Gradual implementation process until 2015

Barcelona's old bus network was in full operation until September 2012, when the first instalment of the *Nova Xarxa* was opened to the public. At that time redundant lines of the old network were eliminated. By December 2015, two more portions of the *Nova Xarxa* had been opened, and two more sets of old redundant lines had been eliminated. Table 7.1 summarizes the characteristics of the new lines, and lists the old lines they replaced.

As Table 7.1 shows, the new lines are being operated with slightly longer headways than those planned for the final phase. This occurs because the agency has to devote bus resources to populate many old lines that cannot be removed because they serve O-D pairs not yet covered by the new network. Since there will be few of these O-D's in the final phase, the idea is to increase the frequency of the new routes to their final targets at that time, when few old lines will have to be retained and populated. As of December 2015, 235 vehicles served the 13 new lines implemented to date.

Table 7.1. Implemented Nova Xarxa lines: key features and removed old lines.

Phase (Date open)	Bus line	Current headway (min)	Design headway (min)	Bidirectional Length (km)	Old bus line (removed)
1 (10/1/12)	H6	6.0	5.0	9.7	L74
	H12	6.0	3.0	11.4	L56
	D20	6.0	4.0	9.2	L57*[c], L157*[c]
	V7	7.0	7.0	5.1	L30
	V21*[a]	7.0	6.0	8.2 (9.5)*[a]	L10
	Total			**84.1**	
2 (11/18/13)	H8	6.5	5.0	13.0	L15
	H10	6.5	3.0	13.2	L43, L44
	H16*[b]	7.5	5.0	Ph. 2: 4.0 - Ph. 3: 12.2*[b]	Ph. 2: L14*[c], L36*[c], L41*[c] - Ph. 3: L9
	V3*[a]	7.0	5.0	7.5 (8.7)*[a]	L72
	V17	7.0	6.0	8.8	L28, L19*[c], L40*[c]
	Partial			98.1	
	Total			**182.2**	
3 (9/15/14)	H14	8.0	8.0	8.1	L141
	V15	6.5	4.0	8.7	L17, L16
	V27	8.0	8.0	11.1	L71
	Partial			61.3	
	Total			**243.5**	

*[a] These lines cross a tunnel where there are no stops. For this reason, the tunnel length is removed. The total bus line length is displayed in parenthesis; *[b] This line was implemented in Phase 2 but was extended in Phase 3, for this reason, two lengths are displayed; *[c] These lines were shortened to avoid overlap with the new lines, but not totally removed.

7.2. Raw data interpretation: the number of bus boardings and the network effect

To see how the network configuration influences travel we tracked the number of ticket validations per month for every line as the network was expanded. In both the old and the new systems, users validate their tickets upon boarding every bus, including transfers. Therefore, validations slightly overstate the number of trips taken by paying customers, since some trips involve more than one boarding. It is important to clarify that the fare system in Barcelona city is complete flat and the transfer is free if this is made in 1 hour and 15 minutes from the beginning of the trip. This fare integration has existed since 2000, therefore, this is not a distinguishing factor between the pre-existing network and the new design.

Data collection started in October 2012 when the first lines were opened to the public, and ended in October 2015. The solid line of Figure 7.3a shows that the total number of validations in the *Nova Xarxa* consistently increased when new lines were opened. This is not surprising since the service was being expanded. A bit more surprising, however, is the fact that if we group the lines by the phase in which they were implemented (see the dotted and dashed lines labelled *Phase 1*, *Phase 2* or *Phase 3*) one can see how after each transition, the validations on each set of lines increased to a new baseline level. The actual changes can be more clearly seen in Figures 7.3b and 7.3c, which superimpose the yearly profiles of these validations. [The 4th year is incomplete. It belongs to Phase 3 and consists of a single month (October) which is

marked in the figures by a thick dot. As one might expect, the dot coincides in both cases with the corresponding point for the previous October, which is also in Phase 3.]

The observed jumps in validations from one phase to the next strongly suggest that the implementation of new bus lines leads to an increase in the boardings of pre-existing lines, most likely due to the new connections and the possibility to link more origin-destination pairs with a single transfer. In other words, the jumps likely are a manifestation of the network effect that arises when high-frequency lines provide extended coverage to an entire region. The evidence is fairly conclusive. In particular, note that the number of boardings for the lines of Phase 1 grew by about 31.7% as Phases 2 and 3 were completed.

The jumps in the curves of Figure 7.3 are unlikely due to seasonal effects since the curves show similar profiles in different years and their jumps are quite pronounced. The only months that do not exactly conform to this pattern are the first months after the implementation of new lines (October 2012 for Phase 1, November 2013 for Phase 2 and September 2014 for Phase 3). In all cases, the validations for these initial months were lower than in the following years. One of the reasons for this is that the new lines did not start their operation until the middle of the moth.

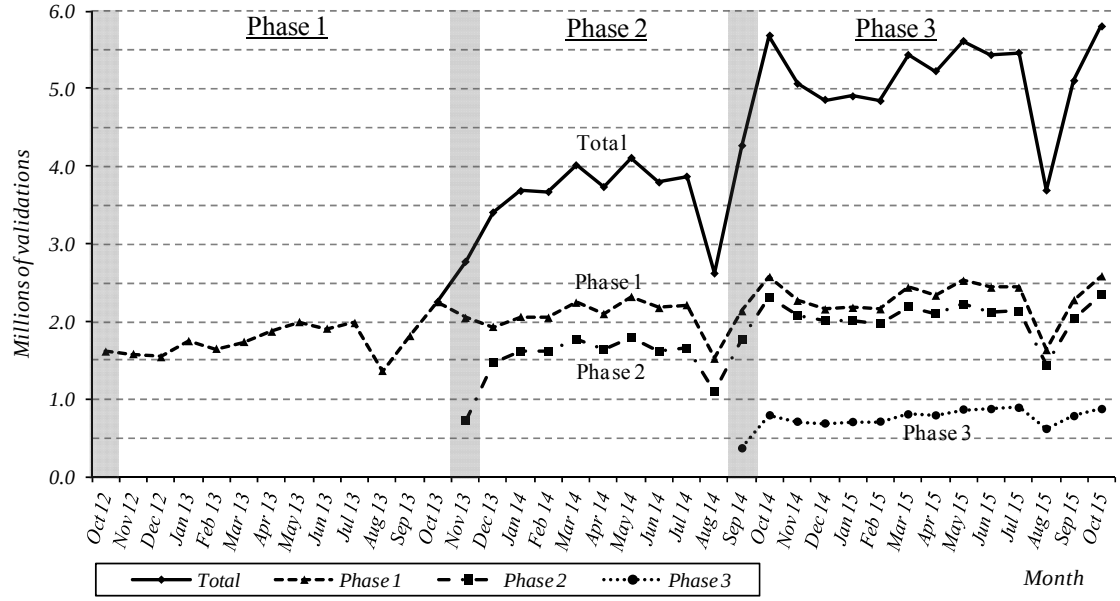

(a) Time series of monthly validations in the Nova Xarxa

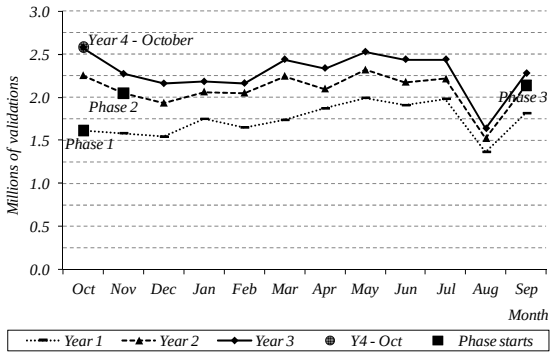

(b) Validation profiles for lines opened in Phase 1

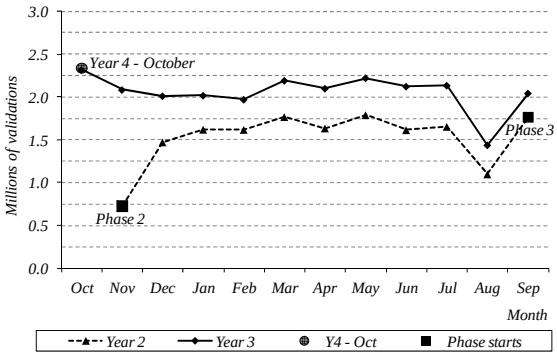

(c) Validation profiles for lines opened in Phase 2

Figure 7.3. Total monthly validations for groups of implemented lines.

Furthermore, this notable growth in boardings for specific lines cannot be attributed to an improving economy or any another factor that could stimulate the demand for transportation. During the study period, Barcelona's overall transit ridership (including Metro, light rail and all bus services) and private vehicle demand levels remained approximately unchanged. This is shown by the solid line of Figure 7.4, which tracks the number of overall transit trips from 2011 until 2014. The line decreases by 2.1% in a very narrow band. The pattern is almost identical for private vehicle trips. This is shown by the dashed line, which decreases by 3.2% between 2011 and 2014. These declining numbers indicate that the boarding increases seen in the *Nova Xarxa* were not the result of a benign economic climate or an overall increase in the city's demand for mobility.

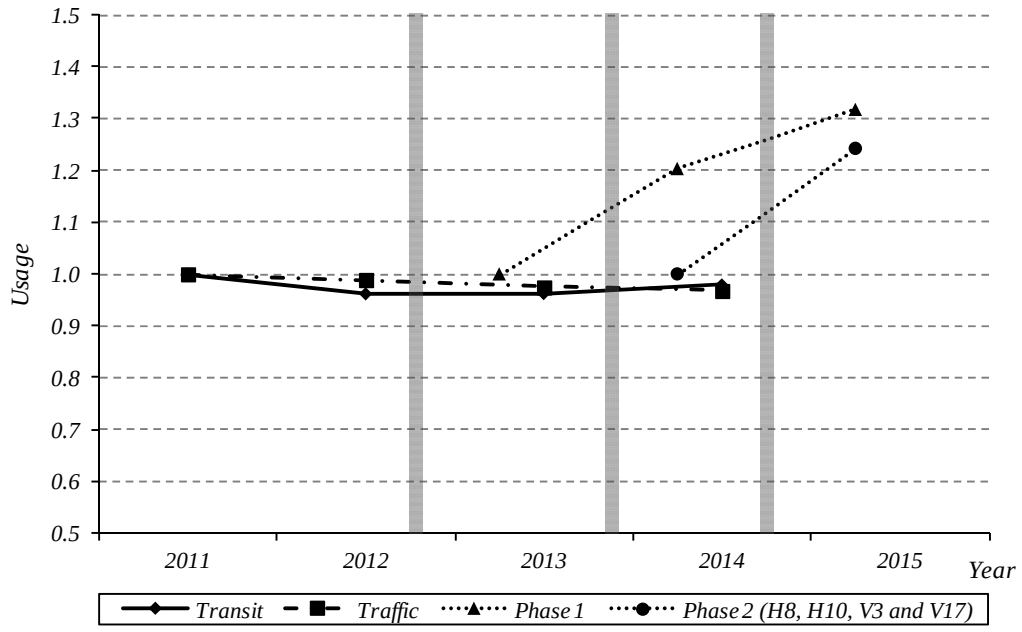

Figure 7.4. Usages of various transport modes from 2011 to 2015: initial usages are set to 1. *(Source for transit and traffic data: Ajuntament de Barcelona - Direcció de Serveis de Mobilitat, 2012-2015)*

Further supporting the presence of network effects is that positive jumps in boardings were consistently observed for all lines and all phases. In particular, as shown by the dotted line marked with triangles in Figure 7.4, the aggregate boardings on Phase 1 lines increased 20.3% from Phase 1 to Phase 2 and by another 9.5% from Phase 2 to Phase 3. The growth in boardings by the lines deployed in Phase 2 is best captured by ignoring line H16 because this line was not held fixed. Line H16 was extended so substantially in Phase 3 that its validations quadrupled. The fixed lines that remained grew by 24.2% from Phase 2 to Phase 3, as depicted by the dotted line marked with circles in Figure 7.4.

In summary, this section has established that the *Nova Xarxa*'s lines exhibit: (i) boarding volumes that have increased at a higher pace than any of their transit or private vehicle alternatives; and (ii) jumps in these boardings that occur as new lines are deployed. All of the above points to the appeal of the new system and the existence of a positive network effect that arises with the implementation of new lines. Passengers must be taking considerable advantage of transferring opportunities. The next section estimates the number of passenger trips taken (the demand) for each line, and the percent that transfer.

7.3. Analysis: Trips taken and the percent that require transfers

Because only ticket validations are observed a model was constructed to break these validations into transfers and initial boardings. Since the latter correspond to trips taken, this breakdown enabled us to assess the growth in travel demand, and in the percent of demand that requires transfers. This section focuses on the results of this model, and only describes its logic qualitatively. A full description is given in Appendix G.

If transit users were to avoid transfers, one would expect demand levels in already deployed lines not to be affected as new lines are implemented. Therefore, it stands to reason that the demand and the percentage of transfers can be teased out from the longitudinally observed growth in validations per line by examining its statistical relationship to the fixed length of the line and the growing length of the connecting lines. As explained in the appendix, a parsimonious two-parameter regression model does the job. The model predicts both, the number of monthly passenger trips and the number of monthly passenger trips with a transfer, for each line during each of the network deployment phases.

The model's two parameters are assumed to be different for each line. Therefore, they were separately estimated across them. Only lines opened in Phase 1 were considered because: (i) they contained sufficient longitudinal information to estimate their parameters (under three different network configurations); and (ii) their basic demand (without transfers) was easier to isolate without specification error because Phase 1 included the fewest connecting lines. Opened in Phase 1, line D20 was excluded because its parameters could not be reliably estimated. D20 is a diagonal line in the periphery that is connected at sharp angles to other lines. As a result, many of its connecting paths are too circuitous to be practical. This feature makes estimation less reliable because it requires assumptions about route choice. This left lines H6, H12, V7 and V21. For maximum statistical efficiency, all data from Phases 1-3 were used. The resulting model was then applied to all the lines and phases, past and future, to predict the demand and the percent that involves transfers.

Table 7.2 displays the predictions. For each line and implementation phase, the table includes the total monthly demand, the number of transfers, and the corresponding percentage. The values obtained indicate that the number of validations involving transfers increases with successive phases to a considerable fraction of the total. In the third phase, 26% of the trips involve a transfer, and for line V7 the number rises to 57%. These values are expected to increase further as new *Nova Xarxa*'s lines are deployed in the phases to come. Ultimately, the model predicts that transfers will represent more than 44% of all trips in the final phase and almost 66% for line V7. Thus, it seems apparent that given the right conditions and contrary to conventional wisdom passengers will embrace transfers. In other words, the results strongly support idea that transit passengers are much less averse to transfers than assumed in current planning practice.

It is also worth noting that transfers seem to be occurring because the network was designed to encourage them. The *Nova Xarxa*'s current 26.4% value already exceeds by a wide margin the transfer percentages of the old bus network, which was about 11% (Transports de Barcelona, 2016). Both the current and forecasted values are also much higher than the percentage of transfers in other urban bus networks that are less transfer friendly: Melbourne 16% (Currie and Loader, 2010), or Boston 1.5%, London 13% and New York 3% (Guo, 2008). These numbers are consistent with the idea that a network designed for transfers can attract

transfers. They also suggest that such a network could also attract more demand than a direct-service network.

Table 7.2. Trips generated and percent of trips with transfers for each line and in total.

	Line	H6	H12	V7	V21	Total
Phase 1	Monthly demand	467,572	407,824	101,765	241,204	1,218,365
	Number of transfers	26,375	50,016	37,018	22,527	135,936
	Percentage transfers	5.6%	12.3%	36.4%	9.3%	11.2%
Phase 2	Monthly demand	499,747	454,308	137,929	268,598	1,360,582
	Number of transfers	58,549	96,500	73,181	49,922	278,153
	Percentage transfers	11.7%	21.2%	53.1%	18.6%	20.4%
Phase 3	Monthly demand	539,051	475,054	150,906	276,433	1,441,444
	Number of transfers	97,854	138,385	86,159	57,757	380,154
	Percentage transfers	18.2%	29.1%	57.1%	20.9%	26.4%
Final phase	Monthly demand	682,823	716,536	189,384	301,701	1,890,445
	Number of transfers	241,626	379.867	124,637	83,025	829,155
	Percentage transfers	35.4%	53.0%	65.9%	27.5%	43.9%

Further analysis confirms this idea. That new demand stimulated by the new network can be seen by comparing the demand of the new lines versus those that they replaced. Before, we verified from the map that the replaced lines had similar or better coverage than the new lines. This is weakly confirmed by the rough similarity in the monthly demands of the new and replaced lines, which are shown on the first two rows of Table 7.3. The values for line V7 are dissimilar because V7 is considerably shorter than the line it replaced. So, to test the idea that a properly designed transfer-based network can induce extra demand, compare now row 1 with row 3, which displays the current total monthly demand of the new lines in Phase 3. This approximates the extra demand due to the improved connectivity, ease of use and level of service of the transfer-based network. As can be seen from the table, the difference exceeds 20% for lines H6, H12 and V7, and is about 6% for line V21. Therefore, this strongly supports the tested idea.

Table 7.3. Monthly demand for the new lines and the old lines they replaced.

Line	H6	H12	V7	V21
Equivalent monthly demand of replaced old lines*[a]	446,856 (L74)	381,897 (L56)	122,086 (L30)	261,093 (L10)
NX monthly base demand (0-transfer)*[b]	441,197	357,808	64,748	218,676
NX total monthly demand (Phase 3)	539,051	475,054	150,906	276,433

*[a] The old lines' demand was provided as the daily number of validations in weekdays, but we also know from data shared by TB that the total number of validations in a week is roughly equal to 5.65 times the number of validations during weekdays in Barcelona. This allowed us to obtain the equivalent monthly demand; *[b] It is the difference between the 7th and 8th lines of Table 7.2.

7.4. Conclusions

Analysis of the *Nova Xarxa* shows that a well-designed transfer-based network can attract more users, and that these users will not be averse to transferring. The acceptance of transfers by transit users not only means that more trips can be completed using a network but that an agency can operate more effectively by consolidating service in well-connected, high-frequency corridors.

In the case of Barcelona, the case study reveals that the new lines are already serving more demand than the pre-existing lines they replaced. Furthermore, the current levels have been reached after a gradual increase concurrent with the expansion of the network. This increases contrasts with a slight declining trend for all transportation modes. This strongly suggests that the growth in demand is due to network effects of the new design and not to other economic, social, or urban factors.

The results also show that the new network is drastically reshaping the demand. While conventional bus networks in big cities exhibit transfer percentages ranging from 1.5% to 16%, the *Nova Xarxa* current percentage is 26%; and this value is projected to rise to 44% when the number of lines is expanded from 13 to 28 at the project's completion in 2018. These considerable numbers support the notion that transit users will transfer if given an attractive chance.

In view of these findings, we can recommend that transfers be systematically considered as an integral part of bus network design. This case study shows that, properly designed, transfer-based bus networks can capture much demand and be an effective mobility solution for many cities.

Part IV: CONCLUSIONS

Chapter 8

Conclusions and future research

This final chapter summarizes the most important results of this thesis, either by the theoretical analysis made in Part II or by evidences obtained from the real case study in Part III. In addition, new research lines are suggested to continue with the comparison between the two network design approaches discussed along the thesis, and others related to design and operation for a transfer-based structure.

8.1. Main contributions

Related to bus network design, there is a discussion about what network structure is the best alternative to supply the most efficient and effective transit system. Two main approaches are confronted. Some planners defend a system based on direct connections since users reject to make transfers. Others support a transfer-based network, characterized by a high readability and simple structures, where a better distribution of travel time among the different steps of the transit chain reduces this total travel time. The main argument to justify this second alternative is the increasing urban dispersion.

In order to clarify this discussion, the thesis develops an analytical model that compares different network structures for different urban dispersion degrees. Based on this model, three basic structures are compared: radial, direct trips and transfer-based scheme. Regarding the representation of urban dispersion, this is modelled just by two parameters ϕ and f_d. The theoretical analysis made in Part II provides some conclusions about what network structure is the most suitable:

- Urban dispersion increases transit mobility costs from agency and user point of view. More resources are needed to serve larger areas of service and longer trips are travelled. As mobility requirements change with urban dispersion, there is no a unique solution with regard to network structure.
- The best network structure depends on the urban dispersion degree of the case study. The theoretical analysis identifies that each structure has a range of urban dispersion in which it is the best solution.
- A simple radial network is the best option to serve a highly concentrated city. It satisfies the mobility requirements in a cheap way, that is, with a few number of resources. However, when the demand starts to spread out, the number of transfers and the trip length shoot up. Therefore, user cost becomes too high.
- A direct trip-based structure appears as the best alternative when the radial network is not effective for users. New lines are introduced over the radial network to serve new displacements that radial lines do not serve fittingly. These new lines remove all transfers and reduce the trip length growth. Although an urban dispersion threshold exists from which the mobility necessities are so dispersed, and to maintain direct connections increases the number of lines and resources needed at the same time as other user times (access and waiting) become longer. Therefore, this strategy is the best alternative in intermediate dispersion degrees.
- This structure initially operates in headways. However, when the region to be directly connected is large, the system works by schedules. In this way, the system can supply a good spatial coverage, though at the expense of an attractive temporal coverage.
- When urban sprawl continues, a network reconfiguration is needed. Transfer appears as an essential step in the transit chain to reach an efficient network design. This allows synergies between transit lines that reduce the agency investment as well as produce a better distribution of user time among the different phases. This second factor gives shorter total travel times.
- As the analytical model idealizes the demand pattern, the actual factor that determines the cut-off dispersion degrees between structures is the size of the central attractant area. In other words, the region directly connected with the whole city or where a complete mesh is developed. In summary, parameter ϕ prevails over parameter f_d.
- These results agree with previous discussions about transit network structure. As Newell (1979) noted, when the attractant areas of a city are so concentrated around a central space, the best solution is a radial (or hub and spoke) scheme. However, at the same time, our comparison shows that a grid becomes a better option for scenarios where peripheral areas have more prominence on mobility; this was already advocated by Thompson (1977). In addition, the intermediate hybrid network is in line with the previous arguments of Newell (1979) and Thompson (1977). Transit lines are focused on a central area where the activities are concentrated, as Newell (1979) argued. Although that central area is no longer a small center or corridor: it becomes ever larger with the evolution of the city. Therefore, it is convenient that this central area has to be served by a grid, as Thompson (1977) proposed.
- It is important to emphasize some assumptions that are accepted in the approach followed in the analytical model. If stop and line spacings were not coincident or the line branching was not defined by that stop spacing, the model would have more freedom to reduce the number of lines or the times that those lines are branched, i.e., a reduction of

the infrastructure length would be possible. Other example is the omission of tangential trips out the central attractant area. In line with the results, these assumptions are conservative with regard to the change from direct trips to transfer trips. Transfer-based networks are longer and deals with higher dispersed mobility patterns better.

These conclusions are obtained for a particular idealized case study. Therefore, this open a new question, if the cut-off dispersion degrees between network structures are constant or depend on the case study characteristics. A second analysis determines the area of applicability for the each structure in function to some characteristics of the case study. This analysis contributes with additional conclusions:

- The dispersion degree from which a change of network structure is the best decision is not constant. It depends on characteristics such as level of demand, city size, transfer penalty, unit agency costs or value of time.
- Radial network gains applicability versus a direct trip-based structure for low demands, small cities, low transfer penalties and when unit agency costs prevails over value of time of users. Although in this case, the dispersion degree of change varies slightly.
- The area of applicability for a network based in direct services grows for high demands, small cities and high transfer penalties. Regarding the relevance of agency or user costs, direct trips gain applicability in extreme scenarios, i.e., when the cost of one stakeholder widely prevails over the other.
- Consequently, a transfer-based scheme is more suitable for low demands, large cities, low transfer penalties and scenarios where agency and users have a more balanced unit costs.
- Too small demand densities change the tendency of the boundary between areas of applicability of direct trip and transfer-based structures. The operation by schedules in the former structure increases its usefulness.
- Well designed transfer points reduce the transfer penalty to low values. Therefore, direct connections lose their raison d'être and are never the optimal solution.

The previous comparison is made atop two different street patterns: grid and ring-radial. In this way, the thesis evaluates possible effects that the street layout has over the suitability of each network structure. The main conclusions are:

- The general guidelines about the applicability for each network structure do not significantly change with regard to the street layout.
- The main difference is related to the hybrid scheme (transfer-based network). In a ring-radial mesh, there is an unbalanced distribution of resources with regard to the demand carried by each line. Only radial lines serve the periphery, therefore, carry greater passenger flows than circular lines. This fact reduces its benefits. However, when the demand is concentrated in the central mesh, an improved balance increases the area of applicability of this structure. In summary, from the comparison of grid and ring-radial street layouts, in the latter it is possible to states in general that: the more centralized the demand is, the lower the dispersion degree from which a transfer-based network is the best solution.

In addition to the analytical study, a parsimonious methodological framework is presented in order to translate the theoretical results from the analytical model to real case studies. First, the methodology checks the monocentric structure of the city, and secondly, measures the urban dispersion degree by two dimensions, concentration and centralization. After analyzing the current scenario for three cities (Barcelona, Palma and Terrassa) by means of O-D matrixes, the conclusion is:

- The three cities are monocentric, at least from the point of view of attracted demand.
- Their central attractant areas vary from 33% in Terrassa to 52% in Barcelona. Although in all the cases, more than 80% of demand is inside that central region.
- The Gini coefficient (measure of concentration) ranges from 0.50 in Barcelona to 0.67 in Terrassa.
- The area based centralization index (measure of centralization) goes from 0.27 to 0.64 in Barcelona and Terrassa respectively.
- The more populated a city is, the more deconcentrated and decentralized, i.e., dispersed.
- All three cases justify the implementation of transfer-based networks. Either by high dispersion degrees or by low demand densities, the best solution in these cities is a redesign of their bus networks from radial schemes or direct services to connections based on transfers. However, to obtain general insights, the analysis of a greater number of cities should be necessary.

After the theoretical analysis, Part III focuses its attention in a real case study: the Barcelona's bus network. The pre-existing network is an example of a direct trip-based structure. Then, this network is compared with two transfer-based redesigns proposed for Barcelona, by means of an adaptation of the analytical model. One redesign proposes a transfer-based structure with only 11 corridors that coexists with most of the pre-existing bus network. One of the main objectives is to supply an intermediate service between conventional bus and metro. The other proposal is a complete transfer-based network composed by 28 corridors that replace almost all the conventional bus lines. The results obtained are:

- An analytical model is a good tool to design transfer-based networks. This gives an idealized sketch that is adapted to the real street network. The comparison between analytical and simulated metrics are similar in uniform demand distributions, with discrepancies below 10%. If the simulated demand follows a real distribution those discrepancies are greater, but below 20%.
- Both network proposals improve the pre-existing level of service for bus demand without more resources. On the one hand, 11 corridors network increases the door-to-door speed by 16% and reduces total travel time by 9%. On the other hand, 28 corridors improves the door-to-door speed by 4% and total travel time by 9%. Therefore, both proposals similarly reduce user cost.
- If all transit demand is taking into account, the same conclusions are obtained. The improvements are smaller, but a change in the bus network structure gets a better supply. A reduction of total travel time above 4% is obtained.
- In any case, the benefits are for the pre-existing users, but the study ignores the transit demand that a transfer-based network can induce due to its greater ease of use.

Finally, the proposal chosen by municipality and agency is the 28 corridors, called the *Nova Xarxa*. A progressive implementation process is followed, and 13 corridors were already working at the moment when this study was made. Real data from those corridors allow to quantify the network effect among them. This is an essential factor for the succeed of this type of network. The main contributions of this analysis are:

- The new lines carry more passengers than the pre-existing lines removed. Their levels of demand have been reached after a gradual increase concurrent with the expansion of the network. This increase is an intrinsic consequence of its design and not due to external factors since the trend for the remainder transport modes is slightly declining.
- The current percentage of transfers in the *Nova Xarxa* is 26%. A value significantly higher than the transfer percentages of conventional bus networks in big cities. These are below 16%.
- The prognosis of number of transfer for the final implementation in 2018 gives levels of transfer around 44%.
- These percentages support the notion that people is not adverse to transfer if given an attractive chance. Well-designed transfer-based network can attract new users.

With all this, the thesis closes a contribution about the discussion related to bus network design. It justifies that a transfer-based structure is an efficient way to face this problem. Well-designed transfer points remove the aversion of users to make them. This acceptance of transfers by transit users means that more trips can be completed using the network as well as the agency can operate the service more efficiently.

8.2. Future research

This thesis leaves opened different research lines. Some of them are suggested below in a short way:

- The transit network design model can be improved in two directions. One of them is related to urban form and demand representation assumed in the analytical model. The main idea is to improve the monocentric structure in order to represent polycentric cities. In this way, we will be able to verify the effects of the emergence of new centralities. Although, in light of the results, polycentric forms would justify a transfer-based network for lower levels of dispersion than the monocentric case.
- The other improvement is related to the transit system. In this thesis, simple networks are considered, where only one structure or strategy of service are accepted. However, the analysis of more complex systems would be interesting. By means of hierarchical and mixed structures, more realistic systems would be analyzed to obtain a better adaptation to mobility requirements. For example, the most demanded zones can be connected to the whole city by direct services, while the rest of trips would be made by a base network where transfers would be an essential step of their paths. That is, whether or not there is a threshold of demand that justifies direct connections in some areas. Although the allocation of resources in those lines would reduce the investment in the complementary transfer-based network, since its number of passengers would be lower.

- Another aspect with regard to the network design model is the inclusion of more decision variables to obtain a better allocation of resources along the network. For example, different stop spacing and line spacing, in line with Badia et al. (2014), or higher frequencies in the corridors that carry more passengers, already studied in Chen et al. (2015).
- Generalization of the study included in Chapter 5 for a greater number of cities. The idea is to know which cities have the characteristics that justify a reconfiguration of their transit networks from radial or direct trip-based structures to transfer-based ones. That is, if the evolution of those cities has changed their urban mobility patterns to more dispersed scenarios.
- A deeper analysis of bus users from Barcelona to know how they are facing the new way to use the system, which is their opinion. By means of surveys to users of the *Nova Xarxa*, we can know the perception of pre-existing and new users and how they have changed the way that they move. In addition, to quantify the induced demand due to the new bus network design.
- Finally, the new design implies to face some operating tasks. The Barcelona's bus network redesign opened some issues. One of the most relevant is a consequence of high frequencies of new lines. A fact that makes it difficult to guarantee a good level of service, avoiding bus bunching. The same happens in the branched sections that the hybrid model proposes. How to maintain the reliable and regular service in the central section when buses come from two different branches.

Bibliography

Abercrombie, P., 1933. Town and Country Planning. Thornton Butterworth, London.

Aguilera, A., 2005. Growth in commuting distances in French polycentric metropolitan areas: Paris, Lyon and Marseille. *Urban studies* 42 (9), 1537-1547.

Ajuntament de Barcelona - Direcció de Serveis de Mobilitat, 2015. Dades bàsiques de mobilitat 2014. Barcelona (In Catalan)

Ajuntament de Barcelona - Direcció de Serveis de Mobilitat, 2014. Dades bàsiques de mobilitat 2013. Barcelona (In Catalan)

Ajuntament de Barcelona - Direcció de Serveis de Mobilitat, 2013. Dades bàsiques de mobilitat 2012. Barcelona (In Catalan)

Ajuntament de Barcelona - Direcció de Serveis de Mobilitat, 2012. Dades bàsiques de mobilitat 2011. Barcelona (In Catalan)

Ajuntament de Barcelona - TMB, 2012. Nova Xarxa de Bus de Barcelona. Primera fase - tardor 2012. (In Catalan)

Ajuntament de Palma, 2003. Pla de Mobilitat Urbana de Palma de Mallorca. (In Catalan)

Aldaihani, M.M., Quadrifoglio, L., Dessouky, M.M., Hall, R., 2004. Network design for a grid hybrid transit service. *Transportation Research Part A* 38 (7), 511–530.

Anas, A., Arnott, R., Small, K., 1998. Urban spatial structure. *Journal of Economic Literature* 36 (3), 1426–1464.

Anselin, L., 1993. *The Moran scatterplot as an ESDA tool to assess local instability in spatial association*. Morgantown, WV: Regional Research Institute, West Virginia University.

Anselin, L., 1995. Local indicators of spatial association – LISA. *Geographical Analysis* 27 (2), 93-115.

ATC - Australian Transport Council, 2006. National Guidelines for Transport System Management in Australia (2nd ed.).

ATM - Autoritat del Transport Metropolità, 2006. Estudi de la Mobilitat Quotidiana 2006. Barcelona (In Catalan)

Badia, H., Estrada, M., Robusté, F., 2014. Competitive transit network design in cities with radial street patterns. *Transportation Research Part B* 59, 161-181.

Badia, H., Estrada, M., Robusté, F., 2016. Bus network structure and mobility pattern: A monocentric analytical approach on a grid street pattern. *Transportation Research Part B* 93, 37-56.

Badia, H., 2016. Diseño de redes de autobús frente a la dispersión de la movilidad urbana. In *Proceedings of the XII Congreso de Ingeniería del Transporte*. Valencia, Spain. (In Spanish)

Badia, H., Argote-Cabanero, J., Daganzo, C.F., 2017. Network effects in bus transit: Evidence from Barcelona's Nova Xarxa. In *Proceedings of the 96th Transportation Research Board Annual Meeting*. Washington, D.C.

Badia, H., Argote-Cabanero, J., Daganzo, C.F., (2017). How network structure can boost and shape the demand for bus transit. Submitted in *Transportation Research Part A*.

Baaj, M.H., Mahmassani, H.S., 1990. TRUST: A LISP Program for the Analysis of Transit Route Configurations. *Journal of the Transportation Research Record* 1283, 125-135.

Baaj, M.H., Mahmassani, H.S., 1991. An AI based approach for transit route system planning and design. *Journal of Advanced Transportation* 25 (2), 187-210.

Baaj, M.H., Mahmassani, H.S., 1992. Artificial intelligence-based system representation and search procedures for transit route network design. *Journal of Transportation Research Board* 1358, 67-70.

Baaj, M.H., Mahmassami, H.S., 1995. Hybrid route generation heuristic algorithm for the design of transit networks. *Transportation Research Part C* 3 (1), 31–50.

Batty, M., Longley, P.A., 1987. Fractal-based description of urban form. *Environment and planning B: Planning and Design* 14 (2), 123-134.

Bauer, K.W., 2009. *City planning for civil engineers, environmental engineers, and surveyors*. CRC Press.

Baumont, C., Ertur, C., Gallo, J., 2004. Spatial analysis of employment and population density: the case of the agglomeration of Dijon 1999. *Geographical Analysis* 36 (2), 146-176.

Bertaud, A., Malpezzi, S., 1999. The spatial distribution of population in 35 World Cities: the role of markets, planning and topography. The Center for urban land and economic research, The University of Wisconsin.

Bertaud, A., 2001. Metropolis: A measure of the spatial organization of 7 large cities. *Unpublished working paper*, 1-22.

Bertaud, A., 2004. The Spatial Organization of Cities: Deliberate Outcome or Unforeseen Consequence?. *IURD Working Paper Series* WP-2004-01, Institute of Urban and Regional Development, Berkeley, CA.

Bontje, M., Burdack, J., 2005. Edge cities, European-style: examples from Paris and the Randstad. *Cities* 22 (4), 317-330.

Brown, J.R., Thompson, G. L., 2008. Examining the Influence of Multidestination Service Orientation on Transit Service Productivity: A Multivariate Analysis. *Transportation* 35 (2), 237-252.

Brown, J.R., Thompson, G.L., 2012. Should Transit Serve the CBD or a Diverse Array of Destinations? A Case Study Comparison of Two Transit Systems. *Journal of Public Transportation* 15 (1), 1-18.

Byrne, B.F., Vuchic, V., 1972. Public transportation line positions and headways for minimum cost. *Traffic Flow and Transportation* (Newell Ed.), American Elsevier Publishing Company, New York, 347-360.

Byrne, B.F., 1975. Public transportation line positions and headways for minimum user and system cost in a radial case. *Transportation Research* 9 (2-3), 97-102.

Byrne, B.F., 1976. Cost minimizing positions, lengths and headways for parallel public transit lines having different speeds. *Transportation Research* 10 (3), 209-214.

Ceder, A. Wilson, N.H.M., 1986. Bus Network Design. *Transportation Research Part B* 20 (4), 331-344.

Ceder, A., Israeli, Y., 1998. User and operator perspectives in transit network design. *Journal of Transportation Research Record* 1623, 3–7.

Ceder, A., 2003. Designing public transport network and routes. Pergamon Imprint, Elsevier Science Ltd., 59-91.

CENIT, 2010. Xarxa de transport públic de Barcelona. Definició i avaluació d'un nou model integrat dels serveis de superfície. Final report, TRA.09P663. (In Catalan)

CENIT, 2013. Nova xarxa d'autobusos per a Barcelona. Anàlisi de la nova xarxa. Final report. (In Catalan)

Cervero, R., 1998. The Transit Metropolis: A Global Inquiry. Island Press, Washington.

Chen, H., Gu, W., Cassidy, M.J., Daganzo, C.F., 2015. Optimal transit service atop ring-radial and grid street networks: A continuum approximation design method and comparisons. *Transportation Research Part B* 81, 755-774.

Clark, C., 1951. Urban population densities. *Journal of the Royal Statistical Society* 114, 490-496.

COST - European Cooperation in Science and Technology, 2011. Buses with High Level of Service. Fundamental characteristics and recommendations for decision-making and research. Brendan Finn (ETTS Ltd.), Odile Heddebaut (IFSTTAR DEST), Arno Kerkhof (UITP), François Rambaud (CERTU), Oscar Sbert Lozano (Consultant), Claude Soulas (IFSTTAR GRETTIA) (Eds.). Final Report, COST action TU0603.

Craig, S.G., Ng, P.T., 2001. Using quantile smoothing splines to identify employment subcenters in a multicentric urban area. *Journal of Urban Economics* 49 (1), 100-120.

Currie, G., Loader, C., 2010. Bus network planning for transfers and the network effect in Melbourne, Australia. *Transportation Research Record* 2145, 8-17.

Daganzo, C.F., 2005. *Logistics Systems Analysis* (4th ed.). Springer, Berlin, Germany.

Daganzo, C.F., 2010. Structure of competitive transit networks. *Transportation Research Part B* 44 (4), 434-446.

Daganzo, C.F., Gayah, V.V., Gonzales, E.J., 2012. The potential of parsimonious models for understanding large scale transportation systems and answering big picture questions. *EURO Journal on Transportation and Logistics* 1 (1-2), 47-65.

Desaulniers, G., Hickman, M.D., 2007. Public Transit. In *Handbooks in Operations Research and Management Science*, G. Laporte y C. Barnhart Eds., *Transportation* 14, Elsevier, Amsterdam, 69-127.

Dickinson, R.E., 1961. The West European City. A Geographical Interpretation (2nd ed.). Routledge and Kegan Paul Ltd., London.

Dodson, J., Mees, P., Stone, J., Bruke, M., 2011. The principles of public transport network planning: a review of the emerging literature with select examples. *Urban Research Program*, Issues Paper 15.

Duranton, G., Overman, H.G., 2008. Exploring the detailed location patterns of UK manufacturing industries using microgeographic data. *Journal of Regional Science* 48 (1), 213-243.

EMT - Empresa Municipal de Transports, 2015. Informe anual 2014. Palma (In Catalan)

Estrada, M., Roca-Riu, M., Badia, H., Robusté, F., Daganzo, C.F., 2011. Design and implementation of efficient transit networks: Procedure, case study and validity test. *Transportation Research Part A* 45 (9), 935-950.

Fairthorne, D. B., 1964. Description and shortcomings of some urban road traffic models. *Journal of the Operational Research Society* 15 (1), 17-28.

Fan, W., Machemehl, R., 2004. Optimal transit route network design problem: Algorithms, implementations, and numerical results. Technical Report SWUTC/04/167244-1, Center for Transportation Research, University of Texas.

Fan, W., Machemehl, R., 2006a. Optimal transit route network design problem with variable transit demand: Genetic algorithm approach. *Journal of Transportation Engineering* 132 (1), 40-51.

Fan, W., Machemehl, R., 2006b. Using a simulated annealing algorithm to solve the transit route network design problem. *Journal of Transportation Engineering* 132 (2), 122-132.

Florence, P.S., 1948. *Investment, Location, and Size of Plant*. Cambridge: Cambridge University Press.

Galster, G., Hanson, R., Ratcliffe, M.R., Wolman, H., Coleman, S., Freihage, J., 2001. Wrestling sprawl to the ground: defining and measuring an elusive concept. *Housing policy debate* 12 (4), 681-717.

Getis, A., 2010. Second order analysis of point patterns: the case of Chicago as a multicenter urban region. In *Perspectives on Spatial Data Analysis*. Springer Berlin Heidelberg, 83-92.

Getis, A., Ord, J.K., 1992. The analysis of spatial association by use of distance statistics. *Geographical analysis* 24 (3), 189-206.

Giuliano, G., Small, K.A., 1991. Subcenters in the Los Angeles region. *Regional science and urban economics* 21(2), 163-182.

Giuliano, G., Narayan, D., 2003. Another look at travel patterns and urban form: the US and Great Britain. *Urban studies* 40 (11), 2295-2312.

González, A., 2008. La difícil inserción de redes de autobuses rápidos en medios urbanos densos: el caso de París. *Ciudad y Territorio, Estudios Territoriales* 40 (156), 313-320. (In Spanish)

Griffith, D.A., Wong, D.W., 2007. Modeling population density across major US cities: a polycentric spatial regression approach. *Journal of Geographical Systems* 9 (1), 53-75.

Guihaire, V., Hao, J.H., 2008. The Transit network design and scheduling: A global review. *Transportation Research Part A* 42 (10), 1251-1273.

Guo, Z., 2008. Transfers and path choice in urban public transport systems. PhD dissertation. Massachusetts Institute of Technology.

Gutiérrez-Domènech, M., 2008. ¿Cuánto cuesta ir al trabajo? El coste en tiempo y en dinero. *Documentos de economía "la caixa"* 11. (In Spanish)

Hasselström, D., 1981. Public Transportation Planning - A Mathematical Programming Approach, PhD dissertation, University of Göteborg, Sweden.

Heddebaut, O., Finn, B., Rabuel, S., Rambaud, F., 2010. The European Bus whit High Level of Service (BHLS): Concept and Practice. *Built Environment*, Lloyd Wright Ed. *Bus Rapid Transit: A public renaissance* 36 (3), 307-316.

Heikkila, E., Gordon, P., Kim, J.I., Peiser, R.B., Richardson, H.W., Dale-Johnson, D., 1989. What happened to the CBD-distance gradient?: land values in a policentric city. *Environment and planning A* 21 (2), 221-232.

Holroyd, E.M., 1967. The optimum bus service: a theoretical model for a large uniform urban area. In L. C. Edie, R. Herman, and R. Rothery (Eds.), *Vehicular Traffic Science,* In *Proceedings of the 3rd International Symposium on the Theory of Traffic Flow*. New York: Elsevier.

Israeli, Y., Ceder, A., 1989. Designing transit routes at the network level. In *Proceedings of the First Vehicle Navigation and Information Systems Conference*. IEEE Vehicular Technology Society, 310-316.

Israeli, Y., Ceder, A., 1995. Transit route design using scheduling and multiobjective programming techniques. In *Computer-Aided Transit Scheduling*. Springer Berlin Heidelberg, 56-75.

Jansson, J.O., 1980. A simple bus line model for optimization of service frequency and bus size. *Journal of Transport Economics and* Policy 14 (1), 53-80.

Jara-Diaz, S. R., Gschwender, A., 2003. From the Single Line Model to the Spatial Structure of Transit Services: Corridors or Direct?. *Journal of Transport Economics and Policy* 37 (2), 261-277.

Jara-Diaz, S. R., Gschwender, A., Ortega, M., 2012. Is public transport based on transfers optimal? A theoretical investigation. *Transportation Research Part B* 46 (7), 808-816.

Jara-Diaz, S. R., Gschwender, A., Ortega, M., 2014. The impact of a financial constraint on the spatial structure of public transport services. *Transportation* 41 (1), 21-36.

Kepaptsoglou, K., Karlaftis, M., 2009. Transit route network design problem: Review. *Journal of Transportation Engineering* 135 (8), 491-555.

Kuah, G.K., Perl, J., 1988. Optimization of feeder bus routes and bus-stop spacing. *Journal of Transportation Engineering* 114 (3), 341-354.

Labbouz, S., Diab, Y., Christen, M., 2006. The Mobilien high-performance bus network. *Nova Terra Connected Cities*, Netherlands Institute for Housing and Planning, Delft, The Netherlands, 31-35.

Lampkin, W., Saalmans, P.D., 1967. The design of routes, service frequencies, and schedules for a municipal bus undertaking: a case study. *Operational Research Quarterly* 18 (4), 375-397.

Lee, B., 2007. "Edge" or "edgeless" cities? Urban spatial structure in US metropolitan areas, 1980 to 2000. *Journal of Regional Science* 47 (3), 479–515.

Li, Z., Chen, Y., Wang, Y., 2013. Optimal Density of Radial Major Roads in a Two-dimensional Monocentric City with Endogenous Residential Distribution and Housing Prices. *Regional Science and Urban Economics* 43 (6), 927-937.

Lorenz, M.O., 1905. Methods of measuring the concentration of wealth. *Publications of the American Statistical Association* 9 (70), 209-219

Lynch, K., 1962. Site Planning. MIT Press, Cambridge, Massachusetts.

Malpezzi, S., Guo, W.K., 2001. Measuring "sprawl": alternative measures of urban form in US metropolitan areas. *Unpublished manuscript*, Center for Urban Land Economics Research, University of Wisconsin, Madison.

Mandl, C.E., 1980. Evaluation and optimization of urban public transportation networks, *European Journal of Operational Research* 5 (6), 396-404.

Massey, D.S., Denton, N.A., 1988. The dimensions of residential segregation. *Social forces* 67 (2), 281-315.

Mazzulla, G., Forciniti, C., 2012. Spatial association techniques for analysing trip distribution in an urban area. *European Transport Research Review* 4 (4), 217-233.

MCRIT, GEE - Gabinet Estudis Econòmics, 2010. Guia per a l'avaluació dels projectes de transport. Barcelona. (In Catalan).

Mees, P., 2000. A very public solution: transport in the dispersed city. Melbourne University Press, Melbourne.

Midelfart-Knarvik, K., Overman, H., Redding, S., Venables. A., 2002. Integration and industrial specialisation in the European Union. *Revue économique* 53 (3), 469–81.

Miyagawa, M., 2009. Optimal hierarchical system of a grid road network. *Annals of Operations Research* 172, 349-361.

Newell, G.F., 1979. Some issues relating to the optimal design of bus routes. *Transportation Science* 13 (1), 20-35.

Nielsen, G., Nelson, J.D., Mulley, C., Tegner, G., Lind, G., Lange, T., 2005. Public transport - Planning the networks. HiTrans Best Practice Guide Vol. 2, Stavanger, Norway.

Nielsen, G., Lange, T., As, C.C., Mulley, O.C., Nelson, J.D., 2006. Network planning and design for public transport success–and some pitfalls. In *European Transport Conference*. Strasbourg, September, 18-20.

Nourbakhsh, S.M., Ouyang, Y., 2012. A structured flexible transit system for low demand areas. *Transportation Research Part B* 46 (1), 204–206.

Ord, J.K., Getis, A., 1995. Local spatial autocorrelation statistics: distributional issues and an application. *Geographical analysis* 27 (4), 286-306.

Pattnaik, S.B., Mohan, S., Tom, V.M., 1998. Urban bus transit route network design using genetic algorithm. *Journal of Transportation Engineering* 124 (4), 368–375.

Park, J., Boyles, S.D., Waller, S.T., 2009. Efficiency of a radial transit route with a focus on the comparison of a trunk with branches and a trunk with feeders route system. In *88th Annual Meeting of Transportation Research Board*. Washington, DC.

Pereira, R.H.M., Nadalin, V., Monasterio, L., Albuquerque, P.H.M., 2013. Urban centrality: a simple index. *Geographical Analysis* 45 (1), 77-89.

Pucher, J., Lefevre, C., 1996. The urban transport crisis in European and North America. Macmillan Press.

Riguelle, F., Thomas, I., Verhetsel, A., 2007. Measuring urban polycentrism: a European case study and its implications. *Journal of Economic Geography* 7, 193-215.

Rodrigue, J.P., Comtois, C., Slack, B., 2006. The geography of transport systems. Routledge, London.

Rueda, S., Latorre, J., Ibarrondo, M., 2009. Diseño e implantación de una nueva red de autobuses en Vitoria-Gasteiz. *Equipamientos y servicios municipales* 146, 30-38. (In Spanish)

Rueda, S., 2010. Mobilitat i ecologia urbana. Jornada Tècnica Operació i Disseny de xarxes urbanes d'autobusos. (In Catalan)

Saka, A., 2001. Model for determining optimum bus-stop spacing in urban areas. *Journal of Transportation Engineering* 127, 195-199.

Schimek, P., 1997. Understanding Differences in Public Transit: Comparison of Boston and Toronto. *Transportation Research Record* 1604 (1), 9-17.

Shih, M., Mahmassani, H.S., 1994. A design methodology for bus transit networks with coordinated operations. Technical Report SWUTC/94/60016-1, Center for Transportation Research, University of Texas, Austin.

Shih, M., Mahmassani, H.S., Baaj M.H., 1998. A planning and design model for transit route networks with coordinated operations. *Journal of Transportation Research Record* 1623, 16-23.

Sitte, C., 1945. The Art of Building Cities. City Building According to its Artistic Fundamentals. Reinhold Publishing Corporation, New York.

Small, K.A., Song, S., 1994. Population and employment densities: structure and change. *University of California Transportation Center.*

Smeed, R.J., 1965. A theoretical model of commuter traffic in towns. *IMA Journal of Applied Mathematics* 1 (3), 208-225.

Tan, T., 1966. Road networks in an expanding circular city. *Operations Research* 14 (4), 607-613.

Thompson, G.L., 1977. Planning considerations for alternative transit route structures. *Journal of American Institute of Planners* 43 (2), 158-168.

Thompson, G.L., Matoff, T.G., 2003. Keeping up with Joneses: planning for transit in decentralizing regions. *Journal of the American Planning Association* 69 (3), 296-312.

Tirachini, A., Hensher, D.A., Jara-Diaz, S.R., 2010. Comparing operator and users costs of light rail, heavy rail and bus rapid transit over a radial public transport network. *Research in Transportation Economics* 29 (1), 231-242.

TMB - Transports Metropolitans de Barcelona, 2009. Basic Data 2009. Barcelona.

TMB - Transports Metropolitans de Barcelona, 2012. Private communication.

TMB - Transports Metropolitans de Barcelona, 2016. Private communication.

Tom, V.M., Mohan, S., 2003. Transit route network design using frequency coded genetic algorithm. *Journal of Transportation Engineering* 129 (2), 186–195.

TRB - Transportation Research Board, 2003. Transit Capacity and Quality of Service Manual - TCQSM (2nd ed.). Kittelson & Associates, Inc., KFH Group, Inc., Parsons Brinckerhoff Quade

& Douglass, Inc., Hunter-Zaworski, K. (Eds.), Transportation Research Board, National Academy Press, Washington, DC.

Tsai, Y.H., 2005. Quantifying Urban Form: Compactness versus 'Sprawl'. *Urban Studies* 42 (1), 141–61.

Tsekeris, T., Geroliminis, N., 2013. City Size, Network Structure and Traffic congestion. *Journal of Urban Economics* 76, 1–14.

Unwin, R., 1914. Town Planning in Practice: An Introduction to the Art of Designing Cities and Suburbs (2nd ed.). TF Unwin, Limited.

Van Nes, R., Hamerslag, R., Immers, B.H., 1988. Design of public transport networks. *Journal of Transportation Research Record* 1202, 74-83.

Van Nes, R., 2002. Design of multimodal transport networks, a hierarchical approach. TRAIL Thesis Series T2002/5, DUP, Delft University, The Netherlands.

Vaughan, R., 1986. Optimum polar networks for an urban bus system with a many-to-many travel demand. *Transportation Research Part B* 20 (3), 215–224.

Vaughan, R., 1987. Urban spatial traffic pattern. Pion Ltd., London.

Vuchic, V., 2005. Urban Transit: Operations, Planning and Economics. John Wiley and Sons, New Jersey.

Vuchic, V., 2007. Urban transit: Systems and Technology. John Wiley & Sons, New Jersey.

Wheaton, W.C., 2004. Commuting, congestion, and employment dispersal in cities with mixed land use. *Journal of Urban Economics* 55 (3), 417-438.

Wirasinghe, S.C., 1980. Nearly optimal parameters for a rail/feeder-bus system on a rectangular grid. *Transportation Research Part A* 14A, 33-40.

Zhao, F., 2006. Large-scale transit network optimization by minimizing user cost and transfers. *Journal of Public Transportation* 9 (2), 107-129.

Zhao, F., Zeng, X., 2006. Simulated annealing-genetic algorithm for transit network optimization. *Journal of Computing in Civil Engineering* 20 (1), 57-68.

APPENDIXES

Appendix A

Nomenclature

Chapter 3 and 4:

H	Headway, H_c and H_p for central and peripheral headway in a grid structure [h]
s	Stop or line spacing in network structures atop the grid street pattern and radial stop spacing or ring line spacing in network structures atop the ring-radial street pattern [km]
θ	Ring stop spacing or radial line spacing in network structures atop the ring-radial street pattern [rad]
d	Swath width or swath-corridor spacing in a direct trip-based network structure [km]
α	Parameter defining the central grid in a hybrid network structure [-]
Z	Total system cost [h/p-h]
C_A	Agency cost [h/p-h]
C_U	User cost [h/p-h]
L	Infrastructure length [km]
V	Kilometers travelled per vehicle and hour [veh-km/h]
M	Number of vehicles working per hour [veh-h/h]
A	Average access time per trip [h]
W	Average waiting time per trip, where W_c and W_p are the average waiting time in central and peripheral regions [h]
T	Average in-vehicle time per trip [h]
E	Average in-vehicle distance per trip, where E_c and E_p are the average in-vehicle distance in central and peripheral regions [km]
v_c	Commercial speed [km/h]
l_s	Average infrastructure length per stop in network structures atop the ring-radial street pattern [km]
e_T	Average number of transfers per trip [-]
O	Vehicle occupancy in the most loaded points of the network [p/veh]
ϕ	Demand decentralization degree that determines the central attractant area size [-]

f_d	Factor of densities between central and peripheral areas [-]
ρ	Portion of generated demand at central area [-]
Λ	Demand during the rush hour [p/h]
λ	Average hourly demand [p/h]
D	Length of the side of square that represents the city with a grid street pattern [km]
R	Radius of the circle that represents the city with a ring-radial street pattern [km]
μ	Value of time [€/h]
δ	Equivalent penalty distance per transfer [km]
v	Cruising speed without considering spent time at stops [km/h]
w	Pedestrian speed [km/h]
$€_i$	Unit agency cost, where $i = L,\ V$ or M [€/km-h; €/veh-km; €/veh-h]
C	Vehicle capacity [p/veh]
SF	Occupancy safety factor [-]
τ	Dwell time per stop [h]
τ'	Boarding (and alighting) time per passenger [h]
w_i	Time perception weight, where $i = A,\ W,\ T$ or t [-]
H_s	Cut-off headway between types of service [h]
h_s	Safety waiting time [h]
f_s	Home waiting time factor [-]
ε_H	Parameter that defines the boundary between both types of service operation in a direct trip-based network structure [-]
O_i	Origin of trip
D_i	Destination of trip
CP_i	Critical point of occupancy
Chapter 5:	
I	Moran's I coefficient, subscripts A and G refer to attracted and generated demand respectively [-]
CoG	Center of Gravity
GC	Gini coefficient, subscripts A and G refer to attracted and generated demand respectively [-]
ACI	Area based centralization index, subscripts A and G refer to attracted and generated demand respectively [-]
Chapter 6:	
D_i	Length of the side of rectangle that represents the city, where subscripts H and V represent the length in horizontal and vertical directions [km]

α_i	Parameter defining the central grid, where subscripts H and V refers to horizontal and vertical directions [-]
s_i	Line spacing, where subscripts H and V represent the spacing between horizontal and vertical lines respectively [km]
s	Stop spacing [km]
p_i	Integer multiple between line and stop spacings, where subscripts H and V represent horizontal and vertical lines respectively [-]
H	Headway [h]
H_{min}	Minimum headway of service in a corridor [h]
N	Maximum number of corridors in the central area [-]
O_i	Vehicle occupancy in the most loaded points of the network, where subscripts H and V represent horizontal and vertical lines respectively [p/veh]
P_i	Portion of trips with regard to the number of transfers, where 0, 1 and 2 refers to zero-transfers trips, one-transfer trips and two-transfers trips respectively.
Chapter 7:	
V_k	Number of validations in line k [p]
X_k	Number of transfers from other lines in line k [p]
D_k	Total demand with origin in line k [p]
$\beta_{0,k}$	Coefficient of zero-transfers demand per length in line k [-]
$\beta_{1,k}$	Coefficient of one-transfer demand per length in line k [-]
l_k	Length of line k [km]
$l_{1,k}$	Length of lines with a point of transfer with line k [km]
$l_{o,k}$	Length of overlapping line to line k [km]
$l_{1,o,k}$	Length of lines with a point of transfer with line k and the other overlapping line to line k [km]
$\eta_{o,k}$	Ratio of overlapping line frequency and the total frequency of service with regard to line k [-]
H_k	Headway of line k [h]
$H_{o,k}$	Headway of overlapping line to line k [h]

Appendix B

Derivation of the analytical formulation atop a grid street pattern

In this appendix, the formulation of the different partial costs are derived for each network structure compared atop a grid street layout. All these costs are estimated with geometric probability tools and are expressed in terms of the model's input parameters and decision variables. Regarding agency costs, the determinant factor is the network structure geometry of Section 3.4.1. For user costs, the user choice paths explained in Section 3.4.2.

Previously, some indications are commented to make easier the following of the formulation's proofs. Cordons are used to identify the location of the trip's origin and destination. These cordons are concentric squares defined by the parameter $\beta \in [0, 1]$. βD is the length of one side of the square and $\beta D/2$ the perpendicular distance from the city center. The cordon $\beta = 1$ is the city edge, $\beta = \phi$ is the edge of the central attractant area, $\beta = \alpha$ is the edge of the central mesh for the hybrid network, and $\beta = \varepsilon_H$ is the boundary between the types of service operation of Section 3.3.1 in a direct trip-based network. In addition, the flow of vehicles that crosses any β-cordon is conserved. However, the number of lines increases when they are branched. In that case, the number of lines is $\beta D/s$.

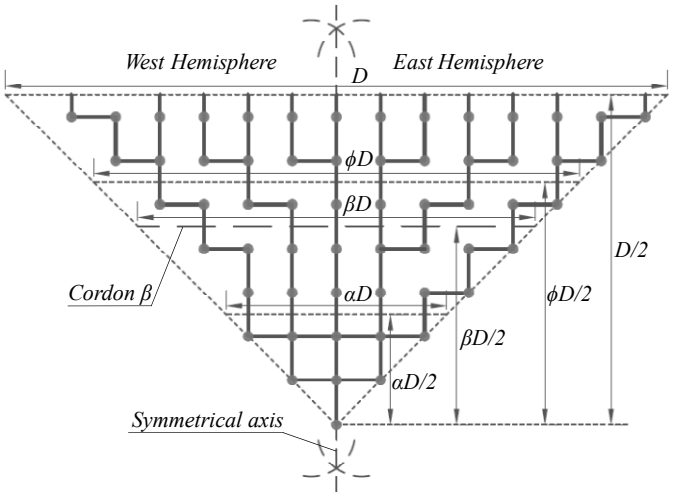

Figure B.1. Network structure layout in North quadrant.

In this street pattern, two divisions of the city are used: (i) in two hemispheres, North-South or East-West, and (ii) into four quadrants, triangular areas from the city center (or from the edge of the central grid in the hybrid structure) to its edge. Figure B.1 shows the North quadrant. Furthermore, two types of lines are distinguished, those that cross the city from its North edge to the South and back, and those that run in the West-East direction and back.

The hybrid scheme is derived first, and then, its two extreme configurations, a radial and a complete grid structures. After, the formulation of the direct trip-based structure is estimated.

B.1. Hybrid network structure

The proposed model for this structure is based on the model presented in Daganzo (2010), and its derivation follows a similar process. In this case, the distinction between central and peripheral areas is made from two different points of view: supply and demand. The former is due to the transit network structure, a grid at the central area and branched lines at the periphery. The decision variable α determines the boundary between both. The latter is a consequence of the demand decentralization degree, where the parameters ϕ and f_d fix the size of the central attractant area and the generated demand distribution respectively. As a consequence, the agency costs are obtained in the same way as Daganzo (2010). However, the user costs presents changes due to the different demand distribution over the city.

Agency costs

Result B.1. The total length of the two-way infrastructure system is given by (B.1):

$$L = D^2(1+\alpha^2)/s \tag{B.1}$$

Proof. In the city center each transfer stop has associated a length $2s$ of two-way infrastructure. In the periphery, each stop has associated just s. We can obtain the total length infrastructure by multiplying the corresponding length by the number of stops contained in each subregion (central area or periphery). This number is equivalent to the ratio of the total area of the subregion and the area associated to one stop. Therefore, we obtain the length in the city center $L_c = 2\alpha^2 D^2/s$, and the length in the periphery $L_p = (1-\alpha^2)D^2/s$. Finally, $L = L_c + L_p$. □

Result B.2. The total vehicle-distance travelled per hour is given by (B.2):

$$V = 2\alpha(3-\alpha)D^2/sH \tag{B.2}$$

Proof. We consider first the central square and then the periphery. As H is constant in the central square, the distance travelled is the ratio between the length of the routes to be covered and that headway. The length of these two-way routes is twice the length of the infrastructure in the central square, that is, $4\alpha^2 D^2/s$. Then, the total distance travelled per hour in the central rectangle is $V_c = 4\alpha^2 D^2/sH$.

The periphery has to be handled differently because the headways are not constant. Lines are branched every s units of distance in the longitudinal direction. Any vehicle runs that distance s longitudinally and an additional lateral displacement in each branching process. When a line is branched, a half of its fleet runs in the lateral direction s units of distance, while the other half

continues in the same direction. Therefore, the average lateral distance is $s/2$. Moreover, this branching process happens $(1\text{-}\alpha)D/s$ times along the periphery. As a consequence, the total distance traveled in the periphery by one vehicle is $3(1\text{-}\alpha)D/2$ on average. On the other hand, the vehicle flow in the vertical direction must remain constant, so that $2\alpha D/sH$, and the same in the horizontal. Then, this flow multiplied by the distance travelled per vehicle gives $V_p = 6\alpha(1-\alpha)D^2/sH$. Adding, $V = V_c + V_p$. □

Result B.3. The number of vehicles in operation during the rush hour is given by (B.3):

$$M = V/v_c \tag{B.3}$$

Proof. The number of vehicles at rush hour is given by the distance traveled per vehicle (V) and the speed with which the vehicle travels that distance (v_c). □

Result B.4. The expected commercial speed during the rush hour is given by (B.4):

$$v_c = 1/[1/v + \tau/s + \tau'(1+e_T)\Lambda/V] \tag{B.4}$$

Proof. As it is made in Daganzo (2010), the commercial speed of the service is the result of reducing the time spent at stops from its upper bound. This bound is the maximum attainable speed on urban streets v, where restrictions, traffic signals and interferences are already taken into account. From this upper bound, the speed decreases due to two reasons: (i) downtime at stops τ, such as acceleration, deceleration and open and close doors, which is prorated per unit of distance, that is, the average distance between stops s; and (ii) boarding and alighting time per passenger τ', this time, also prorated per distance, increases with the number of transfers since users must get on and get off the transit vehicles more times. □

User costs

Now, user costs are evaluated. These are conditioned by the relationship between the parameters α and ϕ. If $\alpha > \phi$, all destinations are located at the gridded central area. Therefore, users can reach their destinations with zero or one transfer. On the other hand, when $\alpha \leq \phi$, some destinations are located between the supply boundary αD and the demand boundary ϕD, that is, at the branched section of the lines. In this case, some trips are completed by means of two transfers. To make easier the derivation, different types of trips are distinguished depending on the locations of their origins and destinations.

In the first case ($\alpha > \phi$), three categories of trips are distinguished. These only depend on the origin location: (1) origin in the attractant central area, whose probability is $P[\text{a.}1] = \rho$; (a.2) origin in the area between demand and supply boundaries, $P[\text{a.}2] = (\alpha^2 - \phi^2)(1-\rho)/(1-\phi^2)$; and (a.3) origin in the periphery from the supply point of view, $P[\text{a.}3] = (1-\alpha^2)(1-\rho)/(1-\phi^2)$. On the other hand, when the attractant central area is larger than the central grid ($\alpha \leq \phi$), three areas are distinguished: the central grid, the intermediate area between supply and demand boundaries, and the rest of the city as the periphery. Therefore, six types of trips are differentiated with regard to the position of their origins and destinations. Three of them have their destinations in the central area, but different location of their origins: (b.1) origin in the central grid, whose probability is $P[\text{b.}1] = \rho\alpha^4/\phi^4$; (b.2) origin in the intermediate area, $P[\text{b.}2] = \rho(\phi^2 - \alpha^2)\alpha^2/\phi^4$; and (b.3) origin in the periphery, $P[\text{b.}3] = (1-\rho)\alpha^2/\phi^2$. The other

three categories have their destinations in the intermediate area and the origin in: (b.4) the central grid, $P[\text{b.4}] = \rho\alpha^2(\phi^2 - \alpha^2)/\phi^4$, (b.5) the intermediate area, $P[\text{b.5}] = \rho(\phi^2 - \alpha^2)^2/\phi^4$; and (b.6) the periphery, $P[\text{b.6}] = (1-\rho)(\phi^2 - \alpha^2)/\phi^2$.

For each cost, two proofs are distinguished: Proof A for the case $\alpha > \phi$ and Proof B when $\alpha \leq \phi$.

Result B.5. The expected number of transfers per trip is given by (B.5):

$$e_T = \begin{cases} 1 - s[\phi^2 D(1+\alpha^2)(1-\rho) + 2\alpha\phi D(\rho - \phi^2) - \alpha s(1-\phi^2)\rho]/\alpha\phi^2(1-\phi^2)D^2, & \alpha > \phi \\ 1 + [D(\phi^2 - \alpha^2) + 2\alpha s](\phi^2 - \rho\alpha^2)/2\phi^4 D - [2\phi^3 D - \rho\alpha^2 s]s/\phi^4 D^2, & \alpha \leq \phi \end{cases} \quad \text{(B.5)}$$

where:

$$P_0 = \begin{cases} s[\phi^2 D(1+\alpha^2)(1-\rho) + 2\alpha\phi D(\rho - \phi^2) - \alpha s(1-\phi^2)\rho]/\alpha\phi^2(1-\phi^2)D^2, & \alpha > \phi \\ [\phi^3 D + \rho\alpha^2(\phi D - s)]s/\phi^4 D^2, & \alpha \leq \phi \end{cases} \quad \text{(B.5.1)}$$

$$P_1 = \begin{cases} 1 - s[\phi^2 D(1+\alpha^2)(1-\rho) + 2\alpha\phi D(\rho - \phi^2) - \alpha s(1-\phi^2)\rho]/\alpha\phi^2(1-\phi^2)D^2, & \alpha > \phi \\ (1+\alpha^2)/2 + \alpha^2(1-\alpha^2)/2\phi^2 - \alpha[(1 + 2\alpha\phi - \alpha^2)D - \alpha s]s/\phi^2 D^2, & \alpha \leq \phi \end{cases} \quad \text{(B.5.2)}$$

$$P_2 = \begin{cases} 0, & \alpha > \phi \\ (\phi^2 - \rho\alpha^2)(\phi - \alpha)[(\phi + \alpha)D - 2s]/2\phi^4 D, & \alpha \leq \phi \end{cases} \quad \text{(B.5.3)}$$

Proof A. Unlike Daganzo (2010), it is assumed that those users with origin and destination in the influence area of the same transit line can travel with zero transfers. This influence area of one transit line is the area whose inner points are nearer than $s/2$ units of distance to that line. Moreover, there are no trips that need two transfers since all the destinations are located at the central grid. Therefore, if the trip is not direct, only one transfer would be required to reach its destination. Then, the expected number of transfers is computed depending on the probability to make 0 or 1 transfer.

Regarding zero-transfer trips, the origins of the users of category (a.1) fall in the influence area of two lines, one horizontal and other vertical. Therefore, their probability of zero transfers is derived from the total area that these two lines serve, $s(2\phi D - s)/\phi^2 D^2$. Regarding users of categories (a.2) and (a.3), only some origins can reach a portion of destinations by direct trips. These origins belong to the influence area of a transit line that crosses the attractant central area. Otherwise, they always need one transfer. To obtain the probability of zero transfers, we have to multiply the probability of those origins and the probability that their destinations are located in the central section of the same line. The former probability for category (a.2) is $2\phi/(\alpha + \phi)$, and ϕ/α for category (a.3). The latter is $s/\phi D$ in both cases. As a result, the zero-transfer probability for these categories is $2s/(\alpha + \phi)D$ and $s/\alpha D$ respectively. Multiplying each one by the probability of each trip category, the total portion of zero-transfer trips is $P_0 = P[\text{a.1}] \cdot s(2\phi D - s)/\phi^2 D^2 + P[\text{a.2}] \cdot 2s/(\alpha + \phi)D + P[a.3] \cdot s/\alpha D$.

Using the total probability theorem, we obtain the one-transfer formula P_1. We subtract the probability of zero transfers from 1. In this case, the average number of transfers e_T is equivalent to the probability of one transfer. □

Proof B. In this scenario, as well as zero and one-transfer trips, some trips need two transfers to be completed. The reason is the existence of some destinations out the central grid. Following the previous classification, trips that belong to group (b.1) and (b.4) present the same behavior as group (a.1). The joint probability of zero transfers is $s(2\phi D - s)/\phi^2 D^2$. Although the transit

lines are branched out the central grid, from a conservative point of view, it is considered that the influence area in the periphery has also a width s. When the origin is located out the central grid, that is, the remainder categories, its joint probability of zero transfers is $s/\phi D$. In this case, from any origin, there is a transit line that crosses the central grid. Weighting each probability by each trip category, $P_0 = (P[\text{b.}1] + P[\text{b.}4]) \cdot s(2\phi D - s)/\phi^2 D^2 + (P[\text{b.}2] + P[\text{b.}3] + P[\text{b.}5] + P[\text{b.}6]) \cdot s/\phi D$ is obtained.

The groups of trip (b.5) and (b.6) need a second transfer when the destination is located out the central grid and in the same or the opposite quadrant with regard to the quadrant of the origin. Obviously, origin and destination do not have to belong to the influence area of the same transit line. The probability for these destinations is $(\phi - \alpha)[D(\phi + \alpha) - 2s]/2\phi^2 D$, and multiplied by the sum of probabilities of categories (b.5) and (b.6) gives the global probability of two-transfer trips P_2.

The portion of one-transfer trips P_1 is obtained by means of the total probability theorem again, removing from 1 the probability of zero and two transfers. As a result, the average number of transfers is $e_T = P_1 + 2 \cdot P_2$. □

Result B.6. The expected walking time at the origin and destination is given by (B.6):

$$A = s/w \tag{B.6}$$

Proof. First, the area of influence of one stop is considered a square of side s. Secondly, it is assumed that the average access distance to a transit stop is the mean between the furthest point, whose distance is s in a L_1 metric, and the closest point that is the stop itself, whose distance is zero. Therefore, the access distance is $s/2$ on average. The egress distance is the same, so the total is double. Finally, the total access time is achieved dividing the previous length by the average pedestrian speed w. □

Result B.7. The expected waiting time per user including the origin and all transfer stops is given by (B.7):

$$W = \begin{cases} H\left[\begin{matrix}\phi^2 D^2[(2+\alpha^3)(1-\rho) + 3\alpha(1+\rho) - 6\alpha\phi^2] - \\ 3\phi D s[\phi(1+\alpha^2)(1-\rho) + 2\alpha(\rho - \phi^2)] + 3\alpha s^2(1-\phi^2)\rho\end{matrix}\right]/6\alpha\phi^2(1-\phi^2)D^2, & \alpha > \phi \\ W = \rho W_c + (1-\rho)W_p, & \alpha \le \phi \end{cases} \tag{B.7}$$

where:

$$W_c = H\left[D^2\left(\phi^4(8\phi + 3\alpha) + \alpha^3(3\alpha^2 - 2\phi^2) - \alpha^3(\phi + \alpha)\right) - 2Ds\left(\phi^3(2\phi + \alpha) + \alpha^3(2\alpha + \phi)\right) + 6\alpha^3 s^2\right]/12\alpha\phi^4 D^2 \tag{B.7.1}$$

$$W_p = H\left[D\left(\phi^3(8\phi + 11\alpha) + \phi^2\alpha(4 + 3\alpha) - \alpha^3(\phi + \alpha)\right) - 2s\left(\phi^2(2\phi + 3\alpha) + \alpha^2(3\phi - 2\alpha)\right)\right]/12\alpha\phi^2(\alpha + \phi)D \tag{B.7.2}$$

Proof A. Transfers are an essential step of the user transit chain in this network structure. Consequently, it is assumed that frequencies should be high; and people arrive independently of the schedule because the system works in headways. This fact implies that the average waiting time at stop will be half of the headway of service. Furthermore, any trip has one or two sections in function to the number of transfers, zero or one. The first section starts at the origin

stop, the other starts in an intermediate stop where users make the transfer. In each section, the waiting time depends on the highest headway between its initial and last stop.

As all destinations are in the central grid, the second trip section has its initial and last stop in that grid. Therefore, its waiting time is always $H/2$. If the origin is also at the central grid, categories (a.1) and (a.2), the initial waiting time is $H/2$ too. However, this does not happen for category (a.3) since its trips start on the branched section of the lines. The waiting time of their initial section is conditioned by the headway of service at its respective origin stop. To estimate that peripheral headway, we know that the vehicle flow that crosses one side of the grid's boundary, cordon αD, is $\alpha D/sH$. This flow is conserved in each peripheral cordon βD. However, it spreads out among a higher number of lines $\beta D/s$. Therefore, the resultant headway per line at one peripheral cordon is $\beta H/\alpha$. The average peripheral headway depends on the demand density function in this area. This function is triangular since the demand is uniformly distributed over that periphery, and its expression is $2\beta/(1-\phi^2)$. Then, that average peripheral headway is $H_p = 2(1-\alpha^3)H/3\alpha(1-\alpha^2)$; and its average waiting time a half of it.

Weighting the waiting time of the first trip section by the different categories of trips, the resultant waiting time at the origin is $[(2+\alpha^3)(1-\rho)+3\alpha(\rho-\phi^2)]H/6\alpha(1-\phi^2)$. And finally, adding the waiting time at intermediate stops for those trips with one transfer, the total expected waiting time per user W is obtained. □

Proof B. On the other hand, when α is smaller than ϕ, the same criterion is accepted. However, in this case, some trips are composed by a third section (a second transfer is needed) and there are destinations on the branched periphery. The average headway in branched sections are estimated in the same way. Now, there are two different headways. One peripheral, beyond the cordon ϕD, that is $H_p = 2(1-\phi^3)H/3\alpha(1-\phi^2)$; and other for the intermediate area between cordons αD and ϕD, $H_i = 2(\phi^3-\alpha^3)H/3\alpha(\phi^2-\alpha^2)$.

Trips (b.1)-(b.3) have all their destinations at central grid. Therefore, the waiting time is conditioned by the origin location. For direct trips, these values are $H/2$ for (b.1), $H_i/2$ for (b.2) and $H_p/2$ for (b.3). When the trip needs one transfer, this happens in the central grid, adding an extra time $H/2$. The destination of trips (b.4)-(b.6) are in the intermediate area. Origins of (b.4) are in the central grid. If only one section composes the trip, its waiting time depends on the destination stop, $H_i/2$. If there are two sections, the first starts and finishes in the central grid, that is, $H/2$ units of time more. For category (b.5), the waiting time of each section of zero and one-transfer trips is $H_i/2$ since these starts or finishes in the intermediate area. Two-transfer trips have an additional section in the central grid, which implies a waiting time of $H/2$. The last category (b.6) has the same behavior as trips (b.5). Only one difference, the origin is in the external periphery. Therefore, the origin prevails over the destination to determine the waiting time for the initial section of these trips, that is $H_p/2$. The resultant waiting time of each category is obtained in function to their percentages of zero, one or two transfer-trips:

$$W(\text{b.1}) = H/2 + H/2 \cdot (1 - s(2\alpha D - s)/\alpha^2 D^2) = H[1 - s(2\alpha D - s)/2\alpha^2 D^2] \quad \text{(B.7.3)}$$

$$W(\text{b.2}) = H_i/2 + H/2 \cdot (1 - s/\alpha D) = H[(2\phi^2 + 5\phi\alpha + 5\alpha^2)/6\alpha(\phi + \alpha) - s/2\alpha D] \quad \text{(B.7.4)}$$

$$W(\text{b.3}) = H_p/2 + H/2 \cdot (1 - s/\alpha D) = H[1/2 + (1 + \phi + \phi^2)/3\alpha(1 + \phi) - s/2\alpha D] \quad \text{(B.7.5)}$$

$$W(\text{b.4}) = H_i/2 + H/2 \cdot (1 - 2s/(\phi + \alpha)D) = H[(2\phi^2 + 5\phi\alpha + 5\alpha^2)/6\alpha(\phi + \alpha) - s/(\phi + \alpha)D] \quad \text{(B.7.6)}$$

$$W(\text{b.5}) = H_i/2 + H_i/2 \cdot (1 - s/(\phi+\alpha)D) + H/2 \cdot (1/2 - s/(\phi+\alpha)D) = H[(8\phi^2 + 11\phi\alpha + 11\alpha^2)/2 - (2\phi^2 + 5\phi\alpha + 5\alpha^2)s/(\phi+\alpha)D]/6\alpha(\phi+\alpha) \quad \text{(B.7.7)}$$

$$W(\text{b.6}) = H_p/2 + H_i/2 \cdot (1 - s/(\phi+\alpha)D) + H/2 \cdot (1/2 - s/(\phi+\alpha)D) = H\big[\big((8\phi^2 + 11\phi\alpha + 7\alpha^2)(1+\phi) + 4(\alpha+\phi)\big)/2(1+\phi) - (2\phi^2 + 5\phi\alpha + 5\alpha^2)s/(\phi+\alpha)D\big]/6\alpha(\phi+\alpha) \quad \text{(B.7.8)}$$

The last step to estimate W in this scenario is to weight each trip category by its respective probability. □

Result B.8. The expected in-vehicle travel time per trip is given by (B.8):

$$T = E/v_c = \begin{cases} D\begin{bmatrix}(6\alpha + \phi^2 + \alpha^2\phi^2)(1-\rho) \\ +8\alpha\phi(\rho - \phi^2)\end{bmatrix}/12\alpha(1-\phi^2)v_c, \ \alpha > \phi \\ D\begin{bmatrix}\big(\alpha^3(2\phi^2(1+\rho) - \alpha^2\rho) + \phi^4(12\phi - 7\alpha)\big)(1+\phi) \\ +6\phi^4(1-\rho)\end{bmatrix}/12\phi^4(1+\phi)v_c, \ \alpha \le \phi \end{cases} \quad \text{(B.8)}$$

The in-vehicle time is obtained dividing the expected travel distance E by the vehicle commercial speed of the network v_c. This speed is estimated in Result B.4. The in-vehicle distance E is derived below.

Proof A. Two different types of trips are distinguished: those that only travel inside the central grid, and those that also run on the branched lines. The former belong to categories (a.1) and (a.2). The in-vehicle distance for trips (a.1) is equivalent to the average distance in a metric L_1 between two random points in the area inside the cordon ϕD. That is $E_1 = 2\phi D/3$. For trips (a.2), this distance is the average between two points where the origin of the trip is randomly located in the intermediate area between cordons αD and ϕD, and the destination only in a smaller one bounded by that second cordon ϕD. Then, $E_2 = (3\alpha^2 + 3\alpha\phi + 4\phi^2)D/6(\phi+\alpha)$.

On the other hand, trips that belong to category (a.3) are divided in two sections: one that starts at the periphery and arrives to one point of the grid's boundary αD, and other that happens on the grid from its boundary to a destination located in the square of side ϕD. The length of the second section is the average distance in a metric L_1 between a random point at cordon αD and a random point in the attractant area. That is $E_{3,c} = (9\alpha^2 + \phi^2)D/12\alpha$. The peripheral path follows the line branching, which is composed by two distances: one in the radial direction and other in the transversal. Considering an origin at cordon βD, the former is the distance between that cordon and the boundary of the grid, $(\beta - \alpha)D/2$. The latter varies in function to the position of the origin from a symmetrical axis of the city (Figure B.1). If the origin is located at this edge, the trip arrives to the grid's boundary at the same axis; therefore, the distance travelled is zero. On the other extreme, when the trip starts on the boundary between two quadrants, the distance to the axis varies from $\beta D/2$ to $\alpha D/2$. The average of this transversal distance is the mean between the lengths of both extremes, $(\beta - \alpha)D/4$. Finally, weighting radial and transversal distances in function to the parameter β, whose density probability function is $2\beta/(1-\alpha^2)$, gives the peripheral length travelled $E_{3,p} = (2 - \alpha - \alpha^2)D/4(1+\alpha)$.

Finally, all these lengths are weighted by the probability of each trip category and added; giving the value of $E = E_1 \cdot P[\text{a.1}] + E_2 \cdot P[\text{a.2}] + (E_{3,c} + E_{3,p}) \cdot P[\text{a.3}]$. □

Proof B. The same reasoning is followed when α is smaller than ϕ. Trips can have one, two or three sections. One of them in the central grid and the remainder in the branches of the lines. In the grid, there are three possible sections: (i) between two inner random points, (ii) from one

point at the grid's boundary to an inner point, and (iii) between two points at the grid's edge. Their average distance in metric L_1 are $E_{c,1} = 2\alpha D/3$, $E_{c,2} = 5\alpha D/6$ and $E_{c,3} = 11\alpha D/12$ respectively. On the other hand, the branched section have one extreme in the grid's edge and the other at a cordon βD, where $\beta>\alpha$. As in previous Proof A, the distance of that section is $(\beta - \alpha)D/2$ in the radial direction and $(\beta - \alpha)D/4$ in the transversal. The extreme of that section can be located in the intermediate area between the cordons αD and ϕD, or in the peripheral zone from that last cordon. In the first case, the p.d.f. of β is $2\beta/(\phi^2 - \alpha^2)$; and $2\beta/(1 - \phi^2)$ in the second. Therefore, the average distance travelled is $E_i = (2\phi^2 - \phi\alpha - \alpha^2)D/4(\phi + \alpha)$ and $E_p = [2(1 + \phi + \phi^2) - 3\alpha(1 + \phi)]D/4(1 + \phi)$ respectively.

Once the average distance travelled for each possible section is known, the average total length for each trip category is obtained as the sum of the distance of the different sections that compose each type of trip:

$$E(\mathrm{b.1}) = E_{c,1} = 2\alpha D/3 \tag{B.8.1}$$

$$E(\mathrm{b.2}) = E(\mathrm{b.4}) = E_i + E_{c,2} = (6\phi^2 + 7\phi\alpha + 7\alpha^2)D/12(\phi + \alpha) \tag{B.8.2}$$

$$E(\mathrm{b.3}) = E_p + E_{c,2} = [6(1 + \phi + \phi^2) - \alpha(1 + \phi)]D/12(1 + \phi) \tag{B.8.3}$$

$$E(\mathrm{b.5}) = 2E_i + E_{c,3} = (12\phi^2 + 5\phi\alpha + 5\alpha^2)D/12(\phi + \alpha) \tag{B.8.4}$$

$$E(\mathrm{b.6}) = E_p + E_{c,3} + E_i = [6\phi(1 + 2\phi + 2\phi^2) + \alpha(6 + 5\phi + 5\phi^2) - \alpha^2(1 + \phi)]D/12(\phi + \alpha)(1 + \phi) \tag{B.8.5}$$

Finally, weighting each trip category by their respective probabilities gives the expected distance travelled E. □

Constraints

Regarding the capacity constraint, Figure 3.5c in Chapter 3 identifies the location of the most critical points from the occupancy point of view in this network structure. The position of these points depends on the relationship between α and ϕ. Their highest levels of occupancy happen at rush hour, whose demand is Λ. These are exacerbated by a safety factor (SF) in order to take into account the own peaks of demand during that hour. Then, the different occupancies are estimated for both possible cases, $\alpha>\phi$ and $\alpha\leq\phi$. In each scenario, the vehicle size is conditioned by the highest occupancy value.

Result B.9. The expected vehicle occupancy on the critical load point during the rush hour is given by (B.9):

$$O = \begin{cases} [H\Lambda s/8\alpha\phi(1-\phi^2)D]max\left\{\begin{matrix} 2\alpha(1-\rho)(2-\phi^2-\alpha^2); \\ (1-\rho)(\alpha+\phi)(2-\alpha^2)+2\alpha(\rho-\phi^2)\end{matrix}\right\}, & \alpha > \phi \\ (H\Lambda/2\alpha\phi^2 D)max\left\{\begin{matrix}\left[\begin{matrix} D\alpha(\phi^2-\alpha^2)(\phi^2-\rho\alpha^2)+ \\ 4s\left(\phi^2\alpha^2(1+\rho)+3(\phi^4-\rho\alpha^4)\right)\end{matrix}\right]/16\phi^2; \\ s(\phi^2-\alpha^2\rho)\end{matrix}\right\}, & \alpha \leq \phi \end{cases} \tag{B.9}$$

Proof A. For $\alpha>\phi$, two critical points exist: one at cordon ϕD, and other at middle point of the central corridors. The flow of the former is composed by all trips generated out of the central attractant area and cross its boundary. Some origins are located on the grid, $\Lambda(1-\rho)(\alpha^2-\phi^2)/(1-\phi^2)$, and others in the periphery where transit corridors are branched, $\Lambda(1-\rho)(1-\alpha^2)/(1-\phi^2)$. Due to that branching in the periphery, the passengers distribution on

the different corridors is not uniform. This dysfunction produces that some corridors carry a double demand than others, so the peripheral demand is multiplied by a factor 2. The central attractant area boundary is crossed in $4\phi D/s$ points, and each is served by $1/H$ vehicles per hour. Therefore, the maximum number of passengers carried per vehicle at this boundary is $Hs\Lambda(1-\rho)(2-\phi^2-\alpha^2)/4\phi(1-\phi^2)D$.

On the other hand, we focus our attention on the demand that crosses the Equator to travel from one Hemisphere to the other, for example North to South. Central corridors, that is, those that serve the attractant area, present higher levels of demand than the rest of them. These corridors are used for those trips whose origins belong to their area of influence, and travel from North to South. This demand is the sum of $\Lambda\rho/4$ passengers from the central attractant area, $\Lambda(1-\rho)(\alpha-\phi)\phi/4(1-\phi^2)$ from the rest of the grid and $\Lambda(1-\rho)(1-\alpha^2)\phi/4\alpha(1-\phi^2)$ from the periphery. In addition, we consider that a half of the users from the rest of the grid cross the Equator by means of these corridors, that is, $\Lambda(1-\rho)(\alpha-\phi)\alpha/8(1-\phi^2)$. However, they carry all the demand from North half of East and West peripheral quadrants that goes to South attractant area, $\Lambda(1-\rho)(1-\alpha^2)/4(1-\phi^2)$. Finally, the total flow of passengers is allocated among the different corridors, $\phi D/s$, and vehicles, $1/H$, taking into account that all peripheral demand has been penalized by a factor 2. As a result, each vehicle carries $Hs\Lambda[(1-\rho)(2-\alpha^2)(\alpha+\phi)+2\alpha(\rho-\phi^2)]/8\alpha\phi(1-\phi^2)D$ passengers at rush hour.

Proof B. For $\alpha \leq \phi$, all trips generated in the periphery cross the critical points at boundary αD. As in this area the generated demand is greater than the attracted, we analyze the flow that comes in to the central grid. All the peripheral generated demand of one quadrant, which is $\Lambda(\phi^2-\rho\alpha^2)/4\phi^2$, crosses the boundary by means of $\alpha D/s$ corridors. As it is explained in Proof A, this volume of passengers is penalized by a factor 2. Therefore, at these points, the demand carried by one corridor is $\Lambda(\phi^2-\rho\alpha^2)s/2\phi^2\alpha D$ passengers during the rush hour.

On the other hand, central critical points are crossed by the demand whose origin and destination belong to different hemispheres, from North to South or from East to West, or vice versa. Among these points, those with the highest volume of demand belong to the most external corridors around the boundary αD. The reason of that is trips with origin in a peripheral quadrant and destination in the same or opposite peripheral quadrants only use these external corridors. The rest of the demand that crosses the Equator is equally allocated among the perpendicular corridors to that Equator. If origin or destination belongs to the periphery, we have to take into account the line branching and multiply this demand by 2. In summary, these demands for each external corridor are respectively: $(\phi^2-\rho\alpha^2)(\phi^2-\alpha^2)\Lambda/32\phi^4$, $\Lambda\rho\alpha^3 s/4\phi^4 D$ and $[3\phi^4+\alpha^2\phi^2(1+\rho)-5\rho\alpha^4]\Lambda s/8\alpha\phi^4 D$. Adding all these demands, we obtain the flow that crosses these critical points during the rush hour.

As headway of service in both critical points is H, the demand carried per vehicle is the previous demand per corridor multiplied by that headway. □

B.2. Radial network structure

This structure is a particular case of the previous hybrid model. Specifically, the value of the decision variable α is null. Therefore, the central grid does not exist, and all the lines are branched such as Figure 3.3a shows. For agency costs, Equations (B.10) and (B.11) give infrastructure length and kilometers travelled respectively. They are directly presented since

their derivations are identical to the branched line section of the hybrid structure. The same formulas (B.3) and (B.4) estimate the fleet and the commercial speed for this scheme.

$$L = D^2/s \tag{B.10}$$

$$V = 6D/H \tag{B.11}$$

Regarding user costs, the access time is calculated by (B.6) again. However, the remainder of costs present changes related to the number of transfers. Here, the estimation is more accurate than in the branched section of the hybrid network. In this case, a better approximation is made since the route branching represents the totally of the network. Then, its proof and the proof for the other user costs are explained. In this network, two types of trips are distinguished: (c.1) origin in the central attractant area, whose probability is $P[\text{c.1}] = \rho$, and (c.2) origin in the rest of the city (or periphery), $P[\text{c.2}] = (1-\rho)$.

Result B.12. The expected number of transfers per trip is given by (B.12):

$$e_T = 1 - s(3+\rho)/3\phi D \tag{B.12}$$

Proof. A direct trip exists when origin and destination are located in the influence area of the same line. Due to the line branching, the more central the stop is, the greater the number of lines that serve that stop. Lines that serve one stop have an influence area of width s at the cordon where the stop is located. However, the total area of influence of those branched lines is wider in external cordons. Therefore, the probability of direct trips between two cordons is conditioned by the inner one.

Focusing the attention on one quadrant, the probability of zero transfers between two cordons $\beta_O D$ and $\beta_D D$ (which represent origin and destination respectively) depends on their relative position. If $\beta_O > \beta_D$, the probability is $s/\beta_D D$, where s is the width of the influence area of one line and $\beta_D D$ the total length of that cordon. Otherwise, that probability is $s/\beta_O D$. If the origin is located in the attractant central area, the destination can be at an inner cordon or at an outer one. As the p.d.f. of β_O and β_D is $2\beta/\phi^2$, the expected probability of zero-transfer trips for category (c.1) is $\int_0^{\phi}(2\beta_O/\phi^2)\left[\int_0^{\beta_O}(2\beta_D/\phi^2)(s/\beta_D D)\,d\beta_D + \int_{\beta_O}^{\phi}(2\beta_D/\phi^2)(s/\beta_O D)\,d\beta_D\right]d\beta_O = 8s/3\phi D$. When that origin is peripheral, trips (c.2), the destination always conditions the probability. That is, $\int_0^{\phi}(2\beta_D/\phi^2)(s/\beta_D D)\,d\beta_D = 2s/\phi D$.

As line runs along two quadrants, one and its opposite, these direct trips happen in two of the four quadrants. Therefore, the previous probabilities are divided by 2. Then, weighting for each trip category, the probability of zero transfers is $s(3+\rho)/3\phi D$. Using the total probability theorem, we obtain the average number of transfers per trip. That is, removing from 1 the probability of zero transfers. □

Result B.13. The expected waiting time per user including the origin and all transfer stops is given by (B.13):

$$W = H\left[15D(1+2\phi+2\phi^2) - 15s(1+\phi) - \rho\left(15D + s(1+\phi)\right)\right]/45s(1+\phi) \tag{B.13}$$

Proof. Transfers are also needed in this network structure, so that, the system works in headways. The headway of service grows with the distance from the city centre with the ratio

$\beta D/s$. Moreover, as in the branched part of lines of the hybrid structure, the headway that determines the waiting time is the highest between both extremes of each section of the trip. Two types of trips are distinguished, direct and one-transfer trip, composed by one or two sections respectively. The latter goes from the origin to the city centre and from that centre to the destination.

The first section of trips (c.2) has its origin in the periphery and goes to the central area. Therefore, the average headway in that periphery determines the waiting time. That headway is $H_p = \int_{\phi}^{1}[2\beta/(1-\phi^2)](H\beta D/s)\,d\beta = 2(1-\phi^3)DH/3s(1-\phi^2)$. If the trip needs a second section, this happens in the central area; whose average headway is $H_c = \int_0^{\phi}(2\beta/\phi^2)(H\beta D/s)\,d\beta = 2\phi DH/3s$. Weighting by the probability of zero and one-transfer trip, the average waiting time for these trips is $W(\text{c. 2}) = \left[H_p + H_c(1-s/\phi D)\right]/2 = H[D(1+2\phi+2\phi^2) - s(1+\phi)]/3(1+\phi)s$.

On the other hand, for one-transfer trips of category (c.1), first section runs from the origin to the central point of the network, and there, the user make a transfer to go to its destination. The average headway in both cases is H_c. However, direct trips only have one section, and the highest headway depends on the relative position between origin and destination. Considering the origin at cordon $\beta_O D$ and the destination at cordon $\beta_D D$, its average headway is $H_{c,0T} = \int_0^{\phi}(2\beta_O/\phi^2)\left[\int_0^{\beta_O}(2\beta_D/\phi^2)(\beta_O DH/s)\,d\beta_D + \int_{\beta_O}^{\phi}(2\beta_D/\phi^2)(\beta_D DH/s)\,d\beta_D\right]d\beta_O = 4\phi DH/3s$. In summary, the average waiting time for these trips is $W(\text{c. 1}) = \left[2H_c(1-4\,s/3\phi D) + H_{c,0T}(4\,s/3\phi D)\right]/2 = 2H[15\phi D - 8s]/45s$.

Finally, the waiting time is $W = W(\text{c. 1})\,P[\text{c. 1}] + W(\text{c. 2})\,P[\text{c. 2}]$. □

Result B.14. The expected in-vehicle travel time per trip is given by (B.14):

$$T = E/v_c = \left[15D(1+2\phi+2\phi^2) - 15s(1+\phi) - \rho\big(15D + s(1+\phi)\big)\right]/30(1+\phi)v_c \qquad \text{(B.14)}$$

Proof . The path followed in this network is the same as in the branched routes of the hybrid structure. The distance travelled between two cordons is $3|\beta_1 - \beta_2|/4$. Trips (c.1) with one transfer travel from one cordon $\beta_O D$ to the central point of the network, and from that point to the destination $\beta_D D$. Being $E_c = \int_0^{\phi}(2\beta_O/\phi^2)(3\beta_O D/4)\,d\beta + \int_0^{\phi}(2\beta_D/\phi^2)(3\beta_D D/4)\,d\beta = \phi D$ their average length. For zero-transfer trips, if origin and destination are located in opposite quadrants, the length is also E_c. However, when they belong to the same quadrant, the trip does not need to arrive to the central point. In this case, the trip length is $E_{c,0T} = \int_0^{\phi}\int_0^{\phi}(2\beta_O/\phi^2)(2\beta_D/\phi^2)(3|\beta_O - \beta_D|D/4)\,d\beta_D\,d\beta_O = \phi D/5$. Weighting by the respective probabilities, $E(\text{c. 1}) = E_c \cdot (1 - 2\,s/3\phi D) + E_{c,0T} \cdot (2\,s/3\phi D) = (15\phi D - 8s)/15$.

For trips (c.2), the same derivation is followed. Then, $E_p = \int_{\phi}^{1}(2\beta_O/\phi^2)(3\beta_O D/4)\,d\beta + \int_0^{\phi}(2\beta_D/\phi^2)(3\beta_D D/4)\,d\beta = (1+2\phi+2\phi^2)D/2(1+\phi)$, and between origins and destinations at the same quadrant $E_{p,0T} = \int_{\phi}^{1}\int_0^{\phi}(2\beta_O/\phi^2)(2\beta_D/\phi^2)[3(\beta_O - \beta_D)D/4]\,d\beta_D\,d\beta_O = D/2(1+\phi)$. Therefore, $E(\text{c. 2}) = E_p(1 - s/2\phi D) + E_{p,0T}(s/2\phi D) = [D(1+2\phi+2\phi^2) - s(1+\phi)]/2(1+\phi)$. All this gives the average distance $E = E(\text{c. 1})\,P[\text{c. 1}] + E(\text{c. 2})\,P[\text{c. 2}]$. □

Constraints

Result B.15. The expected vehicle occupancy on the critical load point during the rush hour is given by (B.15):

$$O = (SF)H\Lambda[6\phi D - s(3+\phi^2)]/24\phi D \quad \text{(B.15)}$$

Proof. The maximum occupancy in this structure occurs in the central point of the network such as Figure 3.5a shows. In one direction, that point is crossed by all the demand from one quadrant. That is, the passengers that go from that quadrant to the others, and those users that go to the same quadrant but need one transfer. Only direct trips with origin and destination in the same quadrant do not cross the center. This demand during the rush hour is $(\Lambda/4)[1-(3+\phi^2)s/6\phi D]$. As vehicles that serve the central point in one direction are $1/H$, the maximum vehicle occupancy is $H\Lambda[6\phi D - s(3+\phi^2)]/24\phi D$; which is increased by the factor (SF). □

B.3. Grid network structure

This structure is also a particular case of the hybrid network. Here, the central grid covers the whole city, i.e., α is equal to one. For this reason, agency and user costs are presented directly in Equations (B.16)-(B.20). However, in this case, not all the corridors work with the same headway. Corridors that cross the central attractant area have a headway H_c, and the rest of them work with a headway H_p. A fact that produces small changes in vehicle-km and waiting time derivations. On the other hand, commercial speed, fleet and access time follow the same Equations (B.3), (B.4) and (B.6) respectively.

$$L = 2D^2/s \quad \text{(B.16)}$$

$$V = 4D^2\big[(1-\phi)H_c + \phi H_p\big]/sH_cH_p \quad \text{(B.17)}$$

$$W = H_c\big[\phi^2D^2\big(1+3\phi+\rho(1-\phi)\big) - 2\phi Ds(\rho+\phi) + \rho s^2(1+\phi)\big]/2\phi^2D^2(1+\phi) + H_p(1-\phi)(1-\rho)/2(1+\phi) \quad \text{(B.18)}$$

$$T = E/v_c = D[3+3\phi+4\phi^2-\rho(3-\phi)]/6(1+\phi)v_c \quad \text{(B.19)}$$

$$e_T = 1 - s[2\phi D(\phi+\rho) - s\rho(1+\phi)]/\phi^2(1+\phi)D^2 \quad \text{(B.20)}$$

In this structure, there are two types of trips: (d.1) origin in the central attractant area, and (d.2) origin out of that area. Their probabilities are $P[\mathrm{d.1}] = \rho$ and $P[\mathrm{d.2}] = (1-\rho)$.

Constraints

Regarding the capacity constraint, this structure has some particularities that imply an explanation of its derivation.

Result B.21. The expected vehicle occupancy on the critical load point during the rush hour is given by (B.21):

$$O = (SF)(\Lambda s/4D)max\{H_c[1+3\phi+\rho(1-\phi)]/2\phi(1+\phi);\ H_c(1-\rho)/\phi;\ H_p(1-\rho)/(1+\phi)\} \quad \text{(B.21)}$$

Proof. Figure 3.5d indicates the three critical points of this structure: two in the central corridors and one in the peripheral. The middle points of the central corridors are crossed by three categories of demand: (i) all the central demand that crosses the Equator $\rho\Lambda/4$, (ii) all peripheral demand from those areas served by central corridors that crosses the Equator by them $(1-\rho)\Lambda\phi(1-\phi)/(1-\phi^2)$, and (iii) half of the demand generated in the areas only served

by peripheral corridors $(1-\rho)\Lambda\phi(1-\phi)^2/8(1-\phi^2)$. Regarding this last demand, users can cross the Equator by the first vehicle, which belongs to the peripheral corridor, or by the second. In this last case, the user transfers to another vehicle of a central line to cross the Equator. Passengers choose interchangeably both paths. Therefore, it is assumed that each one is used by half of that demand. Finally, those three demands are added and allocated among the $\phi D/s$ central corridors and $1/H_c$ vehicles per hour, $H_c[1+3\phi+\rho(1-\phi)]\Lambda s/8\phi(1+\phi)D$ passengers per vehicle.

The other points of the central corridors, located at cordon ϕD, are crossed by all demand generated in the peripheral area served by central corridors and half of the remainder peripheral demand. This last demand follows the same reasoning of the third group of the previous critical point. Therefore, each side of cordon ϕD is crossed by $(1-\rho)\Lambda\phi(1-\phi)/2(1-\phi^2)+(1-\rho)\Lambda(1-\phi)^2/4(1-\phi^2)$ users. Allocating this demand by corridor and vehicle, the number of passengers is $H_c(1-\rho)\Lambda s/4\phi D$.

Finally, the most loaded point in the peripheral corridors carry all the demand generated in one of the four external areas just served by these corridors, $(1-\rho)\Lambda(1-\phi)^2/4(1-\phi^2)$. Half of them in each direction, served by $(1-\phi)D/2s$ corridors with a flow of $1/H_p$ buses per hour. Giving $H_p(1-\rho)\Lambda s/4(1+\phi)D$ users per vehicle. □

B.4. Direct trip-based network structure

Besides the aspects considered at the beginning of this appendix, this network structure has its own characteristics. Following the explanations in Section 3.4.1, the attractant area is divided into concentric swaths of width d. The central one is served by a radial network, where all lines are gathered in the central point of the city and branched as the stop spacing s marks. The remainder swaths are served by different group of lines that collaborate to connect their respective swaths to the external area of the city, as yet unconnected. Figure 3.4 shows this situation and defines three important concepts for the succeeding proofs: swath-quadrant, external-quadrant and swath-corridor. Moreover, this figure shows that each line has two sections: one that runs longitudinally through the swath-corridor, and one that runs through the branched itinerary of the central radial network. Each swath-corridor is identified by its distance from the city center $i \cdot d$, where i=1,2,…,n and n, whose value is $(\phi D-d)/2d$, is the total number of swaths without taking into account the central one.

On the other hand, as Section 3.3.1 explains, two types of services are accepted: in headways or by schedules, depending on whether the headway of service is lower or higher than a fixed value H_s respectively. Therefore, two zones are identified: one around the city center and another external. The parameter ε_H, whose value is $H_s s/HD$, determines the boundary between both zones at a distance $\varepsilon_H D/2$ from the city center, a square cordon of side $\varepsilon_H D$.

Finally, the parameter e_T is null in this network structure since all the trips are direct, and the number of vehicles that serve the network and its average commercial speed are derived in the same way as the previous structures by Equations (B.3) and (B.4). Regarding the latter of these Equations, we should emphasized that there are no transfers in this case, therefore, fewer boardings and alightings.

Agency costs

Result B.22. The total length of the two-way infrastructure system is given by (B.22):

$$L = D^2/s + (\phi^2 D^2 - d^2)/d \tag{B.22}$$

Proof. The central swath is served by a radial network that, as known from Equation (B.10), has a length of D^2/s. For the remainder of the swaths, only the section of the lines that crosses longitudinally the swaths adds length, since the branched section is overlapped with the radial network. In the i-swath, the corridor is located at a distance $i \cdot d$ from the center, and forms a square cordon of side $2 \cdot i \cdot d$. Therefore, the total length of the corridor section is the summation for all the swaths $\sum_1^{(\phi D-d)/2d} 8id = (\phi^2 D^2 - d^2)/d$. □

Result B.23. The total vehicle-distance traveled per hour is given by (B.23):

$$V = [\phi D^2(6 + \phi) - d^2]/dH \tag{B.23}$$

Proof. The vehicle-kilometers traveled by the fleet that serves the central swath is $6D/H$ from Equation (B.11). For the remainder of the swaths, Figure 3.4 shows the distance travelled by one line. To explain this, we focus our attention on the lines of Figure 3.4a, which are gathered in the East swath-quadrant and are branched over the North and South external-quadrants. These lines run completely the East swath-quadrant, and on average half of both adjacent ones; that is, half of the swath-corridor's length. For the i-swath, this distance is $4 \cdot i \cdot d$.

As the line branching is equal to the previous structures, the lines cross the North external-quadrant vertically from its North swath-quadrant to the city boundary. This distance is $(D/2 - id)$. At the same time there are some horizontal displacements. That is, one line runs approximately $s/2$ units of distance horizontally per each s unit of distance vertically. The number of times that a line travels s units of distance vertically is $(D/2 - id)/s$; therefore, the total horizontal distance is $(s/2)(D/2 - id)/s$. This distance is doubled, since the same length is travelled in the South quadrant; then, $2[(D/2 - id) + (s/2)(D/2 - id)/s] = 3(D - 2id)/2$.

As Section 2.2 explains, the number of vehicles that cover these distances per each swath-quadrant in the i-swath is $1/H$. The resultant kilometers travelled is multiplied by two due to the bidirectional service of the lines, and by four because there are four groups of lines per swath, giving $2 \cdot 4 \cdot [4id + 3(D - 2id)/2](1/H) = 4(3D + 2id)/H$. Adding the vehicle-distance traveled in each swath, the total vehicle kilometers in one hour V is $6D/H + \sum_1^{(\phi D-d)/2d} 4(3D + 2id)/H = [\phi D^2(6 + \phi) - d^2]/dH$. □

User costs

Before deriving the user costs, different types of trips are distinguished by their origin's location. There are two groups: (e.1) those whose origins are located at the central attractant area, which generates and attracts demand; and (e.2) those whose origins are peripheral, located at the external area where there is only trip generation. The probability of (e.1) and (e.2) are $P[\text{e.1}] = \rho$ and $P[\text{e.2}] = (1 - \rho)$.

Result B.24. The expected walking time at the origin and destination is given by (B.24):

$$A = (3s + d)/4w \tag{B.24}$$

Proof. As Section 3.4.2 explains, the users take the transit vehicle at the closest stop. The influence area of one stop is a centered square of side s. The average access distance is $s/2$, zero for the closest origin, located at the same stop, and s for the furthest origin, located at one square's vertex. On the other hand, the users alight at stops of a swath-corridor to avoid transfers, although these stops are not always the closest to their destinations. These stops have a rectangular influence area of side s in the longitudinal direction and side d in the perpendicular direction. Following the same reasoning as for the access, the average egress distance is $(s + d)/4$. In some trips, this behavior is reversed, users go to a swath-corridor stop at origin, and they alight at the closest stop to their destinations. The sum of access and egress distances divided by the pedestrian speed gives the expected walking time: $[s/2 + (s + d)/4]/w = (3s + d)/4w$. □

Result B.25. The expected waiting time per user including the origin and all transfer stops is given by (B.25):

$$\begin{aligned}
&\text{if } \varepsilon_H \geq 1 && W = H[5(1 + \phi + \phi^2) - \rho(5 - \phi - \phi^2)]D/15(1 + \phi)s \\
&\text{if } \phi \leq \varepsilon_H < 1 && W = \left[h_s(1 - \varepsilon_H^2) + H\left(2f_s(1 - \varepsilon_H^3) + (\varepsilon_H^3 - \phi^3)\right)D/3s\right](1 - \rho)/(1 - \phi^2) + 2\phi DH\rho/5s \\
&\text{if } \varepsilon_H < \phi && W = [h_s + 2f_s(1 + \phi + \phi^2)DH/3(1 + \phi)s](1 - \rho) + \left[h_s(\phi^4 - \varepsilon_H^4) + 2H\left(2f_s(\phi^5 - \varepsilon_H^5) + \varepsilon_H^5\right)D/5s\right]\rho/\phi^4
\end{aligned} \tag{B.25}$$

Proof. First, we define the headway of service for the different network's stops. In the central radial network, the headway of service increases from the city center, whose value is H, with a slope $\beta D/s$. In a cordon located at a distance $\beta D/2$, the number of points where the transit lines cross one side of this cordon is $\beta D/s$. Moreover, in each cordon, the flow of vehicles is constant, and its value is $1/H$ for one of its sides. This flow is uniformly distributed among the different points crossed. Therefore, the headway of service at stops that belong to the cordon βD is the inverse of the ratio between that number of vehicles and the number of points crossed: $1/[(1/H)/(\beta D/s)] = (\beta D/s)H$. The same happens with the groups of lines that serve the remainder of the swaths. The lines of the same group are gathered with a joint headway H in the swath-corridor, and follow the same branching as the radial network. As a consequence, one stop located at distance $\beta D/2$ from the city center is connected to each inner swath by a headway of service $(\beta D/s)H$.

On the other hand, the waiting time at stops depends on the type of service with which the transit network works. If it works in headways, it is assumed that the waiting time is half of the headway. On the contrary, the waiting time is composed of two terms, such as in Tirachini et al. (2010). These are a constant time h_s independent of the headway, and a variable term as an opportunity cost. This variable term is the result of multiplying a fixed factor f_s by the headway. There is a cut-off headway H_s that indicates how each stop works: in headways if the headway of service at stop is lower than H_s; otherwise, by schedules.

In addition, the parameter ε_H, previously presented, defines how the transit network works. At cordon $\varepsilon_H D$, the headway is $(\varepsilon_H D/s)H$, which is equalized to H_s. Therefore, the value of ε_H is $H_s s/HD$. Given its value, we can distinguish between three scenarios: (E.1) $\varepsilon_H \geq 1$, the whole system works in headways, (E.2) $\phi \leq \varepsilon_H < 1$, the outer section of the periphery works by

schedules, and (E.3) $\varepsilon_H<\phi$, only an inner zone of the central attractant area works in headways. Moreover, ε_H and ϕ define different areas and their probabilities in each scenario. In the case of (E.1), there are only two areas: the same as (e.1) and (e.2); for the scenario (E.2) the peripheral area (e.2) is divided into one outer and one inner zone, whose probabilities are $(1-\varepsilon_H^2)(1-\rho)/(1-\phi^2)$ and $(\varepsilon_H^2-\phi^2)(1-\rho)/(1-\phi^2)$ respectively, and the central area is equivalent to (e.1); and finally, in the case (E.3), its periphery matches with (e.2) and the central area is partitioned in two zones, whose probabilities are $(\phi^2-\varepsilon_H^2)\rho/\phi^2$ for the outer and $\varepsilon_H^2\rho/\phi^2$ for the inner.

The expected waiting time for scenario (E.1) is now derived. At the periphery, the average headway is the weighted headway of each cordon βD, taking into account that the probability density function of β is triangular; that is, $2\beta/(1-\phi^2)$. The result is $H_p=\int_\phi^1\left[\left(2\beta/(1-\phi^2)\right)(\beta D/s)H\right]d\beta=2(1+\phi+\phi^2)DH/3(1+\phi)s$. At the central area, the headway for each trip is the highest between the headways of its origin (β_O) and destination (β_D) stops, where the p.d.f. for both is $2\beta_i/\phi^2$. Therefore, $H_c=\int_0^\phi(2\beta_O/\phi^2)\left[\int_0^{\beta_O}[(2\beta_D/\phi^2)(\beta_O D/s)H]\,d\beta_2+\int_{\beta_O}^{\phi}[(2\beta_D/\phi^2)(\beta_D D/s)H]\,d\beta_D\right]d\beta_O=4\phi DH/5s$. All this leads to obtaining the expected waiting time: $W=\left[H_c\rho+H_p(1-\rho)\right]/2=H[5(1+\phi+\phi^2)-\rho(5-\phi-\phi^2)]D/15(1+\phi)s$.

For the other scenarios, when ε_H is lower than 1, the same process is followed to derive the expected waiting time, only with the exception that some parts of the city work by schedules. If $\varepsilon_H\geq\phi$, this only happens in the outer periphery, and outer and inner average peripheral headways are distinguished related to the trip's origin. These headways are $H_p^o=\int_{\varepsilon_H}^1\left[\left(2\beta/(1-\varepsilon_H^2)\right)(\beta D/s)H\right]d\beta=2(1+\varepsilon_H+\varepsilon_H^2)DH/3(1+\varepsilon_H)s$ and $H_p^i=\int_\phi^{\varepsilon_H}\left[\left(2\beta/(\varepsilon_H^2-\phi^2)\right)(\beta D/s)H\right]d\beta=2(\varepsilon_H^2+\varepsilon_H\phi+\phi^2)DH/3(\varepsilon_H+\phi)$s respectively. On the contrary, all the periphery works by schedules, such as the most external region of the attractant central area. Therefore, in this case, the central average headway is divided into three types of trip: (i) origin and destination in the outer region $H_c^o=\int_{\varepsilon_H}^{\phi}\left(2\beta_O/(\phi^2-\varepsilon_H^2)\right)\left[\int_{\varepsilon_H}^{\beta_O}\left[\left(2\beta_D/(\phi^2-\varepsilon_H^2)\right)(\beta_O D/s)H\right]d\beta_D+\int_{\beta_O}^{\phi}\left[\left(2\beta_D/(\phi^2-\varepsilon_H^2)\right)(\beta_D D/s)H\right]d\beta_D\right]d\beta_O=4(2\varepsilon_H^3+4\varepsilon_H^2\phi+6\varepsilon_H\phi^2+3\phi^3)DH/15(\varepsilon_H+\phi)^2s$, (ii) origin or destination in the outer region and the other in the inner $H_c^{i,o}=\int_{\varepsilon_H}^{\phi}\left[\left(2\beta/(\phi^2-\varepsilon_H^2)\right)(\beta D/s)H\right]d\beta=2(\phi^2+\phi\varepsilon_H+\varepsilon_H^2)DH/3(\varepsilon_H+\phi)s$, and (iii) $H_c^i=\int_0^{\varepsilon_H}(2\beta_O/\varepsilon_H^2)\left[\int_0^{\beta_O}[(2\beta_D/\varepsilon_H^2)(\beta_O D/s)H]\,d\beta_2+\int_{\beta_O}^{\varepsilon_H}[(2\beta_D/\varepsilon_H^2)(\beta_D D/s)H]\,d\beta_D\right]d\beta_O=4\varepsilon_H DH/5s$ when both are in the inner area. The resulting expected waiting times for each scenario are:

$$\begin{aligned}
&\text{if } \phi\leq\varepsilon_H<1 \quad W=\left[\left(h_s+f_sH_p^o\right)(1-\varepsilon_H^2)+H_p^i(\varepsilon_H^2-\phi^2)/2\right](1-\rho)/(1-\phi^2)+\rho H_c\phi^2/2=\\
&\qquad\qquad \left[h_s(1-\varepsilon_H^2)+H\left(2f_s(1-\varepsilon_H^3)+(\varepsilon_H^3-\phi^3)\right)D/3s\right](1-\rho)/(1-\phi^2)+2\phi DH\rho/5s\\
&\text{if } \varepsilon_H<\phi \quad W=\left(h_s+f_sH_p\right)(1-\rho)+\left[(h_s+f_sH_c^o)(\phi^2-\varepsilon_H^2)^2+\left(h_s+f_sH_c^{i,o}\right)2\varepsilon_H^2(\phi^2-\varepsilon_H^2)+H_c^i\varepsilon_H^4/2\right]\rho/\phi^4=[h_s+2f_s(1+\phi+\phi^2)DH/3(1+\phi)s](1-\rho)+\\
&\qquad\qquad \left[h_s(\phi^4-\varepsilon_H^4)+2H\left(2f_s\left(\phi^5-\varepsilon_H^5\right)+\varepsilon_H^5\right)D/5s\right]\rho/\phi^4 \quad \square
\end{aligned} \tag{B.25.1}$$

Result B.26. The expected in-vehicle travel distance per trip is given by (B.26):

$$T=E/v_c=[15(1-\rho)+2\phi(1+\phi)(10+\rho)]D/30(1+\phi)v_c \tag{B.26}$$

Proof. The length of all trips is decomposed in two sections. One runs over a branched route, and the other partially a swath-corridor. The former has the same behavior as in the previous structures: the travelled distance between an origin at the cordon of side $\beta_O D$ and a destination at the cordon of side $\beta_D D$ is one perpendicular $|\beta_O-\beta_D|D/2$ and one transverse $|\beta_O-\beta_D|D/4$ due to the route branching. Regarding the second section, a swath-corridor located at a distance

$\beta D/2$ from the city center shapes a square cordon of side βD. Therefore, the expected distance in the swath-corridor is the average distance between two random points of that cordon by the shortest possible path; that is, βD units of distance.

First, we compute the expected trip length when the origin is located at the periphery. In this case, there is a section of the trip in that periphery and another in the central attractant area. As the parameter β has a triangular density function $2\beta/(1-\phi^2)$, this length is $E_p = \int_{\phi}^{1}\left[\left(2\beta_O/(1-\phi^2)\right)(3(\beta_O-\phi)D/4)\right]d\beta_O + \int_0^{\phi}[(2\beta_D/\phi^2)(3(\phi-\beta_{Dd})D/4)]\,d\beta_D = (3+4\phi+4\phi^2)D/6(1+\phi)$. On the other hand, when origin and destination are in the central attractant area, the average distance is $E_c = \int_0^{\phi}\int_0^{\phi}(2\beta_D/\phi^2)(2\beta_O/\phi^2)[3|\beta_O-\beta_D|D/4 + min(\beta_O,\beta_D)D]\,d\beta_O\,d\beta_D = 11\phi D/15$. Weighting peripheral and central lengths by (1-ρ) and ρ respectively, the expected traveled distance is $E = [15(1-\rho)+2\phi(1+\phi)(10+\rho)]D/30(1+\phi)$. □

Constraints

Result B.27. The expected vehicle occupancy on the critical load point during the rush hour is given by (B.27):

$$\begin{aligned}&\text{if } \left(2d\rho+\sqrt{3\phi^2D^2\rho+d^2\rho^2}\right)/6\rho \le \phi D/2 \qquad O = (SF)\,H\Lambda d\begin{bmatrix} d\rho(9\phi^2D^2-\rho d^2)+\\ \rho^{1/2}(3D^2+d^2)^{3/2}\end{bmatrix}/27\phi^4D^4\rho\\ &\text{if } \left(2d\rho+\sqrt{3\phi^2D^2\rho+d^2\rho^2}\right)/6\rho > \phi D/2 \qquad O = (SF)\,H\Lambda d(\phi D-d)\begin{bmatrix}\phi^2D^2(1-\rho)+\\ 4d\rho(\phi D-d)\end{bmatrix}/2\phi^4D^4\end{aligned} \tag{B.27}$$

Proof. The highest vehicle occupancy in the transit network takes place on the swath-corridors. As explained in Section 3.4.1, all the demand from an external-quadrant whose destination belongs to the same adjacent swath-quadrant is carried by a group of lines that are gathered on the respective swath-corridor. For a corridor located at a distance $i \cdot d$, $(1-\rho)\Lambda/4 + \rho\Lambda[\phi D/2-(id-d/2)][\phi D+(2id-d)]/2\,\phi^2D^2$ is the generated demand from its external-quadrant, and the probability that this demand is attracted by that swath-quadrant is $2id^2/\phi^2D^2$. As Figure 3.4 shows, these lines also connect that external-quadrant to the same and the opposed swath-quadrants. For some users, these lines serve one, the other or a percentage of both. On average, these lines connect half for each; that is, an additional swath-quadrant, so that the demand carried is multiplied by two. This demand is allocated among those transit vehicles that serve the corresponding lines, whose flow is $1/H$. Then, the vehicle occupancy on the swath-corridor i is $H\Lambda id^2\left[\rho\left(\phi^2D^2-d^2(1+4i(i-1))\right)+(1-\rho)\phi^2D^2\right]/\phi^4D^4$.

As the previous expression shows, not all of the corridors carry the same passenger load: it depends on the size of each swath and the size of the external-quadrant that each of them serves. The first determinant increases with the distance from the city center, but the second decreases. The consequence is that the corridors' passenger load shows a concave behavior with distance from the center, i.e., the maximum load is not located at extremes, but at an intermediate distance from the center. The value of i that maximizes the vehicle occupancy is $\left(2d\rho+\sqrt{3\phi^2D^2\rho+d^2\rho^2}\right)/6\rho$; multiplied by d it gives the distance from the city center where the corridor with maximum load is located. If this distance is shorter than $\phi D/2$, there is a corridor around this position. Then, $O_i = H\Lambda d\left[d\rho(9\phi^2D^2-\rho d^2)+\rho^{1/2}(3D^2+d^2)^{3/2}\right]/27\phi^4D^4\rho$ is the maximum occupancy. However, if that position is situated in the periphery where there are no corridors, the corridor with the highest load is around the boundary of the central attractant area. This happens because the occupancy function has an increasing monotonous behavior with

respect to the corridor's position defined by i. In this case, the maximum occupancy is $O_e = H\Lambda d(\phi D - d)[\phi^2 D^2(1-\rho) + 4d\rho(\phi D - d)]/2\phi^4 D^4$.

In addition, the rush hour actually has its own peaks; for this reason, the occupancy is exacerbated by a safety factor (SF). □

Appendix C

Derivation of the analytical formulation atop a ring-radial street pattern

A detailed explanation of the model's formulation is presented below for the three network structures compared atop a ring-radial street layout. Before starting, it is pointed out some indications about how following the formulation's proofs. As in the grid street pattern, cordons are used to identify the trip's origin and destination. The parameter β, which ranges from 0 to 1, defines those cordons. They are concentric circumferences of radius βR with regard to the city center. As it is explained in Section 3.2, the edge of the central attractant area is the cordon $\beta = \phi$. For the hybrid scheme, the edge of the central ring-radial mesh is the cordon $\beta = \alpha$. For the direct trip-based structure, the cordon $\beta = \varepsilon_H$ is the boundary between the type of service operation explained in Section 3.3.1. In addition, the flow of vehicles across all cordons is conserved.

Figures in Section 3.5 help to understand this appendix. The networks are mainly composed by radial (or pendular) lines that go from one point of the city edge to another one at the opposite side of the city through the central area. These lines run over the radial streets and occasionally over perimeter rings in a longer or shorter length. These perimeter sections are a consequence of the line branching in order to cover all the stops. To keep a constant accessibility, the radial lines branch in each s units of distance in the radial direction. All these lines pass through the city center in a radial or a hybrid network. However, only some of them do that in a direct trip-based structure. In this last case, the radial lines have a centripetal direction, but once they reach the central area, they cross that area by means of transversal routes. On the other hand, a second type of lines exist in a hybrid structure, ring or circular lines that complement the radial lines to shape a ring-radial mesh. These lines run complete concentric circles round the city center in both directions.

Then, the proofs of the partial costs for the different network structures are presented. However, a result is previously derived: the ring distance traveled for the radial lines due to their branching.

Result C.1. Ring distance travelled in the line branching at each i-strip is given by (C.1.1) for the hybrid structure and by (C.1.2) for the radial and the direct trip-based structures:

$$\pi(\alpha R + i \cdot s)/2 \tag{C.1.1}$$

$$\pi(s + i \cdot s)/2 \tag{C.1.2}$$

Proof. Focusing initially on the hybrid network, it supplies a constant spatial accessibility in the periphery equal to the central area's boundary. To ensure that, it is necessary to readjust and branch the radial lines from that boundary. The angle θ that separates those lines should be reduced to preserve the same arc length between stops that exists in that boundary. Considering that the periphery is divided into strips of width s, in each of them, the lines travel a ring distance to reach that constant accessibility. For this reason, a preliminary step is to determine the ring route that the radial lines travelled in the peripheral area.

The i-strip is an annulus between the radii $(\alpha R + (i-1) \cdot s)$ and $(\alpha R + i \cdot s)$. As the arc length between stops is equal to that length at cordon αR, the angle between radial lines in the i-strip is $\theta_i = \theta \alpha R/(\alpha R + i \cdot s)$, where i=1,…,n, and the number of strips n is $(1-\alpha)R/s$. Therefore, the number of lines in the strip is $2\pi(\alpha R + i \cdot s)/\theta \alpha R$, an increase of $2\pi s/\theta \alpha R$ in each strip over the previous. Looking at Figure C.1, the network scheme shows the possibility to group the lines with symmetric behavior. The number of groups coincides with the new lines per strip. In this figure, we can see the ring route that the lines draw. The angle covered in the perimeter direction in one group of the i-strip is (C.1.3).

$$2\left[\theta_i\left(1+3+5+\cdots+(2m+1)\right)/2 - \theta_{i-1}(1+2+3+\cdots+m)\right] = \theta_i(m+1)^2 - \theta_{i-1}m(m+1) \tag{C.1.3}$$

The value of m is roughly obtained from the number of lines per group in the corresponding strip, $m = (\alpha R + (i-2)s)/2s$. Substituting m, θ_i and θ_{i-1}, and multiplying by the number of groups in the i-strip, the total angle covered in that strip is obtained, $\pi(\alpha R + is)/2(\alpha R + (i-1)s)$.The lines are bifurcated at the beginning of the strip, at a distance from the center $\alpha R + (i-1)s$. To find the arc length travelled, we multiply the angle covered by the radius, and it gives $\pi(\alpha R + i \cdot s)/2$.

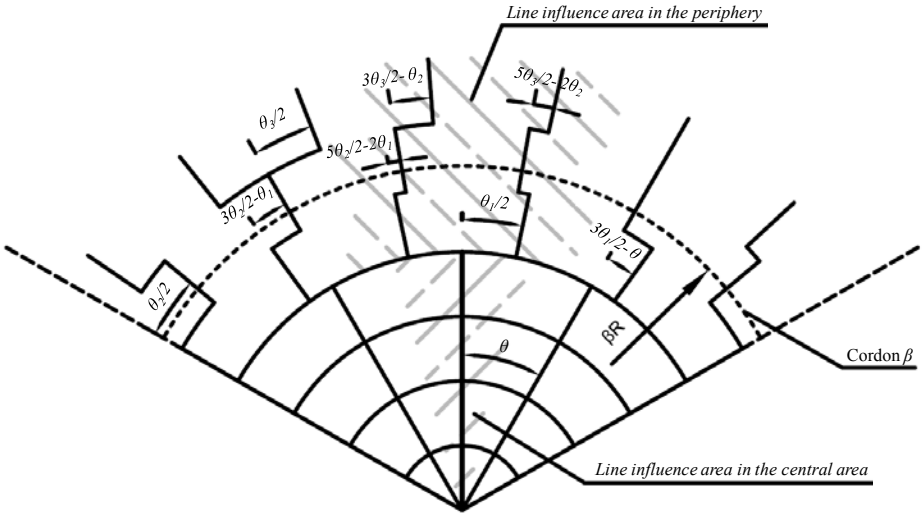

Figure C.1. Branching of the radial corridors in the periphery, and its influence area.

Regarding the other two structures analyzed atop the ring-radial street layout, the radial line branching does not only happen in a peripheral area. This happens along the whole city since the spatial accessibility is always constant. The ring stop spacing is equal to that spacing at a distance s from the city center, that is, θs. Therefore, the ring distance traveled is derived in the

same way as the hybrid scheme with the exemption that the cordon that fixes the ring stop spacing is s instead of αR. □

C.1. Hybrid network structure

As it is explained in Section 3.5.1, this hybrid scheme have two different areas from the supply point of view: a central ring-radial mesh, and a peripheral hub and spoke scheme. In addition to that distinction, the city is divided in two different areas due to the demand distribution. However, unlike the hybrid network atop a grid street layout, in this case, parameter α is always smaller than ϕ. That is, the central ring-radial mesh occupies an area smaller than or equal to the central attractant area. The reason of that is the uselessness of circular lines out of that attractant area. In this structure, in those trips that use a circular line, the shortest path uses the most central circular line between the origin and destination of the trip. Therefore, a circular line out of the attractant area would never be used.

Agency costs

Result C.2. The total length of the two-way infrastructure system is given by (C.2):

$$L = \pi\left[4s\left((1+\alpha^2)R + (1-\alpha)s\right) + \theta\alpha R\left((1+3\alpha^2)R + (1+3\alpha)s\right)\right]/4\alpha s\theta \quad \text{(C.2)}$$

Proof. In the central area, there are $2\pi/\theta$ radial lines of length αR and $\alpha R/s$ circular lines of length $2\pi(i \cdot s)$, where $i=1,\ldots,n$, and n is the number of circular lines. As a result, we get the total length in the central area, $L_c = \pi\alpha R[2s + \alpha R\theta + \theta s]/\theta s$. In the periphery, $2\pi(\alpha R + j \cdot s)/\theta r$ radial lines belong to each strip, where $j=1,\ldots,m$ and m is the number of strips $(1-\alpha)R/s$. Each line travels s units of distance in the radial direction in every strip. For all lines, the total radial distance in the periphery is $L_{pr} = \pi(1-\alpha)[(1+\alpha)R + s]/\theta\alpha$. The total circular distance travelled is obtained from Result C.1, giving $L_{pc} = \pi(1-\alpha)R[(1+\alpha)R + s]/4s$. The sum of the three lengths gives the total. □

Result C.3. The total vehicle-distance travelled per hour is given by (C.3):

$$V = \pi R[4s + \alpha\theta(2s + (1+\alpha)R)]/\theta sH \quad \text{(C.3)}$$

Proof. In the central area, the length of all the lines and the headway are already known. The headway is constant and its value H. Hence, the vehicle kilometers in one hour are $2L_c/H$, i.e., $V_c = 2\pi\alpha R[2s + \alpha R\theta + \theta s]/\theta sH$.

In the periphery, the average distance travelled by one line on one strip can be easily obtained as the sum of a radial distance s and other circular (Result C.1 divided by the number of lines in the respective strip). This gives $s+(\theta\alpha R/4)$ units of distance. There are n strips, where $n=(1-\alpha)R/s$. From here, we get the average length of one line in the periphery, taking into account that it is bidirectional, its distance travelled is $(1-\alpha)R[4s + \theta\alpha R]/2s$. The number of vehicles that circulates in the periphery in one hour is $2\pi/\theta H$, which are those that emerge from the radial lines of the central mesh. Multiplying the number of vehicles per hour by the distance travelled by each one, we obtain the total distance in one hour in the periphery $V_p = \pi(1-\alpha)R[4s + \theta\alpha R]/\theta sH$. The sum of central and peripheral distances gives the total. □

Result C.4. The number of vehicles in operation during the rush hour is given by (C.4):

$$M = V/v_c \tag{C.4}$$

Proof. As in the grid street pattern, the number of vehicles at rush hour is given by the distance traveled per vehicle V and the speed that the vehicle can travel that distance v_c at. □

Result C.5. The expected commercial speed during the rush hour is given by (C.5):

$$v_c = 1/[1/v + \tau/l_s + \tau'(1+e_T)\Lambda/V] = 1/[1/v + \tau\pi[(1+\alpha^2)R + (1-\alpha)s + 2\alpha^2 R]/L\alpha\theta s + \tau'\Lambda(1+e_T)/V] \tag{C.5}$$

Proof. Again, as in the grid street pattern, the commercial speed of the transit service is the inverse of the time that a vehicle needs to travel a unit length during the rush hour. However, while in the previous case the stop spacing along the city is constant, in this hybrid scheme, that spacing increases with the distance from the city center. Therefore, we have to calculate the average infrastructure length per stop l_s. This length l_s is the result of dividing the total infrastructure length ($2L$) by the number of stops. This number is $2\pi[(1+\alpha^2)R + (1-\alpha)s + 2\alpha^2 R]/\alpha\theta s$. Therefore, $l_s = L\alpha\theta s/\pi[(1+\alpha^2)R + (1-\alpha)s + 2\alpha^2 R]$. □

User costs

From this point on, user costs are evaluated. As the case $\alpha \leq \phi$ of the hybrid network atop a grid street pattern, there are also six types of trip here. Again, they differ in the location of their origin and destination. There are three possible areas for that location: (i) the central area served by the ring-radial mesh, where there is a portion $\rho\alpha^2/\phi^2$ of origins and α^2/ϕ^2 of destinations with regard to the total; (ii) an intermediate area between cordons αR and ϕR, which is only served by branched radial lines and generates a portion $\rho(\phi^2 - \alpha^2)/\phi^2$ of origins and attracts a portion $(\phi^2 - \alpha^2)/\phi^2$ of destinations; finally, (iii) the most external area that only generates trips, in a portion $1 - \rho$, but does not attract. Based on this division of the city, when the destination is in the central mesh, there are three different types of trip in function to the origin: (f.1) central, whose probability is $P[\text{f. 1}] = \rho\alpha^4/\phi^4$, (f.2) intermediate, $P[\text{f. 2}] = \rho(\phi^2 - \alpha^2)\alpha^2/\phi^4$, and (f.3) external, $P[\text{f. 3}] = (1-\rho)\alpha^2/\phi^2$. When the destination is in the intermediate area, other three types of trip exist: (f.4) central origin, $P[\text{f. 4}] = \rho\alpha^2(\phi^2 - \alpha^2)/\phi^4$, (f.5) intermediate origin, $P[\text{f. 5}] = \rho(\phi^2 - \alpha^2)^2/\phi^4$, and (f.6) external origin, $P[\text{f. 6}] = (1-\rho)(\phi^2 - \alpha^2)/\phi^2$.

Another aspect to consider is the relative position between origin and destination. Users follow the shortest path, although in some cases they make one transfer more. For this reason, if the angle between origin and destination is smaller than 2 radians, users complete the trip by means of a circular line. Otherwise, they only use radial lines.

Result C.6. The expected number of transfers per trip is given by (C.6):

$$e_T = 1 + [4(\phi^2 - \alpha^2) - \theta(\phi^2 + \alpha^2)]/2\pi\phi^2 - \rho\alpha^2[3R(4+\theta)(\phi^2 - \alpha^2) + 4\alpha s(4-\theta)]/6\pi\phi^4 R \tag{C.6}$$

where:

$$P_0 = (\alpha^2/\phi^2)\left[\theta/\pi + \rho\left(3R\theta(\phi^2 - \alpha^2) + 2\alpha s(4-\theta)\right)/3\pi\phi^2 R\right] \tag{C.6.1}$$

$$P_1 = 1 - [4(\phi^2 - \alpha^2) - \theta(\phi^2 - 3\alpha^2)]/2\pi\phi^2 + \rho\alpha^2[3R\theta(4 - 3\theta)(\phi^2 - \alpha^2) - 4\alpha s(4 - \theta)]/6\pi\phi^4 R \quad \text{(C.6.2)}$$

$$P_2 = (4 - \theta)(\phi^2 - \alpha^2)(1 - \rho\alpha^2/\phi^2)/2\pi\phi^2 \quad \text{(C.6.3)}$$

Proof. In this network, one trip can involve zero, one or two transfers depending on the type of trip. We assume that direct connections (origin and destination in the influence area of the same line) only exist if at least one of the extremes of the trip belongs to the central mesh. Therefore, in categories (f.1)-(f.4). Given an origin or destination, the probability that the other extreme is located around the same radial line is θ/π. In category (f.1), there are also direct trips around circular lines. The area of influence of those lines has a width s, and users only use them if the destination is in less than 2 radians of angular distance from the origin. The probability of these trips is $\int_0^{\alpha R}(2r_o/\alpha^2R^2)\int_{r_o-s/2}^{r_o+s/2}\big((4-\theta)/2\pi\big)(2r_d/\alpha^2R^2)dr_a\,dr_o = 2s(4-\theta)/3\pi\alpha R$. Weighting by the respective probabilities of each trip category, the portion of zero-transfer trips is $P[0T] = (\alpha^2/\phi^2)\big[\theta/\pi + \rho\big(3R\theta(\phi^2 - \alpha^2) + 2\alpha s(4 - \theta)\big)/3\pi\phi^2 R\big]$.

On the other hand, in categories (f.5) and (f.6), there are two-transfer trips. These have origin and destination in the branched section of the radial lines and the angular distance between both extremes is smaller than 2 radians. Therefore, the probability of these trips in each category is $(4 - \theta)/2\pi$. The total portion of them in the network is $P[2T] = (4 - \theta)(\phi^2 - \alpha^2)(1 - \rho\alpha^2/\phi^2)/2\pi\phi^2$. Knowing $P[0T]$ and $P[2T]$, we obtain the probability of one-transfer trips by means of the total probability theorem: $P[1T] = 1 + [\theta(\phi^2 - 3\alpha^2) - 4(\phi^2 - \alpha^2)]/2\pi\phi^2 + \rho\alpha^2[3R\theta(4 - 3\theta)(\phi^2 - \alpha^2) - 4\alpha s(4 - \theta)]/6\pi\phi^4 R$.

Finally, the expected number of transfers per trip is $e_T = P[1T] + 2 \cdot P[2T]$. □

Result C.7. The expected walking time at the origin and destination is given by (C.7):

$$A = [\alpha R\theta(6\phi^2 - \alpha^2 - \rho\alpha^2)/12\phi^2 + s/2]/w \quad \text{(C.7)}$$

Proof. It is assumed that every user connects to the system at its nearest stop. The average distance to one stop is the mean between the closest user and the furthest one. The former is the stop itself, which implies a null distance. The walking distance in the latter is decomposed in two. One radial path whose length is $s/2$ and constant along the central mesh. The other is a perimeter path that varies with the distance from the city center with a ratio $\theta/2$. Therefore, the average walking distance for a stop at a cordon βR is $\beta R\theta/4 + s/4$. As β follows a triangular probability density function $2\beta/\alpha^2$ in the central mesh, the resultant average walking distance in that ring-radial mesh is $\int_0^{\alpha}(2\beta/\alpha^2)(\beta R\theta/4 + s/4)d\beta = \alpha R\theta/6 + s/4$. In the branched section of the radial lines out the central mesh, the accessibility is constant and equal to the boundary αR. Therefore, the average access distance is $\alpha R\theta/4 + s/4$.

On the other hand, the egress cost is the same as the access. The total walking distance is the result of weighting each of the aforementioned distances by the portion of trips generated and attracted in the central mesh and in the periphery. That distance is $(\alpha R\theta/6 + s/4)(1 + \rho)\alpha^2/\phi^2 + (\alpha R\theta/4 + s/4)(1 + \rho)(\phi^2 - \alpha^2)/\phi^2 + (\alpha R\theta/4 + s/4)(1 - \rho) = \alpha R\theta(6\phi^2 - \alpha^2 - \rho\alpha^2)/12\phi^2 + s/2$. Finally, the expected walking time is the previous total distance divided by the pedestrian speed. □

Result C.8. The expected waiting time per user including the origin and all transfer stops is given by (C.8):

$$W = \rho W_c + (1-\rho)W_p \tag{C.8}$$

where:

$$W_c = H\left[4\pi\phi^2(2\phi^3+\alpha^3)R + 3\alpha R\left((4-\theta)\phi^4 - (4+\theta)\alpha^2(2\phi^2-\alpha^2)\right) - 4\alpha^4 s(4-\theta)\right]/ 12\pi\alpha\phi^4 R \tag{C.8.1}$$

$$W_p = H\left[2\pi\left(2\phi^2+(4\phi^3+\alpha^3)(1+\phi)\right) + 3\alpha(1+\phi)\left(4(\phi^2-\alpha^2) - \theta(\phi^2+\alpha^2)\right)\right]/12\pi\alpha\phi^2(1+\phi) \tag{C.8.2}$$

Proof. The waiting time at stops is assumed equal to a half of the headway of service since the system works in headways. This headway of service is constant in the central area, which value is H. However, in the peripheral band where the radial lines branch, that headway increases with the distance from the city center. At cordon βR of that periphery, the headway is $\beta H/\alpha$. This result is a consequence of the assumption that the vehicle flow is constant in any cordon. At boundary of the central mesh the number of lines is $2\pi/\theta$, each served by $1/H$ vehicles. Then, the vehicle flow that goes out of the central area is $2\pi/\theta H$. To maintain a constant spatial accessibility, the angle between radial lines have to decrease with the distance from the center. Approximately, the angle at cordon βR is $(\alpha/\beta)\theta$, that is, $2\pi/(\beta/\alpha)\theta$ radial lines. As the flow is constant, dividing the total flow that leaves from the central mesh by the number of lines at cordon βR, we obtain the number of vehicles per line $\alpha/\beta H$, and the headway of service $\beta H/\alpha$ at stops of that cordon. As it is commented above, we distinguish two areas in the periphery, one intermediate and other external. β has a p.d.f. $2\beta/(\phi^2-\alpha^2)$ in the former and $2\beta/(1-\phi^2)$ in the latter. Therefore, the average headway in each area is $H_i = \int_\alpha^\phi \left(2\beta/(\phi^2-\alpha^2)\right)(\beta H/\alpha)d\beta = 2(\phi^2+\phi\alpha+\alpha^2)H/3\alpha(\phi+\alpha)$ and $H_p = \int_\phi^1 \left(2\beta/(1-\phi^2)\right)(\beta H/\alpha)d\beta = 2(1+\phi+\phi^2)H/3\alpha(1+\phi)$ respectively.

To estimate the waiting time for the different types of trips, these are divided into sections. The first section starts at the origin, and each of the remainder at stop where the user transfers. Furthermore, the waiting time in each section is determined by the highest headway of service between the initial and final stop of the section. Trips (f.1)-(f.4) have zero or one transfer, that is, one or two sections. For zero-transfer trips, categories (f.1)-(f.3) have their destination in the central mesh. Therefore, the origin fixes the waiting time: $H/2$, $H_i/2$ and $H_p/2$ respectively. For category (f.4), the destination fixes the waiting time since the origin is in the central area and the destination in the intermediate; that time is $H_i/2$. When a trip of these categories has one transfer, the additional section starts and finishes in the ring-radial mesh, which implies an additional time $H/2$. On the other hand, trips (f.5) and (f.6) have one or two transfers. The waiting time of the first section depends on the origin and of the last section on the destination: $H_i/2$ and $H_i/2$ for category (f.5), and $H_p/2$ and $H_i/2$ for category (f.6). If an intermediate third section exists, it starts and finishes in the central mesh, therefore, an additional waiting time $H/2$. With all this and the probability of number of transfers from Result C.6, the waiting time for each type of trip is obtained:

$$W(\text{f.}1) = H/2 + H/2\cdot(1-\theta/\pi - 2s(4-\theta)/3\pi\alpha R) = H[1-\theta/2\pi - s(4-\theta)/3\pi\alpha R] \tag{B.8.3}$$

$$W(\text{f.}2) = W(f.4) = H_i/2 + H/2\cdot(1-\theta/\pi) = H[(2\phi^2+5\phi\alpha+5\alpha^2)/6\alpha(\phi+\alpha) - \theta/2\pi] \tag{B.8.4}$$

$$W(\text{f.}3) = H_p/2 + H/2\cdot(1-\theta/\pi) = H[1/2 + (1+\phi+\phi^2)/3\alpha(1+\phi) - \theta/2\pi] \tag{B.8.5}$$

$$W(\text{f.}4) = H_i/2 + H/2\cdot(1-2s/(\phi+\alpha)D) = H[(2\phi^2+5\phi\alpha+5\alpha^2)/6\alpha(\phi+\alpha) - s/(\phi+\alpha)D] \tag{B.8.6}$$

$$W(\text{f.}5) = H_i/2 + H_i/2 + H/2 \cdot (1-(4-\theta)/2\pi) = H[(4\phi^2+7\phi\alpha+7\alpha^2)/6\alpha(\phi+\alpha) - (4-\theta)/4\pi] \quad \text{(B.8.7)}$$

$$W(\text{f.}6) = H_p/2 + H_i/2 + H/2 \cdot (1-(4-\theta)/2\pi) = H\big[\big(2(\phi+\alpha)+(4\phi^2+7\phi\alpha+5\alpha^2)(1+\phi)\big)/6\alpha(\phi+\alpha)(1+\phi) - (4-\theta)/4\pi\big] \quad \text{(B.8.8)}$$

The last step is weighting the partial waiting times per trip category, which gives the total average waiting time W. □

Result C.9. The expected in-vehicle travel distance per trip is given by (C.9):

$$T = E/v_c = \big[\rho E_c + (1-\rho)E_p\big]/v_c \quad \text{(C.9)}$$

where:

$$E_c = R[5\pi\alpha R\theta\phi^2(2\phi^3-3\alpha\phi^2+\alpha^3) + 4s(10\pi\phi^5 - 15\alpha\phi^4 + 10\alpha^3\phi^2 - 3\alpha^5)]/30\pi\phi^4 s \quad \text{(C.9.1)}$$

$$E_p = R\big[\pi\alpha R\theta\big(2\phi^2+(1+\phi)(4\phi^3-6\alpha\phi^2+\alpha^3)\big) + 8s\big(\pi\phi^2+(1+\phi)(2\pi\phi^3-3\alpha\phi^2+\alpha^3)\big)\big]/12\pi\phi^2(1+\phi)s \quad \text{(C.9.2)}$$

Proof. To connect any two points of the city, the undertaken trip is that of a minimum length. Here, the shortest route has priority over others that involve less transfers. A trip is always composed of a central section and sometimes by another peripheral if its origin or destination is outside of the central mesh. At the same time, the peripheral distance is divided in two sections: one from the origin to the central mesh' boundary, and other from that boundary to the destination. Every trip may have these two sections, only one section or none at all. An origin located in a cordon βR travels in the radial direction $(\beta-\alpha)R$ units of distance and in the transverse direction $\theta\alpha(\beta-\alpha)R^2/4s$. The latter is a consequence of the line branching. From result C.1, in each strip, one line runs on average a perimeter length $\theta\alpha R/4$, and this happens $(\beta-\alpha)R/s$ times (the number of strips crossed). As it is known the p.d.f. of β, the average peripheral length traveled from an external origin is $E_p = \int_\phi^1 \big(2\beta/(1-\phi^2)\big)\,[(\beta-\alpha)R + \theta\alpha(\beta-\alpha)R^2/4s]d\beta = R(\alpha R\theta+4s)[2(1+\phi+\phi^2)-3\alpha(1+\phi)]/12s(1+\phi)$. If that origin is located in the intermediate area, that distance is $E_i = \int_\alpha^\phi \big(2\beta/(\phi^2-\alpha^2)\big)\,[(\beta-\alpha)R + \theta\alpha(\beta-\alpha)R^2/4s]d\beta = R(\alpha R\theta+4s)(2\phi^2-\phi\alpha-\alpha^2)/12s(\phi+\alpha)$. Regarding the destination, it can be only located in the intermediate area as a consequence of the attractant demand distribution. The length of this section is also E_i.

Regarding the central section, different routes are followed in the central area with regard to the type of trip. Trips (f.1) have origin and destination randomly located inside the central mesh, whose expected length is $E_{c,1}$. There are two different situations depending on the relative position between the origin $P_O(r_O,\theta_O)$ and the destination $P_D(r_D,\theta_D)$: (i) combination of radial and circular lines in the case that $\theta_O-2<\theta_D<\theta_O+2$, where distance traveled is $|r_D-r_O| + min(r_O,r_D)\cdot|\theta_O-\theta_D|$; and (ii) combination of radial lines exclusively in the case that $\theta_O+2<\theta_D<\theta_O+2\pi-2$, where distance traveled is r_O+r_D. The average distance is weighted from the probability of the respective radius and angle of origin and destination. The p.d.f.'s of the previous variables are $f_{r_O}=2r_O/\alpha^2R^2$, $f_{r_D}=2r_D/\alpha^2R^2$, $f_{\theta_O}=1/2\pi$ and $f_{\theta_D}=1/2\pi$; and finally, it gives $E_{c,1} = \int_0^{2\pi}\int_{\theta_O-2}^{\theta_O+2}\int_0^{\alpha R}\int_0^{r_D} f_{r_O}f_{r_D}f_{\theta_O}f_{\theta_D}[(r_D-r_O)+r_O|\theta_O-\theta_D|]dr_Odr_Dd\theta_Dd\theta_O + \int_0^{2\pi}\int_{\theta_O-2}^{\theta_O+2}\int_0^{\alpha R}\int_0^{r_O} f_{r_O}f_{r_D}f_{\theta_O}f_{\theta_D}[(r_O-r_D)+r_D|\theta_O-\theta_D|]dr_Ddr_Od\theta_Dd\theta_O + \int_0^{2\pi}\int_{\theta_O+2}^{\theta_O+2\pi-2}\int_0^{\alpha R}\int_0^{\alpha R} f_{r_O}f_{r_D}f_{\theta_O}f_{\theta_D}[(r_O+r_D)]dr_Ddr_Od\theta_Dd\theta_O = 4\alpha R(5\pi-4)/15\pi$.

Trips (f.2)-(f.4) have a section in the central mesh where one extreme is inside of it and the other in the boundary of that mesh, and whose average distance is $E_{c,2}$. Trips (f.5) and (f.6) have a central section whose extremes are located in the previous boundary; this section has a length $E_{c,3}$. We follow the same process to calculate both distances. From geometric probability, $E[E_{c,2}|r'] = \alpha R[1 + (E[r']/\alpha R)(1 - 2/\pi)]$ is obtained, where r' is the radius of the cordon where the beginning or end of the inner section lies. To calculate the expectation of r', this radius is weighted based on its p.d.f. $f_{r'} = 2r'/\alpha^2 R^2$. So that, $E_{c,2} = [\alpha R + (1 - 2/\pi)\int_0^{\alpha} f_{r'} r' dr'] = \alpha R(5\pi - 4)/3\pi$. In the case of distance $E_{c,3}$, r' is αR since the central mesh's boundary collects all the peripheral demand, and $E_{c,3} = 2\alpha R(1 - 1/\pi)$.

Once the length of the different possible sections of one trip are estimated, we are able to obtain the distance traveled in each type of trip:

$$E(\text{f.}1) = E_{c,1} = 4\alpha R(5\pi - 4)/15\pi \tag{B.9.3}$$

$$E(\text{f.}2) = E(\text{f.}4) = E_i + E_{c,2} = R[\pi\alpha R\theta(2\phi^2 - 6\alpha\phi - \alpha^2) + 8s(\pi\phi^2 + 2(\pi - 1)\alpha(\phi + \alpha))]/12\pi(\phi + \alpha)s \tag{B.9.4}$$

$$E(\text{f.}3) = E_p + E_{c,2} = R[\pi\alpha R\theta(2 + (2\phi - 3\alpha)(1 + \phi)) + 8s(\pi(\phi + \alpha) - 2\alpha(1 + \phi))]/12\pi(1 + \phi)s \tag{B.9.5}$$

$$E(\text{f.}5) = 2E_i + E_{c,3} = R[\pi\alpha R\theta(2\phi^2 - \alpha\phi - \alpha^2) + 4s(2\pi(\phi^2 + \alpha\phi + \alpha^2) - 3\alpha(\phi + \alpha))]/6\pi(\phi + \alpha)s \tag{B.9.6}$$

$$E(\text{f.}6) = E_p + E_{c,3} + E_i = R[\pi\alpha R\theta(\phi + \alpha + (1 + \phi)(2\phi^2 - \alpha\phi - \alpha^2)) + 4s(\pi(\phi + \alpha) + (1 + \phi)\pi(2\phi^2 + 2\alpha\phi + \alpha^2) - 3\alpha(1 + \phi)(\phi + \alpha))]/6\pi(\phi + \alpha)(1 + \phi)s \tag{B.9.7}$$

Finally, the expected in-vehicle distance traveled per trip E in the network is calculated by means of weighting the length of the different types of trip by their respective probabilities. □

Constraints

Result C.10. The expected vehicle occupancy on the critical load point during the rush hour is given by (C.10):

$$O = (SF)max\{O_{rp};\ O_{cp};\ O_{rc}, if\ r_r < \alpha R;\ O_{cc}, if\ r_c < \alpha R\} \tag{C.10}$$

Proof. The vehicle occupancy is studied in those critical points of the system that present higher passenger loads. Figure 3.9c shows the location of those points in this network. Two possible locations exist: inner point of the ring-radial mesh and in the boundary of that mesh. In addition, as two types of lines compose the network, we distinguish the occupancy of the radial lines and the circular lines. As the generated and attracted curves of demand are different, the occupancy in one direction can be different than in the other. It is easy to check that the generated demand produces higher loads in the radial lines than the attracted. The percentage of generated demand out of the mesh is greater than the attracted, and that demand is only carried by the radial lines. However, regarding circular lines, the attraction determines the highest occupancy for the same reason. The circular lines only serve inside the central mesh where the attracted trips are more than the generated.

Ring-radial mesh's boundary: The demand that crosses this limit through the radial corridors at rush hour coincides with the demand generated out of the central mesh: at the intermediate area $\Lambda\rho(\phi^2 - \alpha^2)/\phi^2$ and at the external periphery $\Lambda(1 - \rho)$. This demand is allocated on the

existing corridors, whose number is $2\pi/\theta$. As corridors are branched, some of them cover a larger area than the others, approximately a double peripheral area such as Figure C.1 shows. For this reason, that demand is multiplied by a factor 2. Finally, such demand is assigned to the number of vehicles that give service $(1/H)$, obtaining the following occupancy $O_{rp} = H\theta\Lambda(1-\rho\alpha^2/\phi^2)/\pi$. Regarding the circular border corridor, the maximum occupancy that a vehicle supports is obtained from the number of trips generated in the influence area of this corridor and the rest of the periphery in an arc of 2 radians, whose destination is situated on an average 1 radian with respect to the analyzed point. Obviously, this demand have to be redistributed by the number of vehicles $(1/H)$, giving an occupancy of $O_{cp} = H\Lambda[4R^2(\phi^2-\rho\alpha^2)+\rho s(4\alpha R-s)][4R^2(\phi^2-\alpha^2)+s(4\alpha R-s)]/32\pi^2\phi^4R^4$.

Inside the ring-radial mesh: The number of passengers that crosses a point of a radial line at distance form then city center r_r is all the demand generated in the area of influence of the radial line beyond that point, and attracted inside the cordon where the point is located and outside that cordon if the destination is spaced angularly in more than 2 radians from that radial line. The former demand is $\theta\Lambda\left[(\rho\alpha^2/\phi^2)(\pi\alpha^2R^2-\pi r_r^2)/\pi\alpha^2R^2+2\left(\rho(\phi^2-\alpha^2)/\phi^2+(1-\rho)\right)\right]/2\pi$; and the latter is $\theta\Lambda[(1-2/\pi)(\pi\phi^2R^2-\pi r_r^2)/\pi\phi^2R^2+\pi r_r^2/\pi\phi^2R^2]/2\pi$. The value of r_r that gives the maximum occupancy is $R\sqrt{\rho(4\phi^2+2\rho\phi^2-\pi\rho\phi^2-2\rho\alpha^2)}/2\rho$. Finally, allocating the passengers to the vehicles that serve the line $(1/H)$, we obtain the maximum occupancy at inner point of a radial line $O_{rc} = H\theta\Lambda[4\phi^2+\rho(\pi\phi^2-2\phi^2-2\alpha^2)]^2/16\pi^2\phi^4\rho$. On the other hand, a circular line at a distance r_c from the city center carries all the demand attracted in its surroundings in an arc length of 2 radians and is generated out of the cordon where the line is located. That is, $(2\Lambda s r_c/\pi\phi^2R^2)[4\phi^2R^2-\rho(2r_c-s)^2]/8\pi\phi^2R^2$. Then, the most loaded line is located at a radius $r_c = s/3+\sqrt{12\rho\phi^2R^2+\rho^2s^2}/6\rho$. As the line is served by $1/H$ vehicles, the most occupied vehicle in a circular line carries $O_{cc} = H\Lambda s\left(2\rho s+\sqrt{\rho(12\phi^2R^2+\rho s^2)}\right)\left(12\phi^2R^2+s\sqrt{\rho(12\phi^2R^2+\rho s^2)}-\rho s^2\right)/108\pi^2\phi^4R^4\rho$.

Finally, from the different analyzed points of the system, the point that presents the greatest occupancy is the determinant in the model's results. However, whether r_r or r_c are located out of the central mesh, the inner points would be in the boundary. Therefore, we only consider O_{rp} and O_{cp}. Furthermore, the rush hour also has its own peaks, for this reason, the occupancy is exacerbated by a safety factor (SF). □

C.2. Radial network structure

The radial structure is composed by radial lines concentrated in the central point of the city and branched as they run away from that center. As Figure 3.7a shows, these lines follow the same branching as the radial lines of the hybrid scheme. Therefore, the agency costs are derived in the same way as these costs in the peripheral band of the previous structure. To derive the cost we have to replace αR by s. Equations (C.11), (C.12) and (C.13) calculate infrastructure length, kilometers travelled and commercial speed respectively. In this case, the number of stops is $2\pi R(R+s)/\theta s^2$. Fleet is also estimated by Equation (C.4).

$$L = \pi[(4+\theta)R(R+s)-2\theta s^2]/4s\theta \tag{C.11}$$

$$V = \pi[(4+\theta)R-\theta s]/\theta H \tag{C.12}$$

$$v_c = 1/[1/v+\tau/l_s+\tau'(1+e_T)\Lambda/V] = 1/[1/v+\tau\pi R(R+s)/L\theta s^2+\tau'\Lambda(1+e_T)/V] \tag{C.13}$$

Regarding user costs, Equation (C.14) gives the access time, the same as the peripheral stops in the hybrid network. However, the remainder costs are again derived since the number of transfers are estimated with more accuracy. First of all, there are two types of trip in this network: (g.1) origin in the central attractant area, whose probability is $P[\text{g. 1}] = \rho$, and (g.2) origin in the periphery out of that central area, $P[\text{g. 2}] = (1 - \rho)$.

$$A = s(1 + \theta)/2w \tag{C.14}$$

Result C.15. The expected number of transfers per trip is given by (C.15):

$$e_T = 1 - 2s\theta(3 + \rho)/3\pi\phi R \tag{C.15}$$

Proof. As atop a grid street pattern, the more central one stop is, the larger its influence area. Therefore, the probability of direct trips between two cordons is determined by the most central one. Given two cordons $\beta_O D$ and $\beta_D D$, if the former is greater, that probability is $\theta s/\pi\beta_O D$, otherwise, $\theta s/\pi\beta_D D$. Knowing that the p.d.f. of β_O and β_D is $2\beta_i/\phi^2$ in the central area, $\int_0^{\phi}(2\beta_O/\phi^2)\left[\int_0^{\beta_O}(2\beta_D/\phi^2)(\theta\, s/\pi\beta_D R)\, d\beta_D + \int_{\beta_O}^{\phi}(2\beta_D/\phi^2)(\theta\, s/\pi\beta_O R)\, d\beta_D\right] d\beta_O = 8s\theta/3\pi\phi R$ is the probability of zero-transfer of trips (g.1). If the origin is peripheral, that probability is always determined by the destination. Therefore, $\int_0^{\phi}(2\beta_D/\phi^2)(\theta\, s/\pi\beta_D R)\, d\beta_D = 2s\theta/\pi\phi R$ is the probability of direct trips in category (g.2). Finally, weighting by each trip category, we obtain the portion of direct trips in this network structure $P[0T] = 2s\theta(3 + \rho)/3\pi\phi R$.

The remainder of trips imply one transfer. The total probability theorem gives their probability, coincident with the expected number of transfers per trip e_T. □

Result C.16. The expected waiting time per user including the origin and all transfer stops is given by (C.16):

$$W = H\left[15\pi R(1 + 2\phi + 2\phi^2) - 30\theta s(1 + \phi) - \rho\left(15\pi R + 2\theta s(1 + \phi)\right)\right]/45\pi s(1 + \phi) \tag{C.16}$$

Proof. The system works in headways and the vehicle flow along the city is constant. This flow at city center is $2\pi/\theta H$. As the lines that cross a cordon at a distance βD is $2\pi\beta R/\theta s$, the headway of one stop at that cordon is $H\beta R/s$. Again, the headway that determines the waiting time is the highest between the extremes of each section that compose the trip. For trips (g.2), the headway at origin always defines the waiting time of the initial section of every trip. The average headway in that periphery is $H_p = \int_{\phi}^{1}[2\beta/(1 - \phi^2)](H\beta R/s)\, d\beta = 2(1 + \phi + \phi^2)RH/3s(1 + \phi)$, and the waiting time a half of it. When the user makes a transfer at city center, the waiting time for that second section is a half of the average central headway $H_c = \int_0^{\phi}(2\beta/\phi^2)(H\beta R/s)\, d\beta = 2\phi RH/3s$. The expected waiting time for category (g.2) weighted by the percentage of direct and transfer trips is $W_p = \left[H_p + H_c(1 - 2s\theta/\pi\phi R)\right]/2 = H[\pi R(1 + 2\phi + 2\phi^2) - 2\theta s(1 + \phi)]/3\pi(1 + \phi)s$.

Two sections compose one-transfer trips of category (g.1). Both sections have origin and destination at central attractant area, that is, two waiting times $H_c/2$. However, for direct trips, there is only one section, and the waiting time is determined by the highest headway of service between the extremes of the trip; that is, $H_{c,0T} = \int_0^{\phi}(2\beta_O/\phi^2)\left[\int_0^{\beta_O}(2\beta_D/\phi^2)(H\beta_O R/s)\, d\beta_D + \int_{\beta_O}^{\phi}(2\beta_D/\phi^2)(H\beta_D R/s)\, d\beta_D\right] d\beta_O = 4\phi RH/5s$. Finally, the expected waiting time for trips (g.1) is $W_c = \left[2H_c(1 - 8s\theta/3\pi\phi R) + H_{c,0T}(8s\theta/3\pi\phi R)\right]/2 = 2H[15\phi R - 16\theta s]/45\pi s$.

Knowing the previous results, the waiting time is $W = W_c\, P[c.1] + W_p\, P[c.2]$. □

Result C.17. The expected in-vehicle travel time per trip is given by (C.17):

$$T = E/v_c = (4+\theta)\begin{bmatrix}15\pi R(1-\phi)(1+2\phi+2\phi^2-\rho)\\ -2\theta s(15-18\phi^2+\rho+2\rho\phi)\end{bmatrix}/90\pi(1-\phi^2)v_c \qquad \text{(C.17)}$$

Proof. The distance traveled in this structure follows the same routing as the periphery of the hybrid scheme. Trips (g.1) with one transfer have two sections, from the origin at cordon $\beta_O D$ to the central point of the network, and from that point to the destination at cordon $\beta_D D$: $E_c = \int_0^{\phi}(2\beta_O/\phi^2)[\beta_O R(4+\theta)/4]\,d\beta + \int_0^{\phi}(2\beta_D/\phi^2)[\beta_D R(4+\theta)/4]\,d\beta = (4+\theta)\phi R/3$. The same distance is traveled for direct trips that pass through the city center, a half of them, those that cross the center to go to the other side of the city. On the other hand, when the trip does not need to arrive to that center, $E_{c,0T} = \int_0^{\phi}\int_0^{\phi}(2\beta_O/\phi^2)(2\beta_D/\phi^2)\left[(4+\theta)\left|\beta_O-\beta_D\right|R/4\right]d\beta_D\,d\beta_O = (4+\theta)\phi R/15$ is the trip length. Weighting by their respective probabilities, $E(c.1) = E_c\cdot(1-4s\theta/3\pi\phi R) + E_{c,0T}\cdot(4s\theta/3\pi\phi R) = (4+\theta)(15\pi\phi R - 16\theta s)/45\pi$.

In the case of category (g.2), we do the same process. Then, $E_p = \int_{\phi}^{1}(2\beta_O/\phi^2)[\beta_O R(4+\theta)/4]\,d\beta + \int_0^{\phi}(2\beta_D/\phi^2)[\beta_D R(4+\theta)/4]\,d\beta = (4+\theta)(1+2\phi+2\phi^2)R/6(1+\phi)$, $E_{p,0T} = \int_{\phi}^{1}\int_0^{\phi}(2\beta_O/\phi^2)(2\beta_D/\phi^2)[(4+\theta)(\beta_O-\beta_D)\,R/4]\,d\beta_D\,d\beta_O = (4+\theta)(5-5\phi+2\phi^3)R/30(1-\phi^2)$, and therefore, $E(c.2) = E_p(1-s\theta/\pi\phi R) + E_{p,0T}(s\theta/\pi\phi R) = (4+\theta)[5\pi(1+\phi-2\phi^3)R - 2\theta s(5-6\phi^2)]/30\pi(1-\phi^2)$. Finally, with these result, we obtain the average distance $E = E(c.1)\,P[c.1] + E(c.2)\,P[c.2]$. □

Constraints

Result C.18. The expected vehicle occupancy on the critical load point during the rush hour is given by (C.18):

$$O = (SF)H\Lambda\theta[3\pi\phi R - \theta s(3+\rho)]/6\pi^2\phi R \qquad \text{(C.18)}$$

Proof. Figure 3.9a shows that the most loaded point of this structure is the central point of the city. All passengers that make a transfer go through that center. In addition, a half of direct trips too, as it is commented in the previous Result C.17. Therefore, the number of passengers during the rush hour at that point is $\Lambda[1-(3+\rho)\theta s/3\pi\phi R]$. All of this demand is allocated along the different corridors at city center $2\pi/\theta$ and the vehicles that serve each of them $1/H$. Therefore, the maximum vehicle occupancy is $H\Lambda\theta[3\pi\phi R-(3+\rho)\theta s]/6\pi^2\phi R$. As in the rest of structures, this value is penalized by the factor (SF). □

C.3. Direct trip-based network structure

From the explanation in Section 3.5, we start now the derivation of the formulas that calculate the costs of this network structure. As in the grid street pattern, the central attractant area is divided into concentric circular swaths of width d. One central served by the previous radial network, and each of the rest of swaths by additional lines. Each of these lines connect its respective swath to an external sector. Figures 3.7b and 3.8 help to understand the arrangement of the lines in detail. In each swath, the lines run a semicircular length in a central swath-corridor. These corridors are located at a distance $i\cdot d$ from the city center, where i=1,2,…,n, being n the number of swaths $(2\phi R-d)/2d$ without considering the central one. The remainder

length of these lines cross in a radial direction the external area of the city. This branched route section is marked by the decision variables s and θ by the central arc length θs.

Another relevant change from the previous structures is the possibility of two types of services: in headways or by schedules. The former happens when the headway of service is lower than H_s, and the latter when it is higher. This fact divides the city in two areas at cordon $\varepsilon_H R$. Inside this cordon the system works in headways and out of it by schedules. The value of ε_H is $H_s s/HR$. We accept to work by schedules in this structure since transfers do not exist; that is, e_T is zero.

The last aspect to comment is that the fleet of the network is estimated by Equation (C.4) derived above.

Agency costs

Result C.19. The total length of the two-way infrastructure system is given by (C.19):

$$L = \pi[(4+\theta)R(R+s) - 2\theta s^2]/4s\theta + \pi(4\phi^2R^2 - d^2)/4d \tag{C.19}$$

Proof. This length is the result to add the swath-corridors length to the initial radial network in Equation (C.11). One swath-corridor is a circumference of radius $i \cdot d$. Therefore, the additional length is $\sum_1^{(2\phi R-d)/2d} 2\pi id = \pi(4\phi^2R^2 - d^2)/4d$. □

Result C.20. The total vehicle-distance traveled per hour is given by (C.20):

$$V = \pi\left[4\phi R^2\left((4+\theta)(2-\phi) + 2\pi\phi\right) - d\left(2d(\pi-2) - \theta(d-4s)\right)\right]/4d\theta H \tag{C.20}$$

Proof. Again, we add the vehicle-kilometers of the remainder of swaths to those done from the central swath, given by Equation (C.12). One line that serve a swath at a cordon $i \cdot d$ runs from the city edge to its swath-corridor a length $\left((4+\theta)s/4\right)\left((R-id)/s\right)$, along that corridor a length πid, and finally, from that swath-corridor to the city edge $\left((4+\theta)s/4\right)\left((R-id)/s\right)$ units of distance. This length is multiplied by 2 due to its bidirectionality. As the number of vehicles that serve a swath is $2\pi/\theta H$, the kilometers traveled from that swath are $2\pi[(4+\theta)R + (2\pi-4-\theta)id]/\theta H$. Adding all the swaths, we obtain $\pi(2\phi R - d)[2R(8+2(\pi-2)\phi + (2-\phi)\theta) + d(2\pi-4-\theta)]/4d\theta H$. The resultant kilometers travelled are the total sum between the radial network and the remainder of swaths, $V = \pi\left[4\phi R^2\left((4+\theta)(2-\phi) + 2\pi\phi\right) - d\left(2d(\pi-2) - \theta(d-4s)\right)\right]/4d\theta H$. □

Result C.21. The expected commercial speed during the rush hour is given by (C.21):

$$v_c = 1/[1/v + \tau/l_s + \tau'\Lambda/V] = 1/[1/v + \tau\pi[4dR(R+s) + s(4\phi^2R^2 - d^2)]/4L\theta ds^2 + \tau'\Lambda/V] \tag{C.21}$$

Proof. In this case, the number of stops is $2\pi R(R+s)/\theta s^2 + \pi(4\phi^2R^2 - d^2)/2\theta ds$, and no transfers exist, i.e., $e_T = 0$. □

User costs

In this structure, we distinguish two categories of trip: (h.1) with the origin in the central attractant area, whose probability is $P[\text{h.1}] = \rho$; and (h.2) when the origin is external, with a probability $P[\text{h.2}] = (1-\rho)$.

Result C.22. The expected walking time at the origin and destination is given by (C.22):

$$A = [s(1+2\theta)+d]/4w \tag{C.22}$$

Proof. The access distance at the beginning of the trip is equal to the access distance in the radial network structure: $s(1+\theta)/4$. However, the egress distance is not coincident. In this case, the final stop is at one swath-corridor. The width of one swath is d, and therefore, the user on average walks in the radial direction a quarter of that width. On the ring direction, the walking distance is $\theta s/4$ since the stop spacing is θs. Finally, adding these distances and dividing by the pedestrian speed, the total access cost is: $[s(1+2\theta)+d]/4w$. □

Result C.23. The expected waiting time per user at a stop is given by (C.23):

$$\begin{aligned}
&\text{if } \varepsilon_H \geq 1 && W = H[5(1-\rho)+\phi(1+\phi)(5+\rho)]R/15(1+\phi)s \\
&\text{if } \phi \leq \varepsilon_H < 1 && W = \left[h_s(1-\varepsilon_H^2) + H\left(2f_s(1-\varepsilon_H^3)+(\varepsilon_H^3-\phi^3)\right)R/3s\right](1-\rho)/(1-\phi^2) + 2\phi RH\rho/5s \\
&\text{if } \varepsilon_H < \phi && W = [h_s + 2f_s(1+\phi+\phi^2)RH/3(1+\phi)s](1-\rho) + \left[h_s(\phi^4-\varepsilon_H^4) + 2H\left(2f_s(\phi^5-\varepsilon_H^5)+\varepsilon_H^5\right)R/5s\right]\rho/\phi^4
\end{aligned} \tag{C.23}$$

Proof. Two aspects are highlighted. First, the headway of service at one stop increases with the distance from the city center due to the line branching. At a cordon βR, the headway is $\beta RH/s$ as in the radial network structure derived above. Secondly, as all of trips are direct, the system can work in headways and by schedules. The former implies a waiting time equivalent to a half of the headway, and the waiting time in the latter follows the expression (3.1) of Section 3.3.1.

Parameter ε_H determines the cordon $\varepsilon_H R$ that delimits a central area where the system works in headways and the external one where works by schedules. Headways inside that boundary are lower than H_s. Therefore, $\varepsilon_H = H_s s/HD$. In function to the value of that parameter, we identify three different scenarios: (E.1) $\varepsilon_H \geq 1$, the system only works in headways, (E.2) $\phi \leq \varepsilon_H < 1$, the most external periphery works by schedules, and (E.3) $\varepsilon_H < \phi$, the system only works in headways in the most internal region of the central attractant area. In the first scenario, the city is divided in the same two areas as in the rest of the proofs, two types of trip, (e.1) and (e.2). However, in the other two scenarios, another area appears. In (E.2) the peripheral area related to (e.2) is divided in two subareas, one external, whose probability is $(1-\varepsilon_H^2)(1-\rho)/(1-\phi^2)$, and other internal, whose probability is $(\varepsilon_H^2-\phi^2)(1-\rho)/(1-\phi^2)$. In this scenario, the central area is (e.1). In (E.3), the periphery is (e.2), but the central area is divided in two, with probabilities $(\phi^2-\varepsilon_H^2)\rho/\phi^2$ for the external and $\varepsilon_H^2\rho/\phi^2$ for the internal.

Focusing our attention on (E.1), the average headways of the periphery and the central attractant area are weighted by the headway of each cordon βD. The probability density function of β is triangular: $2\beta/(1-\phi^2)$ and $2\beta/\phi^2$ respectively. Therefore, those average headways are: $H_p = \int_\phi^1 \left[\left(2\beta/(1-\phi^2)\right)(\beta R/s)H\right] d\beta = 2(1+\phi+\phi^2)RH/3(1+\phi)s$, and $H_c =$

$\int_0^{\phi}(2\beta_O/\phi^2)\left[\int_0^{\beta_O}[(2\beta_D/\phi^2)(\beta_O R/s)H]\,d\beta_D + \int_{\beta_O}^{\phi}[(2\beta_D/\phi^2)(\beta_D R/s)H]\,d\beta_D\right]d\beta_O = 4\phi RH/5s$. Giving an expected waiting time $W = [H_c\rho + H_p(1-\rho)]/2 = H[5(1-\rho)+\phi(1+\phi)(5+\rho)]R/15(1+\phi)s$.

The same derivation is done for the other two scenarios. In (E.2), the average headways in the two subareas of the periphery are: $H_p^o = \int_{\varepsilon_H}^1\left[\left(2\beta/(1-\varepsilon_H^2)\right)(\beta R/s)H\right]d\beta = 2(1+\varepsilon_H+\varepsilon_H^2)RH/3(1+\varepsilon_H)s$ and $H_p^i = \int_{\phi}^{\varepsilon_H}\left[\left(2\beta/(\varepsilon_H^2-\phi^2)\right)(\beta R/s)H\right]d\beta = 2(\varepsilon_H^2+\varepsilon_H\phi+\phi^2)RH/3(\varepsilon_H+\phi)s$. In (E.3), the average of the two central subareas are: $H_c^o = \int_{\varepsilon_H}^{\phi}\left(2\beta_O/(\phi^2-\varepsilon_H^2)\right)\left[\int_{\varepsilon_H}^{\beta_O}\left[\left(2\beta_D/(\phi^2-\varepsilon_H^2)\right)(\beta_O D/s)H\right]d\beta_D + \int_{\beta_O}^{\phi}\left[\left(2\beta_D/(\phi^2-\varepsilon_H^2)\right)(\beta_D D/s)H\right]d\beta_D\right]d\beta_O = 4(2\varepsilon_H^3+4\varepsilon_H^2\phi+6\varepsilon_H\phi^2+3\phi^3)RH/15(\varepsilon_H+\phi)^2 s$, $H_c^{i,o} = \int_{\varepsilon_H}^{\phi}\left[\left(2\beta/(\phi^2-\varepsilon_H^2)\right)(\beta D/s)H\right]d\beta = 2(\phi^2+\phi\varepsilon_H+\varepsilon_H^2)DH/3(\varepsilon_H+\phi)s$, and finally $H_c^i = \int_0^{\varepsilon_H}(2\beta_O/\varepsilon_H^2)\left[\int_0^{\beta_O}[(2\beta_D/\varepsilon_H^2)(\beta_O R/s)H]\,d\beta_D + \int_{\beta_O}^{\varepsilon_H}[(2\beta_D/\varepsilon_H^2)(\beta_D R/s)H]\,d\beta_D\right]d\beta_O = 4\varepsilon_H DH/5s$. Then, the resultant waiting times for these scenarios are:

$$\begin{aligned}
&\text{if } \phi \le \varepsilon_H < 1 \quad W = \left[\left(h_s + f_s H_p^o\right)(1-\varepsilon_H^2) + H_p^i(\varepsilon_H^2-\phi^2)/2\right](1-\rho)/(1-\phi^2) + \rho H_c \phi^2/2 = \\
&\qquad\qquad \left[h_s(1-\varepsilon_H^2) + H\left(2f_s(1-\varepsilon_H^3) + (\varepsilon_H^3-\phi^3)\right)R/3s\right](1-\rho)/(1-\phi^2) + 2\phi RH\rho/5s \\
&\text{if } \varepsilon_H < \phi \quad W = \left(h_s + f_s H_p\right)(1-\rho) + \left[(h_s + f_s H_c^o)(\phi^2-\varepsilon_H^2)^2 + \left(h_s + f_s H_c^{i,o}\right)2\varepsilon_H^2(\phi^2 - \varepsilon_H^2) + H_c^i \varepsilon_H^4/2\right]\rho/\phi^4 = [h_s + 2f_s(1+\phi+\phi^2)RH/3(1+\phi)s](1-\rho) + \\
&\qquad\qquad \left[h_s(\phi^4-\varepsilon_H^4) + 2H\left(2f_s\left(\phi^5-\varepsilon_H^5\right) + \varepsilon_H^5\right)R/5s\right]\rho/\phi^4 \quad \square
\end{aligned} \tag{C.23.1}$$

Result C.24. The expected in-vehicle travel time per trip is given by (C.24):

$$T = E/v_c = \left[(20+5\theta)(1-\rho) + 2\phi(1+\phi)\left(5\pi + \rho(4+\theta-\pi)\right)\right]R/30(1+\phi)v_c. \tag{C.24}$$

Proof. As the line length, a trip also has two sections: one on the swath-corridor and other on the line branching. This second section follows the same path as the radial network. This goes from the most external extreme of the trip to the cordon where the other extreme is located. Its length is $|\beta_O - \beta_D|R$ units of distance in the radial direction and $(\theta s/4)|\beta_O - \beta_D|R/s$ in the circular. The section on the swath-corridor runs from the point of entrance of the previous section to the other extreme of the trip. The distance travelled in this case is on average a quarter of the cordon length, $2\pi\left(min\{\beta_O;\beta_D\}\right)R/4$. With this information, we can estimate the distance travelled for the peripheral trips $E_p = \int_{\phi}^1\left(2\beta_O/(1-\phi^2)\right)(\beta_O-\phi)R(1+\theta/4)\,d\beta_O + \int_0^{\phi}(2\beta_D/\phi^2)[(\phi-\beta_D)R(1+\theta/4) + \pi\beta_D R/2]\,d\beta_D = (4+\theta+2\pi\phi+2\pi\phi^2)R/6(1+\phi)$, and for the central trips $E_c = \int_0^{\phi}\int_0^{\phi}(2\beta_D/\phi^2)(2\beta_O/\phi^2)[|\beta_O-\beta_D|R(1+\theta/4) + \pi min\{\beta_O;\beta_D\}R/2]\,d\beta_O\,d\beta_D = (4\pi+4+\theta)\phi R/15$. Finally, weighting these two lengths by the probability of each trip category, the expected in-vehicle travel distance per trip E is obtained. $\square$

Constraints

Result C.25. The expected vehicle occupancy on the critical load point during the rush hour is given by (C.25):

$$\begin{aligned}
&\text{if } \left(2d\rho + \sqrt{12\phi^2R^2\rho + d^2\rho^2}\right)/6\rho \le \phi R \quad O = (SF)\,H\Lambda\theta d\left[\begin{matrix} d\rho(36\phi^2R^2 - \rho d^2) + \\ \rho^{1/2}(12\phi^2R^2 + \rho d^2)^{3/2}\end{matrix}\right]/216\pi\phi^4R^4\rho \\
&\text{if } \left(2d\rho + \sqrt{12\phi^2R^2\rho + d^2\rho^2}\right)/6\rho > \phi R \quad O = (SF)\,H\Lambda\theta d(2\phi R - d)\left[\begin{matrix}\phi^2R^2(1-\rho) + \\ \rho d(2\phi R - d)\end{matrix}\right]/4\pi\phi^4R^4
\end{aligned} \tag{C.25}$$

Proof. The number of vehicles that connects a swath-corridor, which is at a distance from the city center $i \cdot d$, with its external area is $H\theta/2\pi$. The total demand generated in that swath and in its external area is $\Lambda[4\phi^2R^2 - (4i^2 - 4i + 1)\rho d^2]/8\,\phi^2R^2$. And the probability that this demand has its destination in the swath is $id^2/\phi^2\,R^2$. Mutiplying these three terms, the number of passengers carried by one vehicle is $H\Lambda\theta i d^2[4\phi^2R^2 - (4i^2 - 4i + 1)d^2]/8\,\pi\phi^4R^4$. The most occupied vehicles are those that serve the swath at a distance from the city center $\left(2d\rho + \sqrt{12\phi^2R^2\rho + d^2\rho^2}\right)/6\rho$. When this distance is inside the central attractant area, their occupancy is $O_i = H\Lambda\theta d\left[d\rho(36\phi^2R^2 - \rho d^2) + \rho^{1/2}(12\phi^2R^2 + \rho d^2)^{3/2}\right]/216\pi\phi^4R^4\rho$. Otherwise, the swath with the maximum occupancy is at the central attractant area's boundary since there are no swath-corridors in the periphery. Then, the occupancy in the most external swath-corridor is $O_e = H\Lambda\theta d(2\phi R - d)[\phi^2R^2(1 - \rho) + \rho d(2\phi R - d)]/4\pi\phi^4R^4$. Finally, as in all the cases, a safety factor (SF) is included. □

Appendix D

Sensitivity analysis of the transit network design model

A sensitivity analysis of the analytical model is presented here. A group of graphics are included to show the evolution of different costs with regard to changes on the decision variables. The results are obtained for the base case study of Section 4.1, considering the parameter $\phi = 1$ (therefore, f_d is irrelevant since the central attractant area occupies the whole city). From the optimal solution in that scenario, the decision variables are varied to see their effects on the different components of the objective function: total (Z), agency (C_A) and user (C_U) costs; infrastructure length (L), kilometers travelled per hour (V) and number of vehicles (M); access (A), waiting (W), and in-vehicle (T) times, and number of transfer per trip (e_T); finally, commercial speed (v_c). In each graph, only one decision variable is modified while the others are constant and equal to the optimum. In this way, we observe the influence of each one independently of the others.

The results of this analysis show the model's robustness, the convex behavior of all the network structures and the coherent tendency of all the metrics when the decision variables change. As we can observe, the variation of the total system cost, which is the variable that determines the best network configuration, is not significant around the optimal values. Its curves are flat in that point. Agency and user costs vary in opposite directions, i.e., their changes are counteracted; a fact that restricts the variations of total system costs. In general, the changes are more pronounced when the values of the decision variables are reduced instead of increased.

In addition, the figures also depict the feasible domains in some decision variables due to geometrical or capacity constraints.

D.1. Network structures atop a grid street pattern

In general, the effects of one variable is similar in all the network structures analyzed:

- An increasing headway reduces the fleet needed to serve the service, and obviously, the kilometers travelled by that fleet. The consequences over the users are higher waiting times, and a reduction of the commercial speed (longer in-vehicle times) due to more boardings and alightings per vehicle.

- Longer stop/line spacings produce two immediate changes, less infrastructure length and a higher access cost. However, there are additional effects. A reduction of fleet that is greater in the hybrid and grid structures since a longer stop spacing implies less corridors, and in this structures the headway is related to the corridor and not to a point where the lines are gathered such as in the other schemes. In these other structures, radial and direct trips, there is less branching, and therefore, a reduction of the waiting time. In addition, a faster service, which supposes less fleet and shorter in-vehicle times. However, this increase is limited in the transfer-based structures. In them, less stops improve the speed, but less lines reduce the number of vehicles, i.e., more boardings and alightings per vehicle. Then, the variation of the commercial speed is compensated by these two factors. Finally, the area of influence for each line is larger and the number of transfers decreases.
- For a direct trip-based structure, if the variable d grows, it reduces the number of swath-corridors. This produces a reduction of fleet and the kilometers travelled, and the infrastructure length to a lesser extent. For the users, this variable basically increases the access time.
- In the hybrid scheme, larger central grids imply: more corridors, that is, longer infrastructure lengths due to more stops with double coverage; as headway is defined per corridor, more fleet and kilometers travelled; shorter waiting and in-vehicle times due to less branching and less boardings and alightings respectively; and finally, fewer transfers due to more direct trips and less external two-transfer trips.

Regarding the constraints, problems of capacity appear for high headways, and for long spacings in those structures where the final fleet depends on the number of corridors (hybrid and grid structures). Moreover, for low values of α, there are less corridors and fleet, and the greater peripheral demand makes a greater pressure on the boundary of that area.

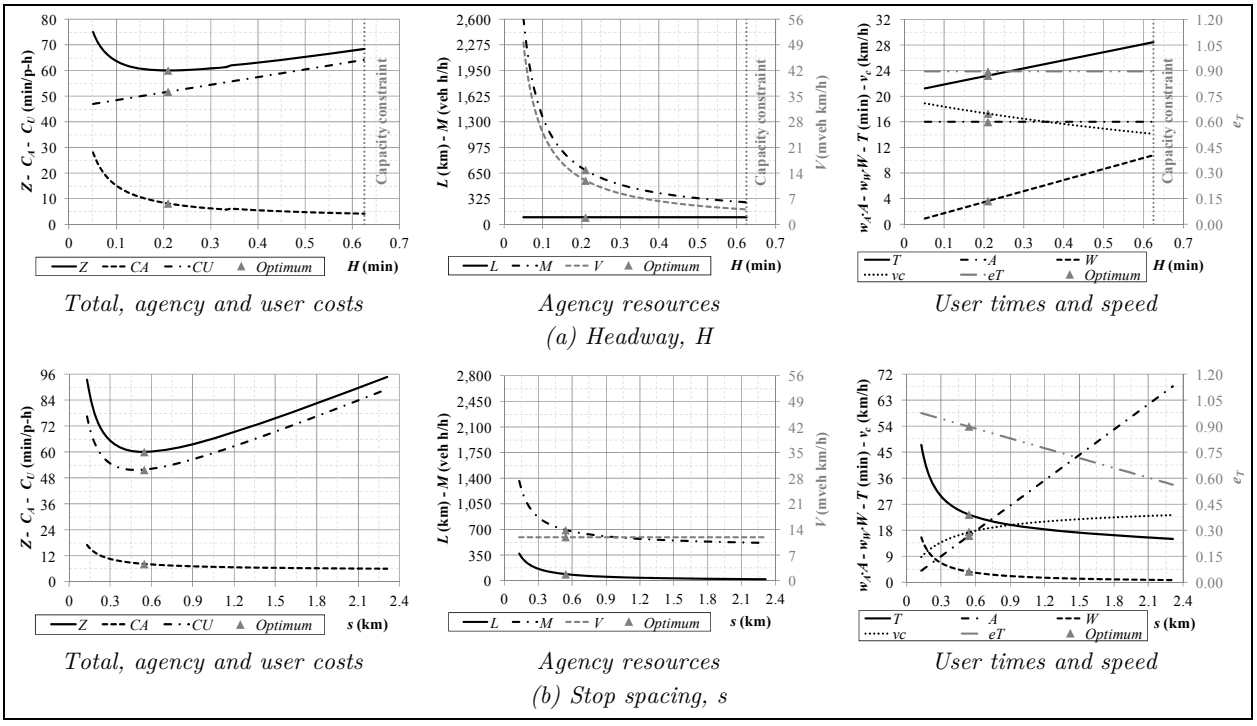

Figure D.1. Sensitivity analysis of the radial network structure.

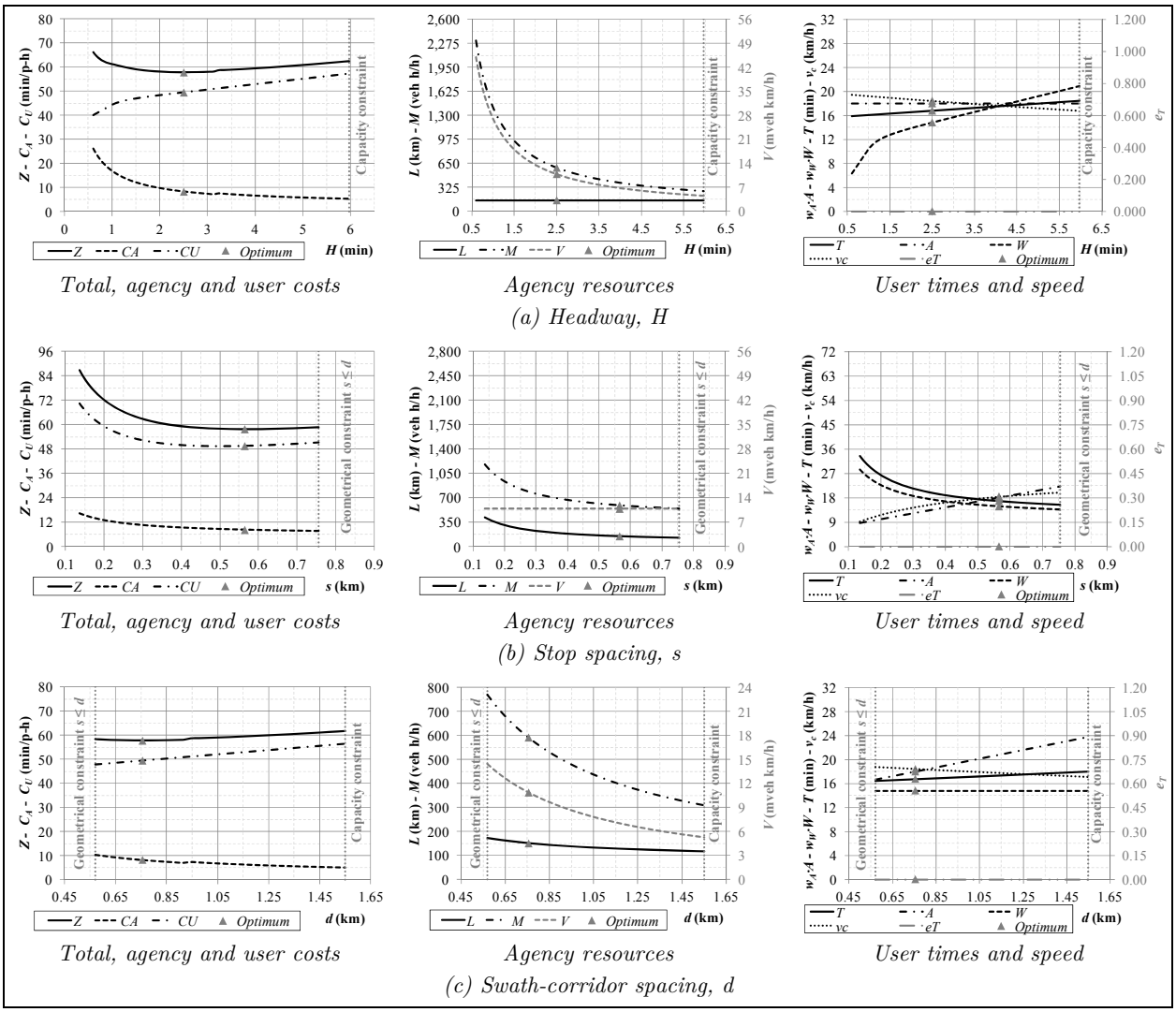

Figure D.2. Sensitivity analysis of the direct trip-based network structure.

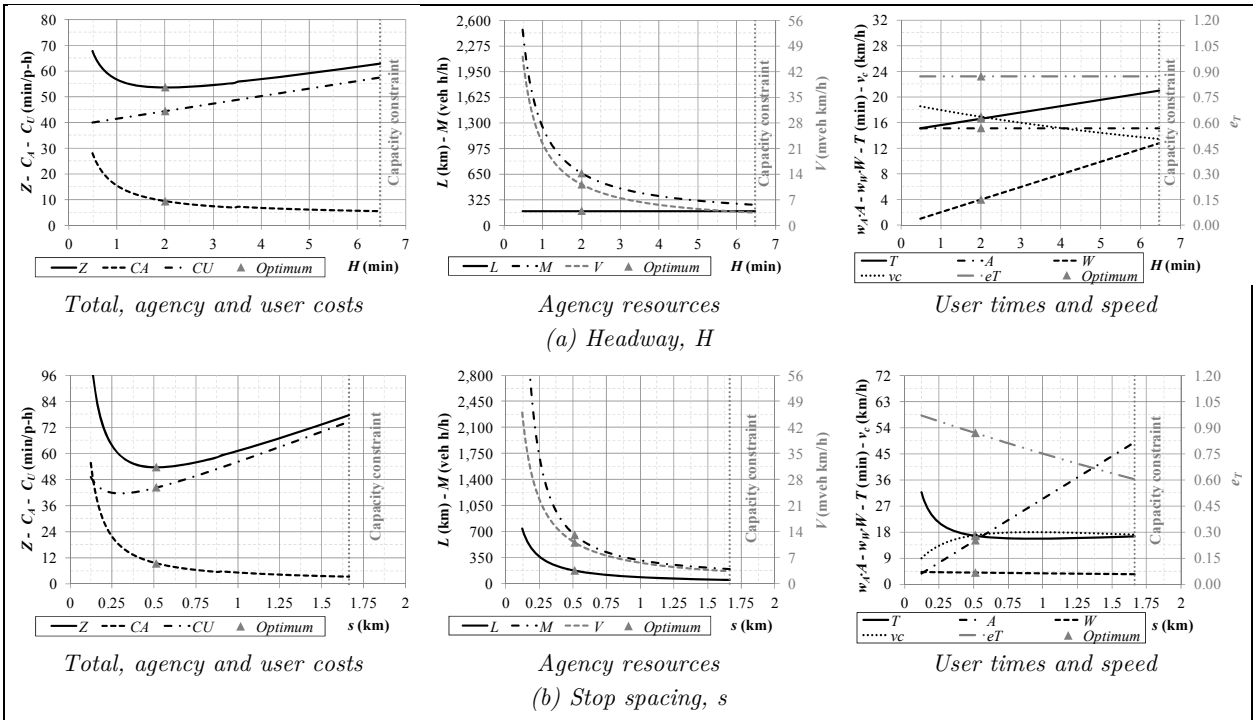

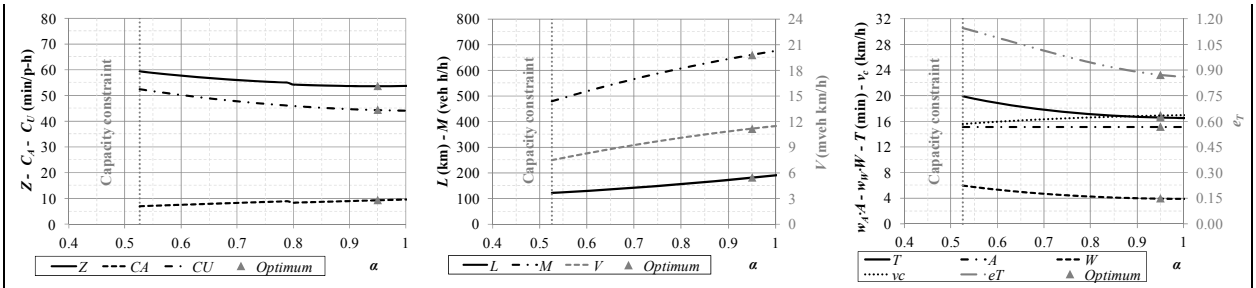

Total, agency and user costs *Agency resources* *User times and speed*

(c) Central area size, α

Figure D.3. Sensitivity analysis of the hybrid network structure.

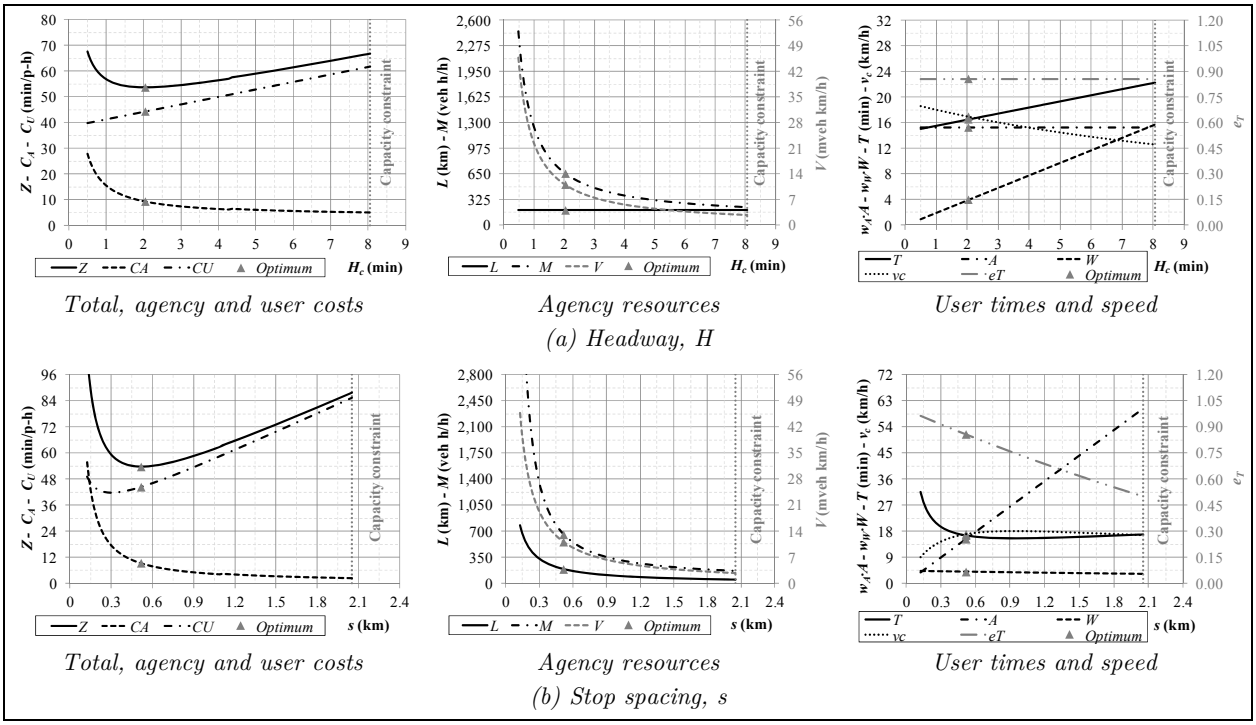

Total, agency and user costs *Agency resources* *User times and speed*

(a) Headway, H

Total, agency and user costs *Agency resources* *User times and speed*

(b) Stop spacing, s

Figure D.4. Sensitivity analysis of the grid network structure.

D.2. Network structures atop a ring-radial street pattern

The evolution of the different metrics in the network structures analyzed atop a ring-radial street pattern is very similar to in the grid street layout. The main differences is the additional decision variable θ. However, as it is a stop spacing, its effects are very analogous to the stop spacing s of the previous section. An increase of this variable produces networks with less infrastructure, and as all of the structures have a headway related to the number of corridors in this street pattern, it supposes a reduction of fleet and kilometers travelled. From the user point of view, greater θ implies longer walking distances and less transfers due to larger influence areas per line. However, the effects on commercial speed and waiting time are limited due to fleet and number of lines are related, that is, less stops at the same time that less vehicles for the same level of demand.

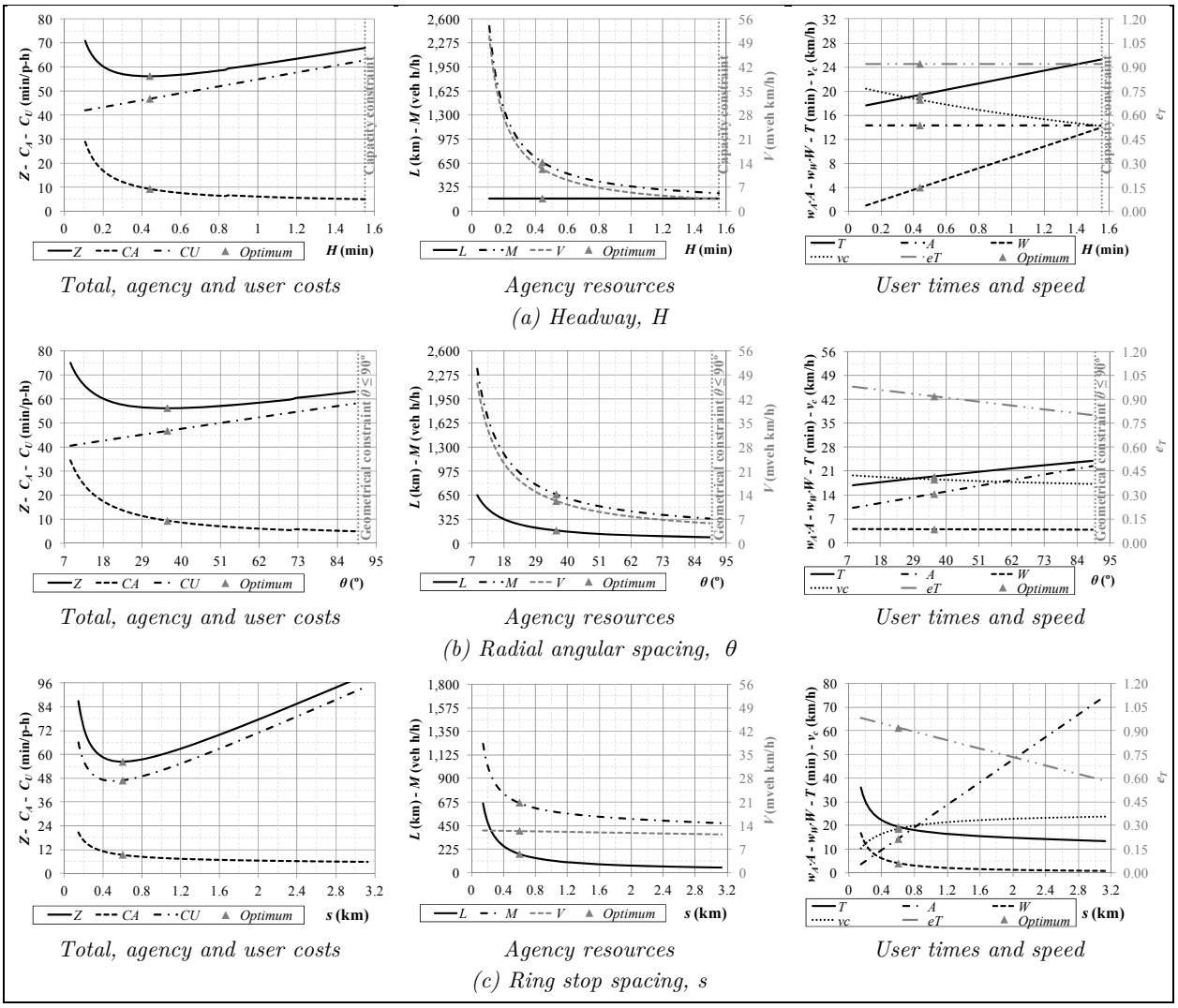

Figure D.5. Sensitivity analysis of the radial network structure.

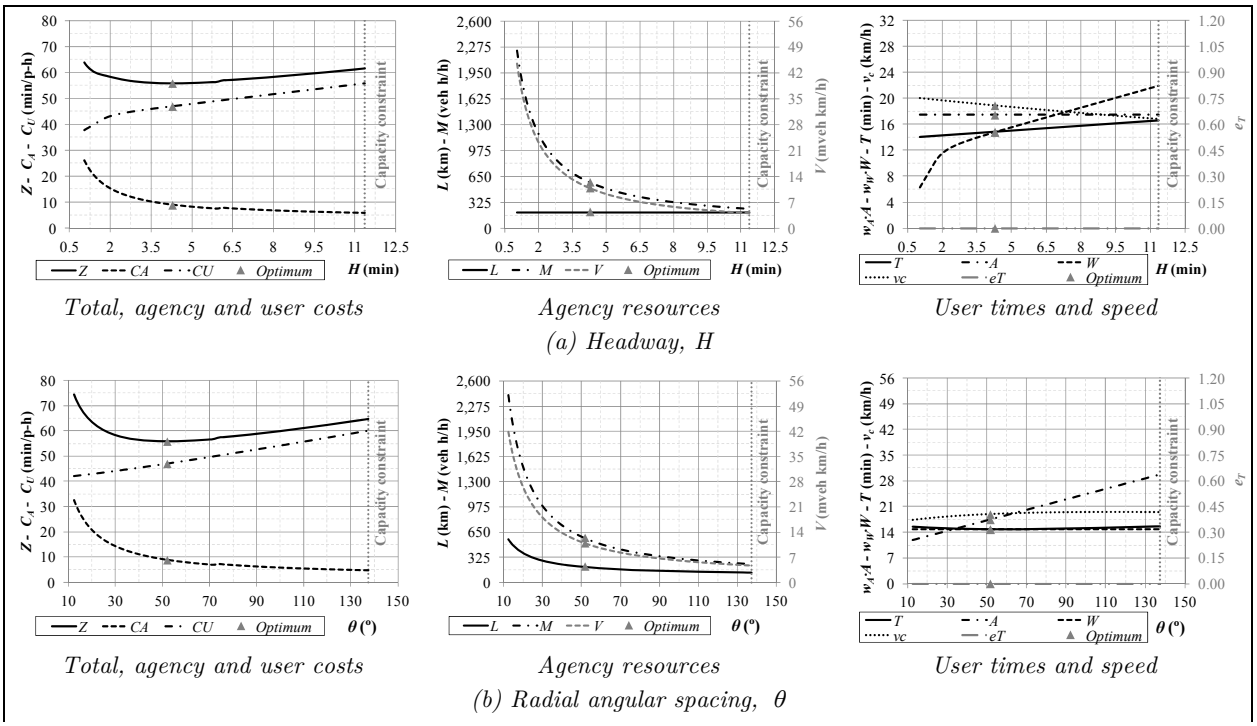

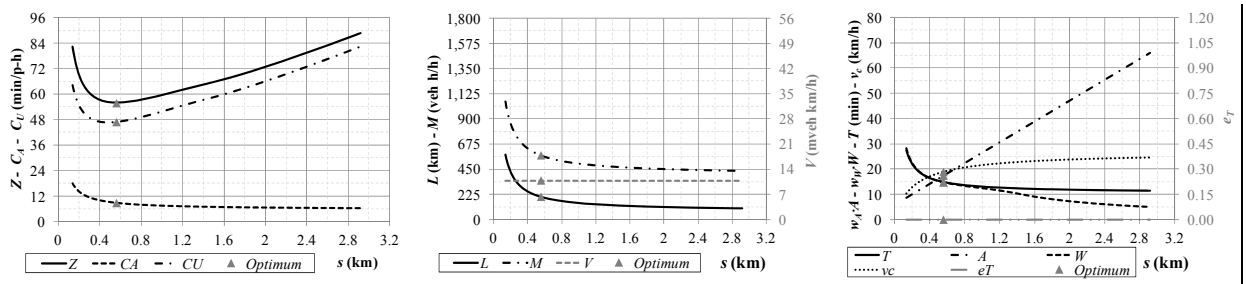

Total, agency and user costs *Agency resources* *User times and speed*

(c) Ring stop spacing, s

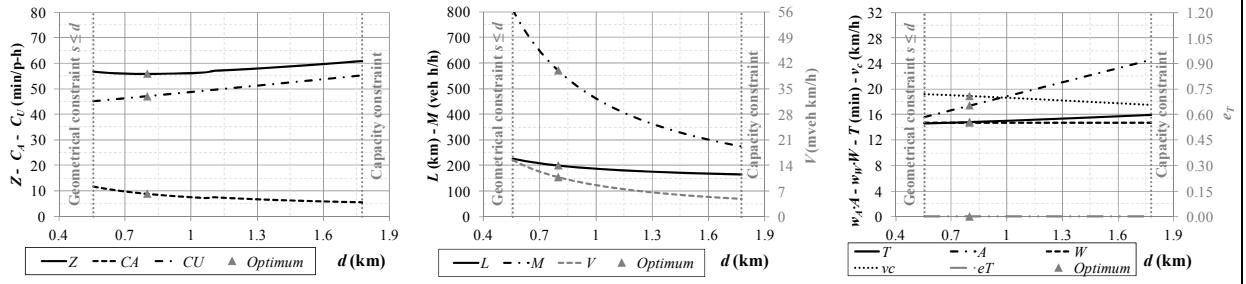

Total, agency and user costs *Agency resources* *User times and speed*

(d) Swath-corridor spacing, d

Figure D.6. Sensitivity analysis of the direct trip-based network structure.

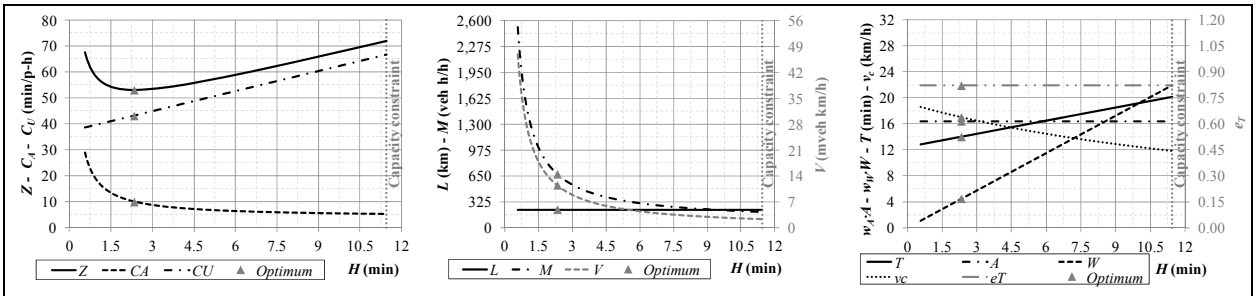

Total, agency and user costs *Agency resources* *User times and speed*

(a) Headway, H

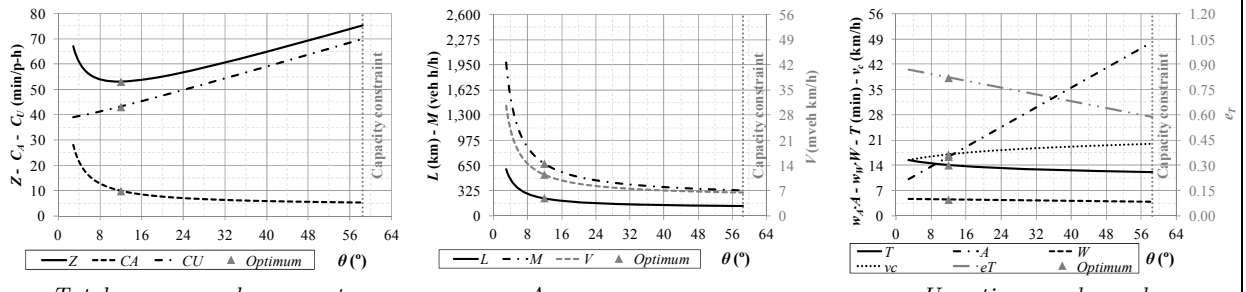

Total, agency and user costs *Agency resources* *User times and speed*

(b) Radial angular spacing, θ

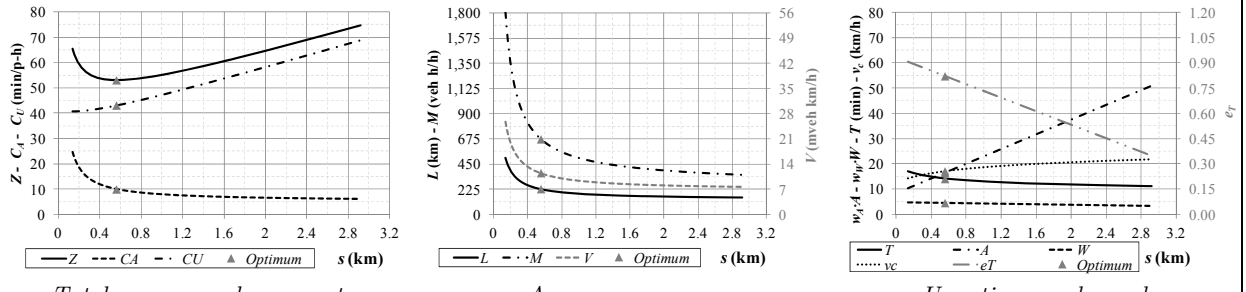

Total, agency and user costs *Agency resources* *User times and speed*

(c) Ring stop spacing, s

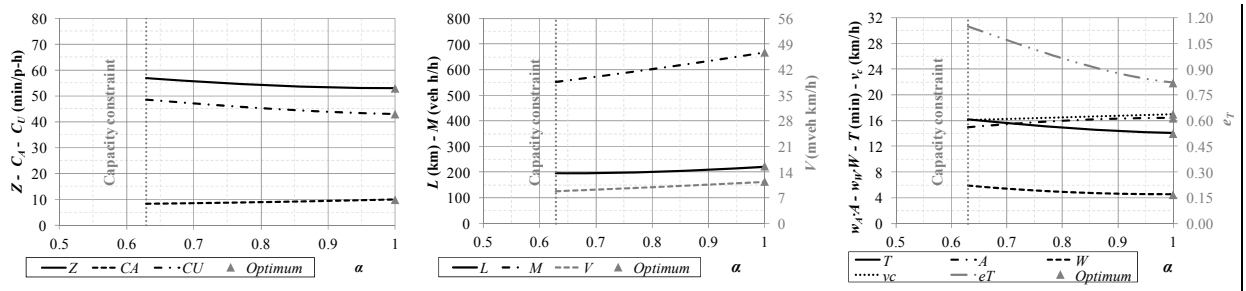

Total, agency and user costs *Agency resources* *User times and speed*

(d) Central area size, α

Figure D.7. Sensitivity analysis of the hybrid network structure.

Appendix E

Additional results of the comparison of transit network structures

Further results about the comparison among network structures are introduced in this appendix. The next figures show the evolution with regard to urban dispersion (parameter ϕ) of the remainder partial costs not included in Chapter 4: network length, kilometers travelled and fleet for agency; access and waiting times for users; and commercial speed. Section H.1 presents the results for the structures designed atop a grid street pattern and Section H.2 for those structures adapted to a ring-radial street layout, complementing Sections 4.2 and 4.3 respectively.

E.1. Comparison atop a grid street pattern

The evolution of these metrics is explained by the evolution of the decision variables in Figure 4.2. Their tendencies or abrupt changes are coincident with the same events in some of those decision variables. However, these results give additional knowledge about each structure. Apart from irregular variations in scenarios of low urban dispersion, then we can emphasize the most significant aspects from Figure H.1. The grid network has the longest infrastructure length due to double coverage in all stops, since stop/line spacing is similar to other networks as Figure 4.2a shows. A hybrid scheme presents a constant growth of its infrastructure length until this length reaches similar values to the grid. This fact is not a consequence of shorter spacings; the reason is larger central grids (Figure 4.2a). Furthermore, a break in the number of vehicles needed and their kilometers travelled happens when this structure works at full capacity from ϕ = 0.34 until ϕ = 0.61. Regarding a direct trip-based network, it has the highest commercial speed, a consequence of longer spacings and less boardings ($e_T = 0$). Therefore, this structure stand out among the others due to greater kilometers travelled. As it is commented in Section 4.2.1, Figures H.1e and H.1f confirms that users walk and wait more in this case.

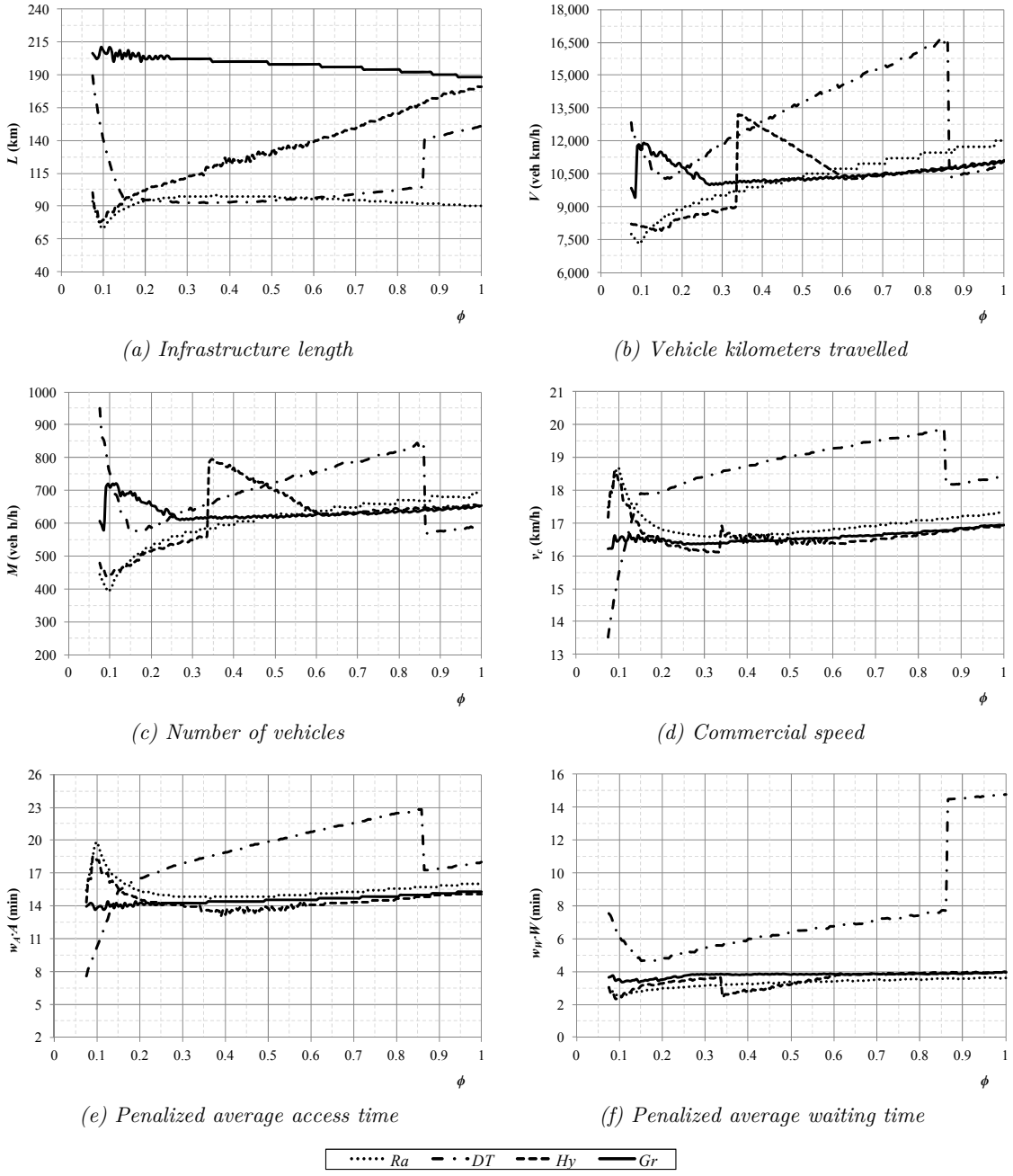

(a) Infrastructure length

(b) Vehicle kilometers travelled

(c) Number of vehicles

(d) Commercial speed

(e) Penalized average access time

(f) Penalized average waiting time

Figure E.1. Evolution of agency and user partial costs and commercial speed with regard to the demand decentralization degree parameter ϕ in a grid street pattern.

E.2. Comparison atop a ring-radial street pattern

The evolution of partial costs in a ring-radial street pattern follows a similar behavior to the other street pattern explained above. Again, the changes on the evolution of partial costs are a consequence of the same factors as the decision variables (Figure 4.8). It is interesting to note the evolution of the infrastructure length for the hybrid structure in Figure H.2a. This cost presents a convex behavior, clearly shown between $\phi = 0.43$ and $\phi = 0.70$. In this range of dispersion, with regard to geometrical decision variables, only the variable α changes; the other two s and θ are practically constant (see Figure 4.8). Therefore, L is convex with α. The different components of L evolve in opposite directions with regard to that decision variable.

The length of circular lines increases with α (more lines), while the length in the radial direction decreases sharply (lines are branched less times). Approximately, during the time that radial length in the periphery prevails over that length in the central mesh, the total length decreases. Its tendency changes when that mesh is larger; and the central radial length is more relevant than the peripheral.

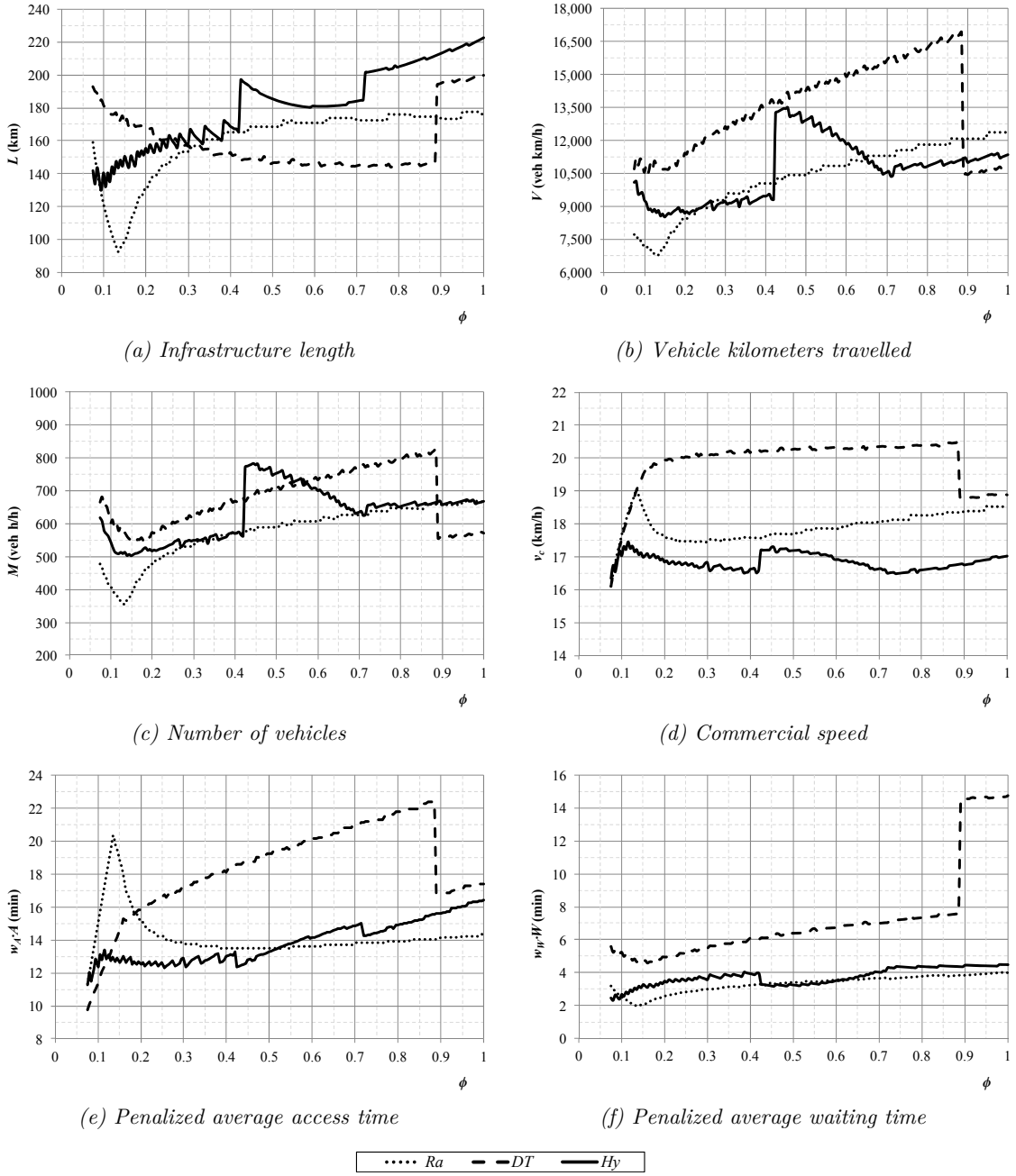

(a) Infrastructure length

(b) Vehicle kilometers travelled

(c) Number of vehicles

(d) Commercial speed

(e) Penalized average access time

(f) Penalized average waiting time

Figure E.2. Evolution of agency and user partial costs and commercial speed with regard to the demand decentralization degree parameter ϕ in a ring-radial street pattern.

Appendix F

Hybrid model formulation in a rectangular grid city

This appendix presents and derives the formulation of the model used in Chapter 6 to design a transfer-based network for Barcelona. That model is an extension of the hybrid structure atop a grid street layout of Chapter 3. In that case, the territory served was a square. However, as Barcelona is roughly a rectangular city, the formulation has to be derived again in order to a better adaptation for that city. Based on that change, the model increases the number of freedom degrees distinguishing the geometrical decision variables between horizontal and vertical directions. In addition, stop and line spacings are different. In this case, the thesis considers a uniform demand distribution over the whole city, both generated and attracted. Therefore, parameters $\phi = 1$ and $f_d = 1$. To derive the formulae, the logic is the same as in Appendix B. For this reason, the formulation is presented directly without an exhaustive explanation.

Agency costs

$$L = D_H D_V (s_H + s_V)(1 + \alpha_H \alpha_V)/2 s_H s_V + D_H D_V (s_H - s_V)(\alpha_V - \alpha_H)/2 s_H s_V$$

$$V = 2\alpha_H D_H D_V [1 + D_H (1 - \alpha_H)/2D_V]/s_V H + 2\alpha_V D_H D_V [1 + D_V (1 - \alpha_V)/2D_H]/s_H H$$

$$M = V/v_c$$

$$v_c = 1/[1/v + \tau/s + \tau'(1 + e_T)\Lambda/V]$$

User costs

$$e_T = P_1 + 2 \cdot P_2$$

where:

$$P_0 = (s_H D_H + s_V D_V)(1 + \alpha_H \alpha_V)/2D_H D_V + (s_H D_H - s_V D_V)(\alpha_V - \alpha_H)/2D_H D_V - \alpha_H \alpha_V s_H s_V / D_H D_V$$

$$P_1 = s_V(-\alpha_V + \alpha_V^2 - 3\alpha_H \alpha_V + \alpha_H \alpha_V^2)/2D_H + s_H(-\alpha_H + \alpha_H^2 - 3\alpha_H \alpha_V + \alpha_V \alpha_H^2)/2D_V + (1 - \alpha_V^2 - \alpha_H^2 + 4\alpha_H \alpha_V - \alpha_H^2 \alpha_V^2)/2 + \alpha_H \alpha_V s_H s_V / D_H D_V$$

$$P_2 = (1 + \alpha_V^2 + \alpha_H^2 - 4\alpha_H \alpha_V + \alpha_H^2 \alpha_V^2)/2 - s_V (1 - \alpha_V)^2 (1 + \alpha_H)/2D_H - s_H (1 - \alpha_H)^2 (1 + \alpha_V)/2D_V$$

$$A = [(s_H + s_V)/4 + s/2]/w$$

$$W = (1 + P_1)[\alpha_H\alpha_V + (1 - \alpha_H^3)(1 - \alpha_V)/3\alpha_H(1 - \alpha_H) + (1 - \alpha_V^3)(1 - \alpha_H)/3\alpha_V(1 - \alpha_V)]H/2 + P_2 \cdot H/2$$

$$T = E/v_c = \Big[\Big((\alpha_V^2 D_V^2 + \alpha_H^2 D_H^2 + 4\alpha_H\alpha_V D_H D_V)/4 + \alpha_H\alpha_V D_H D_V(1 - \alpha_H\alpha_V/2)/3\Big)(1 - \alpha_H^2\alpha_V^2)/(\alpha_H D_H + \alpha_V D_V) + (\alpha_H D_H + \alpha_V D_V)(\alpha_H^2\alpha_V^2)/3 + [D_H(2 - 3\alpha_H + \alpha_H^3) + D_V(2 - 3\alpha_V + \alpha_V^3)]/4\Big]/v_c$$

Occupancy constraint

$$O_V = (\Lambda H/4)max\{s_V(1 + \alpha_H)(1 - \alpha_V)/\alpha_H D_H; (1 - \alpha_H)^2(1 + \alpha_V)^2/8 + s_V(4 - (1 - \alpha_H)^2(1 + \alpha_V)^2 - 2\alpha_H^2\alpha_V^2)/2\alpha_H D_H\}$$

$$O_H = (\Lambda H/4)max\{s_H(1 + \alpha_V)(1 - \alpha_H)/\alpha_V D_V; (1 - \alpha_V)^2(1 + \alpha_H)^2/8 + s_H(4 - (1 - \alpha_V)^2(1 + \alpha_H)^2 - 2\alpha_V^2\alpha_H^2)/2\alpha_V D_V\}$$

Appendix G

Technical analysis for the real demand data from the *Nova Xarxa*

G.1. Demand Model

A parsimonious regression model is proposed. It assumes that the total number of validations in a line, V_k, arises from two demand types: (i) direct trips, where origin-destination pairs can be served without a transfer and therefore must lie in the influence area of line k; and (ii) one-transfer trips for origin-destination pairs requiring transfers.[7] To simplify the analysis, we assume that the generation rates for trips of type (i) and (ii) are uniform in space for each line, although they can vary across lines. Except where indicated, the model shall assume that the influence areas of the various lines, where trips are generated, do not overlap.

Although a detailed analysis would take into consideration the station-to-station O-D demands and a route assignment, this can be avoided here because Barcelona's network closely resembles a homogeneous rectangular grid. To see how this helps, assume for the moment that the grid is perfect with no overlaps and similar frequencies everywhere where people choose the shortest path. Furthermore, since the stop spacing is practically constant, ignore the stops and assume that people walk to/from the closest line. Also let's (reasonably) assume that each line has a catchment area of uniform width where the trip generation rates for direct trips and 1-transfer trips are uniform. These rates are assumed to be proportional to the number of destinations in the respective catchment areas. It is then possible to express the trip generation rate of each type as a function of the length of the line and the combined length of the lines that have a direct connection with it.

To do this, let V_k be the number of boarding validations for line k in some specific month, l_k be the line's length, and $l_{1,k}$ the combined length of the lines that connect with it at the time of observation (see Figure G.1). With the assumptions above, the number of validations should increase linearly with both l_k and $l_{1,k}$. Thus, the proposed regression model is:

$$V_k = \beta_{0,k} l_k^2 + \beta_{1,k} l_k l_{1,k} \tag{G.1}$$

[7] We have verified with a regression analysis not included in this appendix that the number of passengers making more than one transfer is negligible. Therefore O-D pairs requiring more than one transfer are not considered in the model.

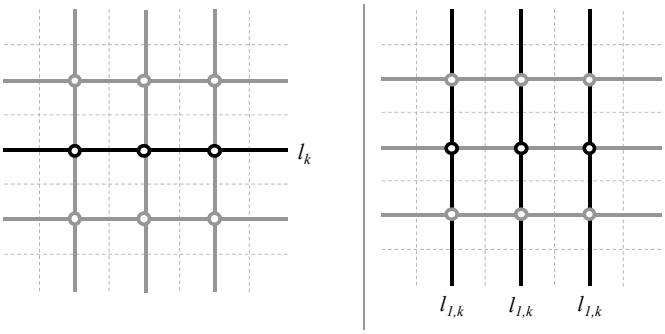

Figure G.1. Graphical representation of the regression model independent variables.

The model specification does not include a constant term because it would make little physical sense. If a lines' length is zero, one should not expect any monthly validations. The first term of (G.1) represents the number of trips generated with destinations along the line, and therefore no transfers. This is the direct demand. The second term represents the number of boardings with origin (or destination) on line k and destination (or origin) on the connecting lines. Note that only one half of these validations are outbound trips from line k. Thus, the formulas for total transfers, X_k, and total demand, D_k, generated by line k are:

$$X_k = 1/2\beta_{1,k} l_k l_{1,k} \tag{G.2a}$$

$$D_k = \beta_{0,k} l_k^2 + 1/2\beta_{1,k} l_k l_{1,k} \tag{G.2b}$$

So far we assume that we have a grid with a well-defined routing for each O-D pair. However, Barcelona is not a perfect grid, and there are a few locations where two lines overlap. This requires a modification of (G.1) because in the region of overlap some people can choose either of the two lines, and this provides a routing option that splits the demand. The modification should consider the length of overlap and take into account the overlapping lines' frequency ratio in order to reflect such demand split.

On account of the overlap, the new model introduces two additional definitions of line lengths: the length of the overlap region, $l_{o,k}$; and the combined length of all lines that connect with this region, $l_{1,o,k}$. These two concepts are illustrated in Figure G.2, where the dashed line is the line that causes the overlap: $l_{o,k}$ is marked on the leftmost diagram; and $l_{1,o,k}$ on the rightmost (the case in the figure includes only one connecting line). It is also necessary to introduce $\eta_{o,k}$ as the fraction of buses flowing on the overlapping region that are not on line k; i.e., the ratio of the overlapping line frequency and the total frequency. This ratio is an approximation for the fraction of the demand that is syphoned away by the overlapping line. In terms of headways, with H_k representing the headway of line k and $H_{o,k}$ the headway of the overlapping line, the expression is:

$$\eta_{o,k} = \left(1/H_{o,k}\right)/\left(1/H_k + 1/H_{o,k}\right) \tag{G.3}$$

With this notation, the specification for the demand of a line k that experiences and overlap of length $l_{o,k}$ is:

$$V_k = \beta_{0,k}(l_k^2 - l_{o,k}^2 \eta_{o,k}) + \beta_{1,k}(l_k l_{1,k} - l_{o,k} l_{1,o,k} \eta_{o,k}) \tag{G.4}$$

$$X_k = 1/2\beta_{1,k}(l_k l_{1,k} - l_{o,k} l_{1,o,k} \eta_{o,k}) \tag{G.5a}$$

$$D_k = \beta_{0,k}(l_k^2 - l_{o,k}^2\eta_{o,k}) + 1/2\beta_{1,k}(l_k l_{1,k} - l_{o,k}l_{1,o,k}\eta_{o,k}) \quad \text{(G.5b)}$$

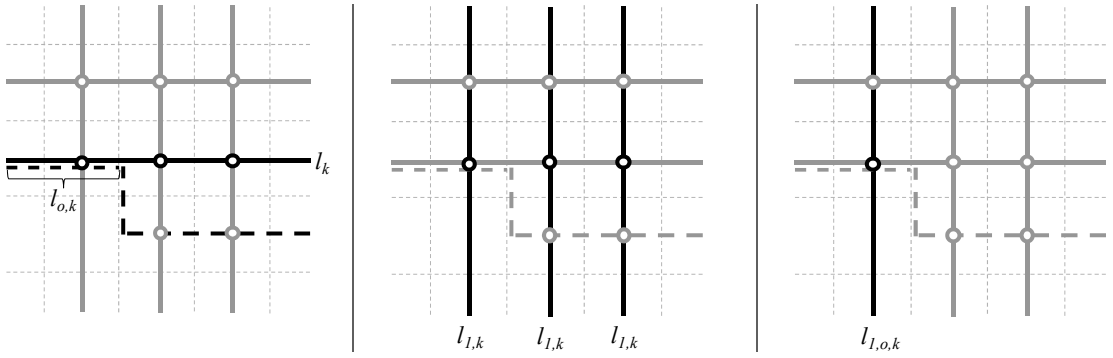

Figure G.2. Graphical representation of the regression model independent variables with overlap.

The least squares regression method has been then used to fit Equation (G.4) to the data from each line and in this way obtain four sets of β-estimates. Table G.1 summarizes these data for lines H6, V7 and V21. These lines do not exhibit significant overlaps and therefore, $l_{o,k} \equiv 0$. The table also includes the dependent variables V_k. For consistency across phases, we have used the average number of validations across the (same) eight months in the middle of each phase. It is not necessary to break validations by month because the explanatory variables stay fixed in every phase.

Table G.1. Estimation data for Lines H6, V7 and V21: $l_{o,k} \equiv 0$.

Line:		H6	V7	V21
l_k (km):		9.70	5.11	8.18
$l_{1,k}$ (km)	Phase 1	13.28	26.87	24.90
	Phase 2	29.48	53.12	55.18
	Phase 3	49.27	62.54	63.84
	Final phase*[a]	121.66	90.47	91.77
V_k (val./month)	Phase 1	493,396	139,880	263,862
	Phase 2	559,272	205,859	316,317
	Phase 3	636,431	240,423	335,337

*[a] The line lengths for the final phase are not used for estimation. They are included because they are used to predict the ultimate performance of the system.

Table G.2 summarizes the data for line H12, which overlaps significantly with line H16. H12 overlaps with H16 for a 1.63 km and then the two lines lie only one or two blocks apart for another 2.54 km. Therefore, the table includes its $l_{o,k}$, $l_{1,o,k}$ and $\eta_{o,k}$ values on separate rows.

Table G.2. Estimation data for Line H12.

Line:	H12	l_k (km):	11.38	
Phase:	1	2	3	Final*[a]
$l_{1,k}$ (km):	17.42	33.61	53.73	139.14
$l_{o,k}$ (km):	-	-	4.17	4.17
$l_{1,o,k}$ (km):	-	-	34.31	42.40
$\eta_{o,k}$:	-	-	0.44	0.44
V_k (val./month):	450,804	563,196	605,949	-

*[a] The line lengths for the final phase are not used for estimation. They are included because they are used to predict the ultimate performance of the system.

G.2. Results

The following tables summarize the results obtained for each line.

Table G.3. Results for line H6.

Regression model H6	R^2	Adjusted R^2	Std. error	F	Significance
	0.996	0.995	38,561	2586	0.000
Explanatory variable	coefficient	Std. error	Significance	Conf. Int. 70%	VIF
$\beta_{0,H6}$	4,689.1	193.4	0.000	4,483.8 - 4,894.4	5.35
$\beta_{1,H6}$	409.5	55.1	0.000	351.0 - 468.0	5.35

Table G.4. Results for line V7.

Regression model V7	R^2	Adjusted R^2	Std. error	F	Significance
	0.994	0.994	16,024	1865	0.000
Explanatory variable	coefficient	Std. error	Significance	Conf. Int. 70%	VIF
$\beta_{0,V7}$	2,479.6	414.5	0.000	2,039.6 - 2,919.5	10.91
$\beta_{1,V7}$	539.2	42.5	0.000	494.1 - 584.2	10.91

Table G.5. Results for line V21.

Regression model	R^2	Adjusted R^2	Std. error	F	Significance
V21	0.990	0.989	32,961	1039	0.000
Explanatory variable	coefficient	Std. error	Significance	Conf. Int. 70%	VIF
$\beta_{0,V21}$	3,268.1	306.3	0.000	2,943.0 - 3,593.3	9.26
$\beta_{1,V21}$	221.2	49.3	0.000	168.9 - 273.6	9.26

Table G.6. Results for line H12.

Regression model	R^2	Adjusted R^2	Std. error	F	Significance
H12	0.999	0.998	26,914	4900	0.000
Explanatory variable	coefficient	Std. error	Significance	Conf. Int. 70%	VIF
$\beta_{0,H12}$	2,762.9	114.6	0.000	2,641.2 - 2,884.5	7.00
$B_{1,H12}$	504.6	36.2	0.000	466.2 - 543.0	7.00

Note from the tables that in all four cases the estimated parameters were statistically significant and the fit is good. Therefore, the parameter values are entered in (G.5) to predict the monthly number of passenger trips (and passenger trips with transfers) generated by each line in the four phases of the project, using the explanatory variables in Tables G.1 and G.2. Tables 7.2 and 7.3 of Chapter 7 in the text contain the results.

G.3. Discussion

All four models have similar explanatory power. The absolute value of the regression coefficients $\beta_{0,k}$ and $\beta_{1,k}$ differs between lines, and these differences are what one might expect. First, differences are expected since the demand levels for bus service are likely to be inhomogeneous throughout the city. Second, differences may be exacerbated because the impact of alternative transit modes may vary considerable across lines. For example, in the case of the *Nova Xarxa*, line H12 lays precisely on top of alternative metro lines. This is probably why its $\beta_{0,k}$ coefficient is 41% smaller than that of line H6.

It is also interesting to see that the ratio $\beta_{1,k}/\beta_{0,k}$ differs considerable across routes. While it was approximately 0.08 for lines H6 and V21, it was about 0.20 for lines V7 and H12. This illustrates that the capacity of each line to generate direct and transfer trips varies considerably. In all cases, however, the direct demand predominates. Most of the variation is due to the $\beta_{0,k}$ coefficients, which change more drastically across lines. This seems reasonable since 0-transfer demand should depend on the line's location within the city, whereas transfer trips have a much broader area of influence, and should predominantly depend on the city's proclivity to transferring.